Microwave Electronics

Design and Development of Compact Asymmetric Coplanar Strip Fed Antennas

A thesis submitted by

DEEPU V

in partial fulfillment of the requirements for the degree of

DOCTOR OF PHILOSOPHY

Under the guidance of

Prof. P. MOHANAN

DEPARTMENT OF ELECTRONICS
FACULTY OF TECHNOLOGY
COCHIN UNIVERSITY OF SCIENCE AND TECHNOLOGY
COCHIN - 682 022, INDIA

April 2009

Dedicated to Almighty,

my parents, teachers and dear ones

DEPARTMENT OF ELECTRONICS
COCHIN UNIVERSITY OF SCIENCE AND TECHNOLOGY,
KOCHI,INDIA.

Dr. P. Mohanan
(Supervising guide)
Professor
Department of Electronics
Cochin University of Science and Technology

Certificate

This is to certify that this thesis entitled "**DESIGN AND DEVELOPMENT OF COMPACT ASYMMETRIC COPLANAR STRIP FED ANTENNAS**" is a bonafide record of the research work carried out by Mr. Deepu.V under my supervision in the Department of Electronics, Cochin University of Science and Technology. The results embodied in this thesis or parts of it have not been presented for any other degree.

Cochin-22
April 2009

Dr. P. Mohanan

Declaration

I hereby declare that the work presented in this thesis entitled "**DESIGN AND DEVELOPMENT OF COMPACT ASYMMETRIC COPLANAR STRIP FED ANTENNAS**" is a bonafide record of the research work done by me under the supervision of Dr. P. Mohanan, Professor, Department of Electronics, Cochin University of Science and Technology, India and that no part thereof has been presented for the award of any other degree.

Cochin-22
April 2009

Deepu.V
Research Scholar
Department of Electronics
Cochin University of Science andTechnology

Acknowledgement

As my teacher puts it "Research is not inventing or discovering anything, it is the process of patient learning of how to solve a problem successfully". This process cannot be successfully completed without the help and cooperation of many people.

Firstly I would like to express my sincere gratitude to my supervising guide Prof.P.Mohanan for offering me a research position, guidance, support and blessings. His alchemy of teaching and research had a great impact on my research career. In addition to science I learned many valuable know how on other important fields of life from him.

My sincere thanks to Dr. K.G. Nair, Director, Centre for Science in Society, Cochin University of Science and Technology and former Head, Department of Electronics, Cochin University of Science and Technology. It was his vision that gave birth to such a wonderful establishment with international facilities.

I am grateful to Prof. K. Vasudevan, Head of the Department of Electronics for his constant encouragement and concern, and for extending the enormous facilities of Department of Electronics for my research. His easily approachable character and his remarkable skill of solving problems was greatly helpful during my research.

My special and sincere acknowledgement goes to Dr. C. K. Aanandan, Professor, Department of Electronics, Cochin University of Science and Technology for his well-timed care in my research, valuable suggestions and constant encouragements to improve my work.

I would also like to thank Prof. K. T Mathew,Prof. P.R.S Pillai, Dr. Tessamma Thomas Mr. James Kurien, Dr. M.H. Supriya and all other faculty members of the Department of Electronics, for their whole hearted support, constant encouragement and valuable suggestions.

I whole heartedly thank Dr.S.Mridula Reader School of Engineering, CUSAT for her support and care. she was instrumental in pushing me back into my full pace.It was her constant support that helped me to complete my work within this short period.

I whole heartedly thank Dr.Gopalakrishnan Nair ,Director Institute of Physics and Maths, Trivandrum for his encouragement and blessings.It was his constant inspiration that helped me tide over my difficulties.

My senior Research scholars Dr.Rohith K Raj,Dr.Suma M N and Mr.Manoj Joseph were like teachers to me. Rohit chettan's views and way of analysis had a strong impact on me. Suma Chechi had given all support to me from my post graduation. I thank them for their love and care.

My dearest Shaheer, Mahendran ,Rijo and Joby were always there with their support and encouragement.

My juniors Sujith,Sarin,Sreenath and Sreejith were always with me through the thick and thin of my career.

,Mrs.Laila D, Mrs.Nisha Nassar ,Mrs. Shameena and Miss.Jitha were always there with support and encouragement.I whole heartedly thank them

I also thank Mrs.Anju Pradeep and Dr. Binu Paul School of Engineering , CUSAT. Anju miss was a real source of inspiration during my difficult times. Binu paul miss has a remarkable way of analyzing things. I really cherish the technical discussions I had with her.

Special thanks to Mrs. Sreedevi K. Menon, Dr. Lethakumary B, M.G. Universtiy, Kottayam and Mr. K. Francis Jacob for their whole hearted support, helps and above all the association with me.

I also would like to acknowledge Dr. Shynu S.V, Dr. Anupam R. Chandran, Mr.GopiKrishanan and Mrs. Deepti Das Krishna for their valuable help, fruitful discussions and constant encouragement.

My words are illimitable to thank every member of Centre for Research in Electromagnetics and Antennas, CUSAT for their encouragement and help rendered to me.

I would also like to thank the colleagues at Centre for Ocean Electronics (CUCENTOL), Microwave Tomography and Material Research Laboratory (MTMR) and Audio and Image Research Lab (AIRL), Department of Electronics, Cochin University of Science and Technology.

I wish to thank Defence Research and Development Organization, Govt. of India, for the financial assistance throughout my research.

My sincere thanks to all non teaching staff of Department of Electronics for their amicable relation, sincere cooperation and valuable helps.

I wish to place on record my gratitude to my teachers, mentors and my friends at all stages of my education.

Above all my great and blessed lab and my lucky analyzer for everything……

Achan, Amma and Divya were always with me with their support, love and faith towards me

Above all there is the god almighty whose blessings and kindness helped me a lot to tide over.

Deepu.V

Preface

With the alarming increase in the number of services provided and with the growing trend of miniaturisation in full swing the need for multi band compact antennas is on a rise. The development of microstrip and other related designs have increased the interest of designers towards these structures and consequently the planar designs replaced the conventional wire antennas. But the present day communication applications require compact and ultra wide band designs which cannot be catered by simple microstrip based designs. PIFAs have solved the problem to some extend, but the field of antennas needs more innovative designs.

In this thesis the design and development of compact planner antenna are presented. Emphasis is given to the design of the feed as well as the radiator resulting in simple compact uniplanar geometries. The Asymmetric coplanar feed used to excite the antennas is found to be a suitable choice for feeding compact antennas.

The main objectives covered in the thesis are:

- The design of compact uniplanar antennas by the effective miniaturization of antenna elements
- Isolation of the best feed for use in compact antennas
- Design of compact single, dual and multi band antennas with uniplanar structure and extension of the design for practical GSM/WLAN applications
- Design of Ultra compact antennas using the above techniques and extension of the design to antennas for practical applications like RFID/DVB-H.

All the above objectives are thoroughly studied. Antennas with ultra compact dimensions are obtained as a result of the study. Simple equations are provided to design antennas with the required characteristics. The design equations are verified by designing different antennas for different applications.

.....ꕥ.....

Contents

Chapter 4

ASYMMETRIC COPLANAR STRIP FED ULTRA COMPACT ANTENNAS

.....ꕥ.....

Chapter 1

INTRODUCTION

Contents

The chapter provides a brief overview of the field of antennas. A brief recollection of the contributions by various eminent researchers to the field of microwaves and antennas is depicted. This is followed by the discussion of various techniques and state of art innovations in the field of planar antennas with related literatures in this field. The chapter also presents the motivation of the Thesis and its organization.

1.1 Introduction

Antennas are indispensable component of any wireless communication device. Thus they are the inevitable component for creating the so called "wireless human network". An antenna is a transducer between the transmitter and the free space waves and vice versa. They efficiently transfer electromagnetic energy from a transmission line into free space.

1.2 Evolution and History

Much boom in the field of electromagnetics, microwaves and antennas - all started with the arguments about the electromagnetic nature of light. The initial foundations were laid by James Clark Maxwell who unified the theories of electricity and magnetism in 1873 [1] and eloquently represented the relations through a set of profound equations best known as "***Maxwell's Equations***". He showed that light is electromagnetic in nature and both light and electromagnetic waves travel with the same velocity. Maxewell's theories were supported by the brilliant experiments of Heinrich Hertz in 1888 [2, 3].

It was Guglielmo Marconi who was the first to commercially use "Air waves" for practical communication in 1897 [4]. He started the first commercial transatlantic wireless communication using radio waves with the help of the large antennas constructed by him in 1901.

Meanwhile Jagadish Chandra Bose a talented Indian Scientist started studies in millimeter waves. He used waveguides, horn antennas, dielectric lenses, various polarisers and even semiconductors for his studies. It is interesting to note that a 1.3 mm multi-beam receiver now in use in the NRAO 12 Metre Telescope, Arizona, U.S.A. incorporates his concepts 100 years back ![5-7].

Karl Jansky of the Bell Labortaries was the first to discover extraterrestrial radio waves using huge antennas designed by him and he is called the "Father of radio astronomy"[8].

These experiments were followed by numerous inventions by scientists and engineers from different parts of the world. The Yagi – Uda antenna is one of the remarkable findings of that period [9].

World War II gave a tremendous push to antenna and radar research. Much of the work remained classified as those were associated with military and defense. Large reflector antennas were built for communications, radar, and radio astronomy. Founded on the developments of World War II and driven by cold war programs, the technology for phased arrays and satellite antennas was refined and realized in several versions. The understanding of array effects was greatly advanced, and the fundamental ideas of adaptive arrays were put into practice. [10 -12]

Another significant development was the introduction of microstrip antennas by Deschamps in 1953[13]. But it took around twenty years for the practical and large scale development of these antennas.

The twentieth century witnessed remarkable and unbelievable progress in antenna technology from the large transceivers used by Marconi to the sub wavelength antennas with dimensions of the order of fraction of wavelength. Another remarkable development during this period is the birth of smart and active arrays [14 -17].

1.3 The State of Art Technologies

This thesis concentrates on the design and development of compact planar antennas. So a brief account of the various planar antenna designs and their methodology is outlined in this section.

Table 1.1 shows the commonly used communication frequencies based on FCC and ITU regulations [18, 19]. The antennas presented in this thesis the design are mainly concentrated in the above bands.

The succeeding section gives a brief account of the various state of art planar antennas.

Table 1.1 Commonly used communication frequencies

Name	Service	Allocated Band
RFID	Radio Frequency identification	865 - 868 MHz, 2.446 -2.454 GHz
DVB-H	Digital video Broadcasting - Handheld	470 MHz – 702 MHz
GSM 900	Global system for mobile	890 MHz -960 MHz
DCS 1800	Digital communication system	1710 MHz-1880 MHz
GPS 1200 GPS 1575	Global Positioning System	1227-1575 MHz 1565-1585 MHz
PCS 1900	Personal Communication System	1850-1990 MHz
3G IMT-2000	International Mobile Telecommunication-2000	1885-2200 MHz
UMTS 2000	Universal Mobile Telecommunications Systems	1920-2170 MHz
ISM 2.4 ISM 5.2 ISM 5.8	Industrial, scientific, medical	2400-2484 MHz 5150-5350 MHz 5725-5825 MHz
UWB	Ultra wide band communication	3.1 -10.6 GHz

1.3.1 Microstrip Antennas

The practical realization of microstrip antennas in the 1970's gave a boost to planar antenna research owing excellent characteristics and low profile of the antenna. The typical geometry of a Microstrip antenna consists of radiating metallic patch and a larger ground plane etched on either sides of a substrate having a fixed dielectric constant and thickness (fig.1.1). The length of the patch is typically about one half of the dielectric wavelength corresponding to the resonant frequency [20,21].

The substrate material has large influence in determining the size and bandwidth of an antenna. Increasing the dielectric constant decreases the size but lowers the bandwidth and efficiency of the antenna while decreasing the dielectric constant increases the bandwidth but with an increase in size.

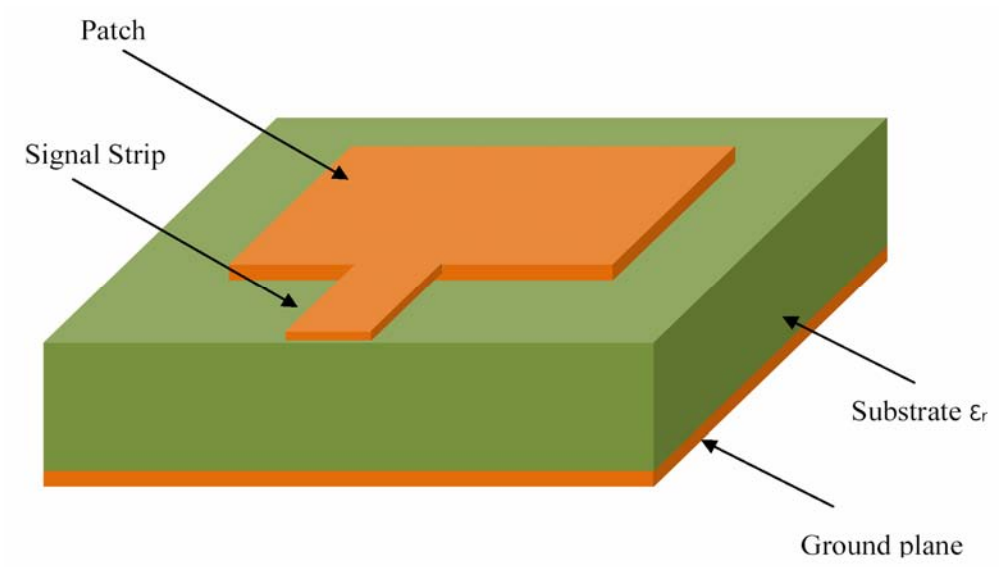

Fig. 1.1 Microstrip Patch antenna

The major reason for the widespread replacement of wire antennas and related designs by the microstrip based configurations is its low profile, light weight nature, conformability to planar and non planar structures and ease of fabrication [22,23]. The ease of integration of MMICs and other active elements is also an added advantage.

But microstrip antennas posses certain disadvantages also. One of the demerits of microstrip antenna is its inherently narrow bandwidth and high Q. This may be reduced by increasing the thickness of the dielectric substrate but only at the cost of decrease in efficiency owing to increase in surface waves [24 , 25]. Another disadvantage is its unipolar radiation characteristic [26 -27]. This bars its use in omni directional radiation applications.

Many studies have been performed to nullify the disadvantages of microstrip antennas. The surface waves in microstrip antennas can be reduced by using cavities as proposed by Mailloux et al [28].

Stacking [29], Aperture coupling [30], Proximity coupling [31] ,Slot coupling [32], addition of parasitic elements [33], use of different feed geometries and slots [34-38] etc are some of the techniques for bandwidth enhancement in microstrip antennas.

The advent of exciting multiple bands using a single antenna fostered the development of dual and multi band microstrip antennas. Many techniques have been proposed to excite dual and multiple bands in microstrip antenna. They include the insertion of shorting pins [39], slots [40] etc. Many designs for producing circularly polarized radiation have also been developed [41].

Even with these modifications the achieved bandwidth of these antennas is still low and they still exhibit unipolar radiation. This defect can be mitigated by the use of truncated ground plane structures [42]. This is discussed in the following section.

1.3.2 Microstrip fed antennas with Truncated ground plane structure

These antennas may be considered as the planar realization of the conventional vertical monopole antennas on a large ground plane. Truncated microstrip configurations are designed by removing a part of the ground plane at the far end of the feed region along the length of the patch (fig.1.2). The signal strip extends beyond the length of the ground plane and the configuration acts similarly as a monopole above a ground plane. The antenna is a quarter wavelength radiator and is hence compact. This configuration reduces the Q of the structure.

The main attractions of truncated ground plane structures are their monopole like radiation characteristics and large band width. The bandwidth of these antennas can be further increased by loading an arbitrary shape on the monopole. The band widths of these antennas are large, capable of easily covering the conventional communication bands [43, 44].

It is also reported that by properly truncating the ground plane width, an additional resonance near the fundamental mode can be excited which can be merged with the fundamental mode to yield more band width [45].

Many interesting dual band and multi band designs have also been developed using truncated microstrip configurations [46 – 50].

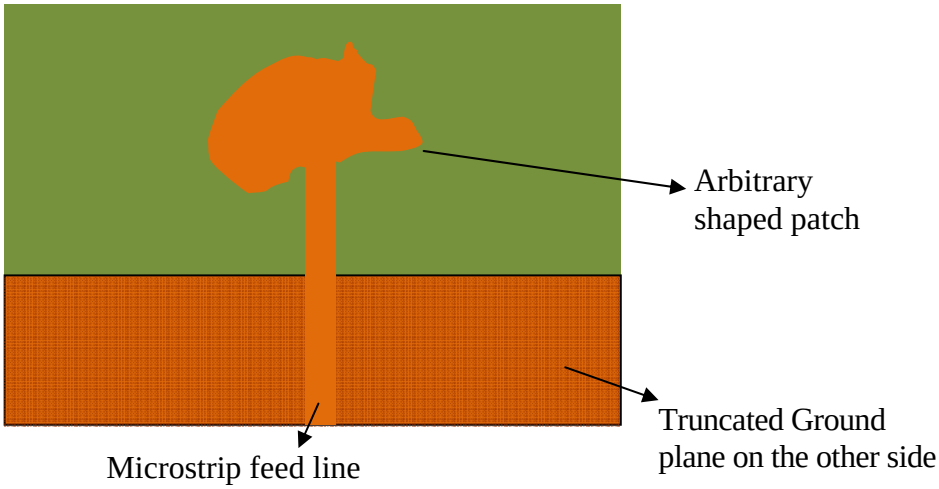

Fig.1.2 An arbitrary patch loaded on a monopole fed by a microstrip with a truncated ground plane

The allocation of the 3.1 GHz to 10.6 GHz band for commercial ultra wide band communications ignited more interest in truncated ground plane structures due to their inherently large band width. Many UWB designs using this geometry have been reported [51-54].

Even though the above mentioned antennas have good reflection and radiation characteristics, these antennas require the careful design of both the ground plane and the radiating structure. Also vias are required for the integration of active devices and MMICs. This has created a greater interest for the design of uniplanar antennas. Uniplanar antennas can be conveniently designed on the single side of a substrate, which makes fabrication and integration of active devices easy. The most widely used uniplanar antennas are the coplanar wave guide fed designs.

1.3.3 Coplanar Waveguide fed (CPW)Antennas

The coplanar wave guide consists of a central signal strip bounded by twin lateral ground strips separated by a small gap. The entire structure can be printed on the single side of a substrate. A typical monopole fed by the CPW feed is given in fig.1.3.

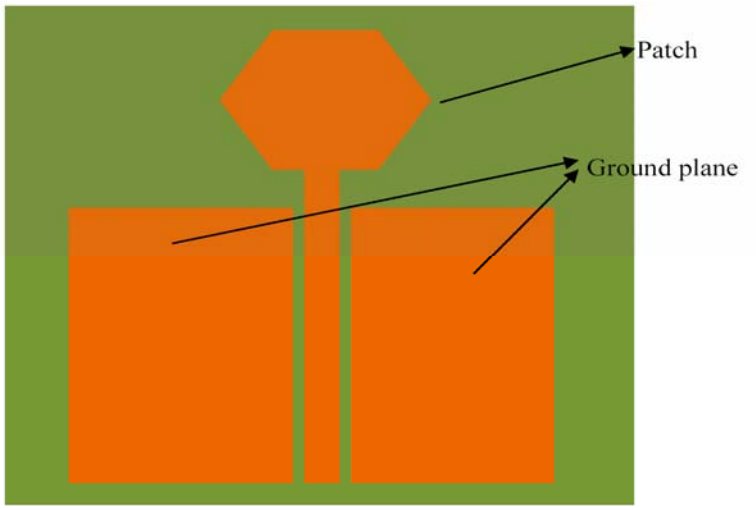

Fig.1.3. Coplanar wave guide fed octagon shaped antenna

Different types of CPW fed designs including single band [55,56] and multi band [57] antennas have been reported in literature.

The microstrip line and the coplanar wave guide are the commonly used transmission lines to transfer power from the power source to the antenna. Based on the challenges and constraints before the designer various interesting modified designs of these transmission lines have been proposed. They include the slotline, Coplanar strips, Asymmetric coplanar waveguide etc [58].

All the above mentioned antennas are half wavelength or quarter wavelength structures. The insertion of these antennas into modern communication devices requires them to be more compact. Various techniques have been proposed to achieve this goal. The use of Photonic Band gap structures, metamaterials and fractal based geometries are most common.

1.3.4 Photonic Band Gap (PBG) structures

The "Photonic Band Gap" (PBG) structures present a very useful feature; they do not allow the propagation of any electromagnetic wave in a frequency range for certain space directions [59, 60].

To enhance the bandwidth in microstrip based structures, methods like increasing the height of the substrate have been proposed. But this method leads to increased surface waves which extract power from the direct radiation degrading the pattern and the efficiency of the antenna. In order to avoid this effect, a PBG structure can be used. The PBG backed microstrip antenna exibit improved antenna efficiency, low side lobe level and and high antenna gain by reducing the surface wave propagation.

Photonic band gap structures are also used to increase the gain or bandwidth of compact planar antenna designs. Various designs of PBG Structures for bandwidth enhancement, size reduction, suppression of unwanted harmonics, reduction of cross polarization etc can be found in literature [61-64].

1.3.5 Metamaterial based antennas designs

Another innovation that is bringing drastic changes in the field of electromagnetics is the introduction of metamaterials. Even though the first metamaterials were developed in the 1940s, widespread research started only in the 1990s. V.G Veselago proposed that materials with simultaneously negative permittivity and permeability are physically permissible and possess a negative index of refraction [65]. He termed these as Left-Handed Media (LHM), because the vectors **E**, **H**, and **k** form a left-handed triplet instead of a right-handed triplet, as is the case in conventional, Right-Handed Media (RHM).

Recently, novel electromagnetic metamaterials have been successfully demonstrated whereby the permittivity and permeability functions are made to be simultaneously negative using an array of resonant cells consisting of thin wire strips and Split-Ring Resonators (SRRs) [66,67].

Materials with such characteristics could enable unprecedented levels of miniaturization of antennas, filters and other devices [68 -70]

1.3.6 Fractal geometry based antenna designs

The term fractal means broken or irregular fragments. Fractals are complex geometric designs that repeat themselves, or their statistical properties on many scales, and are thus “self similar.” The self similarity properties of fractals make them especially suitable for designing multiband antennas. Some fractals have complex, highly convoluted shapes that can enhance radiation when used as antennas. Fractals can improve the performance of antenna or antenna arrays. In antenna design, the use of fractal shapes makes the operational frequency of an antenna, independent of its scale. This means that a fractal antenna can be constructed in small sizes, yet possessing a broad frequency range with enhancement in bandwidth and gain [71, 72].

Fractals geometries like such as Koch curves, Sierpinski triangles and Minkowski fractals etc, have been used to design compact antennas and arrays for multiband, broadband and ultra wide band applications [73 - 80].

Even though several techniques as mentioned above can be found in literature, the practically used antennas are quite different from them. A few types of the practically used antennas are discussed in the following section.

1.3.7 PILA/PIFA designs

The alarming increase in the number of mobile users and the diversity of services offered in addition to voice communication has created greater demand for multi band antennas. Many innovative designs by modifying microstrip configuration [81], coplanar wave guide fed design [82] etc have been reported for enhancing bandwidth and producing multibands. But the above designs are not much compatable to the size of a typical handset.. As the size of handheld devices started decreasing, innovative designs like the Planar inverted-L antenna (PILA) and planar inverted F antenna (PIFA) were found to be promising alternatives to replace the external monopoles.

The Inverted L antenna (ILA) was first devised. The ILA is an end-fed short monopole with a horizontal wire element placed on top that acts as a capacitive load. The design of the ILA has a simple layout making it cost efficient [83-85]. Considering the radiation properties, the ILA have advantages over those of the monopole antenna by radiating in both polarizations. But the bandwidth is low.

To increase the band width, the Planar inverted-F antenna (PIFA) which adds a second inverted-L section to the end of a PILA was introduced (Fig.

1.4). The additional inverted-L segment also introduces a convenient tuning option for a second band and greatly improves the antenna usability.

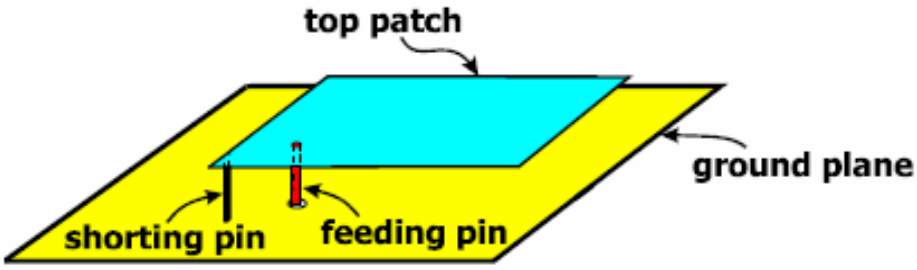

Fig.1.4. Typical structure of a PIFA

The basic PIFA structure is shown in fig.1.4. The PIFA (a "grounded" patch antenna - λ/4 patch instead of the conventional λ/2) consists of a ground plane, a top plate element, a feed wire feeding the resonating top plate, and a shorting plate that is connecting the ground and the top plate at one end of the resonating patch [86,87]. The PIFA is widely used in nowadays' mobile handheld devices.

The photograph of a typical PIFA in a mobile phone is shown in fig.1.5.

Fig.1.5. Typical PIFA in a mobile phone *Courtesy – Ericsson mobile*

PIFAs still suffer from inherently narrow bandwidth. Several techniques such as changing feed type [88], modifying the ground plane [89] etc have been devised to mitigate this limitation.

The multi-banding techniques in PIFAs includes the insertion of slits, stacking etc [90,91]. These techniques have been successfully implemented in practical cases.

1.3.8 Dielectric Resonator based designs

The dielectric resonators have been in existence for almost 25 years, and over that time a great deal of research has been performed in this field. The most attractive feature of dielectric resonators are their inherently low loss behaviour due to the absence of conducting materials which eliminate ohmic losses [92]. Dielectric resonators are useful in communication devices like filters, low noise oscillators, and other circuits [93]. They are highly sought after candidates in space applications and in other wireless gadgets now a days.

Dielectric resonator antennas (DRAs) are miniaturized antennas of ceramics or another dielectric medium for microwave frequencies. Their radiation characteristics are a function of the mode of operation excited in the DRA. The mode is generally chosen based upon the operational requirement. Dielectric resonator antennas offer several advantages over other antennas, such as small size, high radiation efficiency, and simplified coupling schemes for various transmission lines. The bandwidth can be controlled over a wide range by the choice of dielectric constant, and the geometric parameters of the resonator. Designs for increased bandwidth, circular polarization, varying radiation patterns, and for use in arrays have all been demonstrated [94 – 98]. Dielectric resonator antennas can also be made in low profile configurations, making them more aesthetically pleasing than standard whip, helical, or other upright antennas.

1.3.9 Ultra wide band antennas

UWB antennas are gaining widespread popularity because of their various superior qualities [99-101]. According to the definition of the Federal Communications Commission, a UWB device has a fractional bandwidth that is greater than 0.2, or occupies 500 MHz or more of the frequency spectrum, regardless of the fractional bandwidth.The release of an extremely wide spectrum of 3.1–10.6 GHz for emerging commercial microwave UWB applications [102] has greatly spurred the research and development of microwave ultra wideband (UWB) technology for communications, imaging, radar, and localization applications. Henceforth, many techniques to broaden the impedance bandwidth of small antennas and to optimize the characteristics of the broadband antennas have been widely investigated.

The performance of UWB short-pulse systems is superior to that of narrowband systems in multipath environments, because a UWB short pulse allows the retuned from distinct scatterers to be distinguished by using time delay. Many studies have been performed in the design, development and measurement of UWB antennas [103-107].

The ultra wide band antenna designs may be broadly divided as Traveling wave structures like Vivaldi antenna [108,109], Frequency independent structures like the biconical antenna or the bowtie Antenna [110,111], Self-complementary antennas that are characterized by a self-complementary metallization like the logarithmic spiral antenna and fractal antennas [112-114], combinations of the above like the log periodic antenna [115-117] and the electrically small antennas which includes the modified monopoles [118-126]. New designs with frequency notch in the existing WLAN bands in the 5-6 GHz range have also been reported [127,130].

A few typical UWB monopole designs are given in fig.1.6.

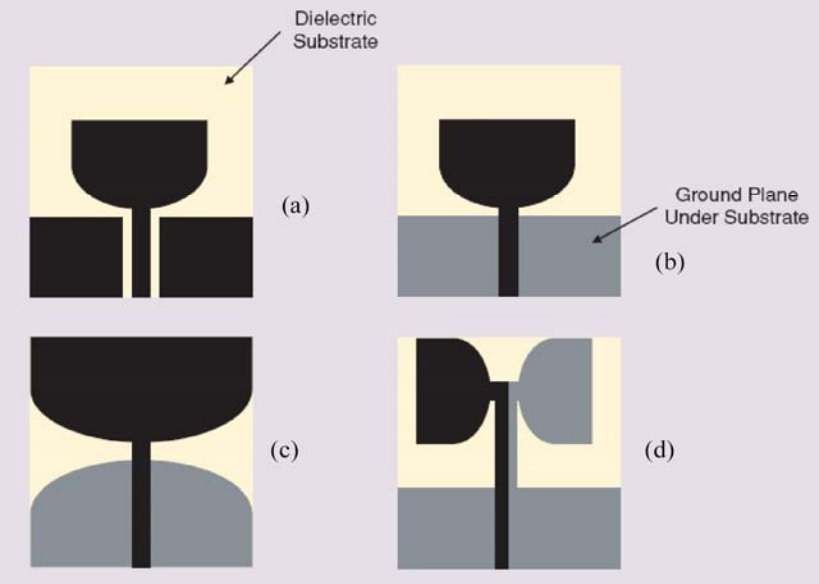

Fig.1.6. Various monopole configuration for ultra wide band applications

1.3.10 LTCC based antenna designs

Low-temperature Co-fired ceramics (LTCC) provides a module technology capable of dramatic volume savings over individual integrated circuit (IC) mounting, by stacking several ceramic substrates each only several µm thick and building-in passive components like resistors, capacitors, inductors etc. LTCC makes it possible to pack the filters and other components used in a mobile phone into a package having dimensions of only a few mm^3 [131].

LTCC technology is based on sintering of multi-layered thick-film sheets (50-250 µm) or so-called green tapes, which are screen-printed with thick-film pastes of conductors, resistors, etc. Many ultra compact antenna designs have been reported using LTCC technology proving it as viable alternative to the conventional miniaturization techniques [132-134].

1.3.11 Mobile phone antenna designs

The mobile phone industry is one of the challenging fields for antenna designers. The trend in cellular-phone technology in the recent years is to dramatically decrease the size and the weight of the handset, forcing designers to come up with highly compact designs.

In the infancy stage (1984), the typical portable cellular phone was nearly 600 cc in volume, and about 850 g in weight. In 2009, cellular handsets having a volume of less than 40 cc and a weight of less than 40 g appeared which is still decreasing rapidly. This remarkable reduction in weight and volume has necessitated a rapid evolution of the antennas used for the handsets. Accordingly, antenna designers encountered difficulty in designing antennas that could maintain their performance unchanged with smaller antenna size [135].

In designing antennas for small mobile terminals, the prime considerations to be taken into account are small size, light weight, compact structure, low profile, robustness, and flexibility. In addition to these, durability against the user's rough handling and environmental conditions should also be taken into account.

Morishita et al has divided the development of mobile phone antennas into three stages [136].

In the first stage, between 1950 and 1960, the antennas used in small portable equipment were mostly a simple monopole of about quarter wavelength. A monopole was usually mounted on the top of the equipment case. Since the case was made of metal in those days, it was s considered as a ground plane. By taking the image of the antenna element into account, the

model was treated as a half-wave dipole. Thus, no particular attention was paid to designing this sort of antenna at that time, and just a quarter-wavelength element was used. Wire monopoles and helical antennas were the typical candidates.

In the second stage, the antenna-design concept had advanced to include the case in the antenna system, as a part of the radiator. The antenna composed of a $\lambda/4$ monopole and the conductive casing was now modelled as an asymmetric dipole, being composed of a long and thin element on one side and a short and thick element on the other side [137]. As a consequence, this antenna system is treated as a parallel combination of a two-dipole system.

In the third stage - from the 1980s to the present - the downsizing of mobile terminals made remarkable progress and, accordingly, the size of the antennas - except for monopole elements -was also forced to be made smaller. The down-sizing of mobile terminals is beneficial for users, However, it is a serious problem for antenna designers, as the antenna design should be such that the antenna's performance should remain unchanged, even though the antenna's size becomes smaller.In this case "the equipment case" is replaced by "conducting materials" existing in the equipment, because almost all of the equipment cases these days are made of plastics, not of metals, and it is the "conducting materials" existing in the equipment that act as a radiator, instead of the equipment case. The typical conducting material in the equipment is a rectangular shielding plate or box, where RF and other circuits are included. Usually a built-in antenna element is placed on this plate or box, and it acts as a ground plane.

As a ground plane performs as a part of a radiator, when a small antenna element is placed on it and induces currents on it, the antenna's size is enlarged and, hence, the antenna's performance is enhanced. The gain and bandwidth

may be increased, although this depends on the size of the ground plane and the type of the antenna. A typical example would be the PIFA [138].

It has to be noted that there are both advantages and disadvantages in utilizing currents on the ground plane inside mobile terminals. The advantage is the enhancement of antenna performance. To the contrary, the disadvantage is the degradation in the performance due to the effect of adjacent materials, including the human body. In fact, more than 6 dB gain degradation has been observed in the talk position of mobile phones, mainly due to the effect of a user's hand. A hand holding a handset varies the currents on the ground plane, and thus the impedance and resonant frequency degrading the antenna gain and efficiency. The human head, when the handset is in a talk position, also varies antenna performance in the same way as does the hand. A decrease in the antenna's gain is also caused by both the hand and the head, which absorb radiation power. Several papers have been reported on human body effects on mobile phone handset antenna performance[139].

Another disadvantage is the possible increase of SAR [specific absorption rate] values in the human head. With the increase in the current distribution on the ground plane inside the handsets, the radiation toward the human head may increase, and so would the SAR. To reduce the undesired radiation toward the human head, the appropriate selection of antenna type, the feed, and mounting of the antenna element on the equipment, are all seriously considered [140,141].

1.3.12 DVB-H antenna designs

Television was the only service missing from mobile phones until recently. But this deficit has also been cleared recently with the innovation of DVB-H services.

DVB-H stands for Digital Video Broadcast - Hand held. DVB-H comprises not only television broadcasting, but it is more like data broadcasting for many users through a single service. It makes possible to view movies, news, music, weather forecasts and other public services. DVB-H system uses the frequency band 470-702 MHz. So, the relative bandwidth is very large. Compared to terrestrial transmission, DVB-T (Digital Video Broadcast-Terrestrial), DVB-H brings more flexibility, which allows its use in portable devices.

The introduction of DVB-H services via mobile phones has brought immense challenge to antenna engineers [142]. The antenna has to be compact and should be integrated inside the limited space available in a mobile phone. Also it should work at comparatively lower frequencies in the 470 – 702 MHz range with better reflection and radiation characteristics. Many designs have been reported in literature.

Yang Kang et al [143] proposed a reconfigurable compact antenna tuned by a multi-states matching network, consisting of switches, capacitors and inductors. By selecting suitable lumped components, the antenna can be dynamically tuned to different resonance frequencies, so that these separate frequency bands combine to cover the DVBH band.

Many related designs using parasitic patches and folded structures have been reported in literature [144-145]. But the trend of miniaturization is forcing designers to go for further ultra compact designs.

In addition to the above designs, many innovative designs for different applications have also been developed. Printed dipoles and printed Yagi antennas [146 - 151] are certain examples. Also the developments in the field of RFIDs have led to greater needs for many compact antennas [152-155].

1.4 Motivation of the work

As the process of miniaturisation of devices is in full swing, antennas cannot remain as standalone devices. Compact designs have to be implemented to cope with the demands of the industry. The main target of designers is the radiating patch. Several techniques like folding, meandering etc are normally performed to decrease the overall size of the antenna.

While designers give much importance to the radiator, the feed region of even the most compact designs still remains untouched. The overall area of an antenna depends on the size of both the radiating element and the feed. The aim of the thesis is the design of compact antennas by effective miniaturisation of the feed as well as the radiating structure. The overall design complexity of the antenna also needs to be reduced for its effective use in a device.

A simple coplanar waveguide fed strip monopole is taken for the initial study. The coplanar wave guide feed is replaced by a suitable feed –The Asymmetric Coplanar Strip feed - to design an antenna occupying less than 50% of the original area, retaining all advantages of the predecessor.Fig.1.7 shows the Asymmetric Coplanar Strip (ACS) and the Coplanar Waveguide (CPW) feeds.

Coplanar Wave Guide Asymmetric Coplanar Strip

Fig.1.7. The coplanar wave guide and the asymmetric coplanar strip transmission line

A thorough study is performed using the ACS fed monopole by comparing it with that of a coplanar waveguide fed monopole. After exhaustive simulation and experimental studies, it is proved that the ACS fed antenna retains all the advantages of the CPW fed antenna along with more compactness.

To prove the capability of using the ACS as an effective feed for dual band and multi band antennas, an F shaped dual band antenna and an inverted C shaped multi band antenna are designed and studied. All the studies provide good and encouraging results. Compact uniplanar antennas of dimensions of the order of $\lambda_d/4$ x $\lambda_d/4$ were obtained in all the above cases, where λ_d is the dielectric wavelength.

To explore the possibility of a resulting imbalance due to the absence of a balun in between the unbalanced coaxial cable and the balanced asymmetric coplanar strip, antennas with and without baluns were studied (section 3.4.10). It was noted that the antenna using the balun shows a slight increase in efficiency and has higher gain but such antennas have larger size and are bulky. It is left to the designer to choose between the balun and balunless configuration based on his requirements.

Different compact ACS fed antennas developed are shown in figure 1.8.

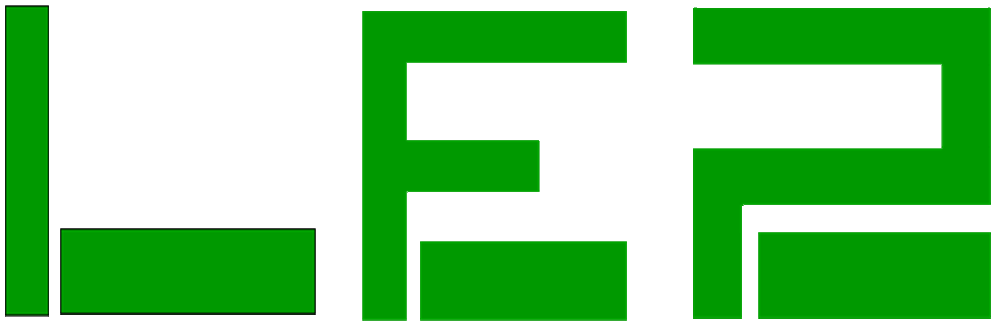

(a) Single band (b) Dual band (c) Triple band

Fig.1.8. Asymmetric Coplanar Strip fed compact antennas

The introduction of services like the digital TV (DVB-H) into mobile phones along with voice and data services has created an immense need for ultra compact antennas working in the 470 – 702 MHz range. The challenge is to design wide band ultra compact antennas with the specifications laid down by operators. Many existing techniques like the use of metamaterials, PBG structures, fractals, meandering etc have been proposed in literature. All the above techniques increase the complexity, cost or size of the device which makes it practically difficult to realize them.

This problem has also been extensively studied by effectively and completely using the available space for the antenna. A loop like structure is finally chosen for the purpose. Dual band and triple band antennas with dimensions of the order of $\lambda_d/5$ x $\lambda_d/10$ or less, highly suitable for RFID/GSM 900/1800 and 2.4 WLAN have been successfully designed and tested.

The above technique is extended to the design of an ultra compact DVB-H antenna which completely satisfies the requirements. Further modifications are made in the design keeping in mind the geometry of a typical handset. It is worth to note that these antennas occupy dimensions of the order of $\lambda_d/7$ x $\lambda_d/22$ or less which is a significant achievement.

The ultra compact designs developed are shown in fig.1.9.Detailed analysis is presented in chapter 4.

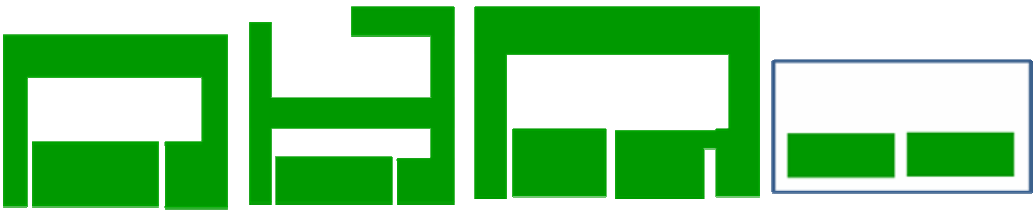

(a) Dual Band (b) Triple band (c) DVBH-I (d)DVBH-II

Fig 1.9. Asymmetric Coplanar Strip fed Ultra compact antennas

In addition to the Asymmetric Coplanar Strip feeding technique another uniplanar feed which has received recent attraction is the Slotline.

The Slot line may be considered as a complementary of the coplanar wave guide. The main advantage of this uniplanar transmission line is the ease of mounting active and passive circuits.

Two different slot line fed planar antenna designs are also studied in the thesis and given as appendices.Fig.1.10 shows the slot line fed antennas.

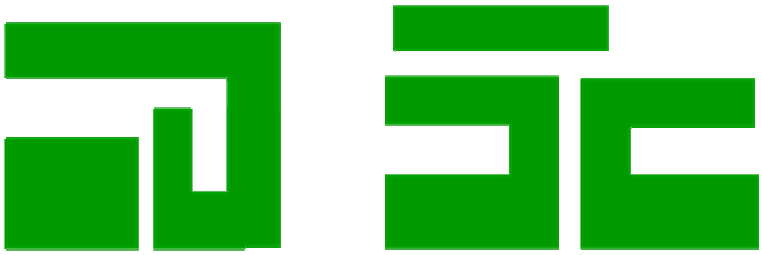

(a) Dual Band antenna (b) Wide Band antenna

Fig.1.10. Slot line fed antennas

1.5 Organisation of the Thesis

The Thesis is organized into five chapters.

Chapter 1 gives a brief introduction about the evolution of planar antennas. Various antenna designs for specific applications have been briefly reviewed along with the motivation of the present work.

Chapter 2 gives an account of the various techniques used for the design fabrication and measurement of antennas. Basic concepts and measurement methodology is briefly outlined in this chapter.

Chapter 3 gives a detailed study of the proposed Asymmetric coplanar strip feeding mechanism. Different types of antennas including Single band ,Dual band and triple band antennas are designed using this feed are studied in detail. The use of balun is also studied in this chapter. The experiments and observations are validated using simulation studies.

Chapter 4 gives details of the design of ultra compact antennas using the asymmetric coplanar feed. Dual band, Triple band antennas for RFID/GSM applications are presented. Various antennas ideal for applications in the DVB-H bands are also designed and studied in detail

Chapter 5 serves as a conclusion of the thesis with directions for future study

The thesis also includes the design and development of slotline fed antennas. A slotline fed wideband dipole is included in appendix 1 and a slotline fed dual band antenna is included in appendix 2.

References

[1] Maxwell, “A Treatise on Electricity and Magnetism”. Macmillan and Co., Oxford University,1873.

[2] Carter, P.S.; Beverage, H.H, “Early History of the Antennas and Propagation Field until the End of World War I, Part I – Antennas” Proceedings of the IRE ,Volume 50, Issue 5, Pp 679 – 682,May 1962

[3] J.D. Kraus, Ronald J. Marhefka, Antennas for all applications, Tata McGraw-Hill , 3rd Edition, pp. 785-788

[4] John D. Kraus, “Antennas since Hertz and Marconi”, IEEE Trans. Antennas and Propagat. vol.33, no.2, pp 131-136, February 1985.

[5] Tapan K. Sarkar arid Dipak L. Sengupta., “An Appreciation of J. C. Bose’s Pioneering Work in Millimeter Waves” IEEE Antennas and Propagation Magazine, Vol. 39, No. 5, pp.55-63,October 1997.

[6] John F. Ramsay, "Microwave Antenna and Waveguide Techniques before 1900," Proc. IRE., Vol.46, No.2, pp. 405-415, February 1958.

[7] G.L. Pearson, and W.H. Brattain, "History of Semiconductor Research," Proc. IRE, 43, pp.1794-1806, 1955

[8] Jansky, K.G "Electrical disturbances apparently of extraterrestrial origin" in Proc. IRE in 1933 (Reprinted in Proc. IEEE, vol. 86, no. 7, pp. 1510-1515, July 1998.

[9] S. Uda, Wireless Beam of short electric waves, J. IEE (Japan), pp. 273-282, March 1926

[10] Schell,A.C, “Antenna developments of the 1950s to the 1980s”, Antennas and Propagation Society International Symposium, IEEE Vol. 1, Pp 30 – 33, July 2001

[11] W. A. Imbriale, “Evolution of the Large Deep Space Network Antennas,” IEEE Antennas and Propagation Magazine, Vol. 33, No. 6. pp. 7- 19, Dec. 1991.

[12] Skolnik, M ,Radar: from Hertz to the 21st century, Antennas and Propagation Society International Symposium, 1988. AP-S. Digest,6-10 Pp:929 vol.3, June 1988

[13] Deschamps G. A , “ Microstrip Microwave Antennas”, III rd USAF symposium on Antennas, 1953.

[14] Guha,D, “Microstrip and printed antennas -recent trends and developments”,. TELSIKS 2003. 6th International Conference on Volume 1, Page(s):39 - 44 vol.1, Oct. 2003 .

[15] Heberling, D, “Modern trends in the development of small and handy antennas” Proceedings of the 2001 SBMO/IEEE MTT-S International, Volume 2, Pp 59 - 64 vol.2,Aug. 2001 .

[16] Edvardsson. O, “Recent advances in handset antennas for satellite communication”; IEEE Antennas and Propagation Society International Symposium,Volume 4, Pp 553 - 556, July 2001

[17] Yongxi Qian and Tatsuo Itoh, “ Progress in Active Integrated Antennas and Their Applications”, IEEE Transactions on Microwave Theory and Techniques, vol. 46, no. 11, Pp 1891 – 1900,November 1998

[18] http://www.itu.int/

[19] http://www.fcc.gov/

[20] Constantine A Balanis "Antenna theory analysis and design" John Wiley and Sons II nd edition

[21] Pozar D.M., “The Analysis and Design of Microstrip Antennas and Arrays”, IEEE press, New York, 1995.

[22] Pozar, D.M, “Microstrip antennas”, Proceedings of the IEEE Volume 80, Issue 1, Pp 79 – 91,Jan. 1992

[23] Fonseca, S.D.A. Giarola, A. “Microstrip disk antennas, Part I: Efficiency of space wave launching”, IEEE Trans. Antennas and Propagat. vol.32, no.6, pp 561- 567, June 1984

[24] Fonseca, S.D.A. Giarola, A. “Microstrip disk antennas, Part II: Efficiency of space wave launching”, IEEE Trans. Antennas and Propagat. vol.32, no.6, pp 568- 573, June 1984

[25] J. Huang, ‘‘The Finite Ground Plane Effect on the Microstrip Antenna Radiation Patterns,’’ IEEE Trans. Antennas Propagat. Vol. AP-31,pp 978-984, July 1983

[26] C A Balanis,” Advanced Engineering Electromganetics”,John Wiley & sons,New york 1989.

[27] Ramesh Garg,Prakash Bhartia and Inder Bahl, “Microstrip Antenna Design Hand book”, 1st ed. MA Artech House, 2001.

[28] R.J .Mailloux," On the use of metallized cavities in printed slot arrays with dielectric Substrates '' IEEE Trans. Antennas Propagat. Vol. AP-35,pp 477-487, May 1987.

[29] S.A Long and M.D.Walton, "A Dual-frequency Stacked circular Disc antenna", IEEE Trans. Antennas Propagat. Vol. AP-27, No.2, pp 270-273, May 1987.

[30] C H Tsao,Y M Hwang,F Kilburg and F .Dietrich, "Aperture Coupled patch antennas with wide bandwidth and Dual Polarisation capabilities", IEEE Antennas and Propogation symposium dig. pp 1220-1223, 1989.

[31] D M Pozar and B Kaufman, "Increasing the bandwidth of microstrip antennas by Proximity coupling," IEE Electronics Lett.Vol.23 pp 1070 – 1072,September 1987.

[32] A.Ittipiboon,B Clarke, and M Cuhaci, "Slot Coupled Stacked microstrip antennas", IEEE Antennas and Propogation symposium dig. pp 63-66, 1983.

[33] C. K. Aanandan, P. Mohanan and K. G. Nair, "Broad band gap coupled microstrip antenna", IEEE Transactions on Antennas and Propagat., Vo. 38, No. 10, pp. 1581-1586,Oct. 1990.

[34] S. Mridula, Sreedevi K. Menon, B. Lethakumary, Binu Paul, C. K. Aanandan, P. Mohanan, "Planar L-strip fed broadband microstrip antenna", Microwave and optical technology letters, Vol. 34, Issue 2 , pp. 115 – 117,Jun 2002,.

[35] B. Lethakumary, Sreedevi K. Menon, C. K. Aanandan, P. Mohanan, "A wideband rectangular microstrip antenna using an asymmetric T-shaped feed", Microwave and optical technology letters, Vol. 37, Issue 1 , pp. 31 – 32,Feb 2003.

[36] Manju Paulson, Sona O. Kundukulam, C. K. Aanandan, P. Mohanan, K. Vasudevan, "Compact microstrip slot antenna for broadband operation", Microwave and optical technology letters, Vol. 37, Issue 4, pp. 248 – 250, March 2003.

[37] Binu Paul, S. Mridula, C. K. Aanandan, P. Mohanan, “A new microstrip patch antenna for mobile communications and bluetooth applications”, Microwave and Optical Technology Letters Volume 33, Issue 4, Pages: 285-286, May 2002.

[38] Latif, S.I.; Shafai, L.; Sharma, S.K, “Bandwidth enhancement and size reduction of microstrip slot antennas”.; IEEE Transactions on Antennas and Propagat.,Volume 53, Issue 3, Pp 994 – 1003,March 2005

[39] J. George, K. Vasudevan, P. Mohanan and K.G. Nair, “Dual frequency miniature microstrip antenna”, Electronics Letters Vol. 34 No. 12, pp. 1168-1170, June 1998

[40] Sona O. Kundukulam, Manju Paulson, C. K. Aanandan, P. Mohanan, “Slot-loaded compact microstrip antenna for dual-frequency operation”, Microwave and optical technology letters, Vol. 31, Issue 5 , Oct 2001, pp. 379 – 381

[41] Nasimuddin, Esselle, Verma, A. K , “Wideband Circularly Polarized Stacked Microstrip Antennas ’’,IEEE Antennas and Wireless Propogat. Lett.,Vol.6,pp 21 – 24, 2007

[42] Zhi Ning Chen; Ammann, M.J.; Xianming Qing; Xuan Hui Wu; See, T.S.P, “Planar Antennas”, IEEE Antennas and Propagation magazine,Vol.7,No.6,pp 59 – 61, December 2006

[43] Ammann, M.J and John, M, “Optimum design of the printed strip monopole”,IEEE Antennas and Propagation magazine,Vol.47,No.6,pp 59 – 61, 2005

[44] M. N. Suma, Rohith K. Raj, Manoj Joseph, P. C. Bybi, and P. Mohanan, “A Compact Dual Band Planar Branched Monopole Antenna for DCS/2.4-GHz WLAN Applications”, IEEE Microwave and Wireless Components Letters, Vol. 16, No. 5, pp. 275-277, May 2006.

[45] Suma M.N, Bybi P.C and P.Mohanan, “A wide Band Printed Monopole antenna for 2.4GHz WLAN Applications” Microwave and Optical Technology Lett. Vol.48, No.5, May 2006. pp 871-873.

[46] Yuehe Ge, Karu P. Esselle and Trevor S. Bird, “A Spiral-Shaped Printed Monopole Antenna for Mobile Communications”, IEEE Antennas and Propagation Society International Symposium Pp 3681 - 3684 July 2006.

[47] Joon II Kim and Yong Jee, “Design of Ultra wide band Coplanar wave guide fed LI- shape planar monopole antennas”, IEEE Antennas and Wireless propagation let., Pp 383-387, vol. 6, 2007.

[48] Raj, R.K., Joseph, M., Aanandan, C.K.; Vasudevan, K.; Mohanan, P.,A New Compact Microstrip-Fed Dual-Band Coplanar Antenna for WLAN Applications, IEEE Transactions on Antennas and Propagat, Volume 54, Issue 12, Pp :3755 – 3762,Dec. 2006

[49] Manoj Joseph, Rohith K.Raj, Suma M.N, C.K.Aanandan, K.Vasudevan And P.Mohanan, “Microstrip-fed dual band folded dipole antenna for DCS/PCS/2.4GHz WLAN applications” International Journal On Wireless and Optical Communications, Volume.4,No.1,pp 43-51,2007.

[50] Y.-L. Kuo and K.-L. Wong, “Printed Double – T monopole for 2.4/5.2 GHz dual-band Operations”, IEEE Trans. Antennas and Propagat., vol. 51, pp. 2187–2192, Sep. 2003.

[51] J.-S. Rowand S.-W.Wu, “Monopolar square patch antennas with wideband operation”, IEE Electron. Lett., vol. 42, no. 3, pp. 139–140, Feb.2006

[52] W. S. Lee, D. Z. Kim, K. J. Kim, and J. W. Yu, "Wideband Planar Monopole Antennas with Dual Band-Notched Characteristics," IEEE Transactions on Microwave Theory Tech., vol.54, no.6, pp2800-2806, June 2006.

[53] D. C. Chang, M. Y. Lin, and C. H. Lin, "A CPW-fed U type Monopole Antenna for UWB Applications," in Proc. IEEE Antennas and Propagation Society Int. Symposium., vol.5A, pp512-515, July 2005.

[54] K. F. Jacob, M. N. Suma, R. K. Raj, M. Joseph and P. Mohanan, “Planar Branched Monopole Antenna for UWB Applications,” Microwave and optical technology letters, vol.49, no.1, pp45-47, Jan. 2007

[55] W. C. Liu and C.-F. Hsu, “Dual-band CPW-fed Y-shaped monopole antenna for PCS/WLAN application”, IEE Electron lett.Vol.No.41,no.7, pp. 390–391, Mar. 2005.

[56] Horng-Dean Chen and Hong-Twu Chen, “A CPW-Fed Dual-Frequency Monopole Antenna”, IEEE Transactions on Antennas and Propagat, Vol.52,No.4,pp 978 – 982, April 2004.

[57] W.-C. Liu and H.-J. Liu, “Compact Triple band slotted monopole antenna with asymmetrical grounds”, IET Electronics lett., Vol. 42 No. 15,pp 78 -79,July 2006

[58] R. Garg, P. Bhartia, and I. Bahl, Microstrip Antenna Design Hand book, 1st ed. Boston, MA: Artech House, 2001, pp. 790–795.

[59] lnrik Chang and Bomson Lec, “Design of Defected Ground Structures for Harmonic Control of Active Microstrip Antenna”, Antennas and Propagation Society International Symposium, 2002. IEEE Volume 2, Pp:852 – 855, June 2002 .

[60] Radisic, V.; Qian, Y.; Coccioli, R.; Itoh, T, Novel 2-D photonic bandgap structure for microstrip lines Microwave and Guided Wave Letters, IEEE ,Volume 8, Issue 2, Pp :69 – 71,Feb. 1998

[61] P. Salonen, M. Keskilammi, L. Sydanheimo, “A low-cost 2.45 Ghz photonic band-gap patch antenna for wearable systems”, IEEE lntemational Conference on Antennas and Propagation, 77-20 April 2001

[62] Y. J. Sung and Y.-S. Kim, “An Improved Design of Microstrip Patch Antennas using photonic Band Gap structures”, IEEE Transactions on Antennas and Propagat,Vol.53,No.5,pp 1799 – 1802, May 2005.

[63] Haiwen Liu, Zhengfan Li, Xiaowei Sun,and Junfa Mao, “ Harmonic Suppression With Photonic Bandgap and Defected Ground Structure” IEEE Microwave and wireless components lett., vol. 15, no. 2, Pp 55-56,february 2005

[64] Debatosh Guha, Manotosh Biswas, and Yahia M. M. Antar, “Microstrip Patch Antenna With Defected Ground Structure for Cross Polarization

Suppression", IEEE antennas and wireless propagation letters, vol. 4, pp 455-458,2005.

[65] V. G. Veselago, "The electrodynamics of substances with simultaneously negative values of e and m," Sov. Phys., vol. 10, no. 4, pp. 509-514, Jan.-Feb.1968.

[66] J. B. Pendry, A. J. Holden, D. J. Robins, W. J. Stewart, "Magnetism from conductors and enhanced nonlinear phenomena," IEEE Trans. on Microwave Theory and Tech., vol. 47, no. 11, pp. 2075-2084, Nov. 1999.

[67] D. R. Smith, W. J. Padilla, D. C. Vier, S. C. Nemat-Nasser, S. Schultz, "Composite medium with simultaneously negative permeability and permittivity," Phys. Rev. Lett., vol. 84, no. 18, pp. 4184-4187, May 2000.

[68] Special issue on Metamaterials, IEEE Trans. On Antennas Propagat., 2003, Vol. 51

[69] Filiberto Bilotti,, Andrea Alú, Membe, and Lucio Vegni, Design of Miniaturized Metamaterial Patch Antennas With μ-Negative Loading, IEEE Trans on Antennas and Propagat., Vo. 56, No. 6, pp. 1640-1586,June 2008.

[70] J. Kim, C.S. Cho and J.W. Lee "5.2 GHz notched ultra-wideband antenna using slot-type SRR", IEE Electron Lett.vol.42,Pp 42-43, No.6,June 2006.

[71] Werner, D.H.; Ganguly, S, " An overview of fractal antenna engineering research", Antennas and Propagation Magazine, IEEE Volume 45, Issue 1, Pp38 – 57,Feb. 2003 .

[72] D. H. Wemer, R. 1. Haupt, and P. L. Wemer, "Fractal Antenna Engineering: The Theory and Design of Fractal Antenna Arrays IEEE Antennas and Propagation Magazine, 41, No.5, pp. 37-59.October 1999.

[73] J.P. Gianviffwb and Y. Rahmat-Samii, "Fractal antennas: A novel antenna miniaturization technique, and applications", Antennas Propagation Magazine 44 (2002), 20–36.

[74] Min Ding, Ronghong Jin, Junping Geng, and Qi Wu., " Design Of A Cpw-Fed Ultrawideband Fractal Antenna", Microwave And Optical Technology Letters , Vol. 49, No. 1, January 2007

[75] C. Puente, J. Romeu, and R. Pous., "Small but long Koch fractal monopole," IEE Electron. Lett., vol. 34, no. 1, pp. 9–10, 1998.

[76] C. Puente, J. Romeu, and R. Pous, "On the behavior of the Sierpinski multiband fractal antenna," IEEE Trans. Antennas Propag., vol. 46, no. 4, pp. 517–524, Apr. 1998.

[77] H. A. Ghali and T. A. Moselhy, "Broad-band and circularly polarized space-filling-based slot antenna," IEEE Trans. Microw. Theory Tech., vol. 53, no. 6, pp. 1946–1950, Jun. 2005.

[78] K.J. Vinoy, K.A. Jose, V.K. Varadan, and V.V. Varadan, "Hilbert curve fractal antenna: A small resonant antenna for VHF/UHF applications," Microwave and Optical Technology Letters., vol. 29, pp. 2 15-2 19, 2000.

[79] K. J. Vinoy, Jose K. Abraham, , and Vijay K. Varadan, "On the Relationship Between Fractal Dimension and the Performance of Multi-Resonant Dipole Antennas Using Koch Curves" IEEE Trans On Antennas And Propagat., Vol. 51, No. 9, September 2003.pp 2296-2303.

[80] P. W. Tang and P. F. Wahid "Hexagonal Fractal Multiband Antenna", IEEE Antennas and Wireless Propagation Letters, Vol. 3, 2004.pp.111-112.

[81] Yijun Liu, Zhongxiang Shen and Choi Look Law, "A Compact Dual-Band Cavity-Backed Slot Antenna" IEEE Antennas and Wireless propag Lett, vol. 5, 2006

[82] Hong-Dean chen,"Compact CPW-fed dual-frequency monopole antenna",IEE Electron. Lett. Vol.38,no.25,December 2002

[83] Z.N.Chen and M.Y.W.Chia,,"Broadband planar inverted-L antennas", IEE proceedings Microw. Antennas Propag., Vol. 148,no. 5, October 2001

[84] Jieh-sen kuo and Kin-lu wong, “Dual-frequency operation of a planar inverted-L antenna with tapered patch width”, Microwave and optical technology letters, vol. 28, pp. 126-127 January , 2001.

[85] Z.N. Chen, “ Note on impedance characteristics of L-shaped wire monopole antenna”, Microwave and optical technology letters,Vol.26, Pp 22_23.July 2000.

[86] Y.J.Cho,Y.S.Shin and S.O.Park,”Internal PIFA for 2.4/5GHZ WLAN applications”, IEE Electron. Lett. vol.42, no.1, January 2006.

[87] Lucas M.Feldner,Christopher T.Rodenbeck,Christos G.Christodoulou and NicolaKinzie,”Electrically Small Frequency Agile PIFA-as-a Package for Portable wireless Devices”, IEEE Trans. Antennas Propagat., vol. 55, no. 11,pp 3310-3319, November 2007.

[88] Byung Chan Kim, Je Hoon Yun and Hyung Do Choi,”Small wideband PIFA for Mobile Phones at 1800 MHz”, Vehicular Technology Conference, 2004. VTC 2004-Spring. 2004 IEEE

[89] F.Wang,Z DU.Q.Wang and K.Gong,”Enhanced –bandwidth PIFA with T shaped ground plane”, IEE Electron. Lett. vol. 40, no.23, November 2004

[90] Benito sanz Izquierdo, John C.Batchelor, Richard J.langley and Mohammed I.Sobhy, ”Single and Double layer planar multi band PIFAs”, IEEE Trans. Antennas Propagat., vol. 54, no. 5,pp 416-422, May 2006.

[91] Dalia Mohammed Nashaat, Hala A. Elsadek and Hani Ghali,”Single Feed Compact Quad-Band PIFA Antenna for Wireless Communication Applications”, IEEE Trans. Antennas Propagat., vol. 53, no. 8, pp. 2631-2635, August 2005.

[92] Long, S.A., Oapos, Connor, E.M., “The History of the Development of the Dielectric Resonator Antenna”, International Conference on Electromagnetics in Advanced Applications, 2007. ICEAA 2007, Issue, 17-21, Pp:872 – 875, Sept. 2007.

[93] Okaya and l. F. Barash ,, “The Dielectric microwave Resonator”, Proceedings of IRE, Vol. 58, No.6, Pp. 922- 923,June 1970.

[94] S.A. Long, M.W. McAllister and L.C. Shen,"The Resonant Cylindrical Dielectric Cavity Antenna," IEEE Trans. Antennas Propagat.,vol. AP-31, pp. 406-412, May 1983.

[95] J. T. H. St. Martin, Y. M. M. Antar, A. A. Kishk, A. Ittipiboon, and M. Cuhaci, "Dielectric resonator antenna using aperture coupling," Electron. Lett., vol. 26, pp. 2015-2016, Nov. 1990.

[96] G. Drossos, Z. Wu, and L. E. Davis, "Theoretical and experimental investigation of cylindrical dielectric resonator antennas," Microwave and optical technology letters vol. 13, pp. 119-123, Oct. 1996.

[97] Ittipiboon, R. K. Mongia, Y. M. M. Antar, P.Bhartia, and M. Cuhaci, "Aperture fed rectangular and triangular dielectric resonators for use as magnetic dipole antennas," Electron. Lett., vol. 29, pp. 2001-2002, Nov. 1993.

[98] Guha, D.; Antar, Y.M.M, “ New Half-Hemispherical Dielectric Resonator Antenna for Broadband Monopole-Type Radiation”, IEEE Transactions on Antennas and Propagation, Volume 54, Issue 12, Pp 3621 – 3628,Dec. 2006 .

[99] Hans Gregory Schantz ,A brief History of UWB Antennas ,IEEE A & E systems magazine Pp 23-26,April 2004

[100] Wiesbeck, W.; Adamiuk, G.; Sturm, C.; “Basic Properties and Design Principles of UWB Antennas”, Proceedings of the IEEE, Volume 97, Issue 2, Pp:372 – 385, Feb. 2009

[101] F. Sabath, E. L. Mokole, and S. N. Samaddar, "Definition and Classification of Ultra-Wideband Signals and Devices”, Radio Science bulletin , No.313, Pp 12-26,June 2005.

[102] Commission of the European Communities, B Commission decision on allowing the use of the radio spectrum for equipment using ultra-wideband technology in a harmonised manner in the community, Official J. Eur. Union, Feb. 21, 2007

[103] Yiqong Shi; Aditya, S.; Law, C.L.; "Time Domain Responses of Printed UWB Antennas", Fifth International Conference on Information, Communications and Signal Processing, Pp:153 – 156,2005

[104] Shlivinski, E. Heyman, and R. Kastner, Antenna characterization in the time domain, IEEE Trans. Antennas Propag.,vol. 45, pp. 1140–1149, Jul. 1997.

[105] Levitas, B, "UWB Time Domain Measurements", European Conference on Antennas and Propagation ,EuCAP 2007,11-16, Pp:1 – 8,Nov. 2007

[106] Debalina Ghosh, Arijit De, Sarkarl,C. Wicks and Eric L. Mokole "Transmission and Reception by Ultra-Wideband (UWB) Antennas", IEEE Antennas and Propagation Magazine, Vol. 48, No. 5, pp 67-99,October 2006

[107] Duroc, Y.; Ghiotto, A.; Vuong, T.P.; Tedjini, S, "UWB Antennas: Systems With Transfer Function and Impulse Response", IEEE Trans. Antennas Propagat., Vol. 55, No. 5, Pp 1449 – 1451, May 2007

[108] Hood, A.Z.; Karacolak, T.; Topsakal, E, "A Small Antipodal Vivaldi Antenna for Ultrawide-Band Applications,; Antennas and Wireless Propagation Lett., IEEE ,Volume 7, Pp:656 – 660,2008

[109] Li Ying; Chen Ai-xin; "Design and application of Vivaldi antenna array Antennas", Propagation and EM Theory, 2008. ISAPE 2008. 8th International Symposium Pp:267 – 270, Nov. 2008

[110] Kiminami, K.; Hirata, A.; Shiozawa, T, "Double-sided printed bow-tie antenna for UWB communications", IEEE Antennas and wireless Propagation Lett., Vol. 3, No. 1, Pp 152 – 153,2004.

[111] Ito, Y., Ameya, M.; Yamamoto, M.; Nojima, "Unidirectional uwb array antenna using leaf-shaped bowtie elements and flat reflector",, IEE Electron Lett.,Volume 44, Issue 1, Page(s):9 – 11,January 2008

[112] Naghshvarian-Jahromi, M. "Novel Wideband Planar Fractal Monopole Antenna", IEEE Transactions on Antennas and Propagat., Volume 56, Issue 12, Pp:3844 – 3849,Dec. 2008

[113] Karlsson, M.; Shaofang Gong, " An integrated spiral antenna system for UWB", Microwave Conference, 2005 European,Volume 3, 4-6 Oct. 2005.

[114] J. Dyson, B "The equiangular spiral antenna", IEEE Trans. Antennas Propag., vol. AP-7 pp. 181–187, Apr. 1959

[115] Shih-Yuan Chen; Po-Hsiang Wang; Hsu, P, "Uniplanar Log-Periodic Slot Antenna Fed by a CPW for UWB Applications", Antennas and Wireless Propagation Lett., IEEE Volume 5, Issue 1, Pp:256 - 259, Dec. 2006

[116] R. Pantoja, A. Sapienza, and F. M. Filho A microwave printed planar log-periodic dipole array antenna, IEEE Trans. Antennas Propag vol. AP-35, pp. 1176–1178, Oct. 1987

[117] Calmon, A.; Pacheco, G.; Terada, M, "A novel reconfigurable UWB log-periodic antenna", Antennas and Propagation Society International Symposium 2006, IEEE, Pp:213 - 216July 2006

[118] Valderas, D.; Alvarez, R.; Melendez, J.; Gurutzeaga, I.; Legarda, J.; Sancho, J.I.; "UWB Staircase-Profile Printed Monopole Design", IEEE Antennas and Wireless Propagation Lett. Volume 7, Pp:255 - 259, 2008

[119] D. Schaubert, E. Kollberg, T. Korzeniowski, T. Thungren, J. Johansson, and K. Yngvesson, Endfire tapered slot antennas on dielectric substrates, IEEE Trans. Antennas Propagat ., vol. AP-33, pp. 1392–1400, Dec. 1985.

[120] N. Behdad and K. Sarabandi, A compact antenna for ultrawide-band applications IEEE Trans. Antennas Propag., vol. 53, pp. 2185–2192, Jul. 2005

[121] Yang, G.M.; Jin, R.H.; Xiao, G.B.; Vittoria, C.; Harris, V.G.; Sun, N.X, "Ultrawideband (UWB) Antennas With Multiresonant Split-Ring Loops",. IEEE Transactions on Antennas and Propagation, Pp 256 – 260, on Volume 57, Issue 1, Jan. 2009

[122] C.-C Lin, Y.-C. Kan, L.-C. Kuo, H.-R. Chuang A planar triangular monopole antenna for UWB communication IEEE Microw. Compon. Lett., vol. 15, pp. 624–626 Oct. 2005.

[123] Wiesbeck, W.; Adamiuk, G.; Sturm, C, "Basic Properties and Design Principles of UWB Antennas", Proceedings of the IEEE Volume 97, Issue 2, Pp.372 – 385 Feb. 2009

[124] Valderas, D.; Alvarez, R.; Melendez, J.; Gurutzeaga, I.; Legarda, J.; Sancho, J.I, "UWB Staircase-Profile Printed Monopole Design" Antennas and Wireless Propagation Lett., IEEE Volume 7,Pp 255 – 259, 2008.

[125] Jia-Yi Sze; Hsu, C.-I.G.; Jen-Yi Shiu, "Small CPW-Fed Band-Notched Ultrawideband Rectangular Aperture Antenna", Antennas and Wireless Propagation Lett., IEEE Volume 7, Pp:513 – 516, 2008

[126] Marchais, C.; Le Ray, G.; Sharaiha, A.; "Stripline Slot Antenna for UWB Communications", IEEE Antennas and Wireless Propagation Lett., Volume 5, Issue 1, Pp:319 – 322, Dec. 2006

[127] Qing-Xin Chu; Ying-Ying Yang, "A Compact Ultrawideband Antenna With 3.4/5.5 GHz Dual Band-Notched Characteristics" IEEE Trans on Antennas and Propagat., Volume 56, Issue 12, Dec. 2008 Page(s):3637 – 3644

[128] Gopikrishna, M.; Krishna, D.D.; Aanandan, C.K.; Mohanan, P.; Vasudevan, K, Compact linear tapered slot antenna for UWB applications, IEE Electron Lett., Volume 44, Issue 20, Pp 1174 – 1175, September 2008

[129] Chow-Yen-Desmond Sim, Wen-Tsan Chung, Ching-Her Lee, " A circular-disc monopole antenna with band-rejection function for ultrawideband application", Microwave and Optical Technology Letters, Volume 51, Issue 6, Date:, Pp: 1607-1613, June 2009

[130] Shameena.V.A, Suma M.N, Rohith.K.Raj, Bybi P.C and P Mohanan "Compact Ultra wide Band Planar Serrated Antenna with Notch band ON/OFF Control" IEE Electron Letters. Volume 42, Issue 23, Pp : 1323 – 1324, November 2006

[131] Jantunen H, Rautioaho R, Uusimäki A & Leppävuori S, " Preparing low loss LTCC material without glass addition", Journal of American Ceramic Society, Vol. 83, No. 11, (2000), pp. 2855-2857.

[132] Gautier, W.; Schoenlinner, B.; Ziegler, V.; Prechtel, U.; Menzel, W, "LTCC Patch Array for RF-MEMS based Phased Array Antenna at 35GHz", 38th European Microwave Conference,. 27-31, Pp:151 – 154, Oct. 2008

[133] Brzezina, G.; Roy, L.; MacEachern, L, " Planar antennas in LTCC technology with transceiver integration capability for ultra-wideband applications" IEEE Trans. on Microwave Theory and Tech, Volume 54, Issue 6, Part 2, Pp:2830 - 2839June 2006

[134] RongLin Li; DeJean, G.; Moonkyun Maeng; Kyutae Lim; Pinel, S.; Tentzeris, M.M.; Laskar, J , "Design of compact stacked-patch antennas in LTCC multilayer packaging modules for wireless application"; IEEE Transactions on Advanced Packaging, Volume 27, Issue 4, Page(s):581 – 589,Nov. 2004

[135] Zhinong Ying, " Progress of multi-band antenna technology in mobile phone industry", Wideband and Multi-band Antennas and Arrays, Pp:1 – 5, IEE 7 Sept. 2005

[136] Morishita, H.; Kim, Y.; Fujimoto, K, " Design concept of antennas for small mobile terminals and the future perspective", Antennas and Propagation Magazine, IEEE Volume 44, Issue 5, Pp:30 – 43, Oct. 2002.

[137] K.Fujimoto, "A Loaded Antenna system applied to VHF portable communication equipment", IEEE Transactions on Vehicular Technology,Vol.17,No.1,Pp 5-12, January 1968.

[138] Yu-Shin Wang; Ming-Chou Lee; Shyh-Jong Chung, " Two PIFA-Related iniaturized Dual-Band Antennas", IEEE Transactions on Antennas and Propagation Volume 55, Issue 3, Part 2, Pp 805 – 811,March 2007

[139] Tofgard, S. N. Hornsleth and J. B. Andersen, "Effects on, Portable Antenna of the Presence of a Person," IEEE Transactions on Antennas and Propagation, AP-41,No.6, pp. 739-746,June 1993.

[140] Kin-Lu Wong; Saou-Wen Su; Chia-Lun Tang; Shih-Huang Yeh, "Internal shorted patch antenna for a UMTS folder-type mobile phone", IEEE Trans on Antennas and Propagat., Volume 53, Issue 10, Pp 3391 – 3394,Oct. 2005

[141] Tzortzakakis, M.; R.J Langley, "Quad-Band Internal Mobile Phone antenna", IEEE Trans on Antennas and Propagat., Volume 55, Issue 7, Pp:2097 – 2103, July 2007.

[142] DVB-The Family of International Standards for Digital Video Broadcasting Reimers, U.H.; Proceedings of the IEEE, Volume 94, Issue 1, Pp 173 – 182,Jan. 2006

[143] Yang Kang; Haipeng Mi; Wenhua Chen; Zhenghe Feng; "A reconfigurable compact antenna for DVBH application",. International Conference on Microwave and Millimeter Wave Technology, Volume 4, 21-24 Pp:1882 - 1885 April 2008.

[144] Jung N. Lee, Jong K. Park, Byoung J. Yim, "Design of the novel DVB-H antenna for mobile handheld terminal", Microwave and Optical Technology Letters Volume 49, Issue 10,Pp 2345- 2350,October 2007

[145] Ma Hanqing and Qing-Xin Chu,, "Compact broadband planar antenna for DVB-H applications", Microwave and Optical Technology Letters Vol. 51, No. 1,Pp 239-243, January 2009

[146] Coplanar waveguide fed coplanar strip dipole antenna, Tilley K, Wu, X.-D, Chang K, IEE Electron Lett., Vol. 30, Issue 3, 3 Feb. 1994 pp.176 - 177

[147] Herraiz-Martinez, F.J.; Garcia-Munoz, L.E.; Gonzalez-Posadas, V.; Segovia-Vargas, D.,"Multi-Frequency Printed Dipoles Loaded with Metamaterial Particles" IEEE conference on Microwave Techniques, 2008. COMITE 2008.,Pp 421– 423-24 April 2008

[148] Zhanwei Zhou; Shiwen Yang; Zaiping Nie, "A Novel Broadband Printed Dipole antenna With Low Cross-Polarization", IEEE Trans on Antennas and Propagat., Volume 55, Issue 11, Part 1, Pp 3091 – 3093 Nov. 2007

[149] Melais, S.E.; Weller, T.M., "A Quasi Yagi Antenna Backed by a Metal Reflector", IEEE Transactions on Antennas and Propagat., Volume 56, Issue 12, Pp 3868 – 3872 Dec. 2008

[150] Lim, S. Iskander, M. F, Design of a Dual-Band, "Compact Yagi Antenna Over an EBG Ground Plane",IEEE Antennas and Wireless Propagation Lett., Volume 8, Pp :88 – 91 , 2009

[151] Kan, H.K.; Waterhouse, R.B.; Abbosh, A.M.; Bialkowski, M.E.; Chung, K.L, " A Simple Broadband Planar Quasi-Yagi antenna", IEEE Region 10 Conference TENCON 2006. 14-17, Pp 1 - 3 Nov. 2006

[152] Nilsson, H.-E.; Siden, J.; Olsson, T.; Jonsson, P.; Koptioug, A, " Evaluation of a printed patch antenna for robust microwave RFID tags", IET Microwaves, Antennas & Propagation, Volume 1, Issue 3, Pp:776 – 781, June 2007

[153] Jung-Chin Hsieh; Ming-Iu Lai; Shyh-Kang Jeng, " An RFID Antenna design for multi-layered printed circuit board applications" IEEE Antennas and Propagation International Symposium, Pp:309 – 312, June 2007

[154] Choi, Y.; Kim, U.; Kim, J.; Choi, J, " Design of modified folded dipole antenna for UHF RFID tag", IEE Electron. Lett. Volume 45, Issue 8 ,Pp:387 - 389, April 2009

[155] Rawal, A.; Karmakar, N.C, "A novel L-shaped RFID tag antenna", European Microwave Conference, 2007. Pp:1003 – 1006, Oct. 2007 .

…….ꕥ……

Chapter 2

DESIGN, FABRICATION AND MEASUREMENT OF ANTENNAS

Contents

The chapter deals with the techniques used for the design, fabrication and measurement of antennas. The design and simulations are performed using the FEM based Ansoft High Frequency Structure Simulator (HFSS). The antennas are fabricated using photolithographic method.VNA HP8510C and Agilent PNA 8362B are used to measure antenna characteristics such as return loss, radiation pattern, gain etc.

2.1 Techniques for the Design and Optimization of Antennas

The design and optimization studies of the antennas presented in this thesis are performed using the commercial software Ansoft High Frequency Structure Simulator (HFSS). HFSS is a high-performance full-wave electromagnetic (EM) field simulator for arbitrary 3D volumetric device modeling.

2.1.1 High Frequency Structure Simulator

Ansoft HFSS utilizes the 3D full-wave Finite Element Method (FEM) with adaptive meshing to compute the electrical behavior of high-frequency and high-speed components [1]. The basic mesh element is a tetrahedron. This allows solving any arbitrary 3D geometry, especially those with complex curves and shapes, in minimum time. Ansoft HFSS can be used to calculate antenna parameters such as S Parameters, radiation pattern, gain, current distributions, fields, efficiency etc. HFSS integrates simulation, modeling, visualization and automation in an user friendly environment. With adaptive meshing and brilliant graphics HFSS gives an unparalleled performance and complete insight to the actual radiation phenomenon in the antenna. With HFSS one can extract the parameters such as S,Y, and Z, visualize 3D electromagnetic fields (near- and far-field), and optimize design performance. An important and useful feature of this simulation engine is the availability of different kinds of port schemes. It provides lumped port, wave port, incident wave scheme etc. The accurate simulation of coplanar and microstrip lines can be done using the port schemes. The parametric set up available with HFSS is highly suitable for an antenna engineer to optimize the desired dimensions.

The first step in simulating a structure in HFSS is to define the geometry of the structure by giving the material properties and boundaries for 3D or 2D elements available in HFSS window. The next step is to draw the intended architecture using the drawing tools available in the software. The designed structure is excited using the suitable port excitation schemes. The next step is

the assigning of boundary scheme. A radiation boundary filled with air is commonly used for radiating structures. The size of air column is taken to be equal to a quarter of the free space wavelength of the lowest frequency of operation. Now, the simulation engine can be invoked by giving the proper frequency of operation and the number of frequency points. Finally the simulation results such as scattering parameters, current distributions and far field radiation pattern can be displayed. The vector as well as scalar representation of E, H and J values of the device under simulation gives a good insight into the structure under analysis.

2.1.2 The Finite Element Method

As mentioned above HFSS uses the FEM technique for the calculation of different parameters. The Finite Element Method is well-established and widely used for the time-harmonic solution of Maxwell's equations. The unstructured nature of the time domain version of FEM gives a clear advantage over numerical computational methods in modeling complex antenna geometries. The main concept of the finite element method is based on subdividing the geometrical domain of a boundary-value problem into smaller sub-domains, called finite elements, and expressing the governing differential equation along with the associated boundary conditions as a set of linear equations that can be solved computationally using linear algebra techniques.

FEM has enjoyed a strong interest for electromagnetic analysis. In fact, over the past 10 years, the greatest progress in computational electromagnetics is based on the development and application of partial

differential equation (PDE) methods such as the finite difference-time domain (FDTD), finite element (FEM) and methods including hybridizations of these with integral equations and high frequency techniques. The major reasons for the increasing reliance on PDE methods stem from their inherent geometrical adaptability, low memory demand and their capability to model heterogeneous (isotropic or anisotropic) geometries. These attributes are essential in developing general-purpose codes for electromagnetic analysis/design, including antennas and their characterization.

FEM is a mature method and is the workhorse of standard analysis and design packages in Mechanical Engineering and Applied Mechanics. In this approach Resistive/material and impedance boundary conditions are readily implemented in a modular fashion. Established hybridizations of the FEM with moment methods and ray methods provide an added advantage by delivering the most adaptable and efficient code when compared to other approaches [2].

The main idea behind the FEM [3,4] is to solve Boundary Value Problems (BVP)s governed by a differential equation and a set of boundary conditions. The representation of the domain is split into smaller sub-domains called the finite elements. The distribution of the primary unknown quantity inside an element is interpolated based on the values at the nodes, provided nodal elements are used, or the values at the edges, in case vector elements are used. The interpolation or shape functions must be a complete set of polynomials.

The accuracy of the solution depends, among other factors, on the order of these polynomials, which may be linear, quadratic, or higher order. The numerical solution corresponds to the values of the primary unknown quantity at the nodes or the edges of the discretized domain. The solution is obtained after solving a system of linear equations. To form such a linear system of equations, the governing differential equation and associated boundary conditions must first be converted to an integro-differential formulation either by minimizing a functional or using a weighted residual method such as the Galerkin approach. This integro-differential formulation is applied to a single element and with the use of proper weight and interpolation functions the respective element equations are obtained. The assembly of all elements results in a global matrix system that represents the entire domain of the BVP.

There are two methods that are widely used to obtain the finite element equations: the variational method and the weighted-residual method.

The variational approach requires construction of a functional which represents the energy associated with the BVP at hand. A functional is a function expressed in an integral form and has arguments that are functions themselves. Many engineers and scientists refer to a functional as being a function of functions. A stable or stationary solution to a BVP can be obtained by minimizing or maximizing the governing functional. Such a solution corresponds to either a minimum point, a maximum point, or a saddle point. In the vicinity of such a point, the numerical solution is stable meaning that it is rather insensitive to small variations of dependent parameters. This translates to a smaller numerical error compared to a solution that corresponds to any other point.

The second method, is a weighted-residual method widely known as the Galerkin method. This method begins by forming a residual directly from the partial differential equation that is associated with the BVP under study. Simply stated,this method does not require the use of a functional. The residual is formed by transferring all terms of the partial differential equation on one side. This residual is then multiplied by a weight function and integrated over the domain of a single element. This is the reason why the method is termed as weighted-residual method. The Galerkin approach is simple and starts directly from the governing differential equation.

2.2 Antenna fabrication

The antennas studied in the thesis are fabricated using the photolithographic technique. This is a chemical etching process by which the unwanted metal regions of the metallic layer are removed so that the intended design is obtained. Depending upon the design of the antenna as biplanar or uniplanar dual or single side substrates are used. The selection of a proper substrate material is the essential part in antenna design.

2.2.1 Characteristics of substrate materials

Recent developments in the microelectronic industry demand high performance microwave materials for substrate and packaging applications. Materials for such applications should have low relative permittivity and low dielectric loss to reduce the propagation delay and to increase the signal speed. In addition the materials should have high thermal conductivity for dissipating heat. Other important substrate characteristics include the thickness, homogeneity, isotropicity and dimensional strength of the substrate [5 - 9].

The selection of dielectric constant of the substrate depends on the application of the antenna and the radiation characteristics specifications. High Dielectric constant substrates causes surface wave excitation and low bandwidth performance. Also as the frequency of operation increases, the loss tangent of the material used for substrates slightly increases, which in turn adversely affects the efficiency of the antenna. Also increasing the thickness of the substrate increases the band width of the antennas at the expense of efficiency owing to increase in surface waves. FR4 with ε_r=4.4 tan, δ=.02, h=1.6 mm and RT Duriod substrate with ε_r=4.4, tan δ=.002, h=1.5 mm are used for the study.FR4 substrate are commonly used for initial studies. The final antennas are fabricated on RT Duroid to enhance the antenna efficiency.

Various methods have been devised to accurately measure the dielectric properties of substrates available in market [10 -11].

The microwave dielectric properties of the sample were measured by the cavity perturbation technique using a vector Network Analyzer. This technique is widely used for the determination of the dielectric characteristics of thin samples of low and medium dielectric loss.

A rectangular S or X-band slotted wave-guide cavity with optimum iris coupling is used for the measurement of dielectric properties of the samples at the microwave frequencies. The resonant frequency and quality factor of the empty cavity were determined for different cavity modes. Then the extremely thin sample having known dimensions is inserted and positioned at the E-field antinode. The new resonant frequency and Q of the sample were again measured. The complex dielectric constant of the sample was calculated using the following equations.

$$\varepsilon_r^{'} = 1 + \left(\frac{V_c (f_0 - f_s)}{2V_s\ f_s} \right) \quad \text{.....(2.1)}$$

$$\varepsilon_r^{''} = \frac{V_c\,(Q_0\ - Q_s)}{4V_s Q_0\, C_s} \quad \text{.....(2.2)}$$

$$\tan\delta = \frac{\varepsilon_r^{''}}{\varepsilon_r^{'}} \quad \text{.....(2.3)}$$

where f_o = resonant frequency of the cavity

f_s = resonant frequency of the samples

V_c = Volume of the cavity

V_s = Volume of the sample

Q_0 = Quality factor of the empty cavity

Q_s = Quality factor of the sample loaded cavity

2.2.2 Photo Lithography

After the proper selection of the substrate material a computer aided design of the geometry is initially made and a negative mask of the geometry to be generated is printed on a transparent sheet. A single or double sided substrate with copper metallization of suitable dimension is properly cleaned using acetone to free from impurities.

A thin layer of negative photo resist solution (1:1 mix of negative photoresit solution and thinner) is coated using spinning technique on copper surfaces and is dried. The mask is placed onto the photo resist and exposed to UV light. After the proper UV exposure the layer of photo-resist material in the exposed portions hardens when it is treated with developer solution

The board is then dipped in dye ink solution in order to clearly view the hardened photo resist portions on the copper coating The board is then washed in water. After developing phase the unwanted copper portions are etched off using Ferric Chloride ($FeCl_3$) solution to get the required antenna geometry on the substrate. The etched board is rinsed in running water to remove any etchant. . $FeCl_3$ dissolves the copper parts except underneath the hardened photo resist layer after few minutes. The laminate is then cleaned carefully to remove the hardened photo resist using acetone solution. The various steps involved in the fabrication process are illustrated in Fig.2.1

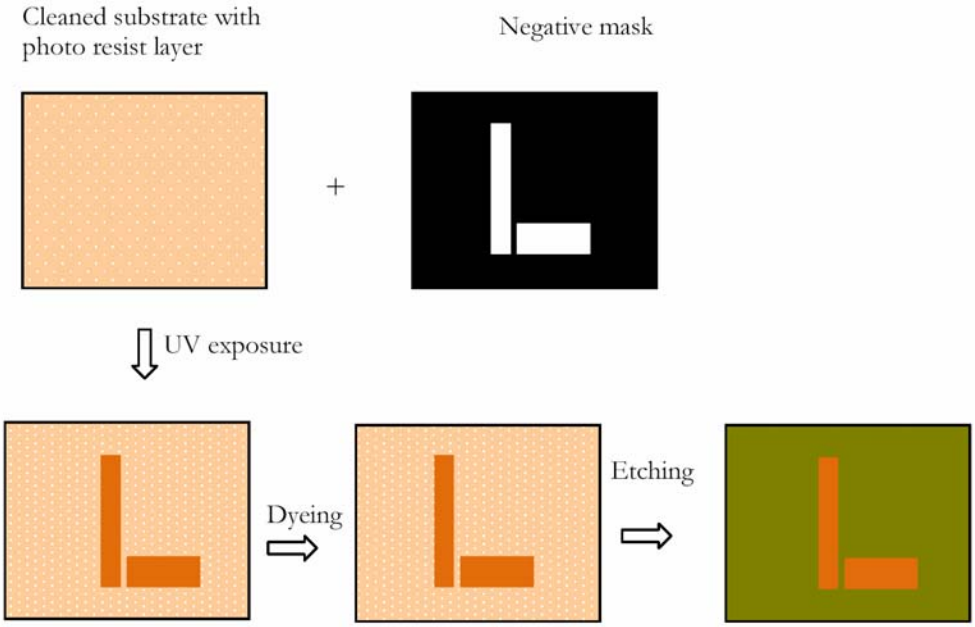

Fig.2.1. Photolithographic technique for antenna fabrication

2.3 Antenna Measurements

This section explains the techniques used for the accurate measurement of antennas under study.

2.3.1 Experimental Set up

An epigrammatic overview of the equipments and facilities used for extracting the antenna reflection and radiation characteristics is presented in this section with details of the measurement procedure. The measurement of radiation characteristics of the antennas were carried out using Network analysers HP 8510C VNA and Agilent 8362B PNA.

2.3.2 HP 8510C Vector Network analyzer (VNA)

HP8510C is sophisticated equipment capable of making rapid and accurate measurements in frequency and time domain [12]. The NWA can measure the magnitude and phase of the S parameters. The 32 bit microcontroller MC68000 based system can measure two port network parameters such as S_{11}, S_{12} , S_{22} ,S_{21} and it's built in signal processor analyses the transmit and receive data and displays the results in many plot formats. The NWA consists of source, S parameter test set, signal processor and display unit. The synthesized sweep generator HP 83651B uses an open loop YIG tuned element to generate the RF stimulus. It can synthesize frequencies from 10 MHz to 50 GHz. The frequencies can be set in step mode or ramp mode depending on the required measurement accuracy. The antenna under test is connected to the two port S parameter test set unit, HP8514B and incident and reflected wave at the port are then down converted to an intermediate frequency of 20MHz and fed to the detector. These signals are suitably processed to display the magnitude and phase information in the required format. These constituent modules are interconnected through HPIB system bus. An in-house developed MATLAB based data acquisition system coordinates the measurements and saves the data in the text format. Schematic diagram of HP8510C NWA and setup for reflection characteristic measurement is shown in Fig.2.2

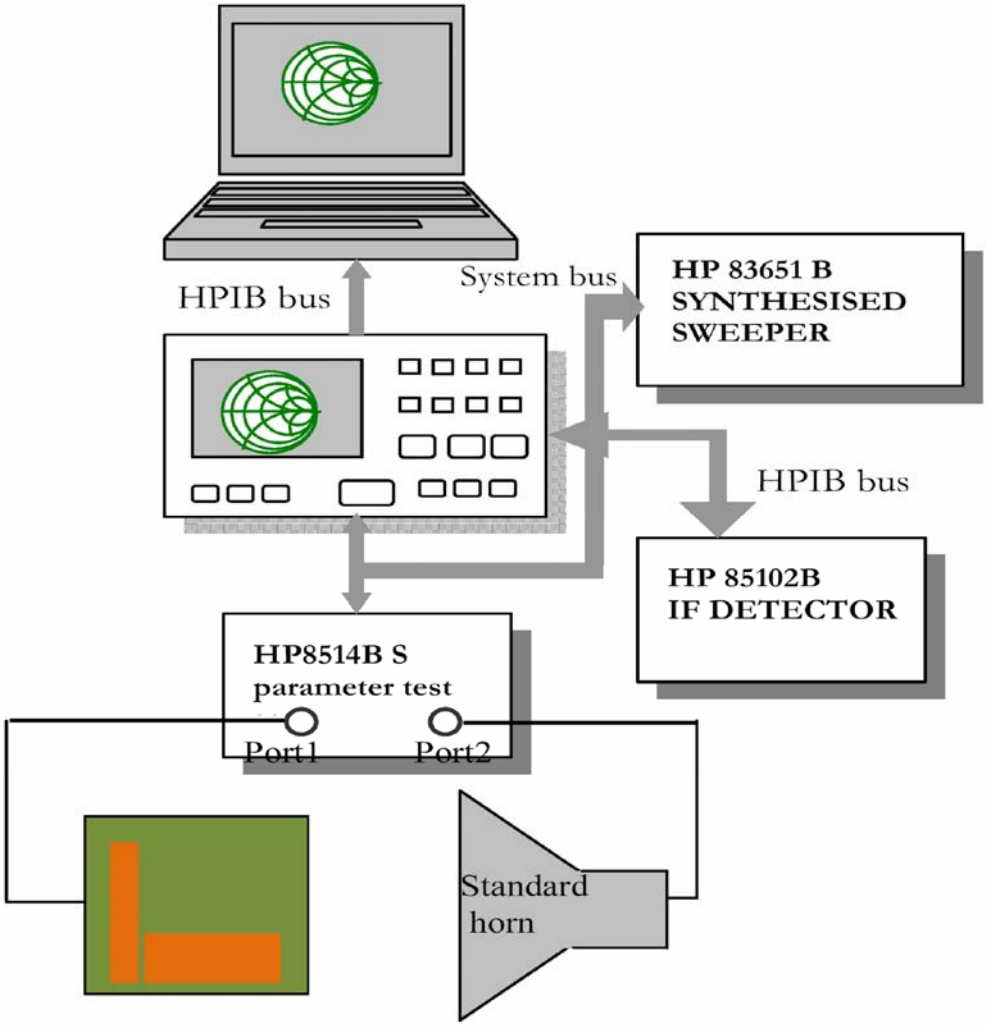

Fig.2.2 Setup for measuring reflection characteristic using HP 8510C VNA

The Antenna characteristics such as return loss, radiation pattern and gain are measured using the HP8510C and associated setup. The indigenously developed CREMA SOFT is used for the automatic measurement of the radiation properties using HP 8510C Network analyzer. The important systems used for the antenna characterization are Vector network Analyzer, Anechoic Chamber, Automated turn table etc.

The antenna under test (AUT) is connected to the port of the S-parameter test set HP8514B and the forward and reflected power at the measurement point is separated and down converted to 20MHz using frequency down converter. It is again down converted to lower frequency and processed in the HP8510C processing unit. All the systems discussed above are interconnected using HPIB bus. A computer interfaced to the system is used for coordinating the whole operation remotely. Measurement data can be saved on a storage medium .

2.3.3 E8362B programmable Network Analyzer (PNA)

The Agilent E8362B Vector Network Analyzer is a member of the PNA Series Network Analyzer platform and provides the combination of speed and precision for high frequency measurements [13]. The operation range is from 10 MHz to 20 GHz. For antenna measurements it provides exceptional results with more points and faster measurement speed. It has 16,001 points per channel with < 26 μsec/point measurement speed and 32 independent measurement channels. Windows operating system and user interface mouse makes measurement procedure much easier. Embedded help system with full manual, extensive measurement tutorials, and complete programming guide helps to carry out accurate measurement of antenna characteristics promptly.

2.3.4 Anechoic Chamber

The anechoic chamber provides a quite zone, free from all types of EM distortions. All the antenna characterizations are done in an Anechoic chamber to avoid reflections from nearby objects.

It is a very big room consisting of microwave absorbers fixed on the walls, roof and the floor to avoid the EM reflections. A photograph of the anechoic chamber used for the study is shown in Fig. 2.3 below.

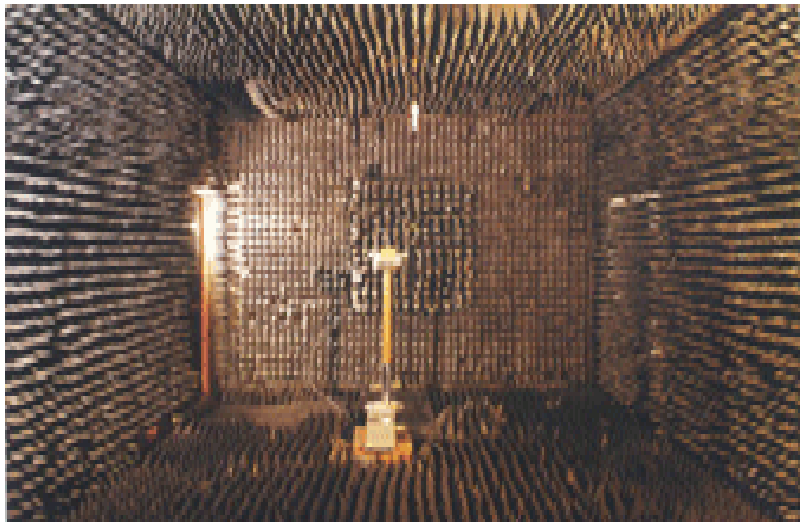

Fig.2.3. Photograph of the anechoic chamber used for the antenna measurements

The absorbers fixed on the walls are highly lossy at microwave frequencies. They have tapered shapes to achieve good impedance matching for the microwave power impinges upon it. The chamber is made free from the surrounding EM interferences by covering all the walls and the roof with aluminium sheet.

2.3.5 Turn table assembly for far field radiation pattern measurement

The turn table assembly consists of a stepper motor driven rotating platform for mounting the Antenna Under Test (AUT). The in-house developed microcontroller based antenna positioner STIC 310C is used for radiation pattern measurement. The main lobe tracking for gain measurement and

radiation pattern measurement is done using this setup. A standard wideband horn (1-18GHz) is used as receiving antenna for radiation pattern measurements. The in-house developed automation software '*Crema Soft*' (Developed at the Centre for Research in Electromagnetics and Antennas, CUSAT, INDIA) coordinates all the measurements.

2.3.6 Experiments

The experimental procedures followed to determine the antenna characteristics are discussed in the following sections. Power is fed to the antenna from the S parameter test set of the analyzer through cables and connectors. The connectors and cables tend to be lossy at higher microwave bands. Hence the instrument should be calibrated with known standards of open, short and matched loads to get accurate scattering parameters. There are many calibration procedures available in the network analyzer. Single port and full two port calibration methods are usually used. Return loss, VSWR and input impedance can be characterized using single port calibration method.

The fabricated antennas are tested to study the various characteristics. Since all the antennas have very compact dimensions of the order of a quarter of the wavelength various factors have to be considered for efficient and accurate measurements.

Ideally, antennas would be measured without any perturbation from measurement cables and connectors. However for cost and speed reasons, most handset and WLAN antennas are measured using a coaxial cable to connect the antenna under test (AUT) to the transceiver. This feed cable

couples to the currents on the AUT and can affect both the antenna match and also the radiation performance. Various techniques have been reported in literature to nullify this effect. A new method of suppressing spurious measurement cable currents has been developed in [14]. This relies on computer simulation to predict the low electric field regions where the measurement cable can be safely attached, and upon comparison between simulation and measurement results the measurement cable spurious surface currents can be accounted. Another common practice is the use of ferrite beads and quarter wave sleeve balm ("bazookas") to be used to suppress the current on the feed cable. But even with all these methods the effects cannot be completely negated [15].

2.3.7 Return loss, Resonant frequency and Bandwidth

The calibration of the port is done for the frequency range of interest using the standard open, short and matched load. The calibrated instrument including the port cable is now connected to the device under test. The return loss characteristic of the antenna is obtained by connecting the antenna to any one of the network analyzer port and operating the VNA in s_{11}/s_{22} mode. The frequency vs reflection parameter (s_{11}/s_{22}) is then stored on a computer using the 'Crema Soft' automation software.

The frequency for which the return loss value is the minimum is taken as resonant frequency of the antenna. The range of frequencies for which the return loss value is within the -10dB points is usually treated as the bandwidth of the antenna. The antenna bandwidth is usually expressed as percentage of bandwidth, which is defined as

$$\%Bandwidth = \frac{f2 - f1}{fc} * 100$$

Where *f2* denotes the higher -10 dB point, *f1* the lower -10 dB point and *fc* the centre frequency having the minimum return loss value.

At -10dB points the VSWR is ~2. The above bandwidth is sometimes referred to as 2:1 VSWR bandwidth.

2.3.8 Radiation pattern measurement

The measurement of far field radiation pattern is conducted in an anechoic chamber. The AUT is placed in the quiet zone of the chamber on a turn table and connected to one port of the network analyzer. The the network analyzer is kept in S_{21}/S_{12} mode with the frequency range within the -10dB return loss bandwidth. The number of frequency points is set according to convenience. The start angle, stop angle and step angle of the motor is also configured '*Crema Soft*'. The antenna positioner is boresighted manually. Now the THRU calibration is performed for the frequency band specified and saved in the CAL set. Suitable gate parameters are provided in the time domain to avoid spurious radiations if any. The *Crema Soft* automatically performs the radiation pattern measurement and stores it as a text file. This is used to plot the 2-D radiation pattern at the required frequency.

2.3.9 Antenna Gain

The gain of the antenna under test is measured in the bore sight direction. The gain transfer method using a standard gain antenna is employed to determine

the absolute gain of the AUT [16-18]. The experimental setup is similar to the radiation pattern measurement setup. An antenna with known gain is first placed in the antenna positioner and the THRU calibration is done for the frequency range of interest. Standard antenna is then replaced by the AUT and the change in S_{21} is noted. Note that the AUT should be aligned so that the gain in the main beam direction is measured. This is the relative gain of the antenna with respect to the reference antenna. The absolute gain of the antenna is obtained by adding this relative gain to the original gain of the standard antenna.

2.3.10 Antenna Efficiency

Conventional antenna radiation efficiency measurement techniques, such as the Wheeler cap, are generally narrowband and, thus, well suited for resonant antennas [19,20].The method involves making only two input resistance measurement of antenna under test: one with conducting cap enclosing the antenna and one without. For the Wheeler cap, a conducting cylindrical box is used whose radius is radiansphere of the antenna and which completely encloses the test antenna. Input impedance of the test antenna is measured with and without the cap using E8362B PNA. Since the test antenna behaves like a series resonant RLC circuit near resonance the efficiency is calculated by the following expression:

$$Efficiency, \eta = \frac{R_{no\_cap} - R_{cap}}{R_{no\_cap}}$$

Where, R_{no_cap} denotes the input resistance without the cap and R_{cap} the resistance with the cap.

References

[1] Ansoft HFSS, http://www.ansoft.com/products/hf/hfss/

[2] Volakis, J.L, Hybrid finite element methods for conformal antenna simulations,Antennas and Propagation Society International Symposium, 1997. IEEE., 1997 Digest Volume 2 ,Page(s):1318 - 1321, July 1997 .

[3] Anastasis C. Polycarpous, Introduction to the Finite Element Method in Electromagnetics, Morgan & Claypool,USA,2006.

[4] Joao pedro a. Bastos and Nelson Sadowski , "Electromagnetic modeling by finite element methods", Marcel Dekker,2003

[5] J. Youngs, G. C. Stevens and A. S. Voughan, "Trends in dielectric research: an international review from 1980 to 2004," J. Phys. D: Appl. Phys. 39 1267-76 (2006).

[6] M. G. Pecht, G, R. Agarwal, P. McCluskey, T. Dishongh, S. Javadpour and R. Mahajan, "Electronic Packaging Materials and there Properties," CRC Press, London, (1999).

[7] T. Hu, J. Juuti, H. Jantunen, and T. Vilkman, "Dielectric properties of BST/polymer composite," J. Eur. Ceram.Soc., 27, 3997-4001 (2007).

[8] D. D. L. Chung, "Materials for Electronic Packaging," Butterworth Heinemann, Washington, (1995).

[9] M. T. Sebastian, "Dielectric materials for wireless communications," Elseiver publishers UK., (2008).

[10] Rao Y, Qu J, Marinis T, Wong C P, " A precise numerical prediction of effective dielectric constant for polymer ceramic composites based on effective medium theory" IEEE Trans. Compon. Packag. Tech Pp 680-683, 2000

[11] Prakash A, Vaid J K Mansingh A, "Measurement of dielectric parameters at microwave frequencies by cavity perturbation technique", IEEE Trans. Microwave Theory and Tech.,vol.27:Pp 791-795, 1979

[12] HP8510C Network Analyzer operating and programming manual, Hewlett Packard, 1988.

[13] http://www.home.agilent.com

[14] Massey, P.J.; Boyle, K.R, "Controlling the effects of feed cable in small antenna measurements", Twelfth International Conference on Antennas and Propagation, Volume 2, 31 Pp:561 - 564 vol.2 April 2003

[15] Kin Seong Leong; Mun Leng Ng; Cole, P.H, "Investigation of RF cable effect on RFID tag antenna impedance measurement" Antennas and Propagation International Symposium, 2007 IEEE, Page(s):573 – 576, 9-15 June 2007

[16] C. A. Balanis, Antenna Theory: Analysis and Design, Second Edition, John Wiley & Sons Inc. 1982

[17] John D. Kraus, Antennas Mc. Graw Hill International, second edition, 1988

[18] Jaume Anguera, Alfonso Sanz, Young-Jik Ko, Carmen Borja ,Carles Puente and Jordi Soler, "Theoretical and practical experiments for a single antenna gain testing method: Application to wireless communication devices", Microwave and optical technology letters Vol. 49, No. 8,Pp 1781 – 1786, August 2007

[19] H.A Wheeler, "The Radiansphere around a small antenna", in Proc. IRE, August 1959, pp 1325-1331.

[20] Hosung Choo; Rogers, R.; Hao Ling; "On the Wheeler cap measurement of the efficiency of microstrip antennas", IEEE Transactions on Antennas and Propagat., Volume 53, Issue 7, Pp:2328 – 2332, July 2005

…….ꕥ…….

Chapter 3

ASYMMETRIC COPLANAR STRIP FED COMPACT ANTENNAS

Contents

The chapter deals with the design and development of compact planar antennas using the asymmetric coplanar strip feed. The chapter starts with a brief introduction of the different types of feeding mechanisms for planar antennas. From the various kinds of feeds described the asymmetric coplanar strip feeding is found to be the best suited candidate for compact antennas. This is validated by comparing the characteristics of a simple strip monopole fed by the Asymmetric Coplanar Strip feed with that of a similar monopole fed by the conventional Coplanar wave guide feed. Compact single band, dual band and multiband antennas are designed by the above feed and thoroughly studied. It can be seen that all these antennas occupy dimensions of the order of only $\lambda_d/4 \times \lambda_d/4$. *The inferences are effectively utilized for the design of different compact antennas for DCS/PCS/UMTS/2.4/5.2/5.8 GHz WLAN applications.*

3.1 Introduction to compact planar antennas

Modern wireless devices are becoming more compact day by day. This trend is forcing designers to miniaturize each and every component of the

device. Antennas which are one of the major components cannot remain as standalone devices. Hence its design too is crucial in deciding the overall performance of the device.

The main characteristic of an antenna is to radiate energy which is launched into its input end (feed). The design of a matched feed is important for transferring maximum power from the source to the radiating antenna. This implies that the feed will play an important role in the design of the antenna. The issue is more crucial in the case of compact antennas.

While designers give much importance to the radiator, the feed region of the most compact designs still remains untouched. The overall area of an antenna depends on the size of both the radiating element and the feed. Hence in this study equal importance is given to the design of the feed and the radiator.

In this chapter the design and development of compact antennas with optimum feed is presented. Single band, Dual band and triple band antennas are developed with the above idea. Exhaustive experimental and simulation studies of the above antennas are also presented and discussed.

3.2 Planar Transmission lines

In this section the different types of antenna feeds are briefly presented. Since the thesis is about the study of planar antennas emphasis is given to planar transmission lines. The widely used planar transmission lines include the microstrip line (Dual layer structure) and the coplanar wave guide (Uniplanar structure).

3.2.1 The Microstrip line

The Microstrip line (MSL) consists of a narrow signal strip on an infinite ground plane separated by a dielectric. The cross section of a typical MSL is shown in fig.3.1.The characteristic impedance of the line depends on the width of the signal strip along with the height and the dielectric constant of the substrate [1].

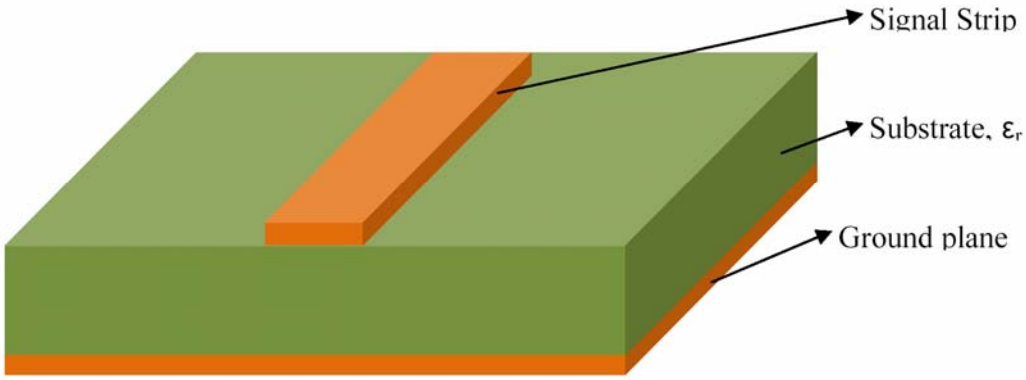

Fig. 3.1. Microstrip transmission line

The term “Uniplanar” or “Coplanar” stands for those transmission lines in which all the conductors lie in the same plane. The members of this category include the Coplanar wave guide (CPW), the SlotLine (SL) etc [2].

3.2.2 The Coplanar Wave guide

The coplanar wave guide consists of a central signal strip bounded by twin lateral ground strips separated by a small gap (Fig.3.2.). The characteristic impedance is determined by the width of the signal strip, the gap between the signal strip and the lateral ground strip for fixed substrate height and dielectric constant [2].

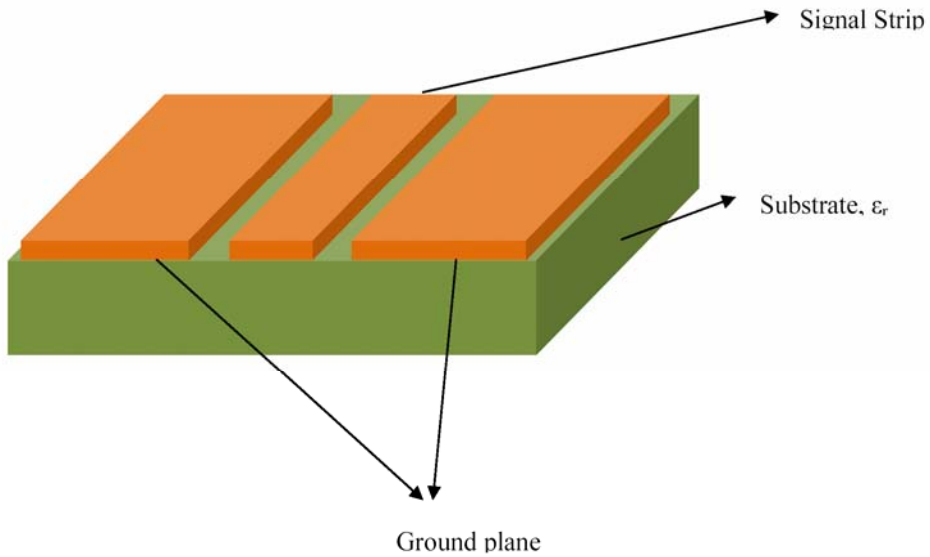

Fig.3.2. The CPW transmission line

3.2.3 The Slotline

The slotline may be considered as a complementary to the CPW (Fig.3.3.). The main advantage of this transmission line is the ease of mounting active and passive circuits into these lines. Here the width of the slot and the height of the substrate determine the characteristic impedance [3].

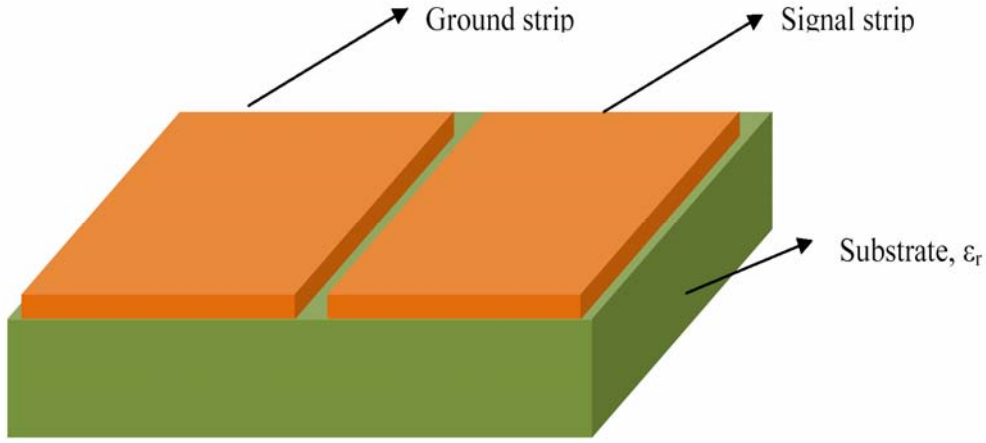

Fig.3.3. Geometry of a Slotline

Many related designs like coplanar strips, conductor backed coplanar wave guide, Asymmetric coplanar strips etc have also been reported in literature.

3.2.4 The Asymmetric Coplanar Strip feed

The Asymmetric Coplanar Strip (ACS) is a modification of the slot line in which the width of one of the lateral strips is narrow. Owing to the simple structure, ease of fabrication and other reasons mentioned below it is more advantageous for compact antenna designs. In this thesis the asymmetric coplanar strip is effectively utilized in the design of compact uniplanar antennas.

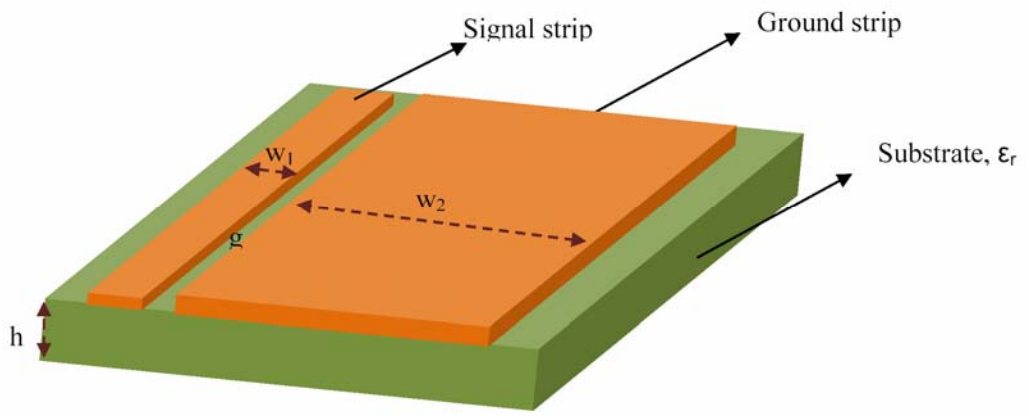

Fig.3.4. Schematic of the Asymmetric Coplanar Strip (ACS) feed

Fig.3.4 shows the schematic of the ACS feed. It mainly consists of a signal strip (w_1) with a single lateral ground plane (w_2) separated by a small gap (g). The characteristic impedance of this transmission line on a substrate of dielectric constant ε_r and height 'h' depends on w_1, w_2 and g [2]. But when the width of one of the strips (say w_2) is very much larger compared to the other (w_1), its effect on the characteristic impedance is found to be less and hence w_2 can be omitted from characteristic impedance calculations, without much error.

The characteristic impedance of the ACS line is given by

$$Zo = \frac{60\pi}{\sqrt{\varepsilon_{re}}} \frac{K^{'}(k)}{K(k^{'})} \quad \text{.....(3.1)}$$

$$k = \sqrt{\frac{w1}{w1+g}} \quad \text{.....(3.2)}$$

Where, $\varepsilon_{re} = 1 + q * (\varepsilon_r + 1)$ .....(3.3)

Also $k^{'} = \sqrt{1-k^2}$ .....(3.4)

$$q = \frac{K(k1)k^{'}(k)}{K^{'}(k1)k(k)} \quad \text{.....(3.5)}$$

$$k1 = \frac{Sinh\left(\frac{\pi w1}{zh}\right)}{Sinh\left(\frac{\pi(w1+g)}{zh}\right)} e^{-\pi g/2h} \quad \text{.....(3.6)}$$

and

$$\frac{K(k)}{K'(k)} = \frac{\pi}{\ln[2(1+\sqrt{k'})]} \; for\, 0 \le k \le 1/\sqrt{2} \quad \text{.....(3.7)}$$

$$\frac{K(k)}{K'(k)} = \frac{1}{\pi} \ln[2(1+\sqrt{k})/(1-\sqrt{k})] \; for\, 1/\sqrt{2} \le k \le 1$$

Hence K(k) and k'(k) are elliptical functions

There are several reasons for using the Asymmetric coplanar strip (Fig.3.4) in place of the coplanar wave guide (Fig.3.2) to feed compact antennas. The first reason is obviously the reduction of area in the feed section. It can be seen that the ACS feed requires lesser area than the CPW feed.

Secondly, as mentioned above, in characteristic impedance calculations of the ACS, if the width of one of the lateral strips is very large compared to the other its width (the width of the larger strip) is found to have less impact on the characteristic impedance. This gives freedom to the designer to select the feed dimensions based on circuit requirements.

Even though the ACS feed is compact, before embedding this feed into a practical antenna system its effect on the overall performance of the antenna has to be analyzed thoroughly and compared with that of an antenna with a conventional feeding mechanism. For this study a simple strip monopole is used as the reference. The simple strip monopole fed by the ACS feed is compared with that of a monopole fed by the CPW feed and studied as given below.

3.3 Coplanar Wave Guide and Asymmetric Coplanar Strip fed Monopole antennas – A comparison

Monopole antennas are attractive in modern wireless applications owing to simple structure, broad bandwidth and nearly omnidirectional radiation characteristics. The monopoles are usually placed vertically to a large ground plane which increases the system complexity, size and volume. Printed monopoles on the other hand, are conformal for modular design and can be fabricated along with the printed circuit board of the system, making fabrication easier. A CPW fed monopole is an ideal example for an uniplanar monopole antenna. Therefore it is used to compare the properties of the Asymmetric Coplanar Strip (ACS) fed monopole.

3.3.1 Geometry of the antennas

Fig.3.5. Shows the geometries of the CPW and ACS fed simple monopole antennas.

In the case of the ACS fed antenna, the monopole is directly fed by the ACS feed. The signal is fed at the point‘s’ and the ground of the coaxial cable is connected to ‘s_1’. The antennas are designed on a substrate of dielectric constant 4.4 and height 1.6 mm.

The length of the monopoles above the ground plane is taken as L_m for both the ACS fed monopole and the CPW fed monopole. The width is taken equal to ‘w’. The ground plane dimensions and the gap of the both the antennas are optimized for good impedance matching.

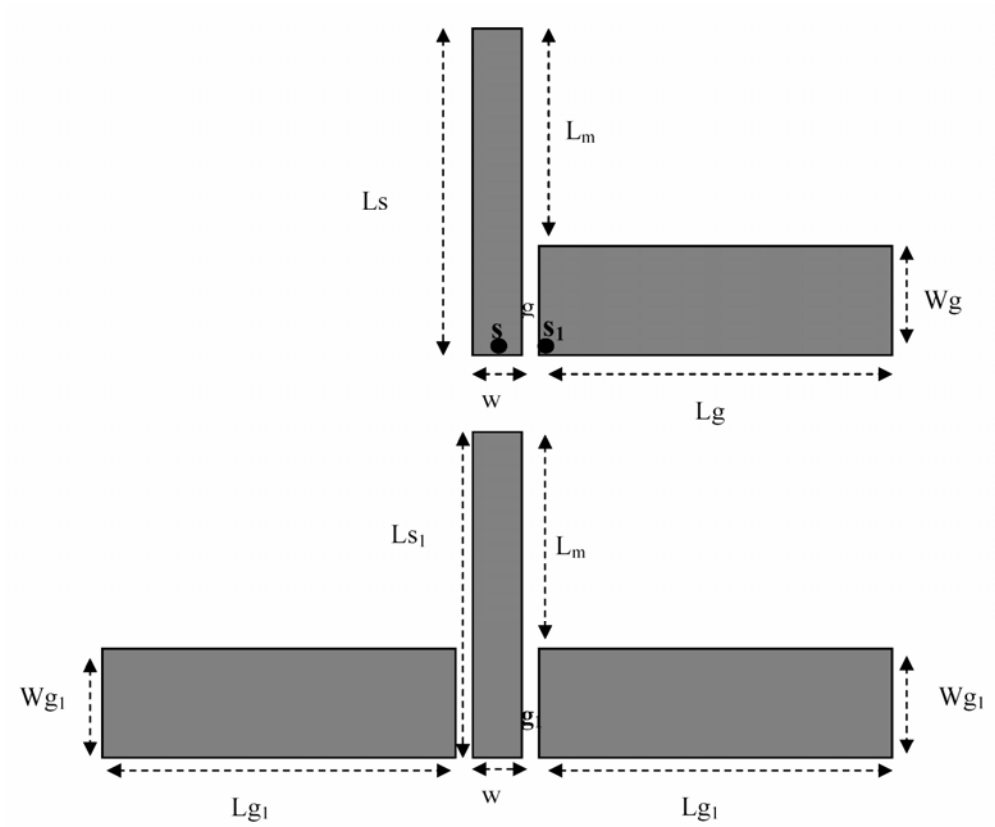

Fig. 3.5. Comparison of the ACS and CPW fed strip monopoles
L_m = 17 mm, Ls = 25 mm, Lg = 25 mm, Wg = 8 mm and w = 3 mm, Ls_1= 25 mm, W=3 mm,,Lg_1 = 25 mm, Wg_1 = 8 mm, g = 0.5 mm, g_1 = 0.3 mm, ε_r =4.4, h= 1.6 mm

3.3.2 Return Loss Characteristics

The Return loss curves of the two antennas are shown in fig.3.6. It can be seen that both the antennas resonate around 2.75 GHz with good impedance matching. The ACS fed antenna exhibits a bandwidth of 20 % while the CPW fed antenna exhibits a band width of 18 %.

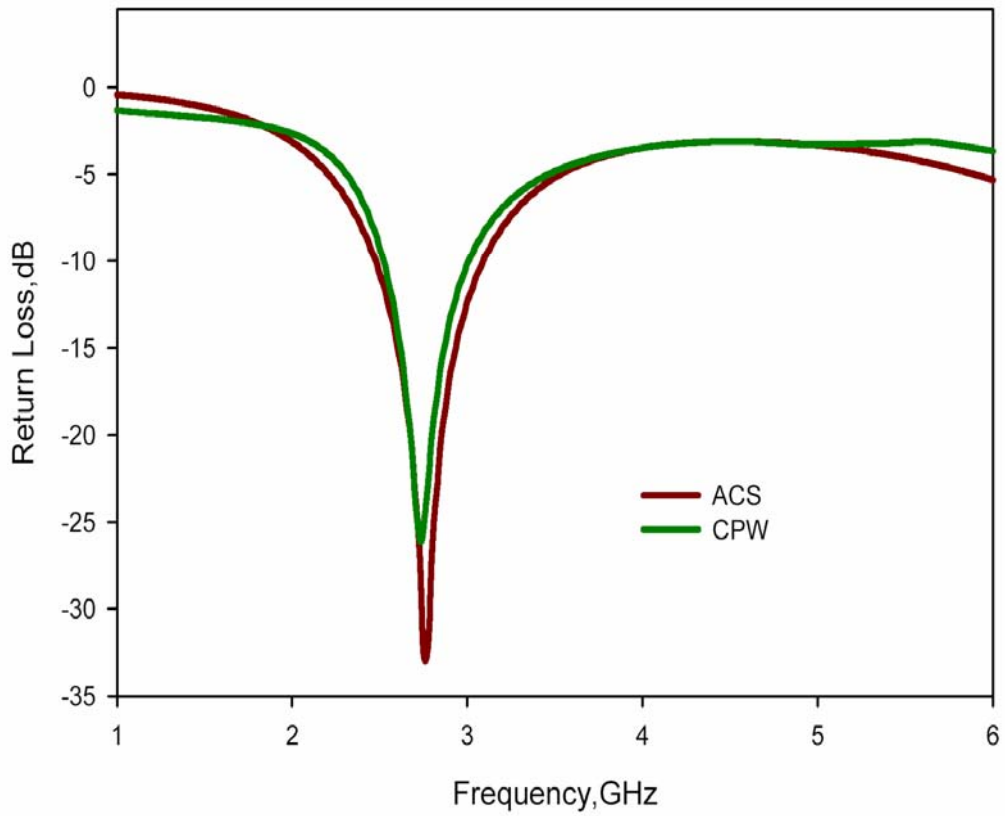

Fig. 3.6. Return Loss curves of the ACS and CPW fed monopole antennas.
Lm = 17 mm, Ls = 25 mm, Lg = 25 mm, Wg = 8 mm and w = 3 mm, εr = 4.4, h=1.6 mm, Ls_1= 25 mm, W=3 mm, Lm_1=17 mm, Lg_1 = 25 mm,Wg_1 = 8 mm,g = 0.5 mm,g_1 = 0.3 mm, ε_r =4.4, h= 1.6 mm

3.3.3 Radiation characteristics

The radiation characteristics of the two antennas are studied in this section. The three dimensional patterns are shown in fig.3.7. Both the antennas exhibit a near figure of eight pattern in the E plane and a non directional pattern in the H plane. The bore sight of CPW fed antenna is directed along X. But the bore sight of the ACS fed antenna is tilted by 45^0. This tilt is due to the asymmetry in the antenna geometry.

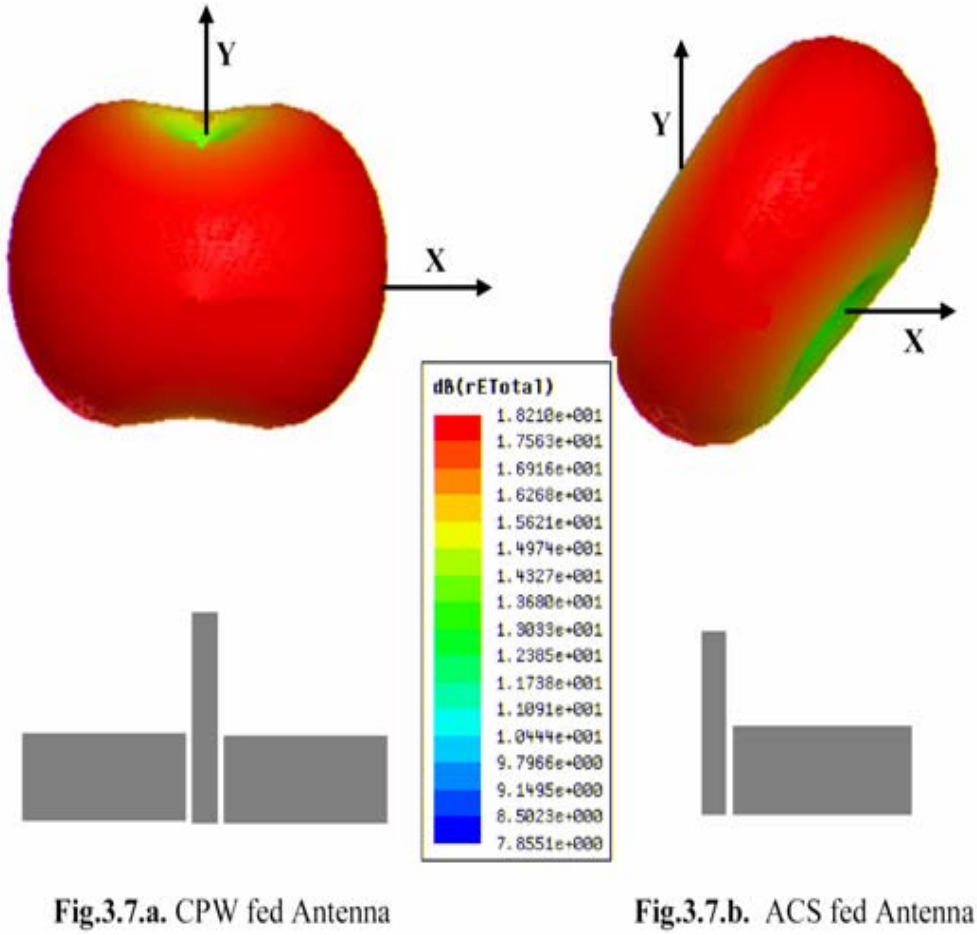

Fig.3.7.a. CPW fed Antenna **Fig.3.7.b.** ACS fed Antenna

Fig.3.7. 3-D Radiation pattern of the CPW and ACS fed antennas

The 2-D radiation patterns of both the antennas are depicted in Fig.3.8.

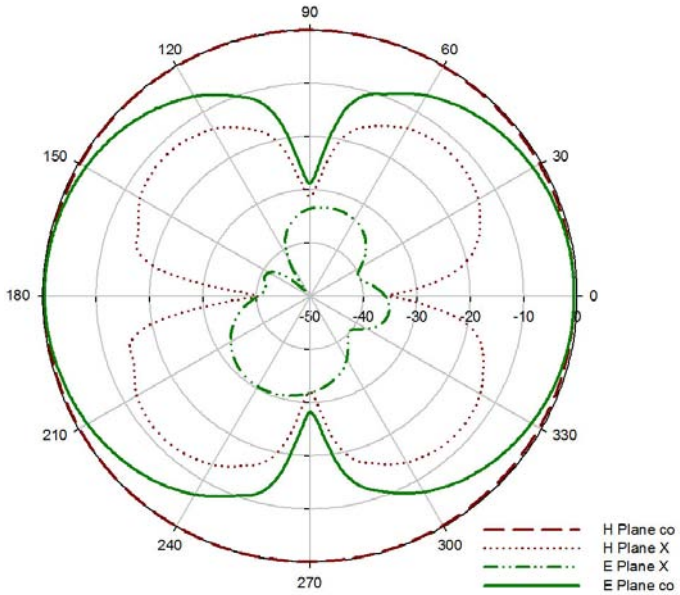

Fig.3.8.a. Principal Plane patterns of the CPW fed Antenna at 2.75 GHz

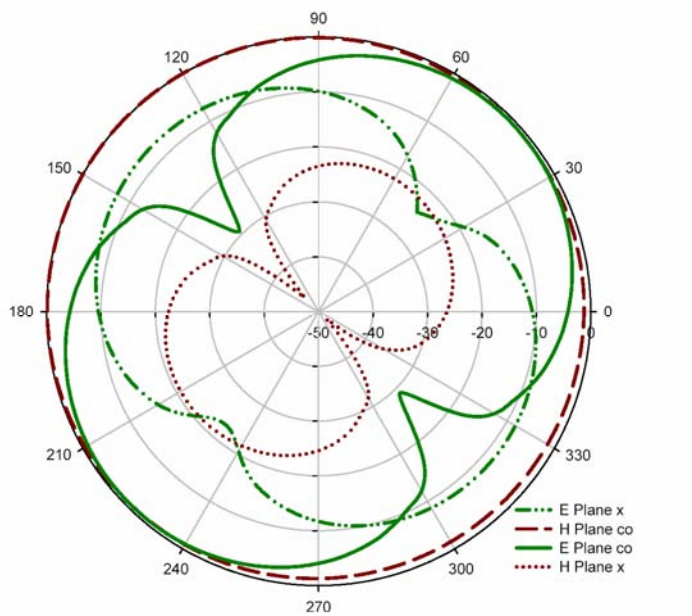

Fig.3.8.b. Principal Plane patterns of the ACS fed Antenna at 2.75 GHz

From fig.3.8 it can be seen that the coplanar wave guide fed antenna exhibits better cross polarization by 15 dB with respect to the ACS fed antenna.

The surface current distributions in the antennas are shown in Fig.3.9.a and 3.9.b. A quarter wave variation is noted in the signal strip in both the antennas. It can be seen that in the case of the CPW fed antenna the current intensity in the ground plane is nearly zero except near the feed. This is not the case with the ACS fed antenna where a nearly equal current intensity variation is found in the signal strip as well as in the ground plane. This means that the ground plane too has predominant effect in the resonance and radiation phenomenon. This is studied in more detail in the succeeding section.

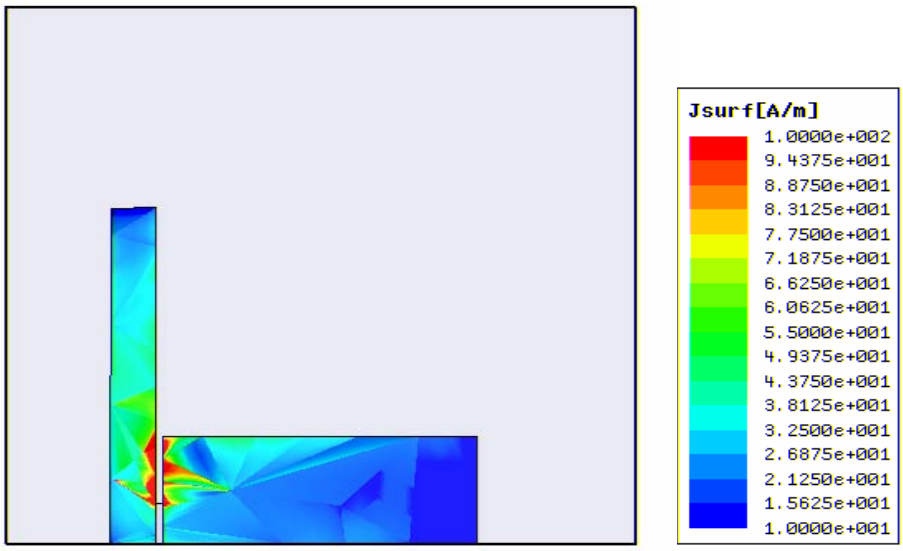

Fig.3.9.a. Current distributions in the ACS fed antenna at 2.75 GHz
Lm = 17 mm, Ls = 25 mm, Lg = 25 mm, Wg = 8 mm and w = 3 mm, εr = 4.4, h=1.6 mm

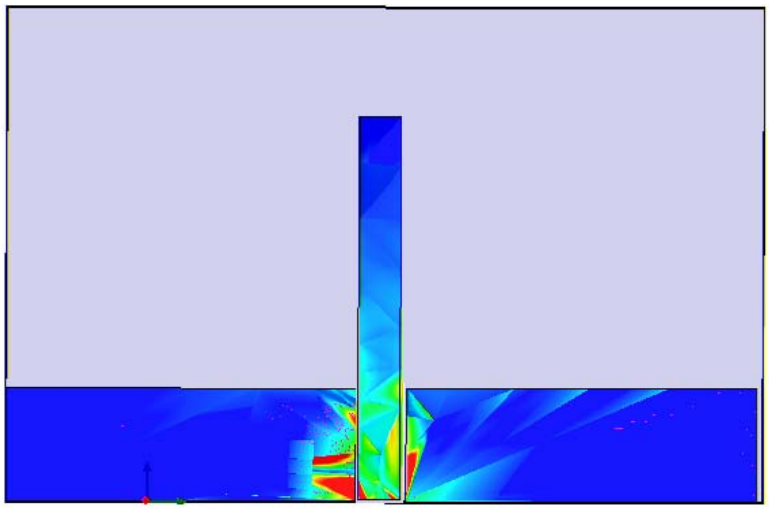

3.9.b. Current distributions in the CPW fed antenna at 2.73 GHz
Ls_1= 25 mm, W=3 mm,Lm_1=17 mm,Lg_1 = 25 mm,Wg_1 = 8 mm,
g = 0.5 mm,g_1 = 0.3 mm, ε_r =4.4 ,h= 1.6 mm

The measured gain and efficiency of the CPW fed antenna 1.89 dBi and 94 % respectively at 2.73 GHz. For the ACS fed antenna they are 1.92 dBi and 90 % respectively at 2.75 GHz.

The results of the above studies are summarized in Table 3.1. It can be seen that the ACS fed antenna retains nearly all the advantages of the CPW fed antenna but within lesser area. In the above study the CPW fed antenna occupies an area of 25 mm x 53.6 mm on a substrate of dielectric constant 4.4 and height 1.6 mm while the ACS fed antenna occupies a dimension of only 25 mm x 28.5 mm on the same substrate. Thus there is a reduction of nearly 46 % in the case of the ACS fed antenna which is highly advantageous in the case of compact wireless devices.

From the above studies it can be concluded that the ACS can be used as a good feed for exciting strip monopoles. To completely understand the resonance and radiation phenomena a thorough study has been performed by varying the different parameters of the antenna and is given in the next section.

Table 3.1. Comparison of the CPW and ACS fed antennas

Characteristics	CPW fed Antenna	ACS fed antenna
Resonant frequency	2.73 GHz	2.75 GHz
Bandwidth	18%	20%
Radiation Pattern	E plane - Figure of Eight H plane - Omnidirectional	E plane - Figure of Eight H plane – Omnidirectional Both Tilted by 45°
HPBW	80°	78°
Cross polarization along beam max	Down by -35 dB	Down by -20 dB
Gain	1.89 dBi	1.92 dBi
Efficiency	94%	90%
Area	25 mm x 53.6 mm, εr = 4.4, h=1.6 mm	25 mm x 28.5 mm, εr = 4.4, h=1.6 mm
Area Reduction	-	Nearly 46% compared to CPW fed antenna

3.4 The Asymmetric Coplanar Strip fed single band antenna

This section highlights the more detailed study of the asymmetric coplanar strip fed monopole (Fig.3.10.).

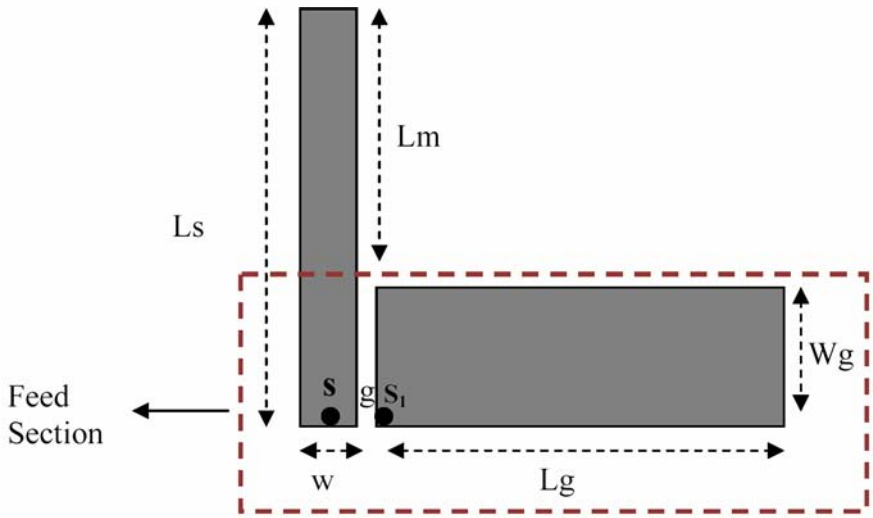

Fig.3.10. The Asymmetric Coplanar Strip fed Monopole Antenna

The length of the monopole, Lm is taken to be equal to a quarter of the dielectric wavelength corresponding to 2.75 GHz in the substrate. For the substrate of dielectric constant 4.4 and height 1.6 mm, the dimensions are chosen as Lm = 17 mm, Ls = 25 mm. The other dimensions are w = 5 mm, Lg = 21 mm, Wg= 8 mm and g = 0.3 mm. The experimental and simulated return loss characteristic of the above antenna is shown in fig.3.11.

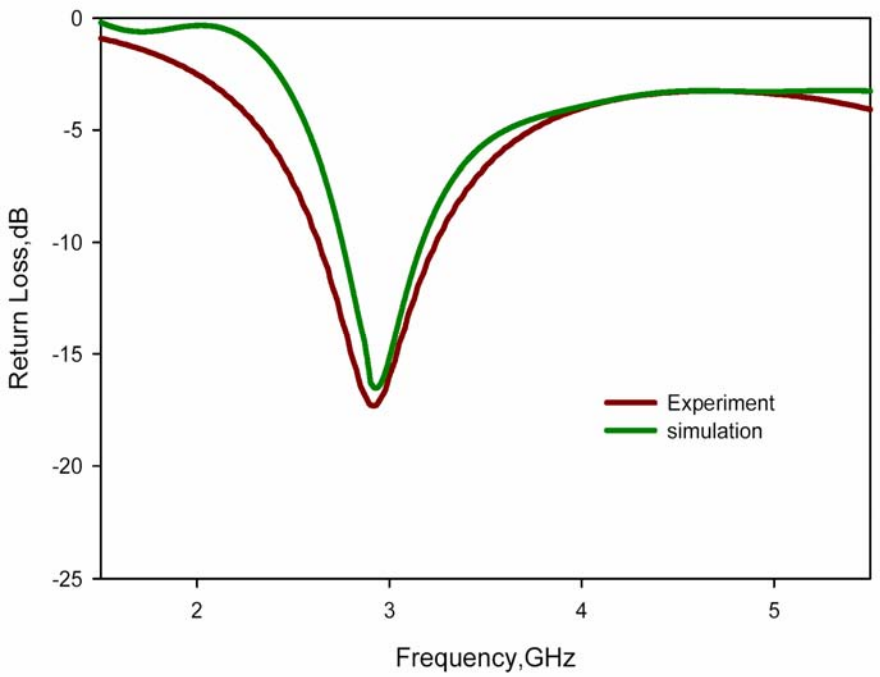

Fig.3.11. Return loss curve of the ACS fed monopole antenna
L_m = 17 mm, L_s = 25 mm, w = 5 mm, L_g = 21 mm, W_g= 8 mm,
g = 0.3 mm, ε_r =4.4 ,h= 1.6 mm

From the return loss curves it can be seen that the antenna resonates at 3 GHz with good impedance matching. But the expected resonance was at 2.75 GHz (due to the quarter wave variation in the length of the signal strip L_m). To find out the possible cause of the shift in the resonance, a detailed parametric study is conducted by varying the different parameters of the antenna. This is outlined in the following sections.

3.4.1 Effect of Signal strip width ('w') on return loss of the antenna

The influence of the width of the signal strip on the resonant frequency of the antenna is shown in Fig.3.12.It can be seen that the matching deteriorates when the strip width is increased or decreased beyond an optimum value as shown in figure. It is because, as mentioned earlier, the width of the signal strip too affects the impedance of the Asymmetric coplanar strip. Also the band width is slightly effected for larger values of 'w'. Good matching is noted when the strip width is kept as 7 mm. But in this study the lesser matched dimension (w = 3 mm) is taken as a compromise between the matching and compactness. In all the cases resonant frequency is independent of 'w'. But there is an increase in bandwidth with increase in width of the signal strip as evident from the figure.

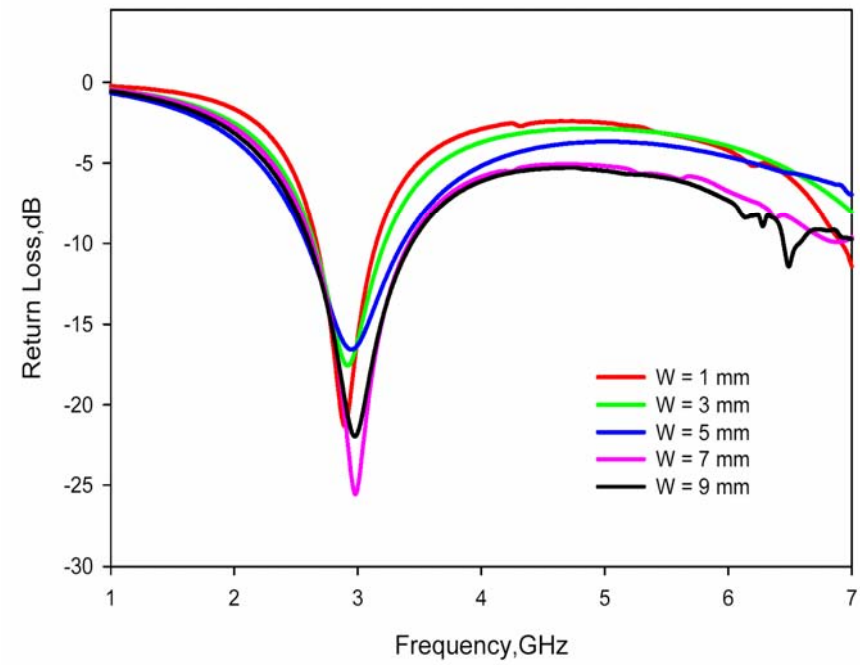

Fig. 3.12. Effect of varying the signal strip width, 'w'
L_m = 17 mm, L_s = 25mm, L_g = 21 mm, W_g= 8 mm and g = 0.3, ε_r =4.4 ,h= 1.6 mm

3.4.2 Gap width (g) variation studies

The gap width 'g' is varied and its effect in the return loss characteristic of the antenna is given in Fig.3.13. The characteristic impedance depends on the gap width and remains nearly constant for higher gap widths. The optimum value is taken as 0.5 mm on a substrate of dielectric constant 4.4 and height 1.6 mm when the signal strip width is 3 mm.

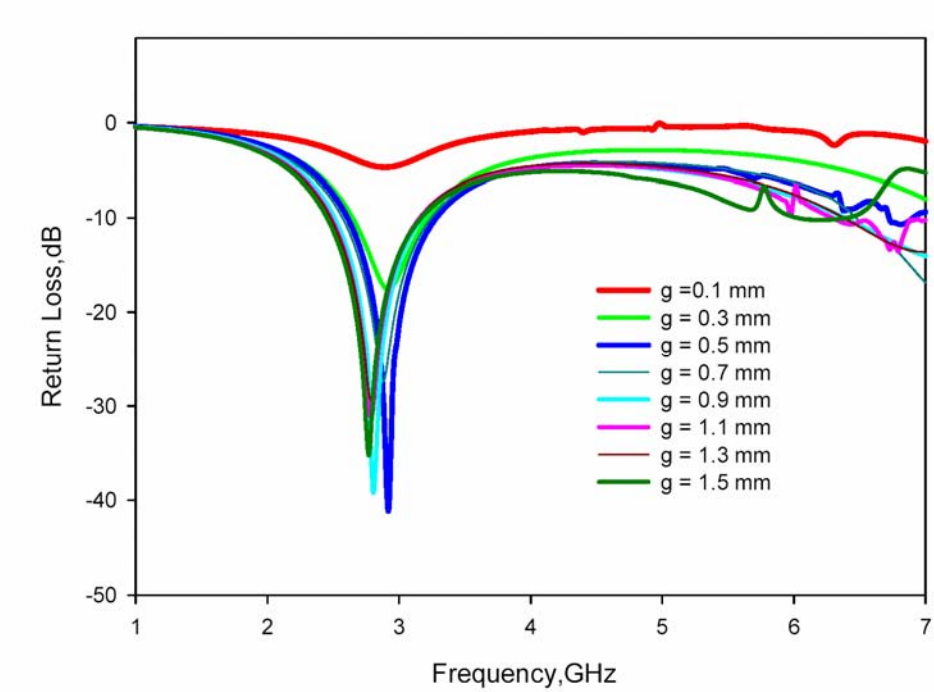

Fig.3.13. Gap width 'g' variation studies
L_m = 17 mm, L_s = 25 mm, w = 3 mm, L_g = 21 mm, W_g= 8 mm, ε_r =4.4 ,h= 1.6 mm

3.4.3 Signal strip Length ('Ls') variation studies

The resonant frequency of the antenna highly depends on the length of the strip as evident from the graph (Fig.3.14). The resonant frequency decreases with increase in length of L_s as expected. It has to be noted that for small values of L_s ($L_s \leq W_g$) the system is not acting as an antenna. It moreover acts like a

transmission line terminated by an open circuit. As L_s is increased beyond W_g, the resonant frequency decreases with increase in L_s. Thus this study proves that the length of the signal strip is primarily deciding the resonant frequency.

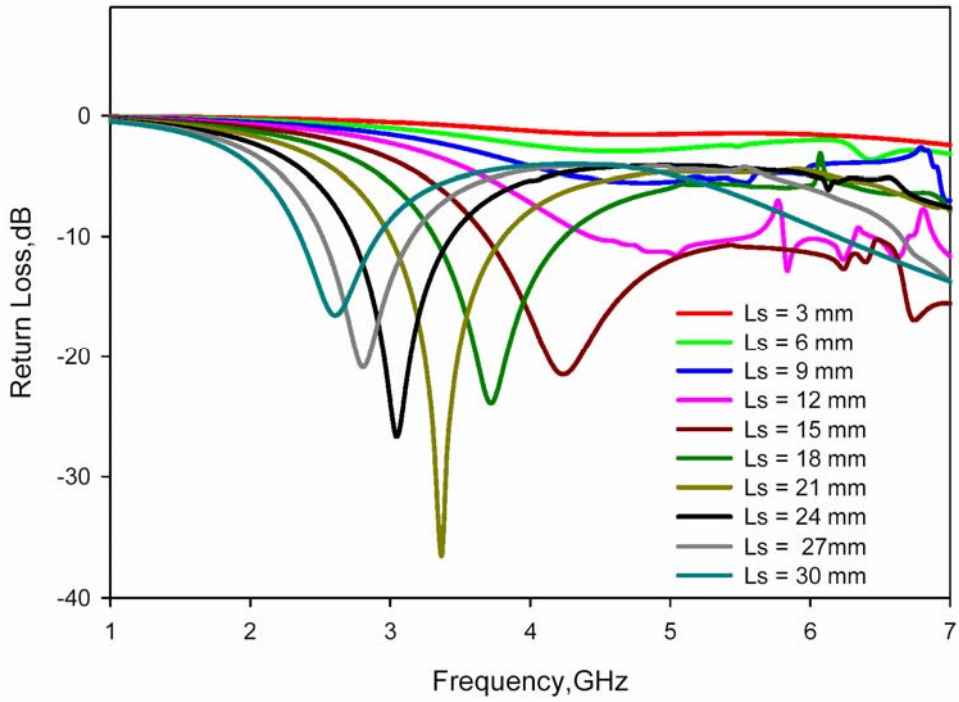

Fig.3.14. Effect of varying the length of the signal strip, Ls
w = 3 mm, L_g = 21 mm, W_g= 8 mm and g = 0.5 mm,
ε_r =4.4 ,h= 1.6 mm

3.4.4 Ground plane width (Wg) variation studies

As mentioned earlier the ground plane dimension is an important factor while the design of compact antenna is concerned. The Asymmetric Coplanar Strip uses only a single lateral ground strip compared to the twin lateral ground strips in the Coplanar Wave Guide feed. Hence the dimension of this single ground plane is expected to have far more effect on the performance of the antenna. The variation of return loss with the ground plane width is shown in Fig.3.15. The band width of

the antenna varies with the ground plane width, W_g but the resonant frequency remains more or less the same even after large variations.

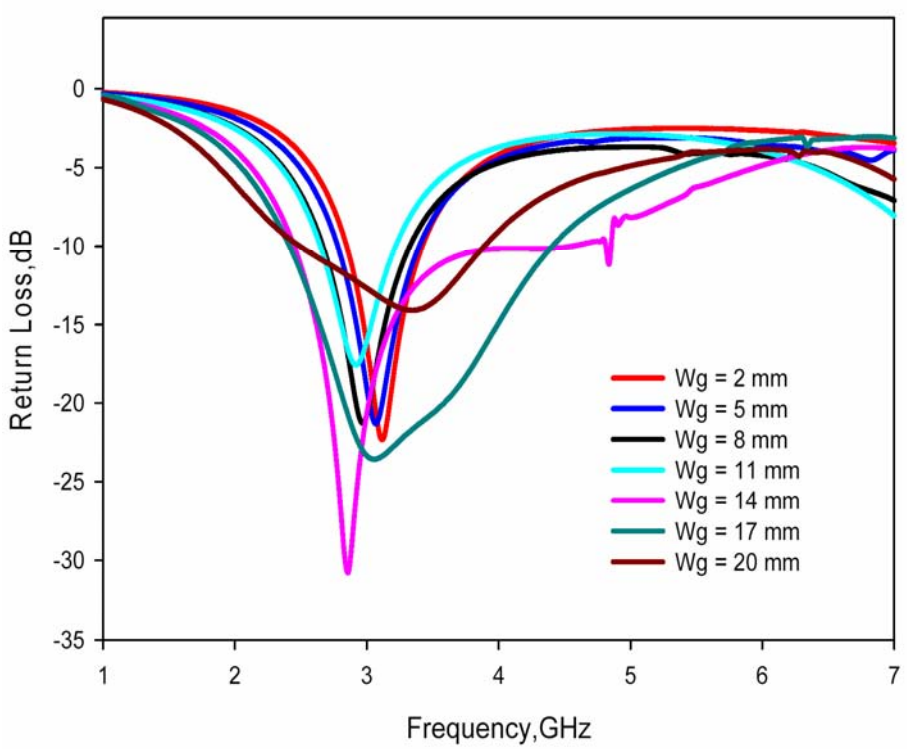

Fig.3.15. Ground width , Wg variation studies
Lm = 17 mm, Ls = 25 mm, w = 3 mm, Lg = 21 mm, and g = 0.5 mm, ε_r =4.4 ,h= 1.6 mm

Since bandwidth enhancement is not the intension of our study, the optimum dimension is taken as Wg ≈ 0.3 L_g keeping in mind the compactness and impedance matching of the antenna.

3.4.5 Ground plane Length (Lg) variation studies

The length of the ground plane is also found to be an important parameter affecting the resonant frequency and compactness of the antenna. It can be noted from Fig.3.16 that the ground plane length significantly affects the resonant frequencies and matching conditions of the antenna. As mentioned

earlier when Lg is very much larger than 'w', the width of the signal strip, its effect on the characteristic impedance is less. Also the resonant frequency decreases with increase in the length of the ground plane and vice versa.

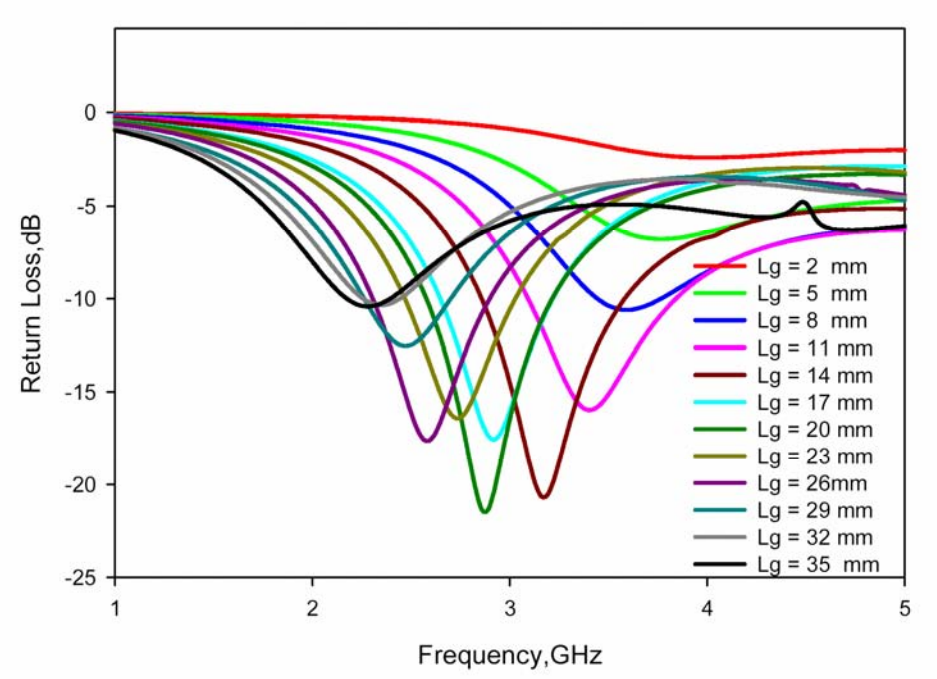

Fig.3.16. Ground plane length Lg variation studies
Lm = 17 mm, Ls = 25 mm, w = 3 mm, Wg= 7 mm and g = 0.5, ε_r =4.4, h= 1.6 mm

This study also explains the cause for the shift in the resonant frequency of the antenna in section 3.4 (fig.3.10) even when the length of the strip above the ground plane, L_m was taken equal to a quarter of the dielectric wavelength corresponding to the resonant frequency at 2.75 GHz. In this case the ground plane length, Lg is taken as 21 mm and not 25 mm as in the previous case (fig.3.5).This causes the shift in the resonant frequency from 2.75 GHz to 3 GHz.

From the above studies It can be assumed that the total length of the antenna (monopole length L_m plus ground plane length L_g) may be determining the resonant frequency of the antenna. Thus the resonant frequency of the antenna is not simply due to the vertical strip L_m alone, but due to the combined effect of the ground plane and the signal strip.

To ascertain the above assumptions the current distribution in the antenna is pictured in fig.3.17.

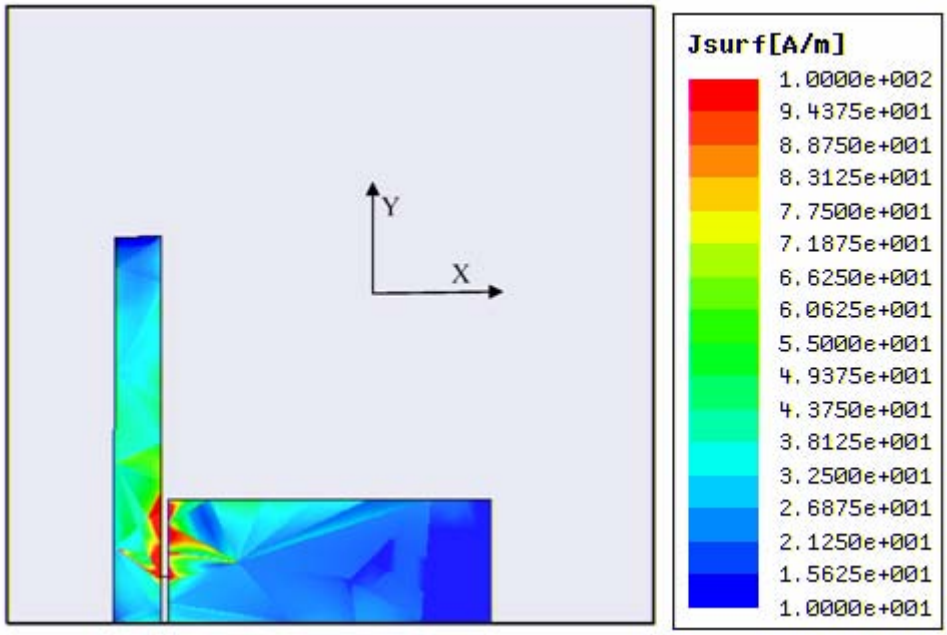

Fig.3.17. Current distribution in the antenna at the resonant frequency Lm = 17 mm, Ls = 25 mm, Lg = 21 mm, w = 3 mm, Wg= 7 mm and g = 0.5, ε_r =4.4 ,h= 1.6 mm

It can be seen from the current distribution in the antenna that there is a quarter wave variation in the signal strip. In addition to this, there is a similar variation along the length of the ground plane also. But it is worth noting that the current variation in the ground plane is only along the edge, which therefore

doesn't perturb the asymmetric coplanar strip line characteristics. The antenna acts moreover like a dipole. This is a modification to the earlier assumption that the antenna acts like a quarter wavelength monopole.

From exhaustive studies it is found that the resonant frequency corresponds to nearly half of the dielectric wavelength corresponding to the total length of Lm + Lg of the antenna as shown in Fig.3.18.

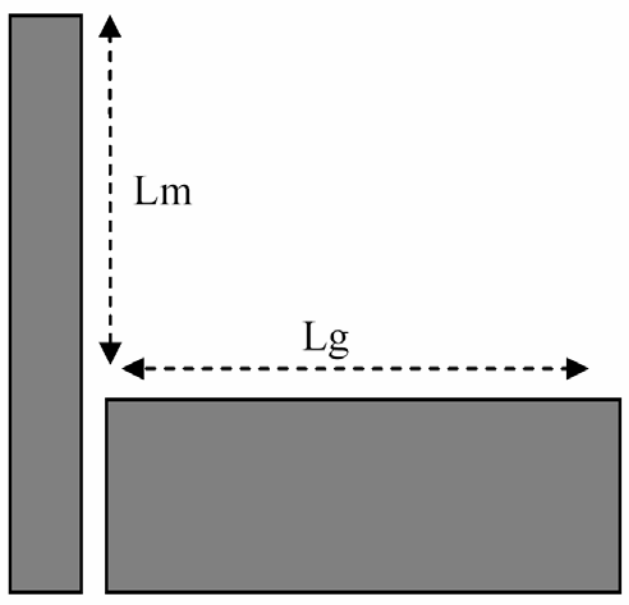

Fig.3.18. Current path in the antenna

The observations may be mathematically given as

$$F = 0.55 \times \frac{30}{L \times \sqrt{\varepsilon eff}} \quad \text{.....(3.8)}$$

where $L = L_m + L_g$ and $\varepsilon_{eff} = (\varepsilon_r + 1 + 1)/3$ is the relative dielectric constant. where ε_r and 1 are the relative dielectric constant of the substrate and air and F is the resonant frequency. The antenna is fabricated on a substrate of dielectric constant 4.4 and height 1.6 mm.

It is also found that different combinations of the signal strip length and the ground plane length can give the same resonant frequency. To find out the optimum relation between L_m and L_g, a set of variation studies have been performed keeping the total length constant and is given in Fig.3.18.

3.4.6 Effect of various combinations of L_m and L_g on antenna performance

In this study the total current path (L_1 + L_g) is kept constant and the matching conditions are studied for various values of L_g and L_m. It is noted that the best matching is obtained when the ground plane length Lg is made equal to Lm + Wg/2 .i.e, when the mean length of both the arms are equal. When the ground plane length is far different from the vertical strip length the matching gets distorted. The optimized width of the ground plane is nearly taken as one third of its length.

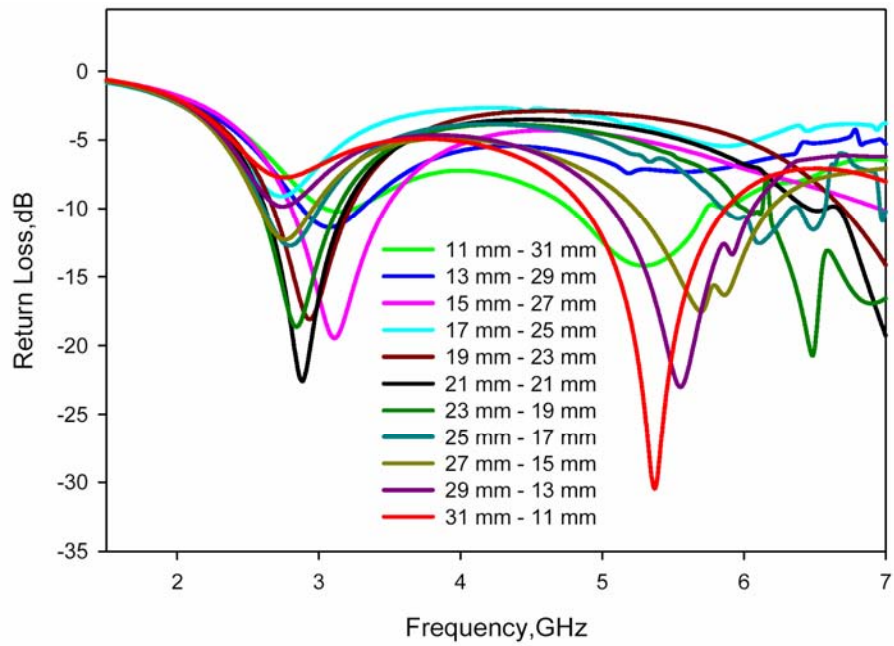

Fig.3.19. Ground plane variation studies keeping Lm + Wg/2 + Lg a constant ((Lm + Wg/2) – Lg variations are shown)
w = 3 mm, Wg= 8 mm and g = 0.5 mm, ε_r =4.4 ,h= 1.6 mm

The following conclusions can be derived from the above studies.

The resonance is due to the combined length of the signal strip (L_m) and the ground plane (Lg).

Good performance is noted when the length of the ground plane (Lg) is kept nearly equal to the strip length ($L_m + W_g/2$)

The above design offers more freedom for an antenna designer. For instance, once can design an antenna with a smaller radiating strip by increasing Lg . Also the resonance of the antenna is independent of Wg. So an optimum feed length can be selected based on the communication system space allocation.

3.4.7 Effect of the substrate height on antenna performance

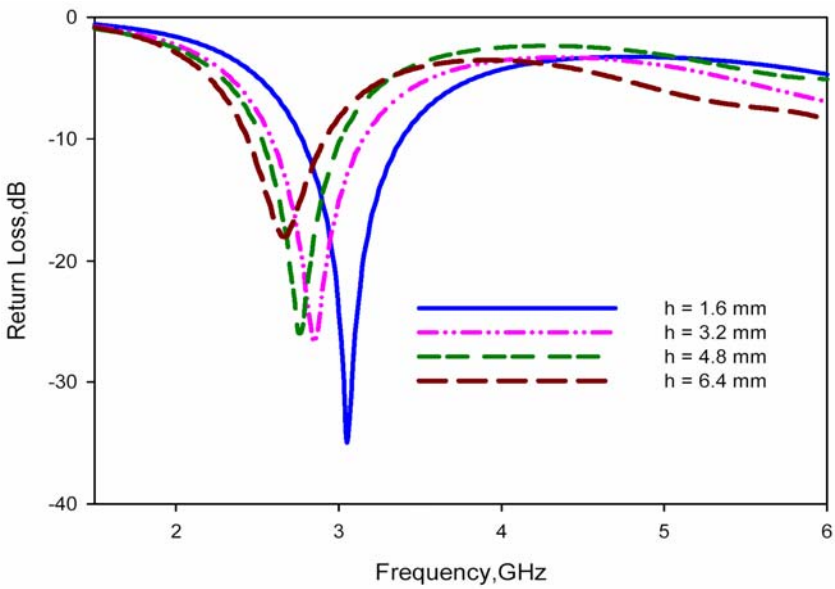

Fig.3.20. Effect of varying the height 'h' of the substrate
Lm = 17 mm, Ls = 25 mm, w = 3 mm, Wg= 8 mm, Lg = 25 mm and g = 0.5 mm, ε_r =4.4

The effect of the height of the substrate on the performance of the antenna is depicted in Fig.3.20. The frequency decreases with increase in substrate

thickness. The resonance at 3 GHz (for h =1.6 mm shifts to 2.7 GHz when the height is increased to 6.4 mm. Thus there is nearly 10 % frequency variation when the thickness is increased eight times.

3.4.8 Effect of varying the dielectric constant of the substrate

The return loss characteristic of antenna for different substrates is shown in Fig.3.21. When ε_r=2.2 the antenna is resonating at 3.3 GHz. The resonant frequency is found to be decrease with increase of dielectric constant as expected.

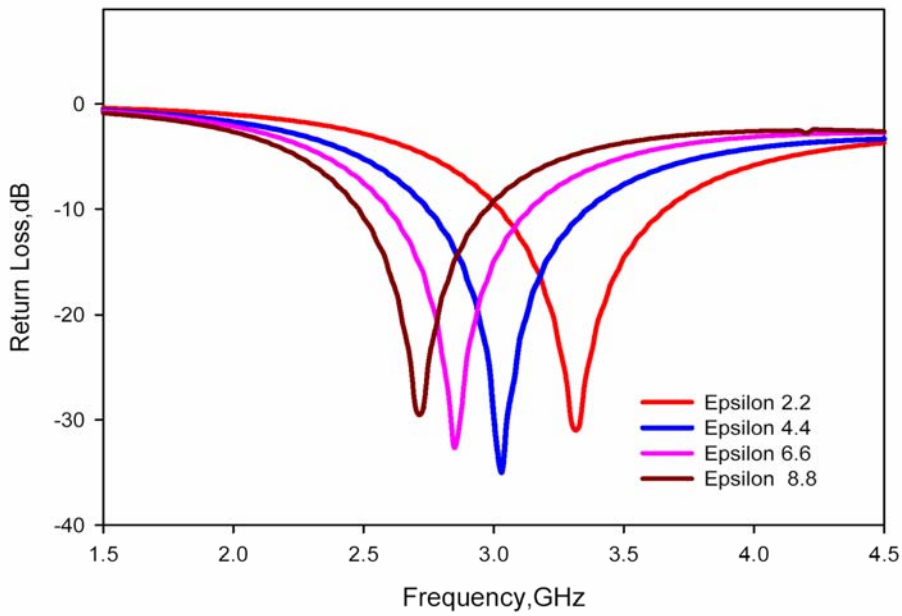

Fig.3.21. Variation of the resonant frequency with the dielectric constant of the substrate
Lm = 17 mm, Ls = 25 mm, Lg = 25 mm w = 3 mm, Wg= 8 mm, Lg = 25 mm and g = 0.5 mm, h= 1.6 mm

3.4.9 Radiation performance of the antenna

The radiation pattern of the antenna at the resonant frequency is depicted in Fig.3.8.b. As mentioned earlier the pattern is similar to that of a dipole, but with a 45° tilt. The tilt in the pattern is due to the asymmetry in the feed

structure. The current distribution (Fig.3.17.) shows that the nearly equal X and Y directed currents are responsible for the 45° tilt in the radiation pattern. This also increases the cross polar level compared to conventional monopoles.

3.4.10 Unbalanced to balanced transformation in the Antenna –Use of Balun

From the current distribution in the antenna shown in fig.3.17, it can be seen that there is equal intensity current in the signal strip as well as the ground strip and the antenna is behaving nearly as a dipole. In all the above studies the antenna is directly fed using the coaxial connector. Since the Asymmetric Coplanar Strip feed is a balanced feed and the coaxial connector an unbalanced, the problem of unbalanced to balanced transformation arises. Hence a balun has to be used to compensate for this unbalance.

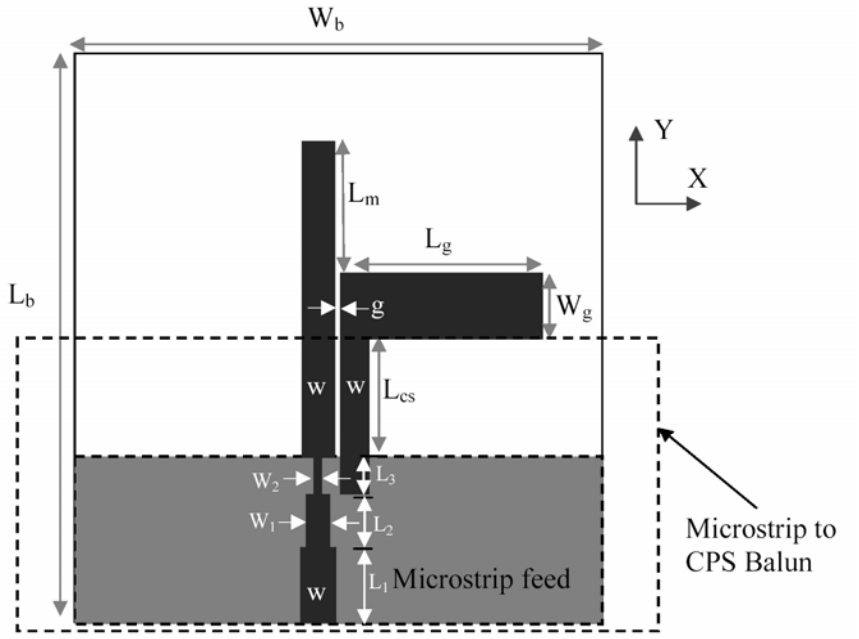

Fig.3.22. Geometry of the ACS fed Monopole with a Microstrip – CPS Balun
L_b= 75 mm, W_b=47mm, L_{cs} = 25 mm,w = 3 mm, Lg = 21 mm,
W_g = 7 mm, L_m = 17 mm,L_1=5mm, L_2=5mm, L_3=5mm,
w_1=2mm, w_2=0.5mm, g = 0.3 mm, ε_r =4.4 ,h= 1.6 mm

But in all the previous studies even though a balun is not used, the antenna doesn't show any degradation in performance. In order to substantiate this, the characteristics of the antenna are studied with and without a balun in this section.

Fig.3.22 shows the geometry of a ACS fed monopole with the balun mentioned in [4]. The Asymmetric coplanar strip fed monopole described in the previous section [section 3.4] is studied with and without a balun. The back to back S parameter characteristic of the microstrip to coplanar strip balun is given in fig.3.23. It has to be noted that the back to back insertion loss twin balun system is -1.4 dBi at 3 GHz. Thus a single balun system has an insertion loss of -0.7 dBi.

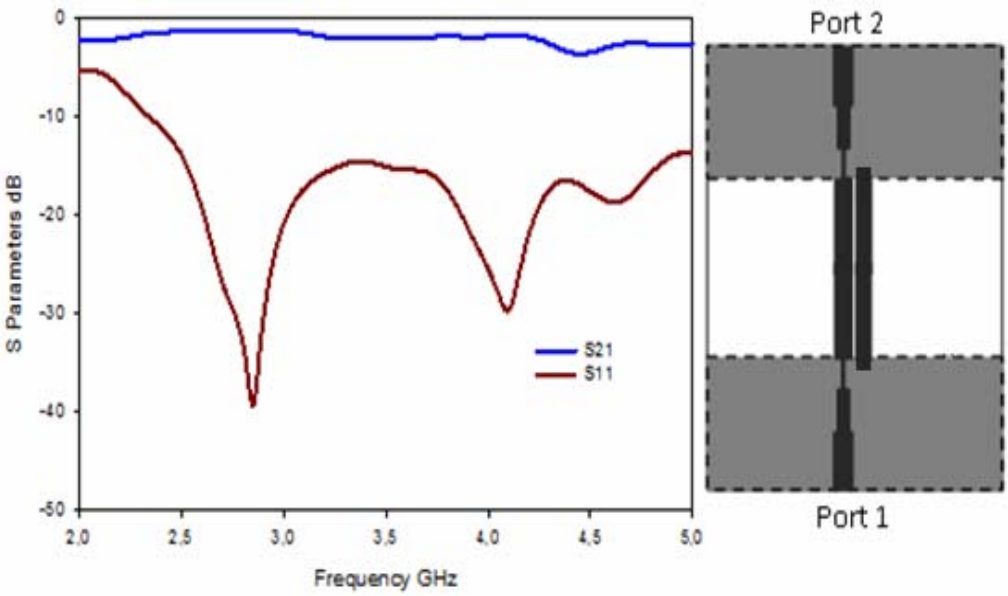

Fig.3.23. Back to back S parameters of the microstrip to CPS transition

L_b= 75 mm, W_b=47mm, L_{cs} = 25 mm,w = 3 mm, Lg = 21 mm, W_g = 7 mm, L_m = 17 mm,L_1=5mm, L_2=5mm, L_3=5mm, w_1=2mm, w_2=0.5mm, g = 0.3 mm, ε_r =4.4, h= 1.6 mm

The return loss curve of the antenna with and without the balun is shown in fig.3.24. Both the antennas resonate at around 3 GHz. The use of balun excites higher order modes as shown in figure. Also a spurious resonance at 3.8 GHz is excited owing to the balun configuration. From the return loss curve it can be inferred that the antenna without the balun too exhibits nearly same impedance matching as that of the antenna using the balun.

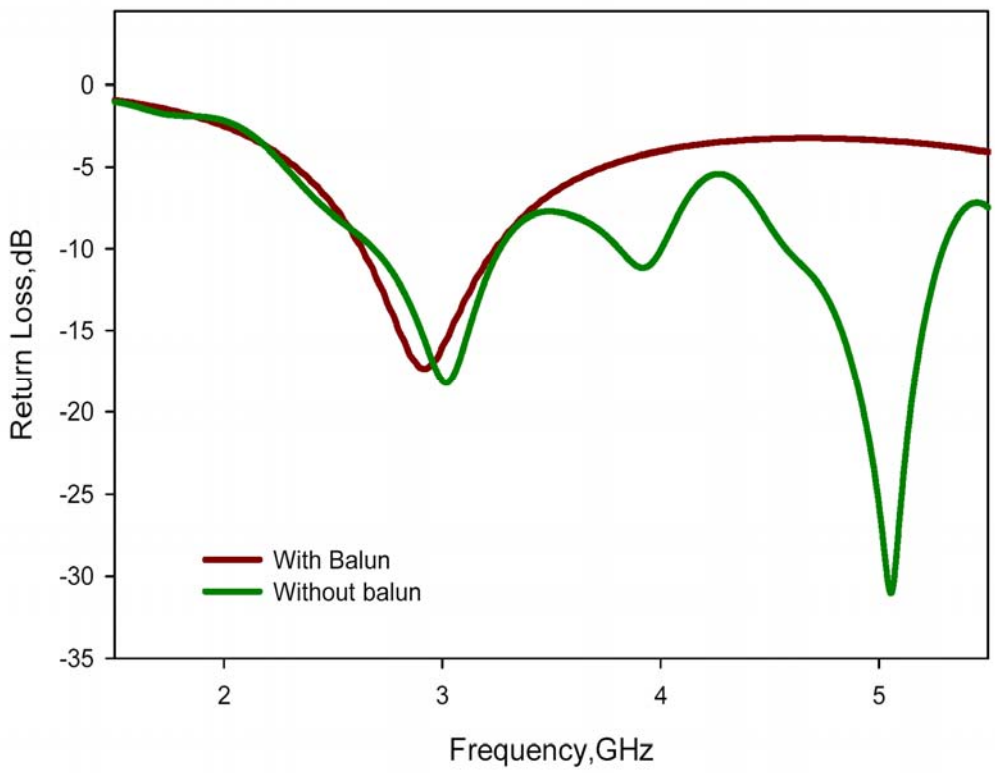

Fig.3.24. Return loss Curves of the antennas with and without the balun

L_b= 75 mm, W_b=47mm, L_{cs} = 25 mm,w = 3 mm, Lg = 21 mm, W_g = 7 mm, L_m = 17 mm,L_1=5mm, L_2=5mm, L_3=5mm, w_1=2mm, w_2=0.5mm, g = 0.3 mm, ε_r =4.4 ,h= 1.6 mm

To explore the effect of the balun on the radiation characteristics of the antenna the 3- D radiation pattern of the antenna is studied and shown in fig.3.25.

The radiation pattern remains nearly the same in both cases as evident from the figure. Here also the tilt in the pattern is noted. This tilt is due to the asymmetry in the feed region of the antenna due to the use of the ACS feed.

The antenna with the balun has a gain of 2.87 dBi while that without balun gives a gain of 1.92 dBi.

The antenna with the balun has an efficiency of 94% while that without the balun shows an efficiency of 90%.

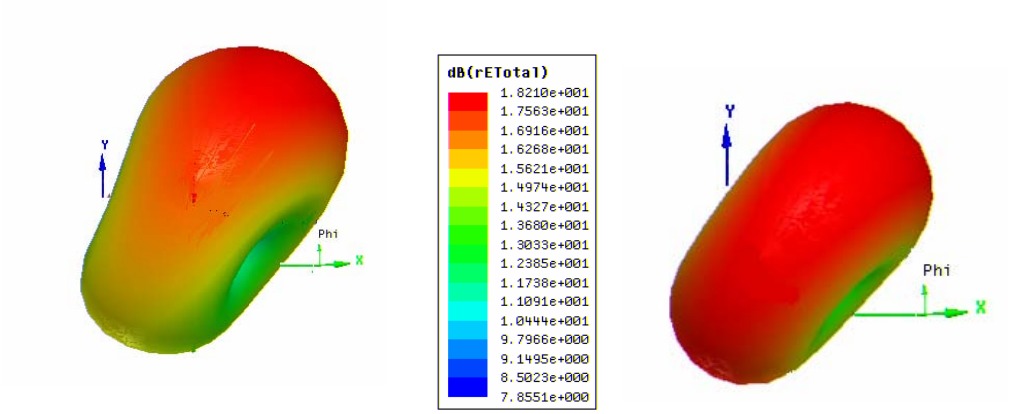

(a) Antenna with balun (b) Antenna without balun

Fig.3.25. 3- D Radiation pattern of the antennas

The antenna with the balun shows an increased gain of 0.95 dBi with a 4 % increase in efficiency. But it has to be noted that the overall size of the antenna on a substrate of dielectric constant 4.4 and height 1.6 mm is 75 mm x 47 mm while that of the antenna without the balun on the same substrate is only 25mm x 24.5 mm. Thus the integration of a balun increases the size of the antenna more than five times.

Table 3.2 Comparison between the antennas with and without balun

Characteristics	ACS fed Antenna (With Balun)	ACS fed antenna (Without Balun)
Resonance and Return loss	At 3.03 (-18.1 dB)	At 2.94 GHz (-17.3 dB)
Radiation Pattern	E plane - Figure of Eight H plane –Non directional (Both Tilted by 45°)	E plane - Figure of Eight H plane –Non directional (Both Tilted by 45°)
Gain	2.87 dBi	1.92 dBi
Area	75 mm x 47 mm ε_r =4.4, h= 1.6 mm	25 mm x 24.5 mm ε_r =4.4, h= 1.6 mm
Area reduction	-	Nearly 80 % compared to the antenna with balun
Efficiency	94%	90%

Table 3.2 summarizes the difference between the antennas with and without the balun. It can be seen that there is no appreciable enhancement in the impedance matching of the antenna by using the balun. But the gain and efficiency increases by 0.95 dBi and 4 % respectively These enhancements are achieved at the cost of increased area. Thus it is the discretion of the designer to choose the suitable configuration. The ACS fed antenna without the balun is highly useful in applications where compactness is a great concern, but at the cost of lesser gain. Since compact antenna design is our primary aim the balun less configuration is taken for the study.

3.4.11 Conclusion

Finally it can be concluded that the Asymmetric Coplanar Strip Fed antenna exhibits all the advantages of conventional monopoles with nearly 46 % area reduction except a tilt in the radiation pattern. Owing to the

uniplanar nature many integrated devices can be embedded into these antennas. All the reflection and radiation characteristics of the Asymmetric Coplanar Strip fed antenna are similar to antennas using conventional feeding mechanisms.

3.5 Asymmetric Coplanar Strip fed dual band antenna

The efficacy of the Asymmetric Coplanar Strip as the feed for a single band antenna has been proved in the previous section. To confirm the ability of this feed in multi band antennas, the design of Asymmetric Coplanar Strip fed dual and multiband antennas are also presented and discussed in the following sections.

This section deals with the design of asymmetric coplanar strip fed dual band antenna. Creation of two different current paths is employed here for the design of the dual band antenna

3.5.1 Design of the single band inverted L antenna

As mentioned in the previous section an ACS fed monopole resonates when the total length of the structure is nearly equal to half of the dielectric wavelength. For a given area, say L x W, maximum compactness is obtained when the signal strip is bent in the form of an inverted L [5]. So an inverted L monopole (Fig.3.26) is chosen as the starting design in the place of a simple strip monopole.

It is aimed to design a dual band antenna working at 2.4/5.2 GHz. Therefore the total length of the inverted L structure plus the ground plane (L_g + L_2 + L_1) is taken equal to 0.55 times the dielectric wavelength corresponding to 2.4 GHz (Equation 3.8).

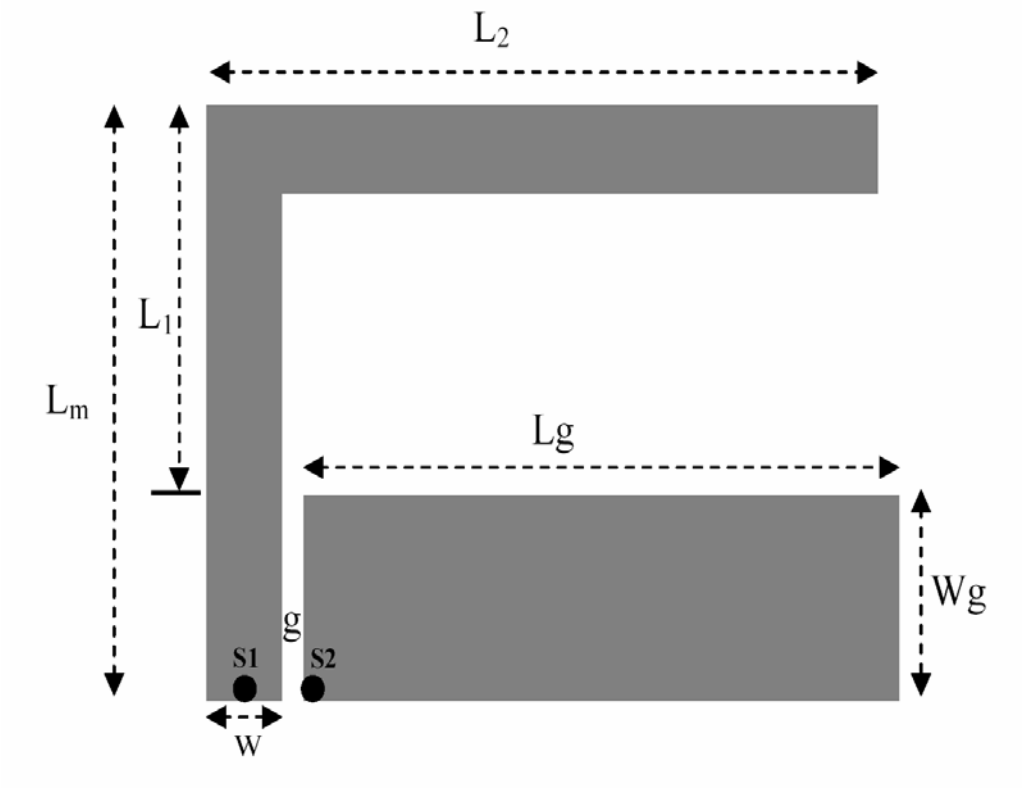

Fig.3.26. ACS fed Inverted L antenna
L_g = 15.5 mm, w = 3 mm, L_m = 21 mm, L_1= 16 mm, L_2=19 mm,
W_g = 5 mm, g = 0.5 mm, ε_r =4.4, h= 1.6 mm

After a set of experimental and simulation studies it is found that for an ACS fed inverted L antenna better performance is achieved when the length of the horizontal arm (L_2) is nearly equal to the ground plane length (L_g) plus the signal strip width (w). i.e.

$$L_2 = L_g + w \quad (3.9)$$

This eventually helps to calculate the length of the vertical strip L_1. To validate the above assumptions a thorough study has been performed by varying the height (L_1) to the strip length (L_2) of the antenna.

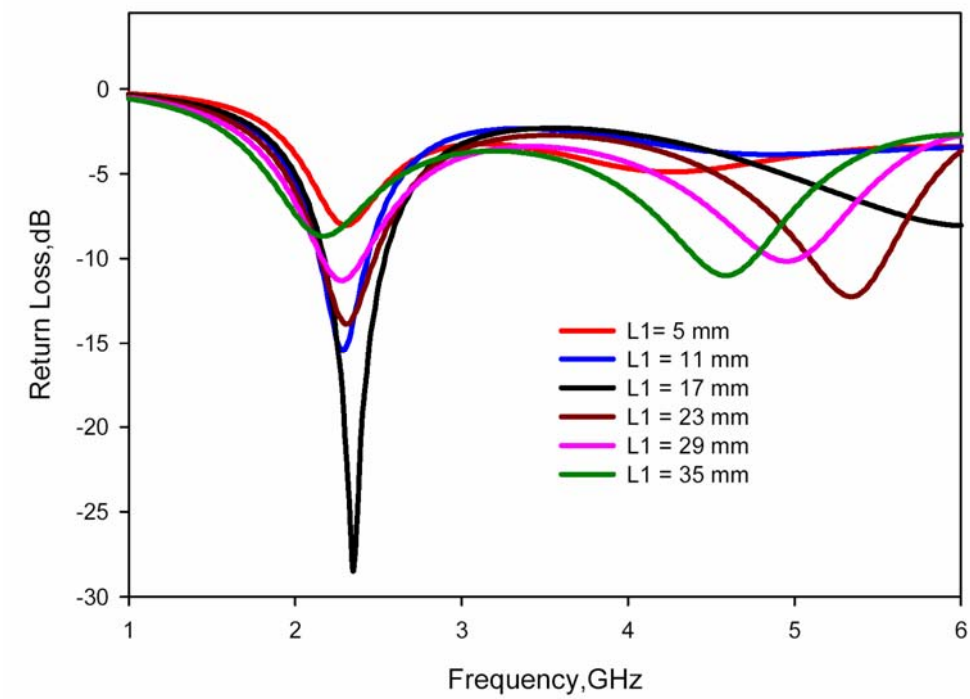

Fig.3.27. Return loss variation in the antenna with different lengths of the vertical strip L_1
Lg = 15.5 mm, w = 3 mm, Wg = 5 mm, g = 0.5 mm, ε_r =4.4 , h= 1.6 mm

From fig.3.27 it can be concluded that best matching is obtained when the height to horizontal strip length ratio (L_1/L_2) is maintained nearly as 0.8.The matching deteriorates when the horizontal strip becomes too closer to the ground plane ($L_1 < 0.1\lambda_d$). The above observations are found to be similar in the case of other inverted L structures like planar inverted L antennas [5].

It has to be noted that the impedance matching of the antenna is affected by the coupling between the strips L_g and L_2. Typical variation of the impedance curve with variation in L_1 is shown in fig.3.28.

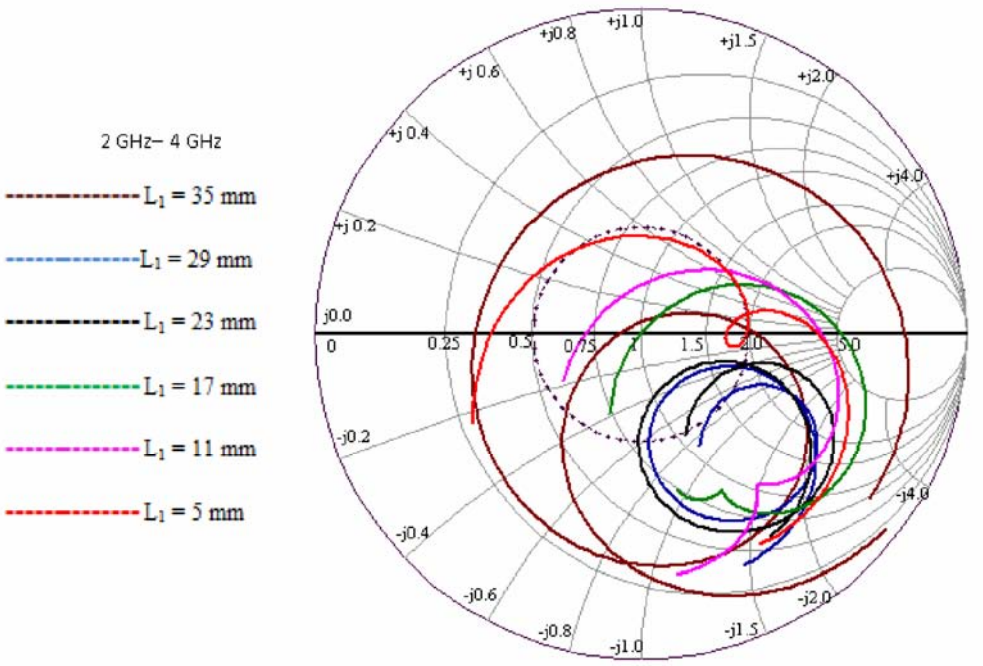

Fig.3.28. Variation in the impedance of the antenna at different heights (L_1). Lg = 15.5 mm, w = 3 mm, Wg = 5 mm, g = 0.5 mm, ε_r =4.4 , h= 1.6 mm

The input impedance of the antenna varies with the shape and position of the signal strip, L_1. It can be seen that while the strip monopole is placed vertically (L_1= 35 mm, Fig.3.29 (a)), the reactance of the antenna is capacitive. As the strip is bent in the form of an inverted L (Fig.3.29(c)), the reactance become more inductive. Better matching is observed when L_1/L_2 is maintained nearly as 0.8 (Fig.3.29 b).

(a) (b) (c)

Fig.3.29. various possible combinations of the ACS fed Antennas
Lg = 15.5 mm, w = 3 mm, Wg = 5 mm, g = 0.5 mm, ε_r =4.4, h= 1.6 mm (a)L_m = 35 mm,L_2=0 mm (b) L_m = 17 mm,L_2=18 mm (c) L_m = 5mm,L_2=20 mm

Note that in all the above studies, the ground plane length is chosen purely based on the circuit requirements. Even though the length of the ground plane plays an important role in determining the input impedance of the Asymmetric Coplanar strip transmission line, the effect is found to be less for larger ground plane lengths (L_g), compared to the signal strip width (w) as mentioned in the previous section. The characteristic impedance mainly depends on the width of the shorter strip (w in this case) and the gap g. This gives flexibility to the designer to choose ground plane dimensions based on the circuit constraints.

From the experimental and simulation studies the following design conditions are derived for an ACS fed inverted L antenna

$$L_g + L_1 + L_2 = 0.55\,\lambda_{d1}, \quad (3.10)$$

The term $L_2 + L_1 + L_g$ denotes the total length of the signal strip and the ground plane and λ_{d1} is the dielectric wavelength corresponding to the first resonance

$$\lambda_{d1} = \lambda / ((\varepsilon_r+1+1)/3)^{0.5} \quad (3.11)$$

The expression in 3.11 is the average dielectric constant. ε_r stands for the dielectric constant of the medium. The term 1 in the equation denotes the dielectric constant of air above and below the substrate.

The ground plane width W_g is taken nearly 0.3 times L_g as in the previous section.

3.5.2 Reflection characteristics of the single band inverted L antenna

Using the above relations the dimensions of the ACS fed inverted L antenna for 2.4 GHz is obtained as L_2 = 19 mm, L_m = 21 mm, L_g = 15.5 mm and W_g= 5 mm, w=3 mm,g=0.5 mm and L_s=21 mm on a substrate of dielectric constant 4.4 and height 1.6 mm. The return loss curve of the antenna so obtained is as shown in fig.3.30.

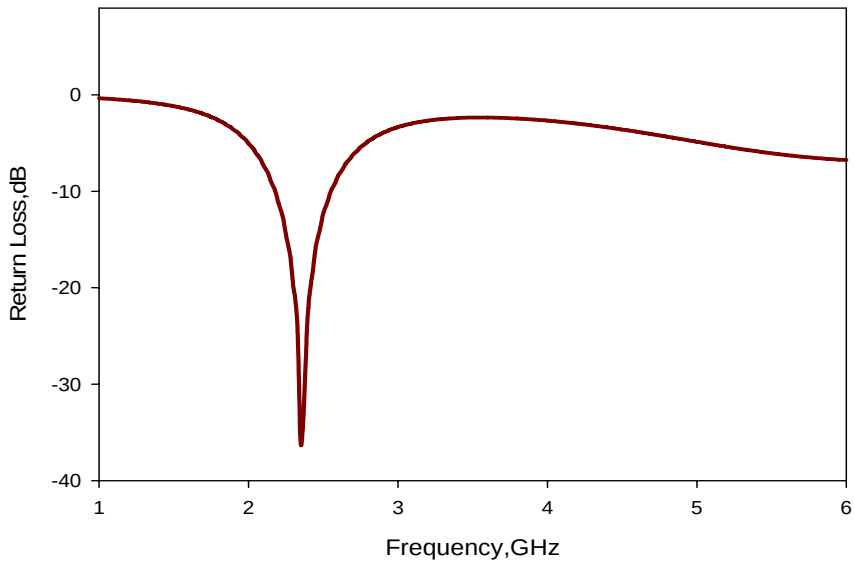

Fig.3.30. Return Loss characters of the inverted L antenna
L_2 = 19 mm, L_1 = 16 mm, L_g = 15.5 mm and W_g= 5 mm. and L_s=21 mm,w=3mm , εr = 4.4, h=1.6 mm

The antenna resonates at 2.33 GHz with good matching as shown above. The 2:1 VSWR ranges from 2.18 GHz to 2.55 GHz.

The current distribution in the antenna is as shown in fig.3.31. It is clear from the figure that there exists a near half wave variation along the total length $L_g + L_1 + L_2$. Here too the current variation in the ground strip is along the edge of the strip which doesn't affect the asymmetric coplanar strip line mode.

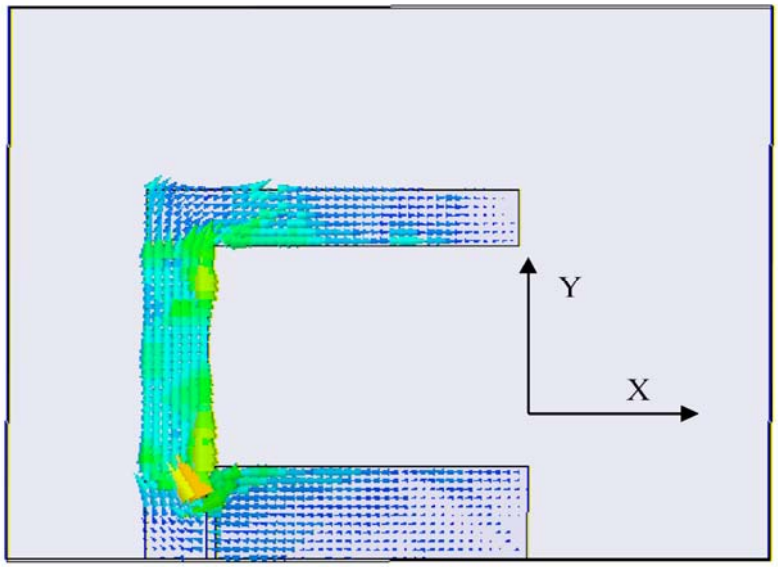

Fig.3.31. Current distribution in the antenna
L_2 = 19 mm, L_m = 21 mm, L_g = 15.5 mm and W_g= 5 mm and L_s=21 mm, εr = 4.4, h=1.6 mm

3.5.3 Radiation characteristics of the single band inverted L antenna

The 3-D radiation pattern of the antenna is shown in figure 3.32. Note that the tilt in the pattern as in the case of the vertical strip fed by the ACS feed in the earlier section (Fig.3.7.b) is absent. This is because the X directed currents in the ground plane and in the strip L_2 are in opposite directions and cancel each other in the far fields. Thus the current along the strip L_1 predominates; producing pattern similar to a Y directed monopole. Thus the use of the inverted L structure can reduce the overall size of the antenna and removes the tilt of the radiation pattern. This is an important achievement.

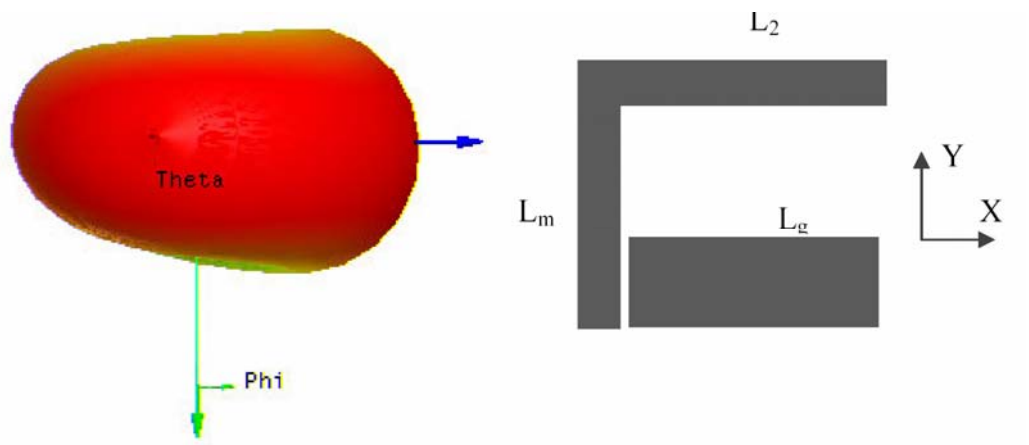

Fig.3.32. 3D radiation pattern of the inverted L antenna
L_2 = 19 mm, L_m = 21 mm, L_g = 15.5 mm and W_g= 5 mm,
εr = 4.4, h=1.6 mm

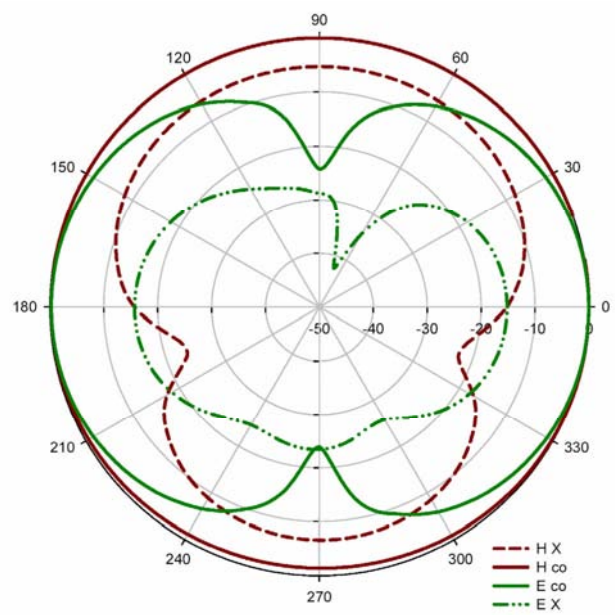

Fig.3.33. E and H plane patterns of the inverted L antenna

The 2 D radiation pattern of the antenna at the centre frequency (2.33 GHz) is shown in Fig.3.33. A near figure of eight pattern is obtained in the E plane. The cross polar level is found to be better than the ACS fed strip monopole in the previous section

The gain and efficiency of the antenna is also measured. The average gain of the antenna in the band is 1.9 dBi. The efficiency of the antenna is noted as 72 % at 2.33 GHz. The decrease in efficiency is due to the coupling between the ground plane and the Strip L_2.

3.5.4 Design of the dual band antenna-Excitation of the second resonance

The next step is to excite another resonance at 5.2 GHz in the same structure without affecting the compactness of the antenna.

An additional strip is attached to the above inverted L antenna as shown in fig.3.34.The strip is added at the point of minimum field intensity so that the first resonance is not perturbed. The position and length of the strip is taken in such a way that the total resonant length due to the addition of the strip ($Lg+L_{11}+L_{22}$) is nearly equal to 0.55 times the dielectric wavelength corresponding to the second resonance.

The dimensions of the final antenna are taken as L_2 =19 mm, L_m = 21 mm, L_g=15.5 mm, W_g = 5 mm, L_{11} = 5 mm, L_{22} = 4.5 mm, g=0.5mm and w =3 mm.

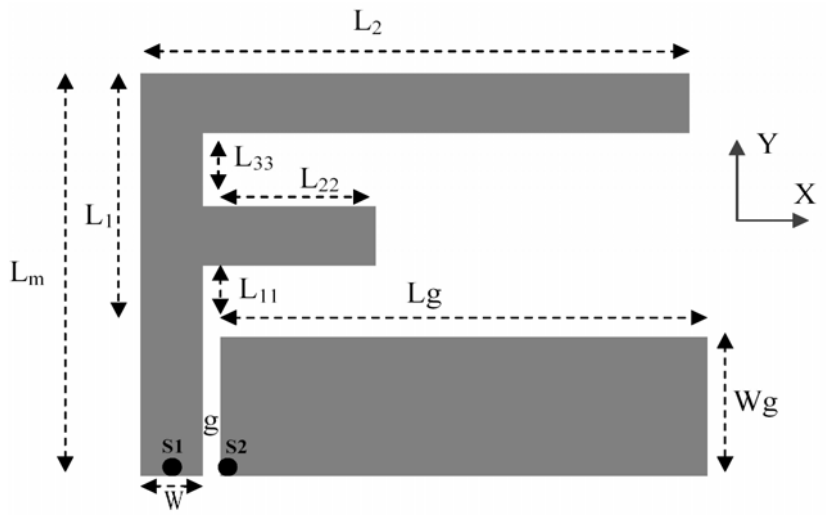

Fig.3.34. Final ACS fed F shaped dual band antenna
L_2 =19 mm, .L_m = 21 mm, L_g=15.5 mm, W_g = 5 mm, L_{11} = 5 mm, L_{22} = 4.5 mm, w =3 mm, εr = 4.4, h=1.6 mm

The effect of the position and length of the strip L_{22} on the characteristics of the antenna is studied and shown in Fig.3.35. The total current path ($Lg+L_{11}+L_{22}$) is kept as a constant in the studies. As can be seen from the figure the input impedance of the antenna is severely affected with the position of the strip L_{22}. It can be noted that the reactance changes from inductive to capacitive as the strip is moved away from the ground plane (Increasing L_{11}) as shown below.

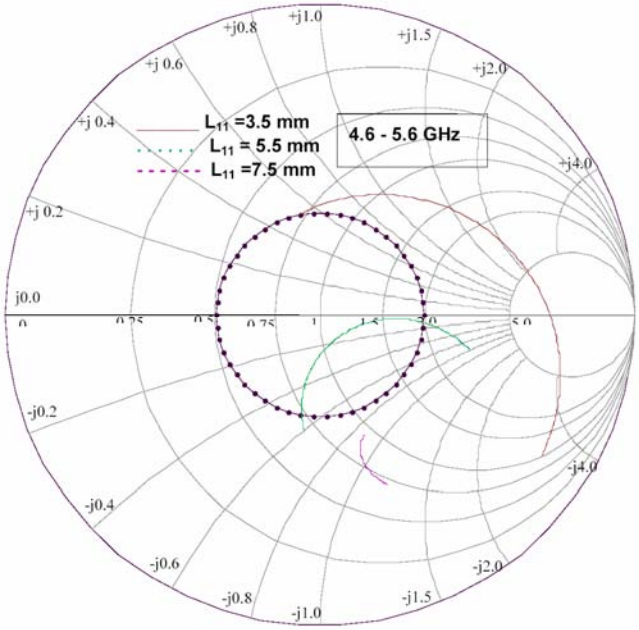

Fig.3.35. Impedance variations in the antenna with the position of the strip L_{22}
L_2 =19 mm, L_m = 21 mm, L_g=15.5 mm, W_g = 5 mm, w =3 mm, g = 0.5 mm εr = 4.4, h=1.6 mm

3.5.5 Return Loss characteristics of the dual band antenna

The return loss characteristic of the resulting dual band antenna is shown in fig.3.36. The antenna resonates at 2.33 GHz and 5 GHz with a 2:1 VSWR bandwidth from 2.24 GHz to 2.55 GHz and from 4.64 GHz to 5.39 GHz with

good impedance matching. The uniplanar nature and compact structure of the antenna make it highly suitable for 2.4/5.2 GHz WLAN applications.

Comparing fig.3.36 and 3.30 it can be seen that the addition of the second strip doesn't produce any affect on the first resonance at 2.33 GHz.

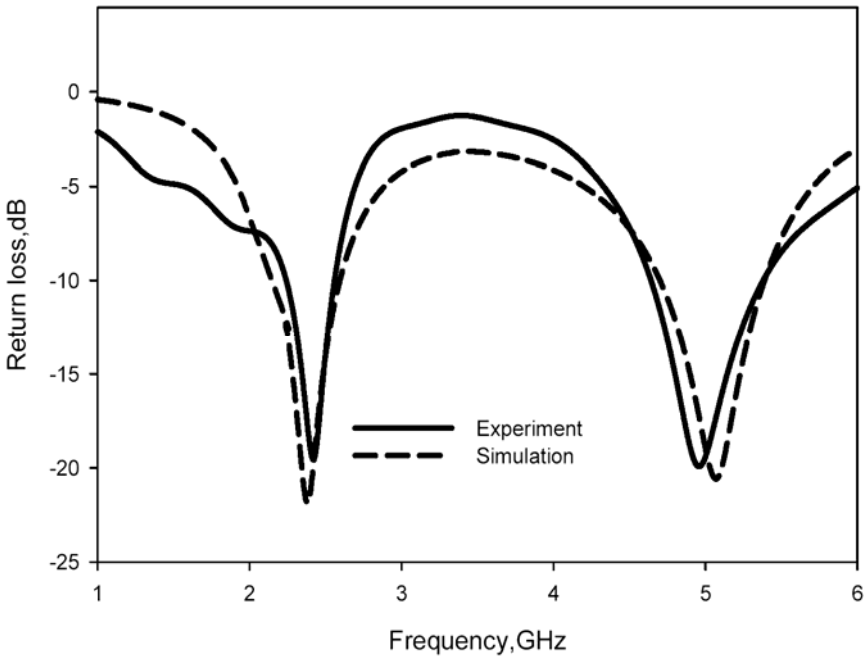

Fig.3.36. Return Loss characteristics of the Dual Band F shaped antenna L_2 =19 mm, .L_m = 21 mm, L_g=15.5 mm, W_g = 5 mm, g=0.5 mm, w =3 mm, εr = 4.4, h=1.6 mm

The current distribution (fig.3.37) too confirms this observation. Corresponding to the first resonance there is very little intensity in the additional strip $L_{22.}$

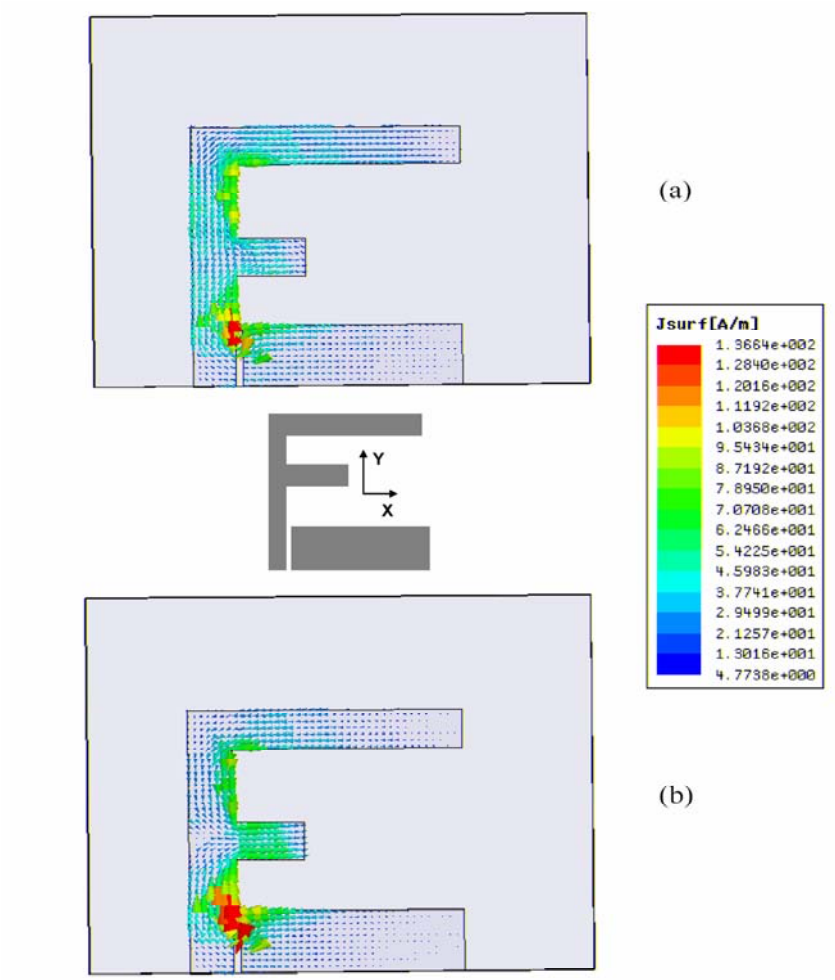

Fig.3.37. Current distribution in the final ACS fed F shaped dual band antenna. (a)At 2.33 GHz (b) At 5 GHz

3.5.6 Effect of the longer strip on second resonance

The effect of the strip L_2 on the second resonance has to be studied for the better understanding of antenna performance. The variation in the return loss characteristic with the length of the strip L_2 is shown in fig.3.38. As expected the first resonant frequency decreases with increase in the length of L_2. Small effect is seen in the case of the second resonance. This is due to the shift in the position of minimum field intensity in the antenna owing to the variation of L_2.

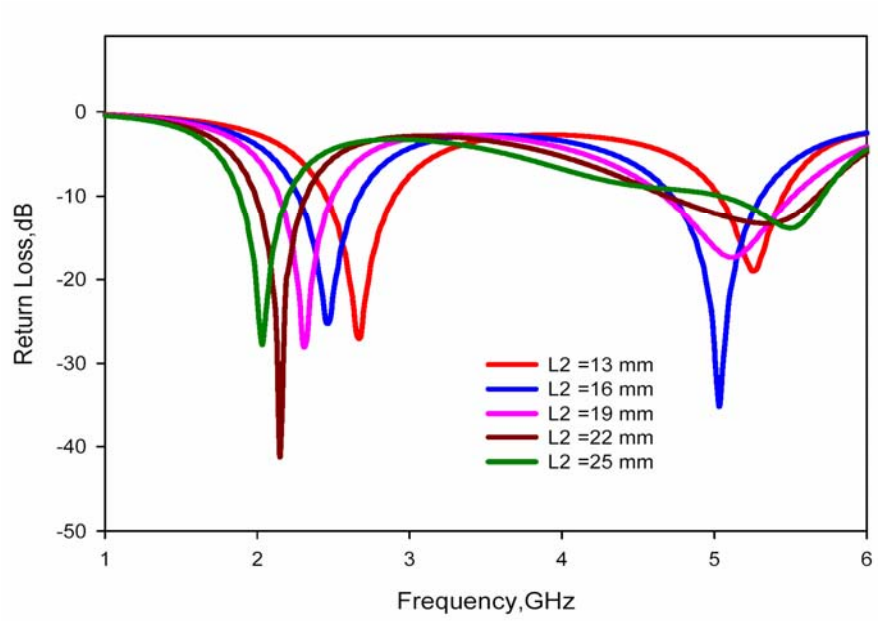

Fig.3.38. Effect of the strip L_2 on second resonance
L_m = 21 mm, L_g=15.5 mm, W_g = 5 mm, w =3 mm, g=0.5 mm
εr = 4.4, h=1.6 mm

3.5.7 Radiation pattern of the dual band antenna

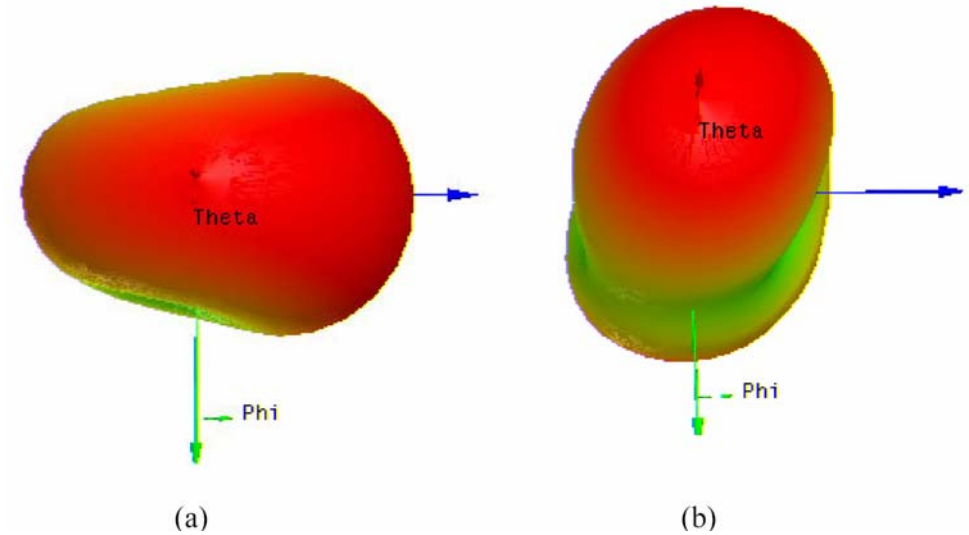

Fig.3.39. 3-D radiation pattern of the antenna
(a)At 2.4 GHz (b) At 5 GHz

The 3-D radiation pattern of the antenna is shown in fig 3.39.a at 2.4 GHz.

There is not much change in the pattern corresponding to the first resonance at 2.4 GHz (Fig.3.39 (a)).The pattern remains consistent as in the case of the single band antenna (Fig.3.32.)

In the case of the second band the polarization of the antenna is tilted by 90° (Fig.3.39.(b)). The pattern is similar to a X oriented dipole.

This can be explained from the current distribution in fig.3.37.(b). Corresponding to the second resonance, the currents along the strips $L_2 + L_{33}$ and $L_g + L_{11}$ are in opposite directions and they cancel each other in the far field. The contribution is only the X-directed current in the strip L_{22}.This produces the pattern as in fig.3.39.b.

The 2-D radiation patterns of the final dual band antenna for the two bands are shown in fig.3.40. The cross polar level corresponding to the second resonance is found to be high. This is evident from the current distribution (Fig.3.32.b.). Note that even though the currents along the strips $L_2 + L_{33}$ and $L_g + L_{11}$ cancel each other at the far fields, there is a slight difference in the current intensities in the strips L_{11} and L_{33}.This is the cause for the higher cross polar level in the second band.

The antenna is polarized along the Y axis for the first band and along the X axis for the second band. This confirms the explanation given above.

The average gain of the antenna is 1.92 dBi in the first band and 2.2 dBi in the second band respectively. Corresponding measured efficiencies of the antenna are 73 % and 83 % at 2.33 GHz and 5 GHz respectively.

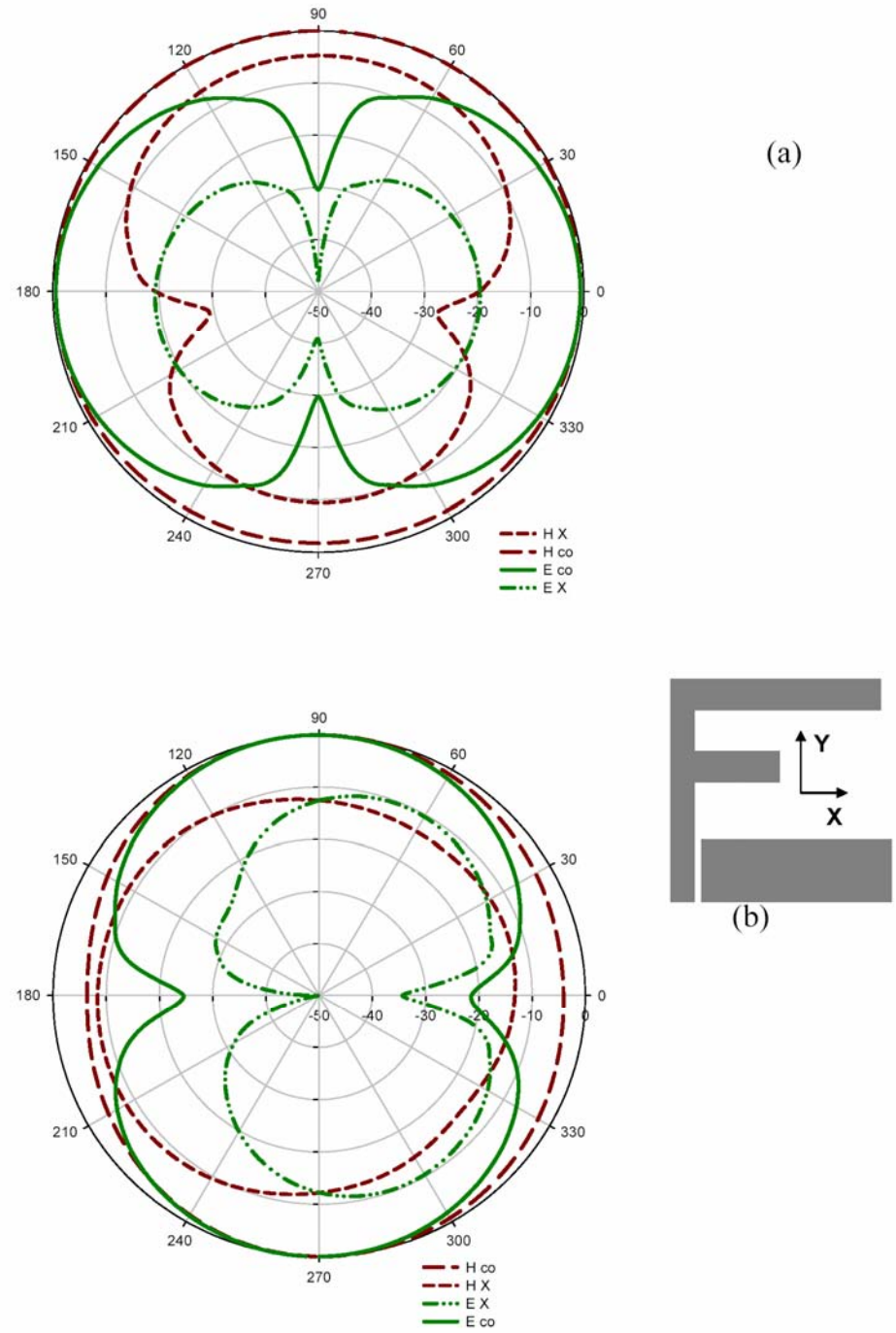

Fig.3.40.2-D radiation pattern of the antenna
(a) At 2.33 GHz (b) At 5 GHz

3.5.8 Conclusion

The design of the Asymmetric coplanar strip fed dual band antenna was thoroughly studied in this section. Bending the signal strip in the form of an inverted L also removes the 45° tilt in the monopole mentioned in section 3.4.The antenna is compact and exhibit good reflection characteristics also.

3.6 Compact asymmetric Coplanar strip fed multi band antenna

The design and analysis of Asymmetric coplanar strip fed triple band antenna is presented in this section. The inverted L monopole in the previous section is taken as the starting design. The technique employed here is the production of different current paths by the insertion of a slot on a wide patch.

3.6.1 Initial design – Single band Inverted L

The geometry of the inverted L antenna working at 2 GHz is shown in Fig. 3.41

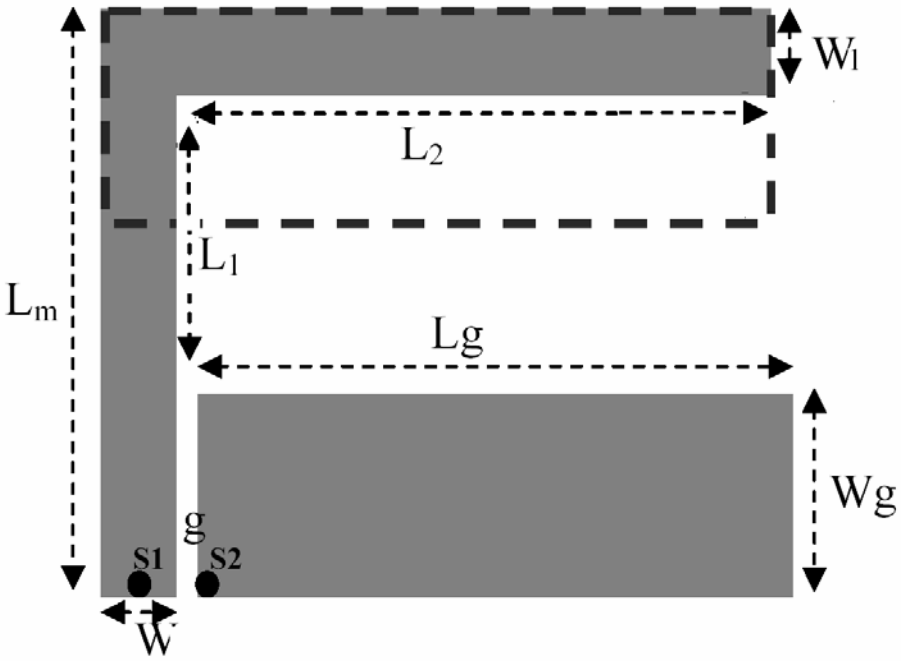

Fig.3.41. ACS fed Inverted L antenna
L_m = 23 mm L_2 = 20 mm, L_g = 16.5 mm and W_g = 6 mm, w= 3 mm,W_1=3 mm, g=0.5 mm, εr = 4.4, h=1.6 mm

The dimensions of the antenna are taken as per the design equations given in the previous section (Equations 3.9 - 3.11).The calculated dimensions on a substrate of dielectric constant 4.4 and height 1.6 mm are L_m = 23, L_2 = 20 mm, L_g = 16.5 mm, w= 3 mm,W_1=3 mm and W_g = 6 mm.

The return loss of the resulting antenna is shown in fig.3.42.The antenna resonates at 2.08 GHz with good impedance matching.

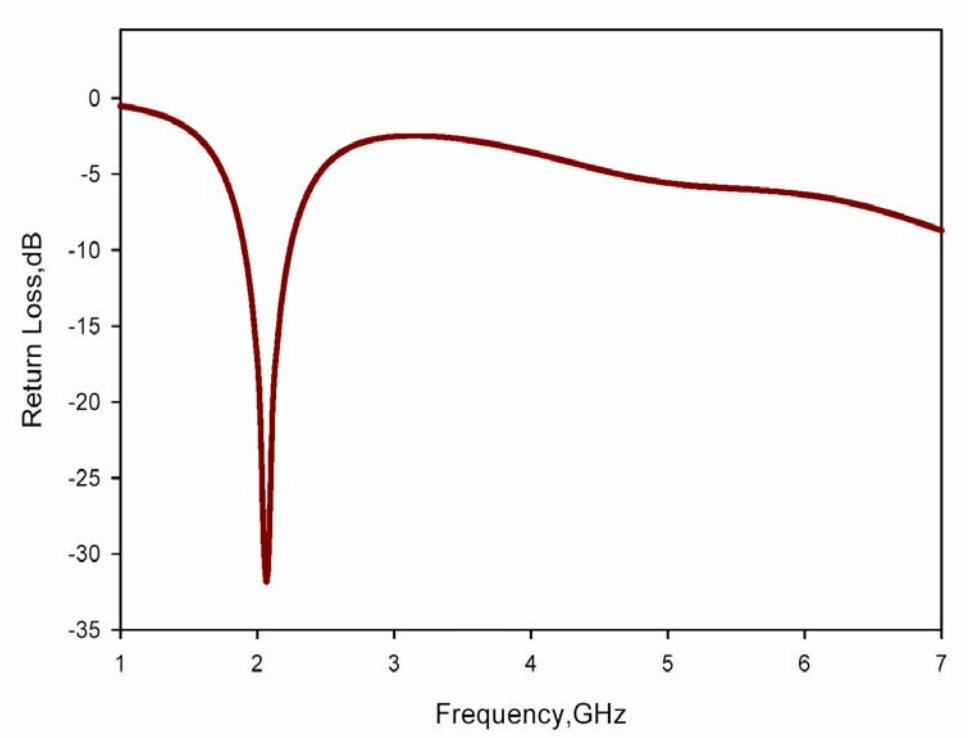

Fig.3.42. Return loss characteristics of the Inverted L antenna in fig.3.41.
L_m = 23 mm, L_2 = 20 mm, L_g = 16.5 mm ,W_2 = 3 mm, W_g = 6 mm, g=0.5 mm, w= 3 mm,W_1=3 mm εr = 4.4, h=1.6 mm

To explore the possibility of exciting different current paths in the same structure the width of the strip W_1 is increased keeping 'L_m' constant. The result of increasing the width of the strip, W_2 is shown in dotted lines in fig.3.43.

It is evident from the figure that the widening of the strip doesn't excite additional resonances in this antenna. Also there is a slight increase in the resonant frequency with the increase in the width W_2.This is due to the decrease in the current path of the antenna because in all these studies L_m is kept constant so that the overall compactness of the antenna is not affected. As a result as W_2 increases, L_1 decreases thereby increasing the resonant frequency.

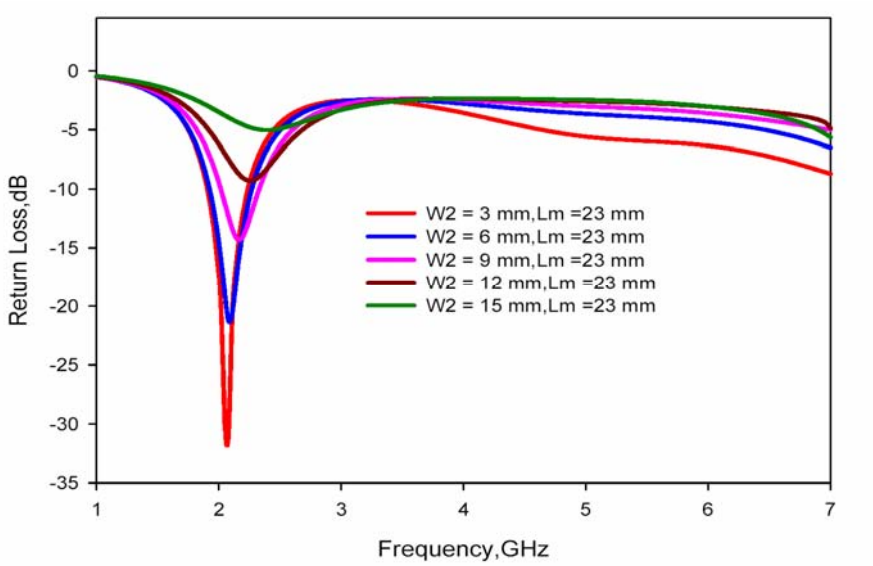

Fig.3.43. Varying the width of the strip W_1
L_m = 23, L_2 = 20 mm, L_g = 16.5 mm W_g = 6 mm, w=3 mm
g=0.5 mm, εr = 4.4, h=1.6 mm

Note that the matching of the antenna deteriorates as W_2 increases owing to the increased coupling between the strips L_2 and L_g as discussed in the previous section.

The next step to explore the possibility of exciting multiband resonance is the introduction of slot in the structure. To explore this method a slot of dimensions X x Y (in this case 0.5 W_1 x 0.5 L_2) is inserted symmetrically in the above strip L_2 x W_1 at different positions as in Fig.3.44.

3.6.2 Slot Insertion - the position

Fig.3.44. shows the different configurations of the inverted antenna with the symmetric slot.

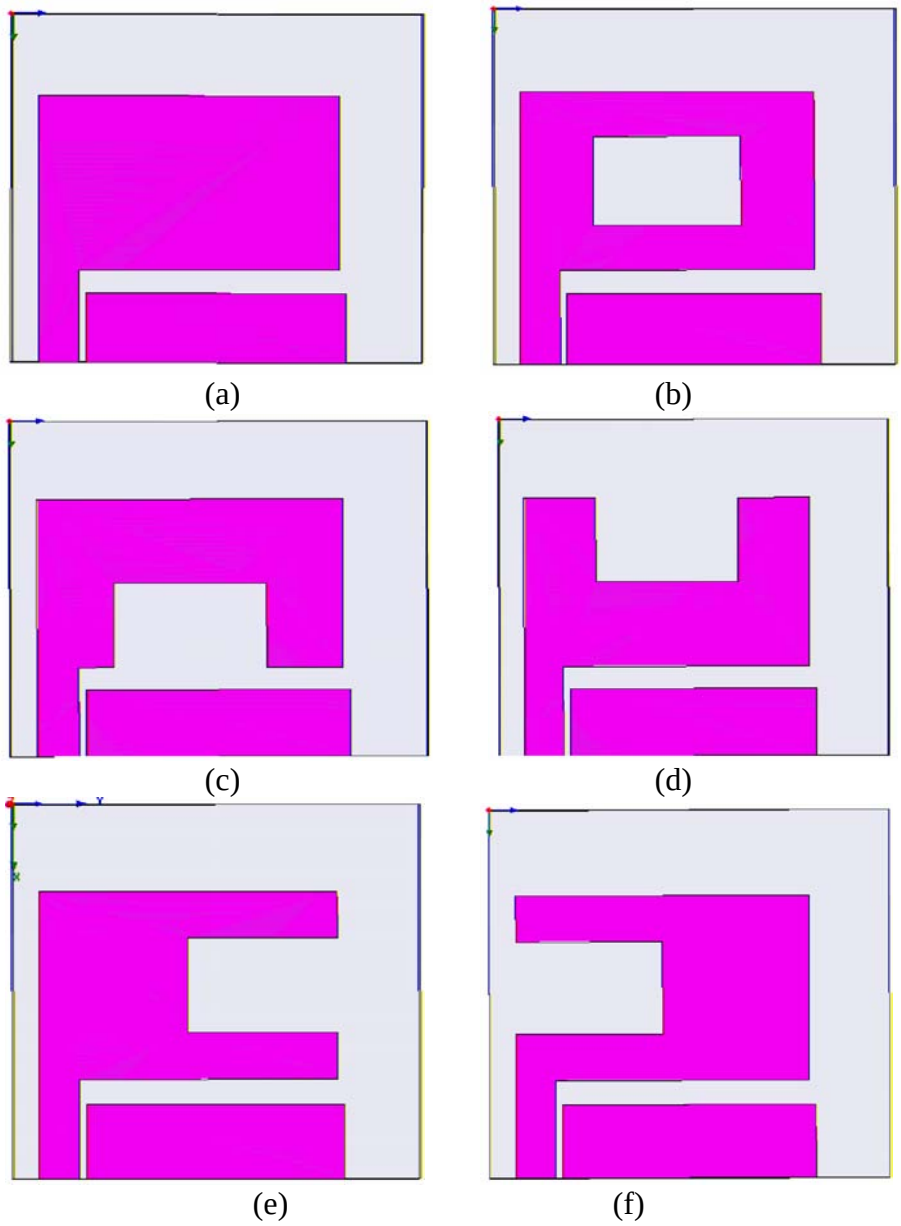

Fig.3.44. Different positions of the slot

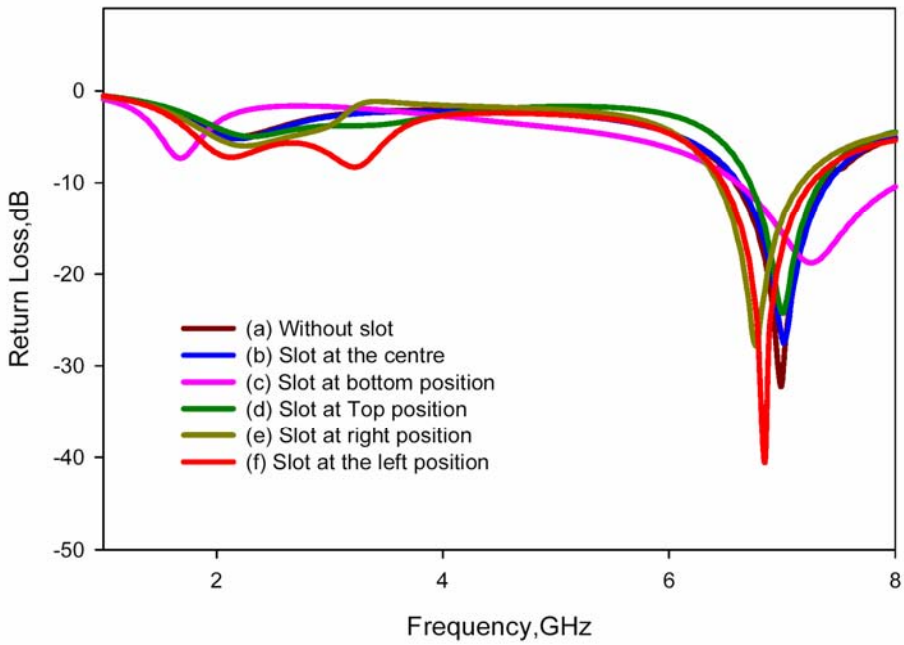

Fig.3.45. Effect of slot insertion at different positions of the strip L_2 x W_1 L_m = 23, L_2 = 20 mm, L_g = 16.5 mm W_g = 6 mm, w=3 mm,g=0.5 mm, εr = 4.4, h=1.6 mm, W_1=15 mm

The return loss curves of the above antenna obtained by the insertion of the slot are shown in fig.3.45.

Fig.3.45.a shows the return loss characteristics of the antenna without the slot but with W_1 = 15 mm.

Symmetric insertion of the slot at the centre doesn't produce much effect in the resonances as evident from the curve 3.45. (b)

Inserting slots in the bottom (fig.3.44.c) and top position (fig.3.44.d) shows the same effect as in curves 3.45. (c) and 3.45.(d).

Slot insertion as in Fig.3.44.(e) produces larger band width (curve 3.45.(e)). But this is similar to the case of the F shaped dual band antenna discussed in the previous section.

Among all the above techniques predominant effect is noted only in the last case (curve 3.45. (f)) and this structure is studied in detail.

The geometry of the final antenna with the slot is shown in fig.3.46.

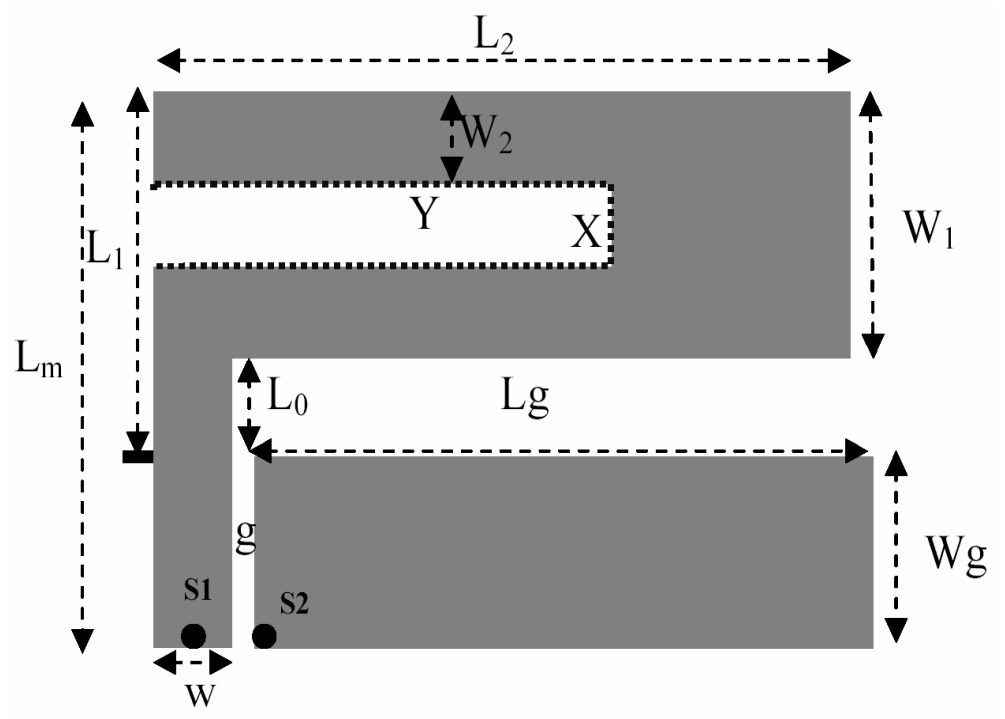

Fig.3.46. ACS fed Inverted L antenna with the slot
L_m = 23, L_1 = 17 mm, L_2 = 22 mm, L_g = 16.5 mm, W_g = 6 mm, W_2 =3.75, W_1 =15 mm, L_0 = 2 mm, X = 7.5 mm,Y = 10 mm, εr = 4.4, h=1.6 mm

3.6.3 Effect of Slot insertion in the antenna

Fig.3.47. shows the return loss characteristics of the antenna with and without the slot. An additional resonance is excited in the final antenna with the slot. The resonances in the antenna without the slot are at 2.23 GHz and 6.99 GHz. The insertion of the slot excites an additional resonance at 2.82 GHz in addition to the above mentioned frequencies

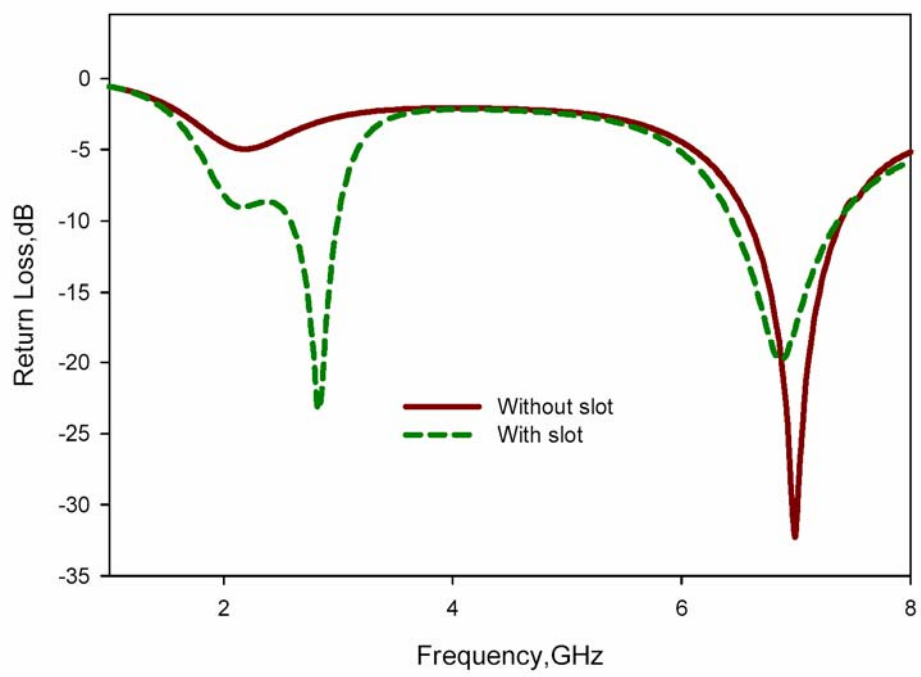

Fig.3.47. Return loss of the antenna with and without slot
L_m = 23, L_1 = 17 mm, L_2 = 22 mm, L_g = 16.5 mm, W_g = 6 mm, W_2 =3.75, W_1 =15 mm, L_0 = 2 mm, X = 7.5 mm, Y = 10 mm, εr = 4.4, h=1.6 mm

3.6.3.1 Current distribution in the antenna

(a) Antenna without the slot

The current distribution in the antenna without the slot is shown in fig.3.48.a (i) and fig.3.48.a (ii). Corresponding to the first resonance there is a half wave variation along the signal strip and the ground plane. Corresponding to the second resonance there are three half wave variations along the edge of the ground plane and the adjoining signal strip.

Note that there is no two half wave variation in the antenna. The second mode is suppressed owing to the high input impedance corresponding to that resonance. This is discussed in more detail in the next chapter.

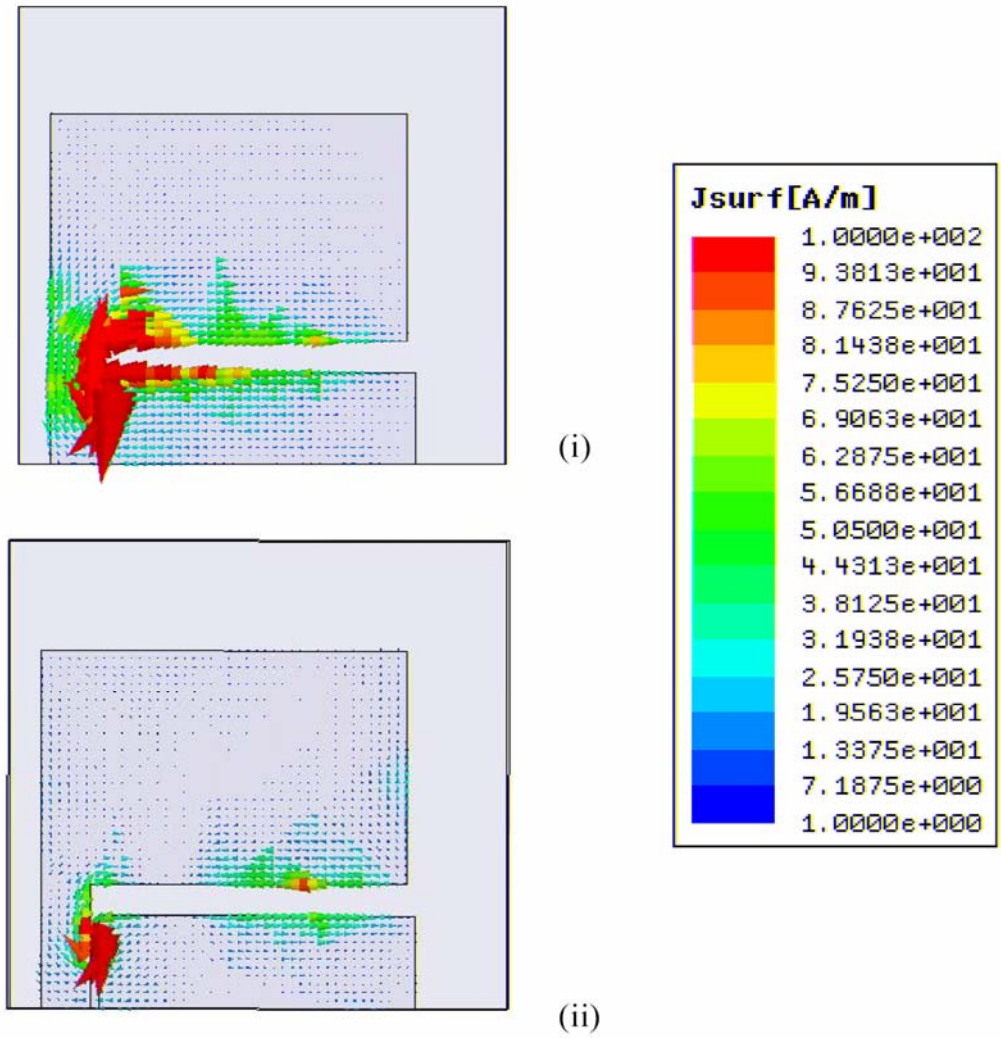

Fig.3.48.a. Current distribution in the antenna without slot insertion
(i) 2.19 GHz (ii) 7 GHz
L_m = 23, L_1 = 17 mm, L_2 = 22 mm, L_g = 16.5 mm, W_g = 6 mm,
W_1 =15 mm, L_0 = 2 mm, εr = 4.4, h=1.6 mm

(b) Antenna with the slot

When a slot is inserted into the above structure an additional resonance is excited owing to the creation of a different current path. Current distribution corresponding to this resonance shows a half wave variation around the slot as

in fig.3.48.b.This idea is used in the design of the multi band antenna as detailed in the following section.

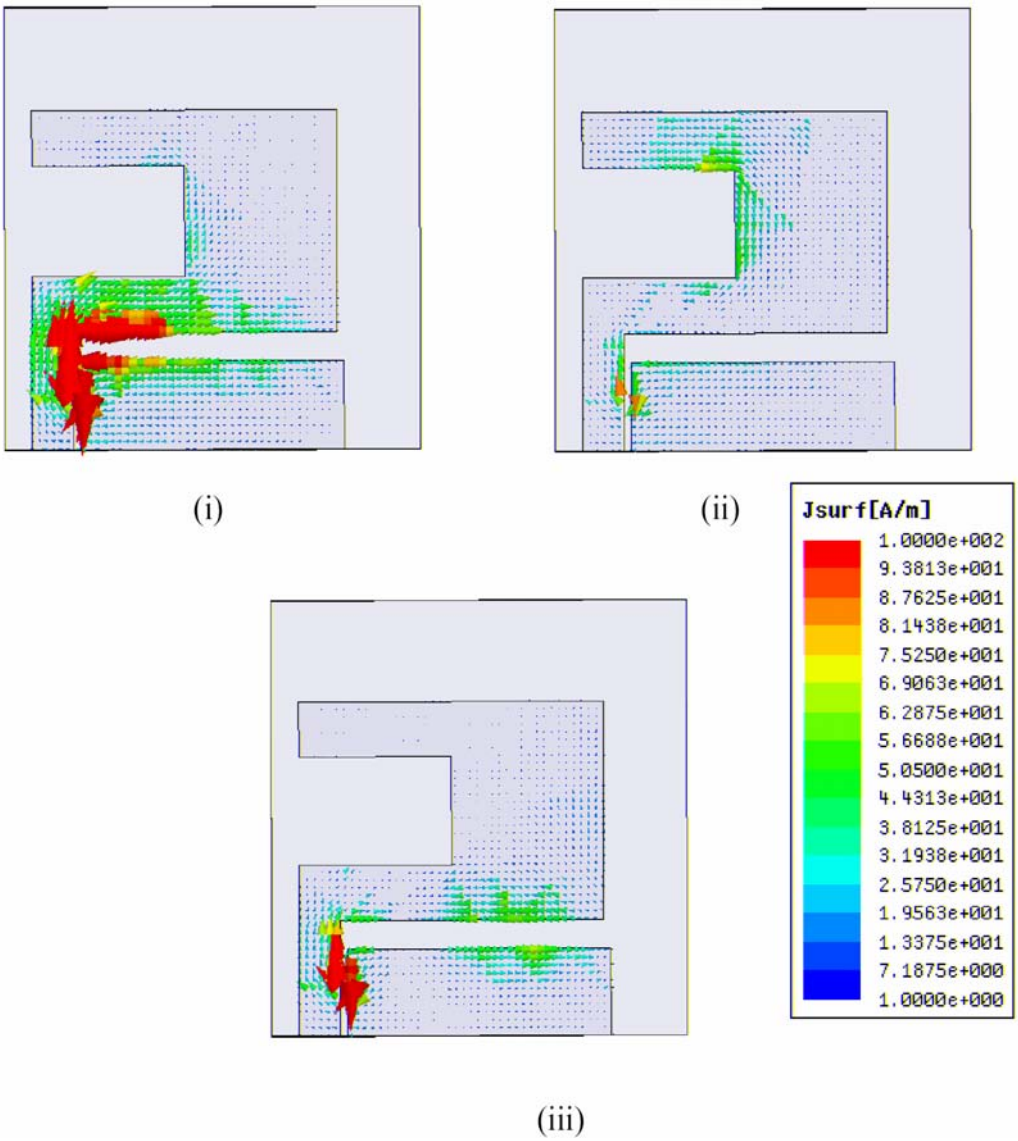

Fig.3.48.b. Field distribution in the antenna after slot insertion (i)At 2.12 GHz (ii) At 2.92 GHz (iii) At 6.88 GHz L_m = 23, L_1 = 17 mm, L_2 = 22 mm, L_g = 16.5 mm, W_g = 6 mm,W_2 =3.75, W_1 =15 mm, L_0 = 2 mm, X = 7.5 mm,Y = 11 mm, εr = 4.4, h=1.6 mm

The above studies confirm that slot insertion is an effective way to induce multiple resonances. To completely understand the behavior of the antenna a set of studies were performed by varying the different parameters of the antenna as given below.

3.6.4 Design and Analysis of the triple band antenna

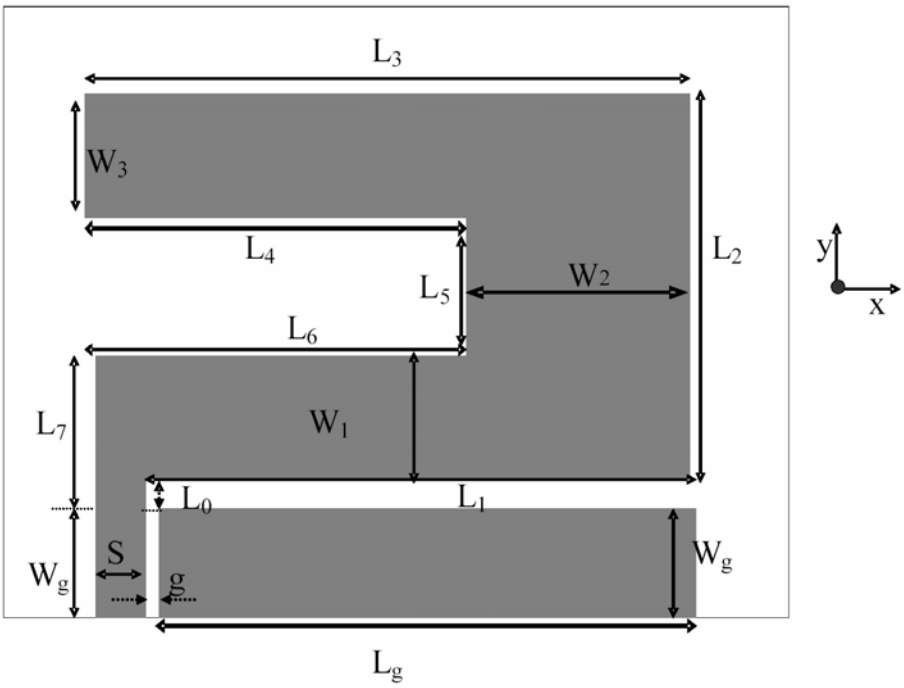

Fig.3.49. Geometry of the proposed multi band antenna
Lg=19 mm, Wg=6 mm, S=3 mm, g=0.5 mm Lo=2.mm, L_1=19mm, W_1=3.75 mm, L_2=15 mm, W_2=11 mm, L_3=22 mm, W_3=3.75 mm,L_7 = 8mm,L_4 = 11mm, L_5=7.5 mm, L_6=11 mm, εr = 4.4, h=1.6 mm

The geometry of the final multiband antenna is shown in fig.3.49.

The ACS feed comprises of the ground plane of length Lg and width Wg separated by a small gap g from the signal strip. The other parameters include strips of dimensions L_1 x W_1, L_2 x W_2 and L_3 x W_3.The lengths of the individual strips are optimized to resonate at the desired frequencies.

Each of the above parameters are varied to study their effect in the performance of the antenna.

3.6.4.1 Effect of the length of the slot L_5 x L_6, (W_2 variation studies)

In this section the length of the slot is varied. This is brought about by changing the width of the strip L_2 x W_2, since an increase in W_2 corresponds to a decrease in the length of the slot L_6.

As the length of the slot L_6 increases, (W_2 decreases) the second resonant frequency decreases. But the first and third resonance nearly remains the same. Thus this length is decisive as far as the bandwidth and merging of the first two resonances are concerned. This implies that the second resonance greatly depends on the slot dimensions.

From the study we have chosen the optimum value of W_2 = 8 mm considering the merging of the first two resonances.

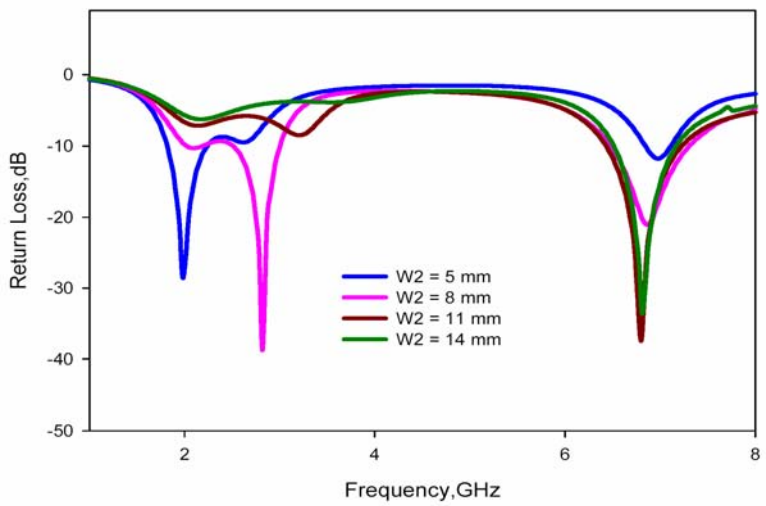

Fig.3.50. Slot length variation studies
Lg=19 mm, Wg=6 mm, S=3 mm, g=0.5 mm Lo=2.mm, L_1=19mm, W_1=3.75 mm, L_2=15 mm, L_3=22 mm,W_3=3.75 mm,L_7 = 8mm, L_4 = 11mm, L_5=7.5 mm, L_6=11 mm, εr = 4.4, h=1.6 mm

3.6.4.2 Effect of the width of the slot L_5 x L_6

Variation in the width of the slot produces small variations in the first and second resonances. But the third resonant frequency is slightly affected by the width of the slot. But varying L_2 is found to affect the first and second resonances.

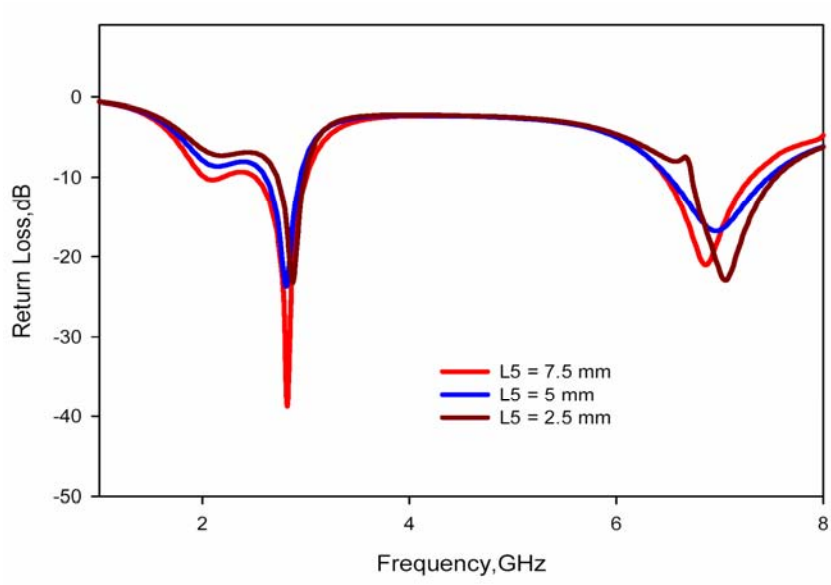

Fig.3.51. Slot width variation studies, L_5 variation studies
Lg=19 mm, Wg=6 mm, S=3 mm, g=0.5 mm Lo=2.mm, L_1=19mm, W_1=3.75 mm, L_2=15 mm, W_2=11 mm, L_3=22 mm,W_3=3.75 mm, L_7 = 8mm,L_4 = 11mm, L_6=11 mm, εr = 4.4, h=1.6 mm

3.6.4.3 Effect of the horizontal strip L_3 xW_3

The effect of the length of the horizontal strip L_3 is studied in this section. It can be seen that the second resonant frequency is mainly affected by the length L_3. This is because varying L_3 also varies the length of the slot and hence the current around the edges of the slot. The width of the strip W_3 is also varied and studied. The optimized width W_3 is taken as 0.3 times L_4 for maximum bandwidth.

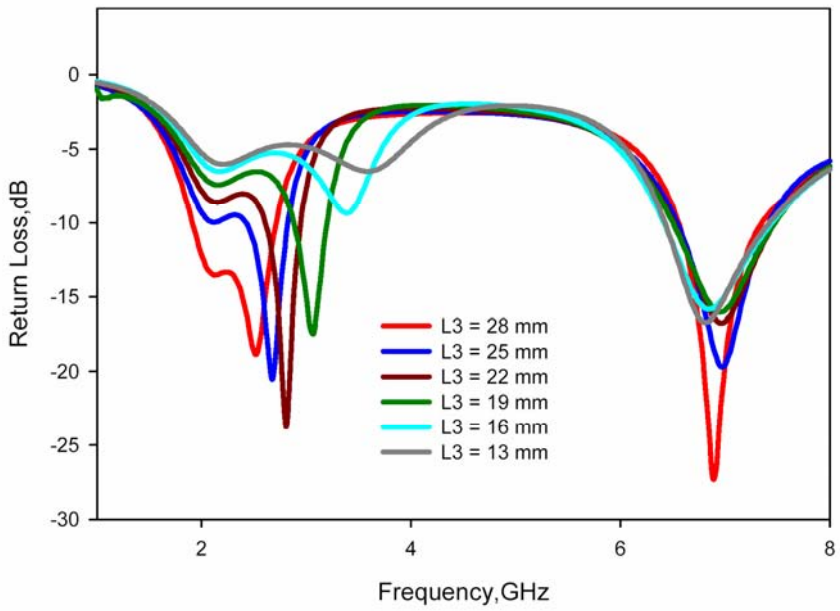

Fig.3.52. Horizontal strip length L_3 variation studies

Lg=19 mm, Wg=6 mm, S=3 mm, g=0.5 mm Lo=2.mm, L_1=19mm, W_1=3.75 mm, L_2=15 mm, W_2=11 mm, L_3=22 mm, W_3=3.75 mm, L_7 = 8mm, L_4 = 11mm, L_5=7.5 mm, L_6=11 mm, εr = 4.4, h=1.6 mm

3.6.4.4 Effect of the horizontal strip L_1 xW_1

Varying the length of the strip produces variation in all the three resonances as evident from fig.3.53. This is because there is current intensity in this strip corresponding to all the three resonances. This is evident from the current distribution in strip shown in fig.3.48.b.Increasing L_1 decreases all the three resonances. It is also found that the performance of the antenna deteriorates when the length of this strip L_1 is far different from the length of the ground plane, L_g. The field distribution in the antenna gets perturbed in this case i.e, when L_1 is far different from L_g. The width of the strip W_1 is also varied and studied. Small variations in the first and second resonances are noted. The optimum width W_1 is taken as 0.3 times L_1+S for maximum bandwidth.

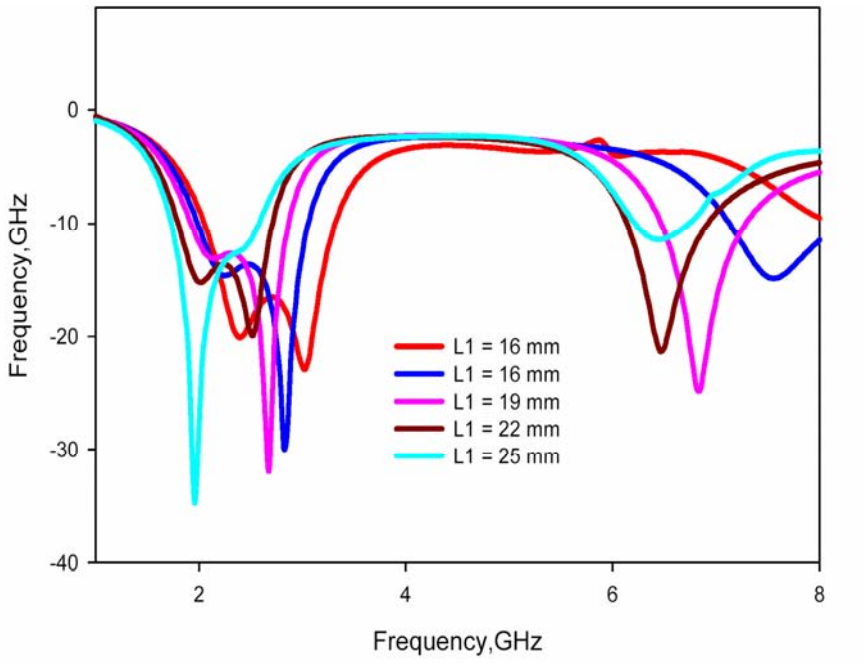

Fig.3.53. L_1 variation studies
Lg=19 mm, Wg=6 mm, S=3 mm, g=0.5 mm Lo=2.mm, L_1=19mm, W_1=3.75 mm, L_2=15 mm, W_2=11 mm, L_3=22 mm,W_3=3.75 mm,L_7 = 8mm,L_4 = 11mm, L_5=7.5 mm, L_6=11 mm, εr = 4.4, h=1.6 mm

3.6.4.5 Effect of varying the separation Lo

The length L_0 denotes the separation of the strip L_1 x W_1 above the ground plane L_g x W_g. It can be seen that varying L_0 affects the three resonances. The first resonance and the third resonance are mainly due to the strips L_1 x W_1 and L_g x W_g and hence they are affected by $L_{0.}$ variation. The second resonance first increases and then decreases with L_0. Also this separation affects the merging of the first two bands. In this case the optimized spacing is taken as L_0 = 2 mm for best performance.

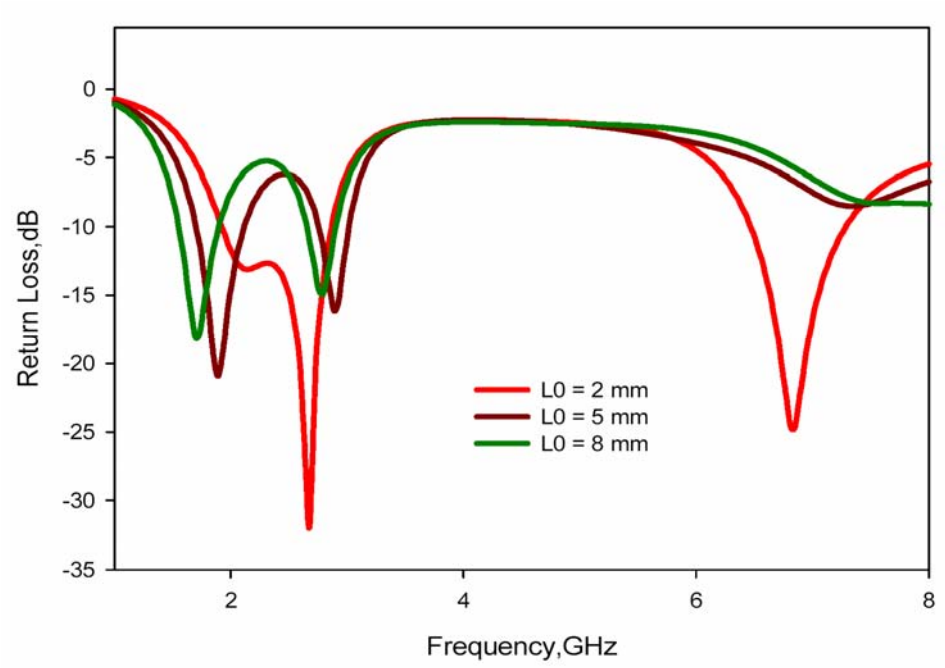

Fig.3.54. Effect of varying the separation L_0
Lg=19 mm, Wg=6 mm, S=3 mm, g=0.5 mm Lo=2.mm,
L_1=19mm, W_1=3.75 mm, L_2=15 mm, W_2=11 mm, L_3=22 mm,
W_3=3.75 mm,L_7 = 8mm,L_4 = 11mm, L_5=7.5 mm, L_6=11 mm,
εr = 4.4, h=1.6 mm

The dependence of the ground plane on antenna characteristics is also an important aspect while realizing the antenna into practical circuits. Hence the dimensions of the antenna are also varied and studied as shown below.

3.6.4.6 Effect of varying ground plane width Wg

Increasing the width of the ground plane increases the bandwidth of the third resonance as evident from fig.3.55. It can be seen that there is only a small change in the first two resonant frequencies. The optimized dimension of the ground plane is taken as W_g = 0.3L_g, considering the compactness and the merging of the first two resonances.

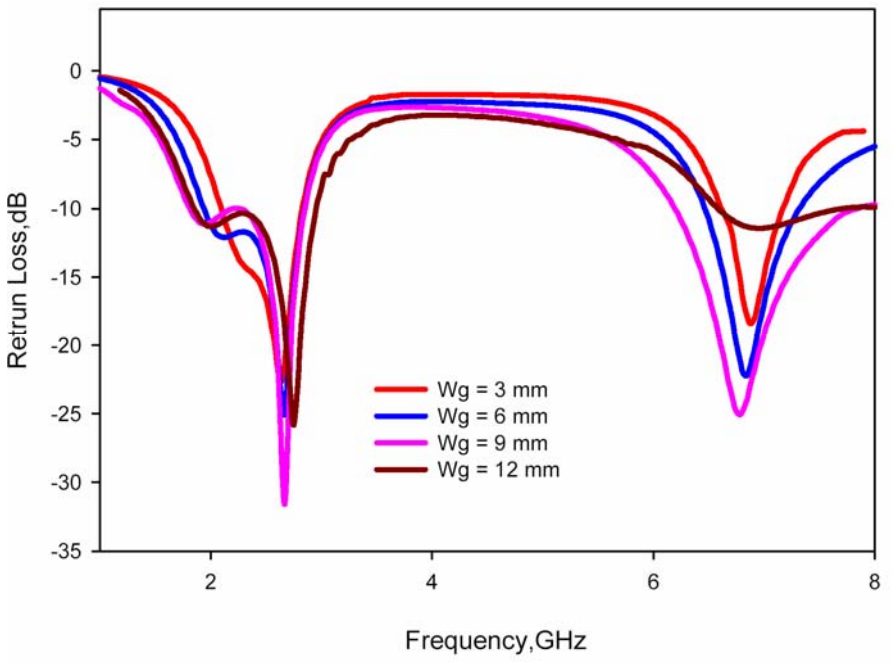

Fig.3.55. Ground plane width, Wg variation studies
Lg=19 mm, S=3 mm, g=0.5 mm Lo=2.mm, L_1=19mm, W_1=3.75 mm, L_2=15 mm, W_2=11 mm, L_3=22 mm, W_3=3.75 mm,L_7 = 8mm,L_4 = 11mm, L_5=7.5 mm, L_6=11 mm, εr = 4.4, h=1.6 mm

3.6.4.7 Effect of varying ground plane length L_g

This is one of the critical factors affecting the compactness of the antenna. As the length of the ground plane L_g is increased the first and third resonant frequencies shift to the lower side. This decrease in resonant frequency is because the first and the third resonances are mainly due to the combined effect of the signl strip and the ground strip L_1 x W_1 . Similar effects were noted in the case of L_1.The second resonance is not much affected since this resonance is due mainly due to the currents around the slot.

The above inferences are to be kept in mind while realising the antenna into circuit boards.

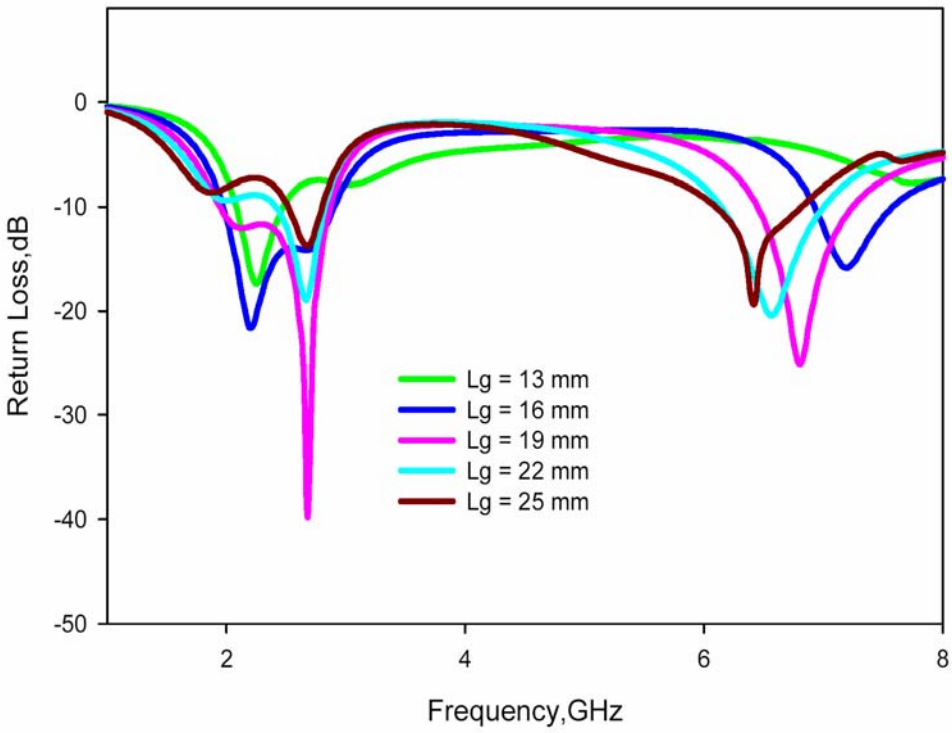

Fig.3.56. Ground plane length , Lg variation studies
Lg=19 mm, Wg=6 mm, S=3 mm, g=0.5 mm Lo=2.mm, L_1=19mm, W_1=3.75 mm, L_2=15 mm, W_2=11 mm, L_3=22 mm, W_3=3.75 mm, L_7 = 8mm,L_4 = 11mm, L_5=7.5 mm, L_6=11 mm, εr = 4.4, h=1.6 mm

From the above parametric studies and from the current distributions in the antenna the following conclusions can be reached.

The first resonance is mainly due to the strips L_g x W_g, L_o x S, L_1 x W_1 and L_2 x W_2. A half wave variation is noted along these strips corresponding to this resonant frequency. The second resonance is due to the current path through the outer edge of the slot and there is also a half wave variation corresponding to the resonance along the length L_4 + L_5 +L_6. The third resonance is due L_g + L_o + L_1 and this length is equal to 1.30 times the dielectric wavelength at that frequency. i.e,

$$L_g + L_1 + L_2 + L_3 = 0.60\ \lambda_{d1} \quad (3.12)$$

$$L_4 + L_5 + L_6 = 0.50\ \lambda_{d2} \quad (3.13)$$

$$L_g + L_o + L_1 = 1.30\ \lambda_{d3} \quad (3.14)$$

where λ_{d1}, λ_{d2} and λ_{d3} are the dielectric wave length corresponding to the first, second and third resonant frequencies.

To confirm the validity of the above studies a triple band antenna working at 1.8GHz/2.4 GHz/5.5 GHz is designed as per the above equations.

The antenna has an overall dimension of 28 x 30 mm^2 including the ground plane when constructed on a substrate of dielectric constant 4.4 and thickness 1.6 mm.

3.6.5 Reflection characteristics

The measured return loss characteristics of the prototype antenna are shown in Fig.3.57. The simulation results obtained from Ansoft HFSS is also depicted. The experimental curve obtained shows that antenna has three resonances at 1.74 GHz, 2.34 GHz and 5.58 GHz respectively. The first two bands coalesce to give a wide bandwidth of 62 % (1.32 GHz to 2.50 GHz, 1188 MHz) while the third band has a bandwidth of 17 % (5.13 GHz to 6.08 GHz, 960 MHz).

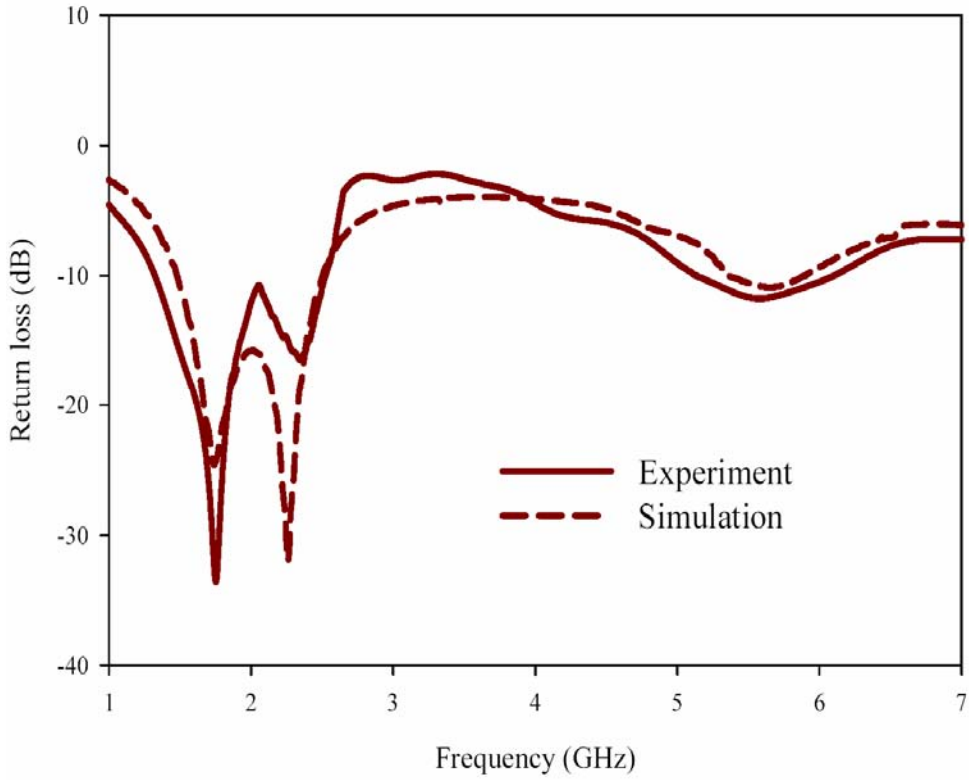

Fig.3.57 Return loss characteristics of the antenna
Lg=22.5 mm, Wg=7 mm, S=3 mm, g=0.5 mm Lo=3.4.mm, L_1=21.5mm, W_1=6.5 mm, L_2=17.6 mm, W_2=7 mm, L_3=26 mm, W_3=6.38 mm, L_4 = 19 mm, L_5=4.85 mm, L_6=16.5mm, L=28 mm, W=30mm, εr = 4.4, h=1.6 mm.

The current distributions in the antenna for the three resonant frequencies are depicted in fig.3.58. As mentioned earlier predominant variations are seen in the strips L_g x W_g , L_o x S, L_1 x W_1 and L_2 x W_2, corresponding to the first resonance. In the case of the second resonance the variation is along $L_4 + L_5 + L_6$ while the third resonance is along the length $L_g + L_o + L_1$.

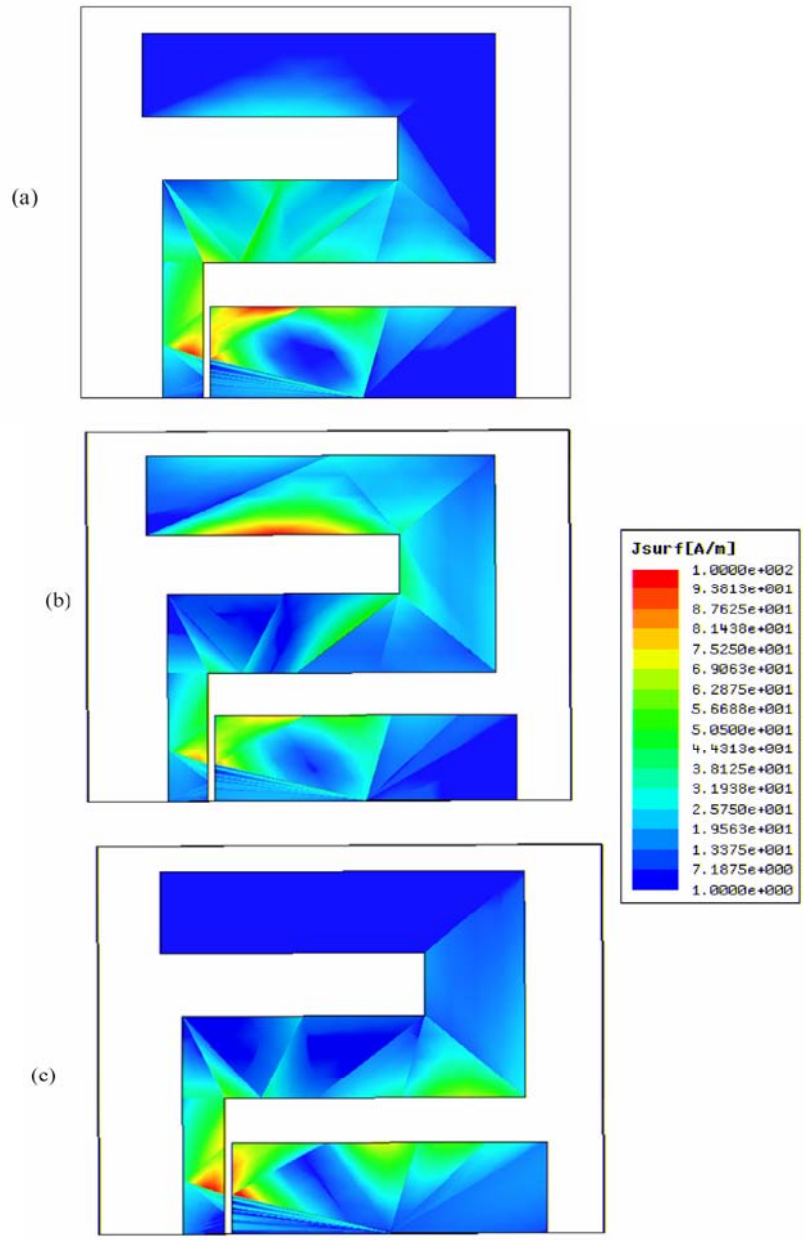

Fig.3.58. Current distribution in the final antenna
(a) At 1.74 GHz (b) At 2.34 GHz and (c) At 5.5 GHz
Lg=22.5 mm, Wg=7 mm, S=3 mm, g=0.5 mm Lo=3.4.mm, L_1=21.5mm, W_1=6.5 mm, L_2=17.6 mm, W_2=7 mm, L_3=26 mm, W_3=6.38 mm, L_4 = 19 mm, L_5=4.85 mm, L_6=16.5mm, L=28 mm, W=30mm, εr = 4.4, h=1.6 mm.

3.6.6 Radiation characteristics

The 3-D radiation pattern of the antenna is shown in fig.3.59.

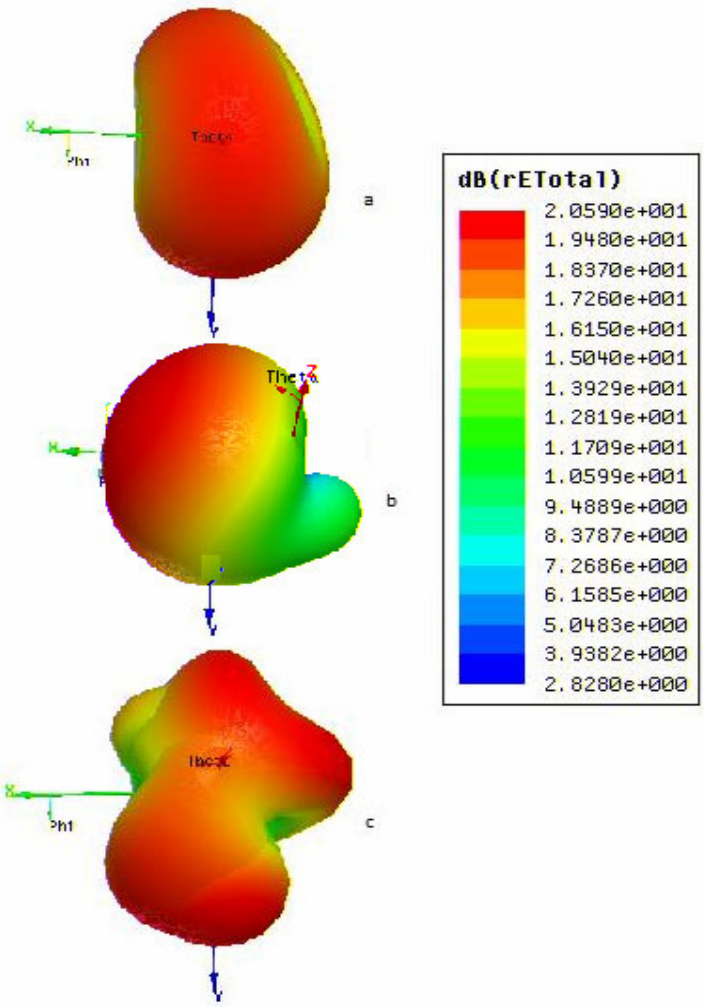

Fig.3.59. 3-D radiation pattern of the multiband antenna
(a) At 1.74 GHz (b) At 2.34 GHz and (c) At 5.5 GHz

The radiation pattern is similar to that of a dipole in at the first resonance. This is nearly similar to the case of the inverted L antenna mentioned in the previous section. The pattern corresponding to the second resonance, due to the slot, exhibits null. The third resonance is due to higher harmonic and is somewhat distorted. The measured 2-D radiation pattern is also shown in fig.3.60.

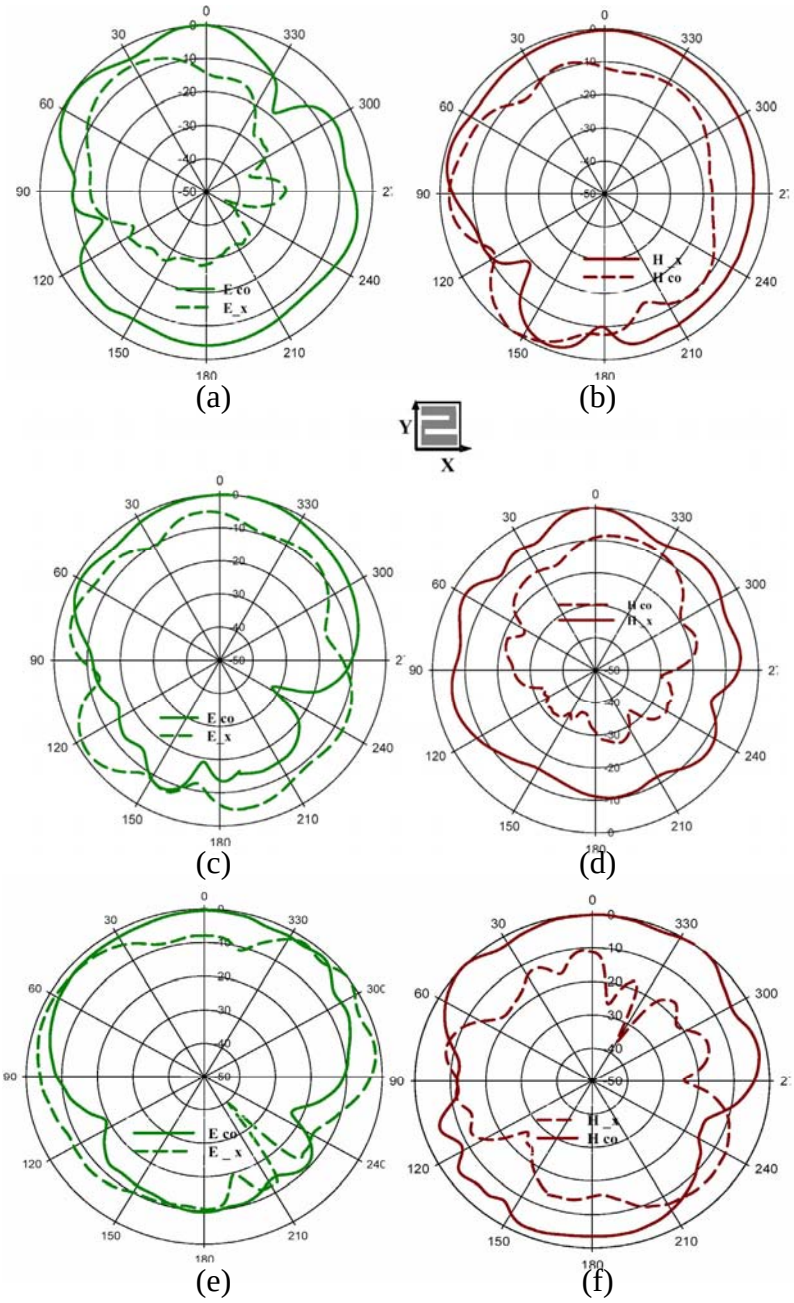

Fig.3.60. 2-D radiation pattern of the final antenna
(a)E plane pattern at 1.74 GHz (b) H plane pattern at 1.74 GHz
(c)E plane pattern at 2.34 GHz (d) H plane pattern at 2.34 GHz
(e)E plane pattern at 5.5 GHz (f) H plane pattern at 5.5 GHz

The cross polar level of the antenna is comparatively higher compared to the previous designs. This is due to nearly equal current in the X and Y directions corresponding to the three resonances. Also the half power beam width of the antenna in the first band is 40° in the E plane and 80° in the H plane. In the second band they are around 80° in the E plane and 30° in the H plane and the for the third band the measured HPBWs are 100° and 110° along E and H planes respectively.

The polarization of the antenna is also experimentally determined and it is found that the antenna is polarized along the Y direction for the three bands.

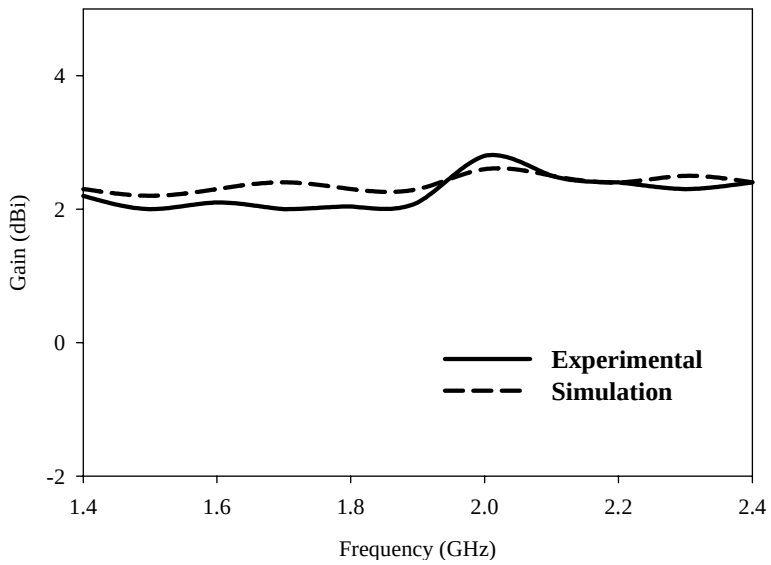

Fig.3.61. Measured and simulated gain of the triple band antenna in the first band

The measured and simulated gains of the antenna in the two bands are given in fig.3.61 and 3.62. The gain in the band remains almost constant. The antenna has an average gain of 2.5dBi in the first band and 1.95dBi in the second band. The efficiency of the antenna is 85 % at 1.74 GHz, 80 % at 2.34 GHz and 77% at 5.5 GHz .

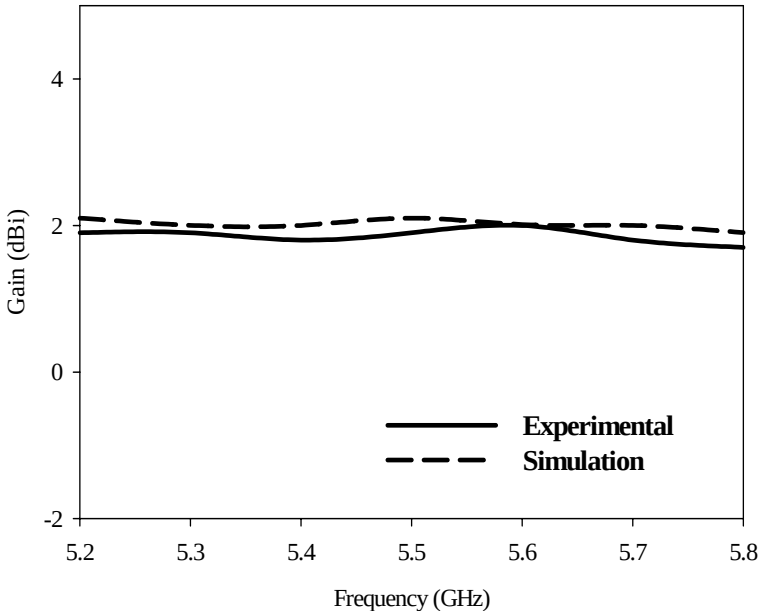

Fig.3.62. Measured and simulated gain of the triple band antenna in the second band

3.6.7 Conclusion

The chapter provides a detailed study of the Asymmetric coplanar strip fed antennas. Various planar feeding mechanisms have been explored. The Asymmetric coplanar strip is chosen as the best suited for feeding compact uniplanar antennas. Single band, dual band and multi band antennas are designed using the above feed and studied thoroughly. These antennas exhibit good radiation and reflection characteristics. The ACS fed antenna designs gives 46 % area reduction compared to other designs using conventional feeds and are thus ideal candidates for compact wireless applications.

References

[1] Constantine A Balanis "Antenna theory analysis and design" John Wiley and Sons II nd edition

[2] Ramesh Garg,Prakash Bhartia and Inder Bahl,Microstrip Antenna Design Hand book, 1st ed. MA Artech House, 2001.

[3] Mariani, E.A. Heinzman, C.P.; Agrios, J.P, Cohn, S.B, “SlotLine characteristics”, IEEE Transactions on Microwave Theory and Techniques, Volume 17, Issue 12 Page(s):1091 – 1096, Dec 1969

[4] Wen-Hua Tu, and Kai Chang, Balun Wide-Band Microstrip-to-Coplanar Stripline/Slotline Transitions IEEE transactions on Microwave theory and techniques, vol. 54, no. 3, march 2006

[5] Zhi Ning Chen And Michael Y. W. Chia, “Broad band planar antennas design and applications" John Wiley & sons , Ltd

…….ꕥ……

Chapter 4

ASYMMETRIC COPLANAR STRIP FED ULTRA COMPACT ANTENNAS

Contents

The chapter presents the design and development of Asymmetric coplanar strip fed Ultra compact antennas with sizes of the order of $\lambda_d/5 \times \lambda_d/18$ and less. The previously studied inverted L antenna is taken as the starting design here also. This design is effectively modified for constructing ultra compact antennas for RFID/GSM and DVB-H applications.

4.1 Introduction

The present day wireless communication devices require ultra compact designs owing to the drastic decrease in size of wireless gadgets. Metamaterial based structures, electronic band gap based designs etc are being developed to cater to the growing demands of compact antennas. But they offer low band width and are difficult to be mounted in practical devices. Also this increases the cost and

complexity of the gadget as a whole. Hence designers are still in search of viable alternatives for designing ultra compact ultra wide band antennas.

In this chapter the design and development of ultra compact planar antennas using the Asymmetric coplanar strip feed is discussed in detail. Emphasis is given to the design of the feed as well as the radiating structure by effectively using the entire real estate available for antennas. As a result wide band compact designs of the order of $\lambda_d/5 \times \lambda_d/18$ and less with simple structures have been realized. The antennas exhibit good reflection and radiation characteristics in the entire operating band and can be effectively used in compact wireless gadgets.

4.2 Planar ACS fed inverted L antenna

To design the ultra compact antenna the inverted L monopole discussed in the previous chapter is taken as the starting design. A simple inverted L strip excited by the ACS is shown in Fig.4.1

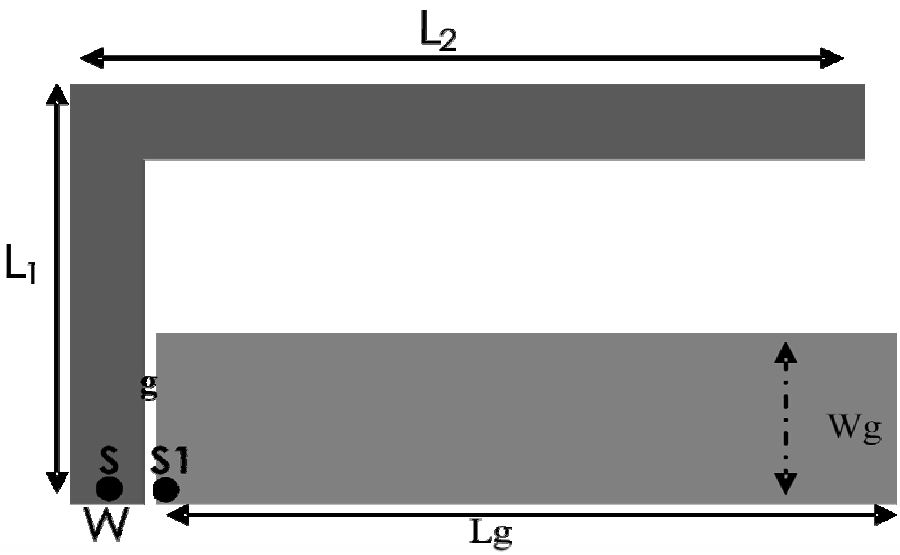

Fig.4.1. ACS fed Inverted L antenna
L_1=20 mm, L_2=42mm, W=3 mm, L_g =38.5, Wg = 6 mm,g =0.5 mm, h=1.6 mm, ε_r =4.4

The centre conductor of the coaxial connector is connected to the point S and the ground to S1. The dimensions of the antenna are chosen for operating at 1.1 GHz.

The return loss curve of the antenna is shown in fig.4.2. The antenna resonates at 1.17 GHz and 3.6 GHz. Note that the impedance matching is poor compared to the previous inverted L antenna because the design criteria given in the previous chapter (chapter 3) is not completely considered here (only the total length, $L= L_g+L_1 + L_2$ is taken to be equal to 0.55 times the dielectric wavelength corresponding to the first resonant frequency).

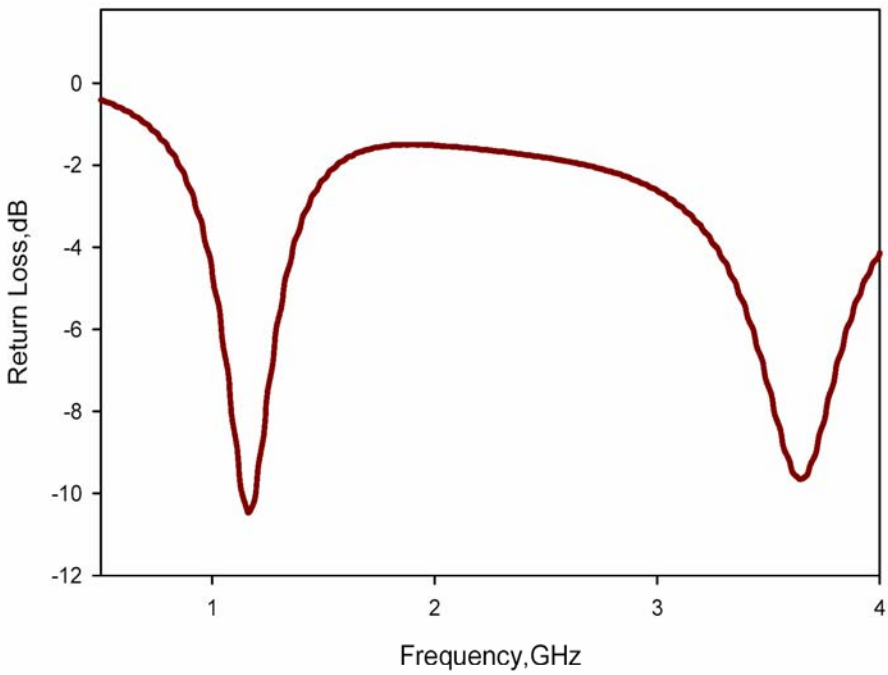

Fig.4.2. Return Loss curve of the ACS fed Inverted L antenna
L_1=20 mm, L_2=42mm, W=3 mm, L_g =38.5, Wg = 6 mm,
g =0.5 mm, h=1.6 mm, ε_r =4.4

The current distribution of the antenna is given in fig.4.3. The modes excited are indentified to be of the first and third order from the figure.

4.2.1 Current distribution in the inverted L antenna

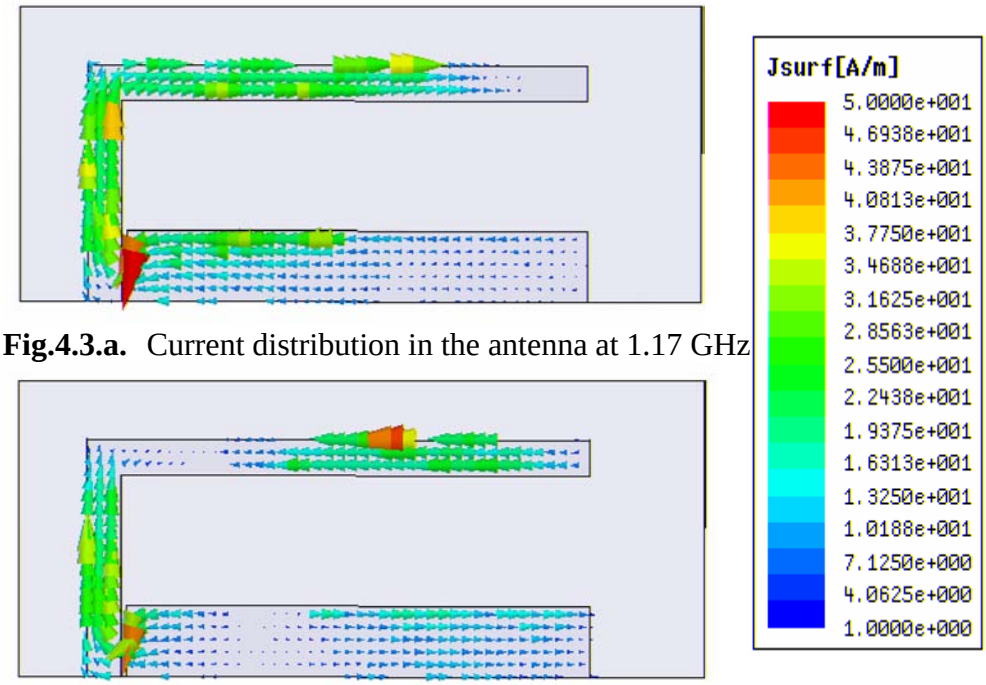

Fig.4.3.a. Current distribution in the antenna at 1.17 GHz

Fig.4.3.b. Current distribution in the antenna at 3.56 GHz
L_1=20 mm, L_2=42mm, W=3 mm, L_g =38.5, Wg = 6 mm,g =0.5 mm, h=1.6 mm, ε_r =4.4

The figure clearly shows the excitation of one half wave variation corresponding to 1.17 GHz (Fig.4.3.a.) and three half wave variations corresponding to 3.56 GHz (Fig.4.3.b.).It is interesting to note that the second harmonic is not excited.

To explore the reason for the absence of the second harmonic the input impedance of the inverted L antenna is studied.

4.2.2 Input Impedance variation in the inverted L antenna

The input impedance of the antenna in the entire band is plotted in fig.4.4. From the figure it can be seen that the input impedance of the antenna corresponding to the second harmonic is high of the order of 600 Ω.

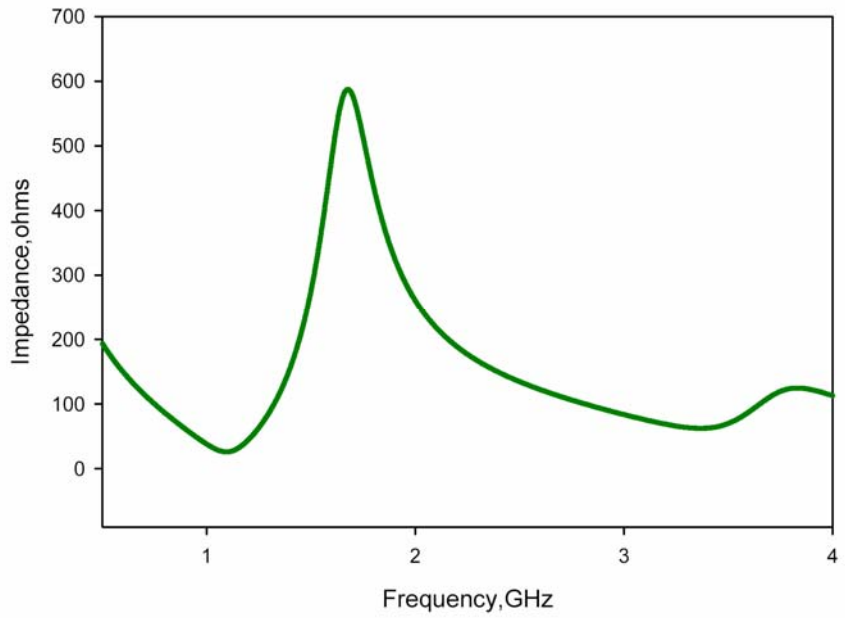

Fig.4.4. Input impedance of the ACS fed inverted L antenna
L_1=20 mm, L_2=42mm, W=3 mm, W_g =38.5, Lg = 6 mm,
g =0.5 mm, h=1.6 mm, ε_r =4.4

The above behavior can be explained by approximating the inverted L antenna as a two wire transmission line with the signal strip connected to one terminal and the ground plane to the other. The schematic is shown in fig.4.5.

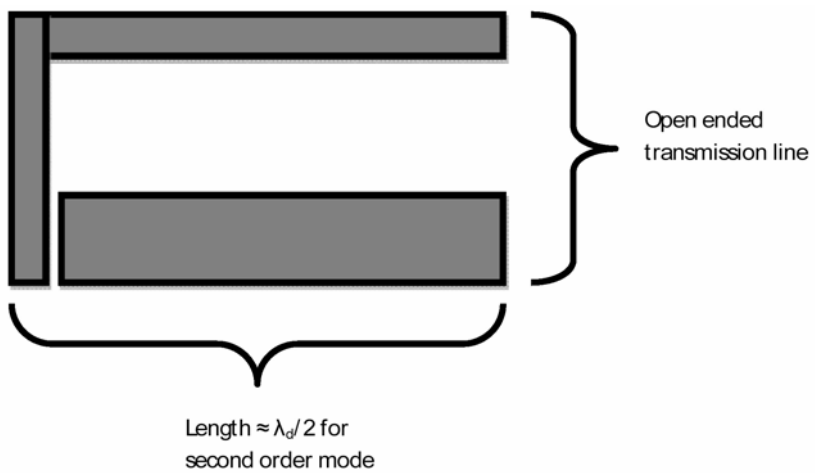

Fig.4.5. Schematic of the ACS fed inverted L antenna

Corresponding to the second order mode the total length of the transmission line becomes nearly equal to $\lambda_d/2$. This is similar to the case of an open ended transmission line having a length $\lambda_d/2$.The input impedance of such a transmission line is given by

$$|Z_{in}| = Z_o \cot(\beta L) \quad \text{.....(4.1)}$$

where Z_{in} is the input impedance, Z_o is the characteristic impedance, β is the phase constant and L is the length of the transmission line. The phase constant β is given as

$$\beta = 2\pi/\lambda_d \quad \text{.....(4.2)}$$

Where λ_d is the dielectric wavelength

When the length L approaches $\lambda_d/2$, the input impedance approaches infinity.

A similar effect is noted in the case of the ACS fed inverted L antenna and this causes the input impedance to be high corresponding to the second harmonic.

If the above assumption is true the reverse phenomena should occur when the open ends of the ACS fed antenna are shorted. i.e, the input impedance should be high for odd modes.

To study this effect the signal strip is shorted to the ground plane as shown in fig.4.6.

4.3 Planar ACS fed shorted inverted L antenna

The validity of the above assumption also necessitates the excitation of only even modes in the case of shorted inverted L antenna. Hence the inverted L strip is bent and shorted to the ground plane as shown in Fig.4.6.

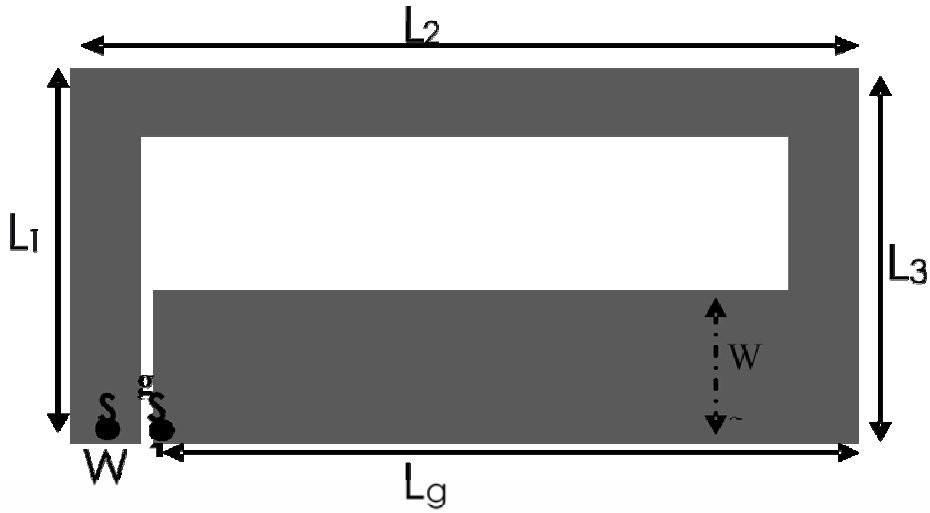

Fig.4.6. ACS fed loop antenna
L_1=20 mm, L_2=42mm, L_3=20 mm W=3 mm, L_g =38.5, Wg = 6 mm, g=0.5 mm, h=1.6 mm, ε_r =4.4

The return loss curve of the above antenna is shown in fig.4.7. The resulting antenna resonates at 2.58 GHz with good matching.

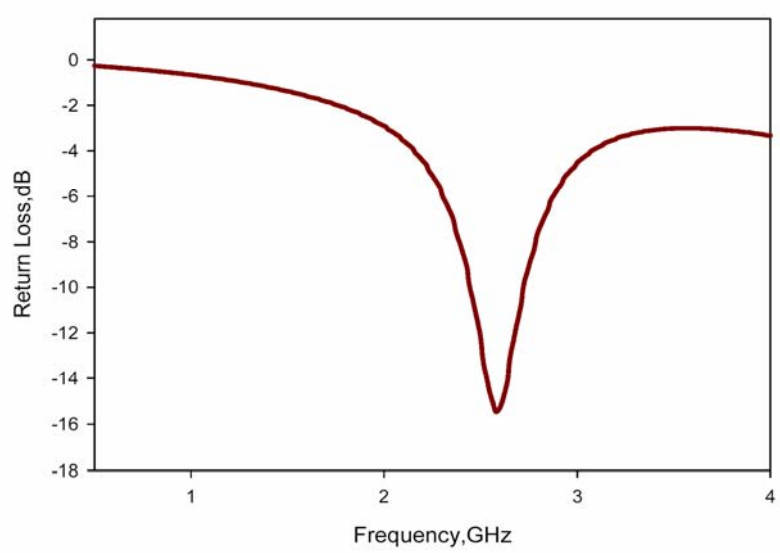

Fig.4.7. Return Loss characteristics of the ACS fed shorted inverted L antenna
L_1=20 mm, L_2=42mm, L_3=20 mm W=3 mm, L_g =38.5, Wg = 6 mm, g=0.5 mm, h=1.6 mm, ε_r =4.4

To identify the mode excited the current distribution in the antenna is also plotted.

From the current distribution in the antenna in fig.4.8 the excited mode is identified to be of the second order.

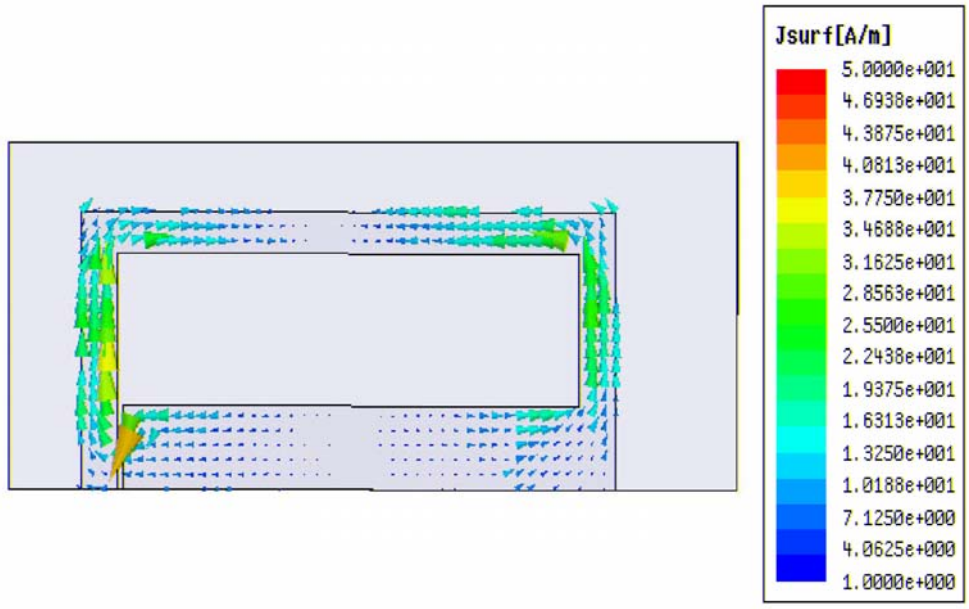

Fig.4.8. Current distribution in the shorted inverted L antenna at 2.57 GHz L_1=20 mm, L_2=42mm, W=3 mm, L_g =38.5, Wg = 6 mm,g =0.5 mm, h=1.6 mm, ε_r =4.4

Also from the return loss curve it is clear that the first and third harmonics at 1.1 and 3.5 GHz respectively are not excited. The input impedance of the antenna in this configuration is also plotted in fig.4.9. From the figure it is evident that the input impedance corresponding to the first harmonic is very high (capacitive reactance) compared to the second harmonic and hence is not excited. The impedance of the third harmonic is also high (capacitive reactance).

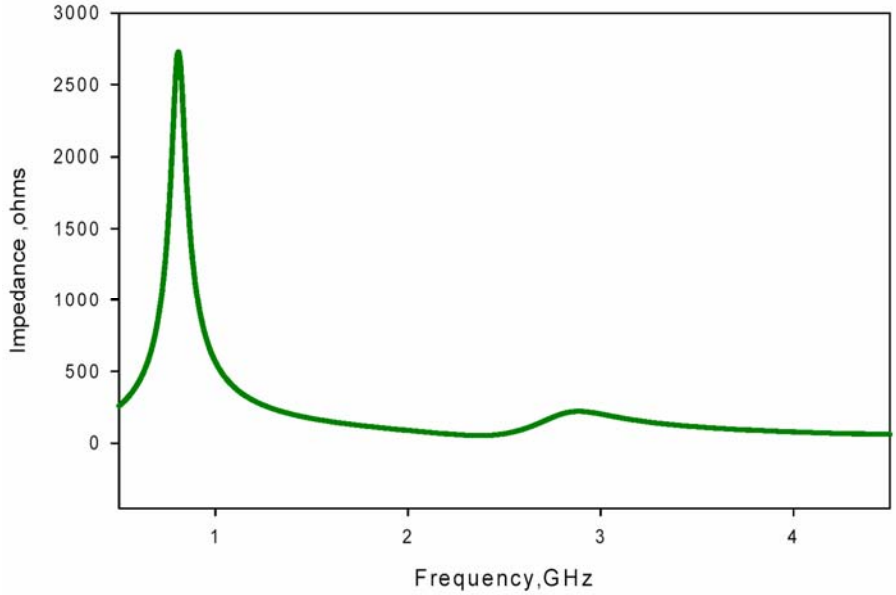

Fig.4.9. Input impedance of the ACS fed shorted inverted L antenna L_1=20 mm, L_2=42mm, L_3=20 mm W=3 mm, L_g =38.5, Wg = 6 mm, g=0.5 mm, h=1.6 mm, ε_r =4.4

4.3.1 L_1,L_3 variation studies in the shorted inverted L antenna

To find out the possibility of compensating the input impedance (changing the coupling) by varying the height of the geometry of the structure, the length of the strips L_1 and L_3 are varied simultaneously as shown in fig.4.10. But these variations do not bring about much effect in the impedance and hence the matching of other harmonics are not improved. Only the impedance matching of the second mode is affected. Also the resonant frequency decreases with increase in the value of L_1 and L_3.

The impedance curve in fig.4.9 shows very high capacitive reactance corresponding to the first harmonic. To compensate for this high capacitive reactance, a viable technique will be to suitably insert a small slot in the structure. Thus a narrow slot is inserted in the shorted inverted L antenna. The geometry of the resulting structure is shown in the next section in fig.4.11.

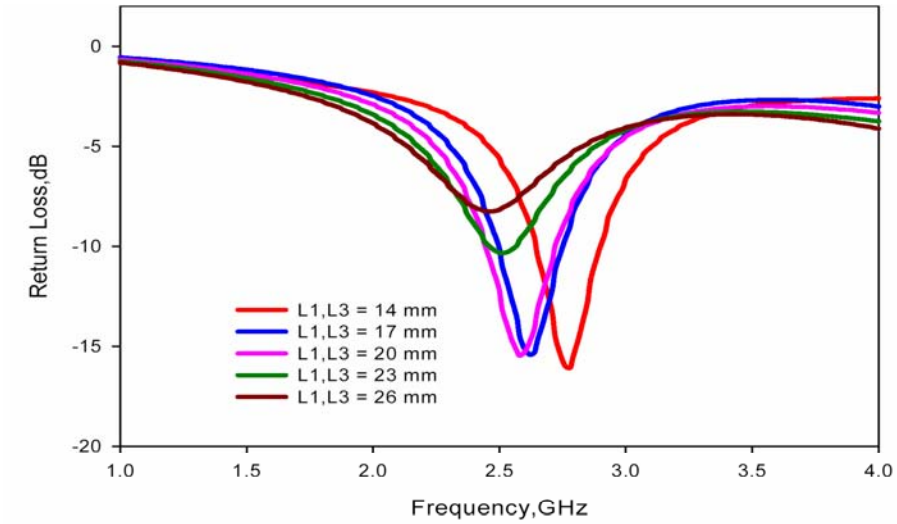

Fig.4.10. Variation of L_1, L_3 in the Loop antenna
L_1=20 mm, L_2=42mm, L_3=20 mm W=3 mm, L_g =38.5, Wg = 6 mm, g=0.5 mm, h=1.6 mm, ε_r =4.4

The position of the slot is chosen to be at the point of minimum current intensity obtained from fig.4.8.

4.4 Planar ACS fed shorted inverted L antenna with the slot

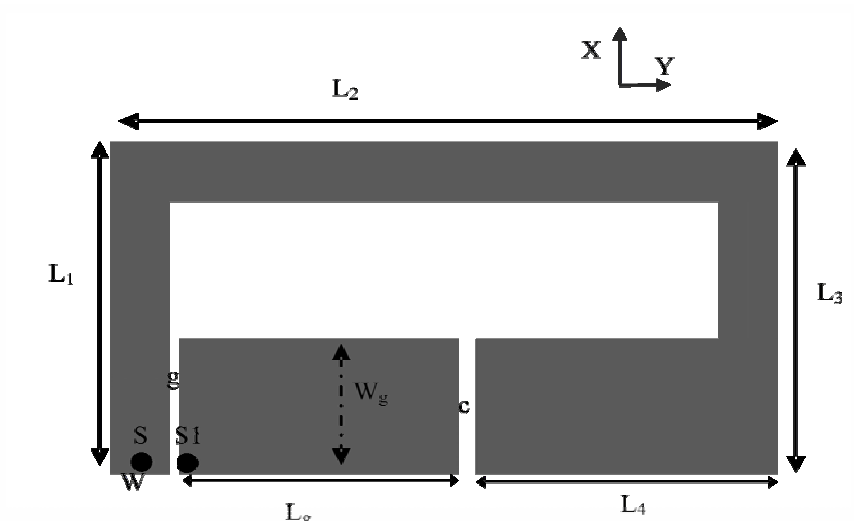

Fig.4.11. ACS fed inverted L antenna with the slit 'c'
L_1=20 mm, L_2=42mm, L_3=20 mm, L_4 =24 mm, W=3 mm, c = 1 mm, L_g =13.5, Wg = 6 mm, h=1.6 mm, ε_r =4.4

The geometry of the antenna with the slot is shown in the fig.4.11.The dimensions of the slot are chosen as C x W_g.. The insertion of the slot excites dual resonances centered at 830 MHz and 2.58 GHz with good impedance matching. The return loss of the antenna is shown in fig.4.12.

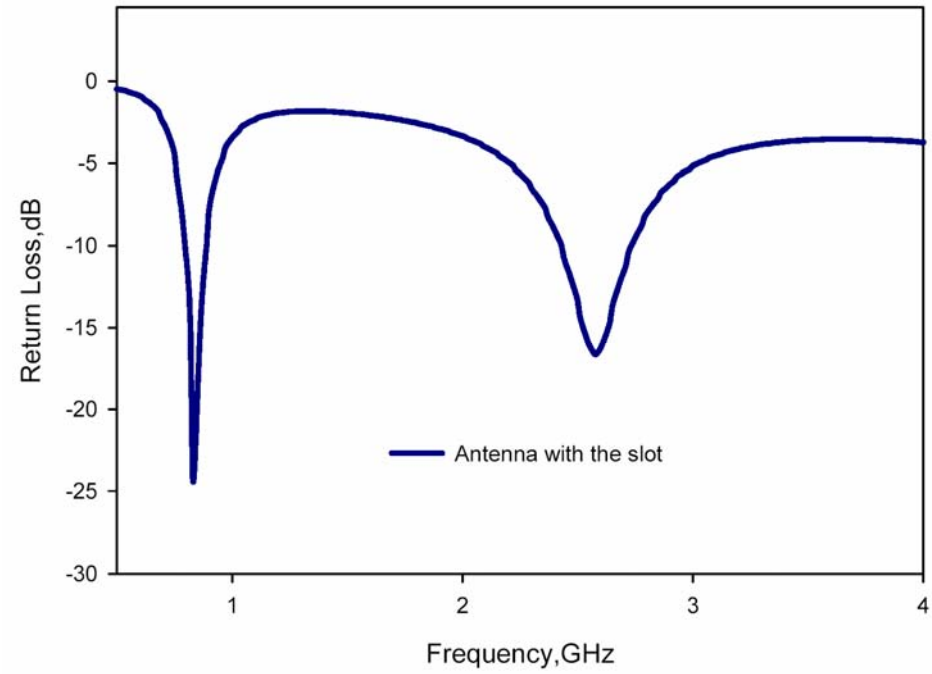

Fig.4.12. Return loss curve of the shorted inverted L antenna with the slot L_1=20 mm, L_2=42mm, L_3=20 mm, L_4 =24 mm, W=3 mm, c = 1 mm, L_g =13.5, Wg = 6 mm, h=1.6 mm, ε_r =4.4

4.4.1 Impact of the position of the slot

From fig.4.8 it can be seen that there are two positions of current minimum in the antenna structure. The first position is obviously in the ground strip along L_g. The second current minimum position is along the strip L_2.

To find out the impact of the position of the slot, the return loss characteristics of the antenna (with the slot in both the positions of minimum

current intensity) are shown in fig.4.13. It can be observed from the figure that the better matching for the first resonance is noted when the slot is inserted in the strip L_g. Also the second resonance is shifted to the band of interest (2.4 GHz WLAN) Hence the antenna with the slot along L_g is chosen as the final design.

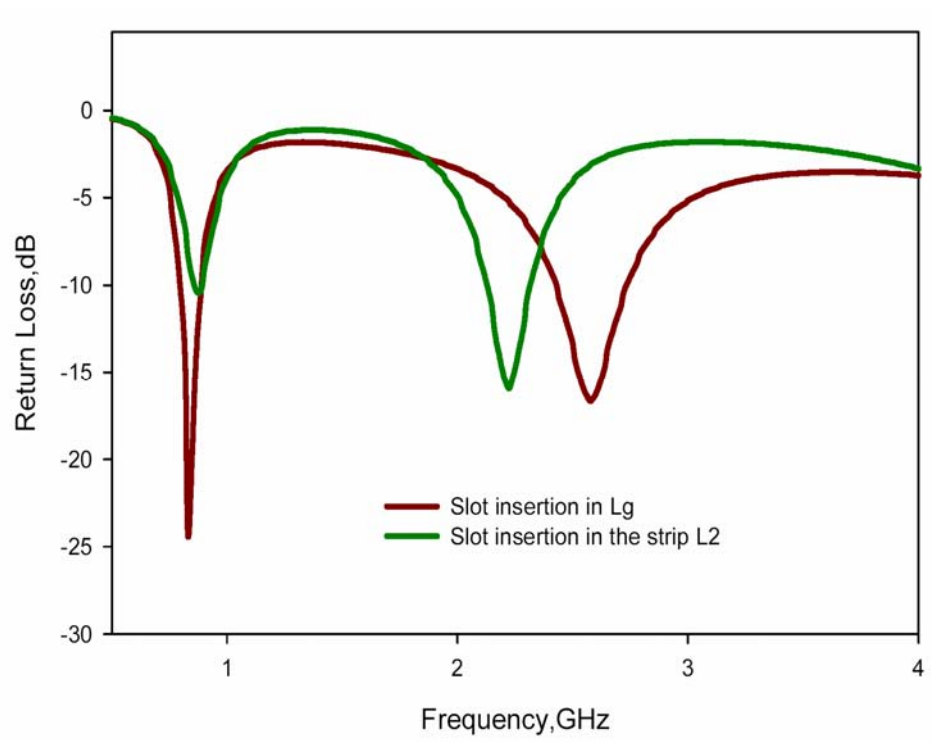

Fig.4.13. Return loss of the inverted L antennas with the slot 'c' at different positions
L_1=20 mm, L_3=20 mm, L =24, w=3 mm, c = 1 mm, Wg = 6 mm, h=1.6 mm, ε_r =4.4

The input impedance of the final antenna with the slot is shown in fig.4.14. Comparing with the input impedance of the shorted inverted L antenna in fig.4.9, it can be seen that the high impedance corresponding to 900 MHz has been nullified by the slot.

The resulting impedance, after slot insertion, corresponding to the third harmonic is found to be capacitive and hence it is not excited.

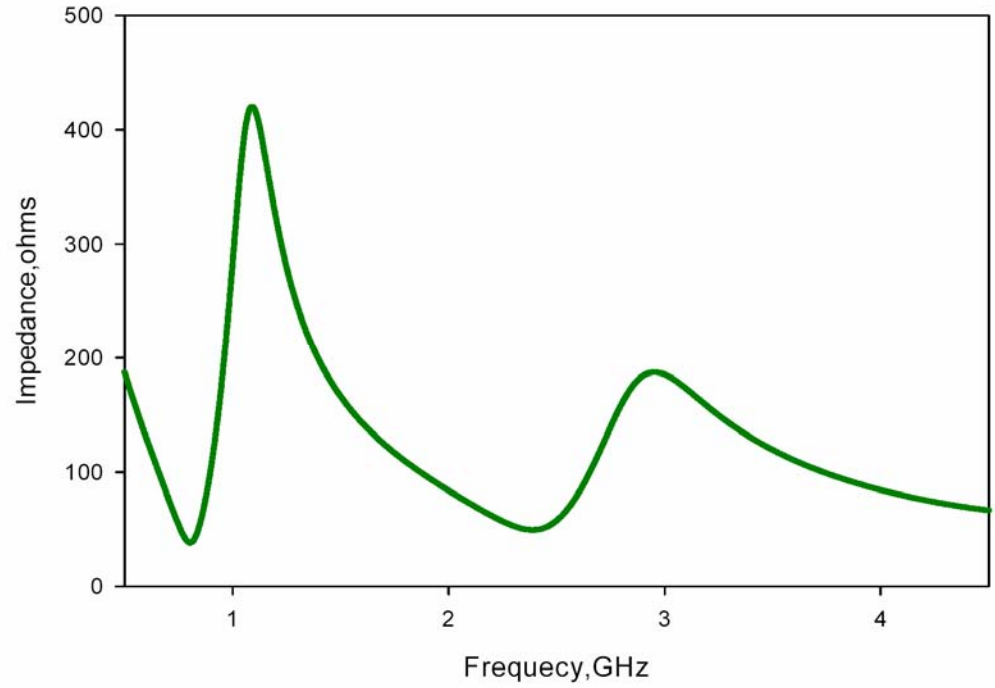

Fig.4.14. Input impedance of the ACS fed inverted L antenna
L_1=20 mm, L_2=42mm, L_3=20 mm, L_4 =24 mm, W=3 mm,
c = 1 mm, L_g =13.5, Wg = 6 mm, h=1.6 mm, ε_r =4.4

To clearly understand the characteristics of the antenna and to obtain optimum dimensions a thorough study has been performed by varying the different parameters of the slot.

4.4.2 Effect of position of the slot

The position of the slot highly determines the characteristics of the two resonances. The variation in the return loss characteristics of the antenna for various positions of the slot ‘c’ from the feed point is shown in Fig.4.15.

The first resonance nearly remains the same in all the cases and therefore it can be concluded that this resonance is due to the total length of the inverted L structure.

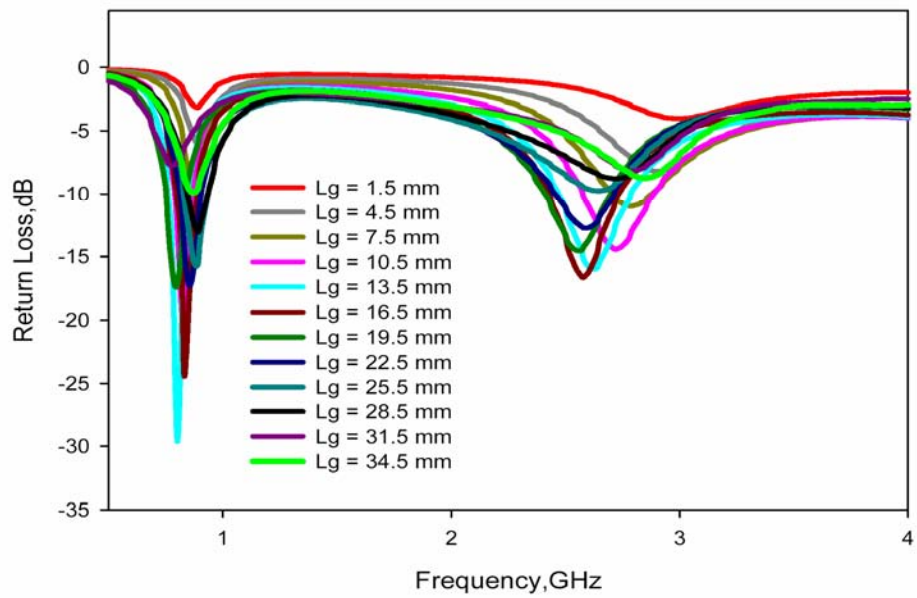

Fig.4.15. Slot position variation studies
L_1=20 mm, L_2=42mm, L_3=20 mm, L4 =3 mm, W=3 mm, c = 1 mm, Wg = 6 mm, h=1.6 mm, ε_r =4.4

The second resonance varies with the position of the slot. It is found that as the slot is moved away from the current minimum position, along both sides, the resonant frequency increases. It is observed that the insertion of the slot at high current intensity positions perturbs the field distribution in the antenna thereby increasing the resonant frequency. Best performance is obtained when the slot is inserted nearly at L_g= 13.5 mm (i.e, when L_g =0.13 L, where L = $L_1+L_2+L_3+L_4+Lg$ is the total length of the loop structure).

It can be observed that a small range of frequency tuning is possible for the second resonance by shifting the slot on either sides of the optimum slot

position. In this case the second resonant frequency can be varied by 10% by varying the position of the slot without deteriorating the matching of the first and the second resonances. This is highly desirable while realizing the antenna for practical applications.

The current distributions in the antenna for the two resonances are given in fig.4.16. A clear half wave variation can be seen in the entire structure corresponding to the first resonance and two half wave variations can be observed corresponding to the second resonance.

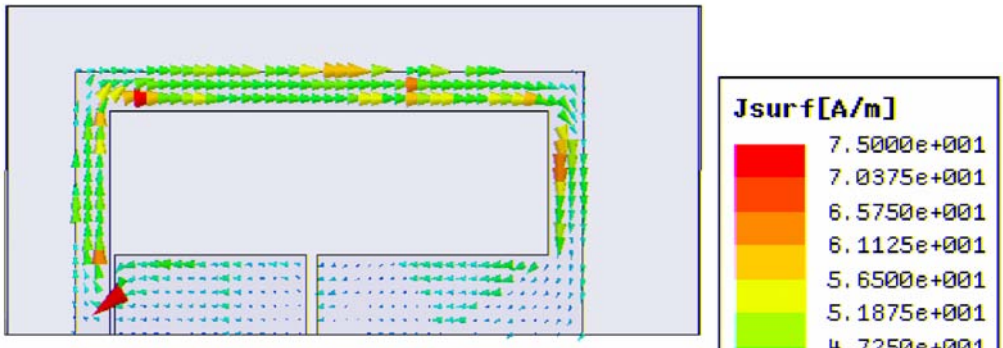

Fig.4.16.a. Current distribution at 830 MHz

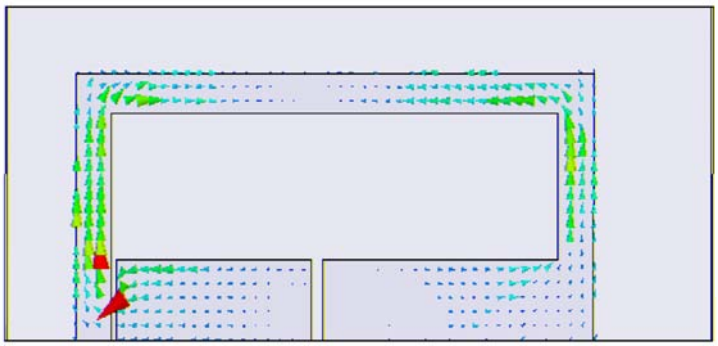

Fig.4.16.b. Current distribution at 2.58 GHz

L_1=20 mm, L_2=42mm, L_3=20 mm, L_4 =3 mm, W=3 mm,
c = 1 mm, Wg = 6 mm, L_g = 13.5 mm, h=1.6 mm, ε_r =4.4

4.4.3 Effect of Slot width

The influence of the width of the slot in the impedance matching of the antenna is shown in fig.4.17.

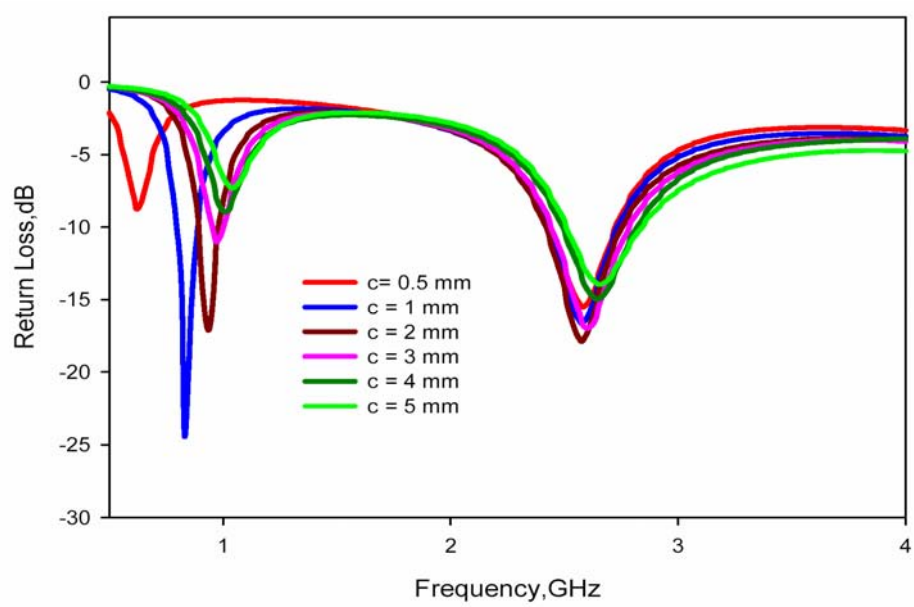

Fig.4.17. Variation in the response of the antenna with the slot width 'c' L_1=20 mm, L_2=42mm, L_3=20 mm, L4 =3 mm, W=3 mm, c = 1 mm, W_g =34.5, Lg = 6 mm, h=1.6 mm, ε_r =4.4

The impedance matching of the first resonance changes appreciably with the width of the slot. The matching deteriorates with larger slot widths owing to the increase in capacitive reactance. In the case of this design the optimum slot width is taken as 1 mm.

There is also a slight variation in the first resonance along with the slot width. This is due to the variation in the total length of the antenna. The effect of the slot is found to be less in the case of the second resonance. From the above studies the following inferences can be drawn upon.

The first resonance is due to the total length of the loop structure

i.e, $L_1+L_2+L_3+L_4+Lg = 0.5\ \lambda_{d1}$ .....(4.3)

The second resonance corresponds to the second harmonic and is given by

$L_1+L_2+L_3+L_4+Lg = 1.5\ \lambda_{d2}$ .....(4.4)

where λ_{d1} and λ_{d2} are the dielectric wavelengths corresponding to the first and second resonant frequencies.

From exhaustive experimental and simulation studies the ratio of L_1/L_2 is maintained as 0.5 for better performance.

In the case of the second resonant frequency, the resonance can be varied by 10% by changing the position of the slot without deteriorating the matching of the first and the second resonances.

It has to be noted that the antenna is resonating at 870 MHz and 2.5 GHz which are nearer to the 900/2400 MHz frequency bands. These bands are of high interest to designers working in the field of RFID antennas. Also the antenna occupies ultra compact dimensions of 42 mm x 20 mm on a substrate of dielectric constant 4.4 and height 1.6 mm. These dimensions come to the order of $\lambda_d/5$ x $\lambda_d/18$, corresponding to the lowest working frequency of the antenna. The antenna also has moderately larger band width and impedance matching which is very difficult to achieve using the conventional design methodologies reported in literature. Moreover, the design is simple and uniplanar. All the above factors portray the antenna as an ideal choice for compact wireless applications.

The inferences obtained from the above studies are used to design a dual band antenna for RFID applications in the UHF/2.4GHz bands. The dimensions are optimized as L_1=14 mm, L_2=48 mm, L_g=30.5 mm, L_3 =14 mm,L_4=13 mm, W =3 mm, Wg = 6 mm, c=1 mm, h=1.6 mm, ε_r =4.4.

4.4.4 Reflection characteristics of the ACS fed dual band antenna

The return loss characteristics of the dual band antenna are shown in fig.4.18. The antenna operates with a 2:1 V**S**WR bandwidth from 800 MHz to 1 GHz and from 2.24 GHz to 2.50 GHz with good impedance matching. The antenna can be effectively used for the RFID applications in the 860 to 930MHz band and in the 2.4 GHz range.

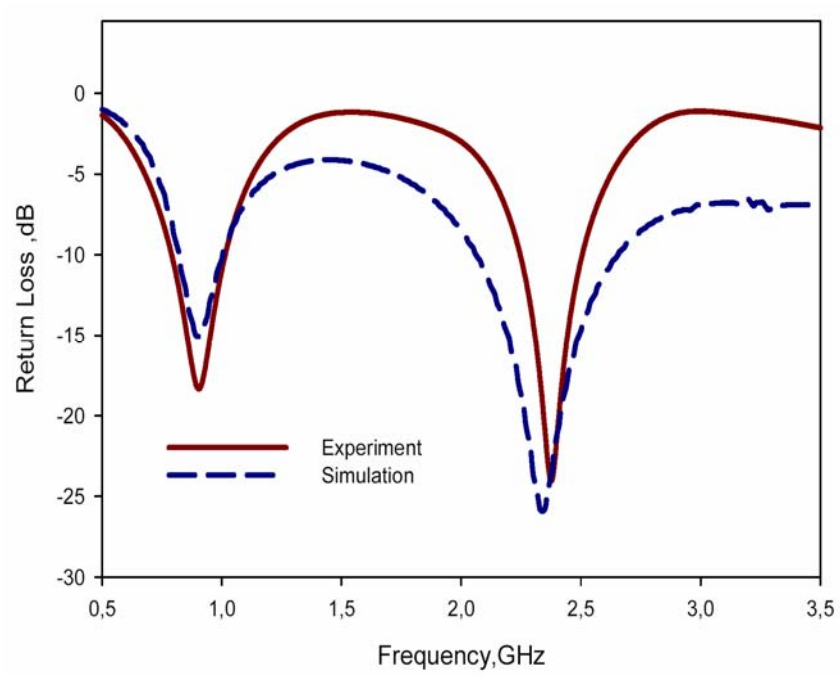

Fig.4.18. Return Loss characteristics of the dual band antenna
L_1=14 mm, L_2=48 mm, W_g=30.5 mm, L_3 =14 mm,L_4=13 mm,
W =3 mm, Wg = 6 mm,L_g = 30.5 mm,c=1 mm, h=1.6 mm, ε_r =4.4.

4.4.5 Radiation characteristics of the ACS fed dual band antenna

The 3-D radiation patterns of the antenna for the two resonances at 860 MHz and 2.4 GHz are shown in fig.4.19.

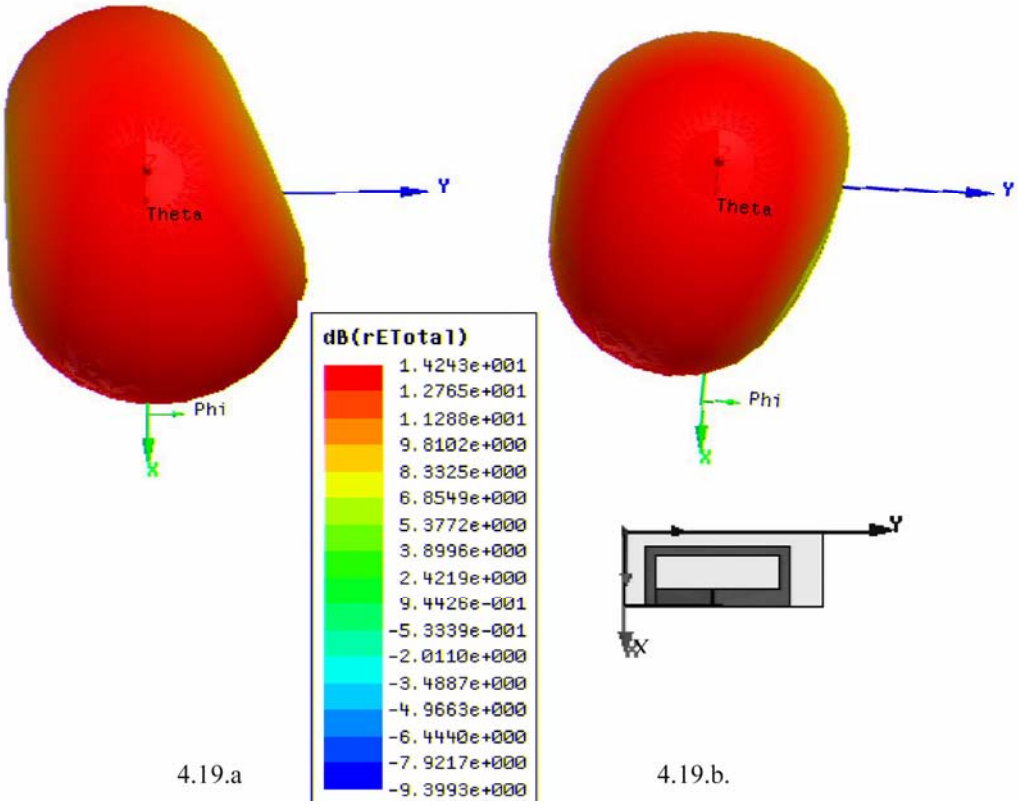

Fig.4.19. 3-D radiation pattern of the antenna at (a) at 860 MHz (b) at 2.4 GHz

The 2 –D radiation patterns of the antenna are shown in fig.4.20. The cross polar levels are found to be high in the case of the second band owing to equal intensity X and Y directed currents in the antenna, which is evident from the current distribution in fig.4.16.b.

The gain of the antenna is found to be 0.6 dBi at 860 MHz and 2.1 dBi at 2.4 GHz with an efficiency of 42 % and 74 % respectively.

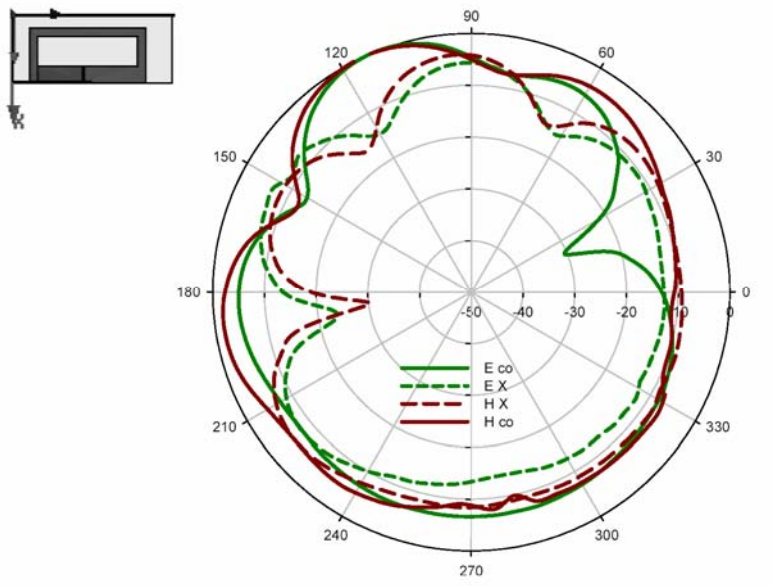

Fig.4.20.a 2-D Radiation pattern of the antenna at 860 MHz

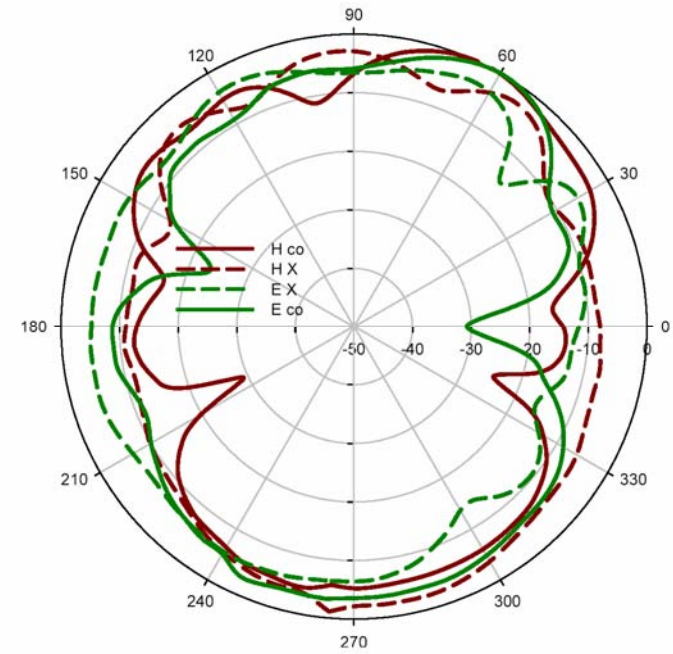

Fig.4.20.b 2-D Radiation pattern of the antenna at 2.4 GHz

To conclude it is worth to note that this compact antenna has a size of only 48 mm x 14 mm when printed on a substrate of dielectric constant 4.4 and height 1.6 mm. The experimental 2:1VSWR bandwidth ranges from 800 MHz to 1 GHz (23 %) and from 2.24 GHz to 2.50 GHz (11%) easily covering the UHF/2.4 GHz RFID bands. The uniplanar nature and the ultra compact size is also an added advantage. The antenna has an overall size of only $\lambda_d/5$ x $\lambda_d/18$ corresponding to the lowest operating frequency, which is far better than the corresponding Metamaterial based and related designs [1]. The antenna also has moderate gain and efficiency in the operating bands which is superior to other compact antenna designs.

4.5 Asymmetric Coplanar Strip fed ultra compact Triple band antenna

The antenna mentioned in the previous section was intended for dual band operations. In this section the design and development of a triple band antenna intended to work in the 900/1800/2400 MHz communication bands is presented.

To design the triple band antenna the method employed here is the creation of an additional current path. A simple technique is the addition of a simple strip to the existing design at the point of minimum electric field intensity without affecting the dual band nature of the antenna.

To find out the position of minimum field intensity the electric field distribution a dual band antenna working at 860 MHz and 2.4 GHz is studied and given as fig.4.21.

4.5.1 Electric field distribution in the dual band antenna

Fig.4.21.a. shows the electric field distribution in the dual band antenna at 860 MHz and Fig.4.21.b show the same at 2.4 GHz.

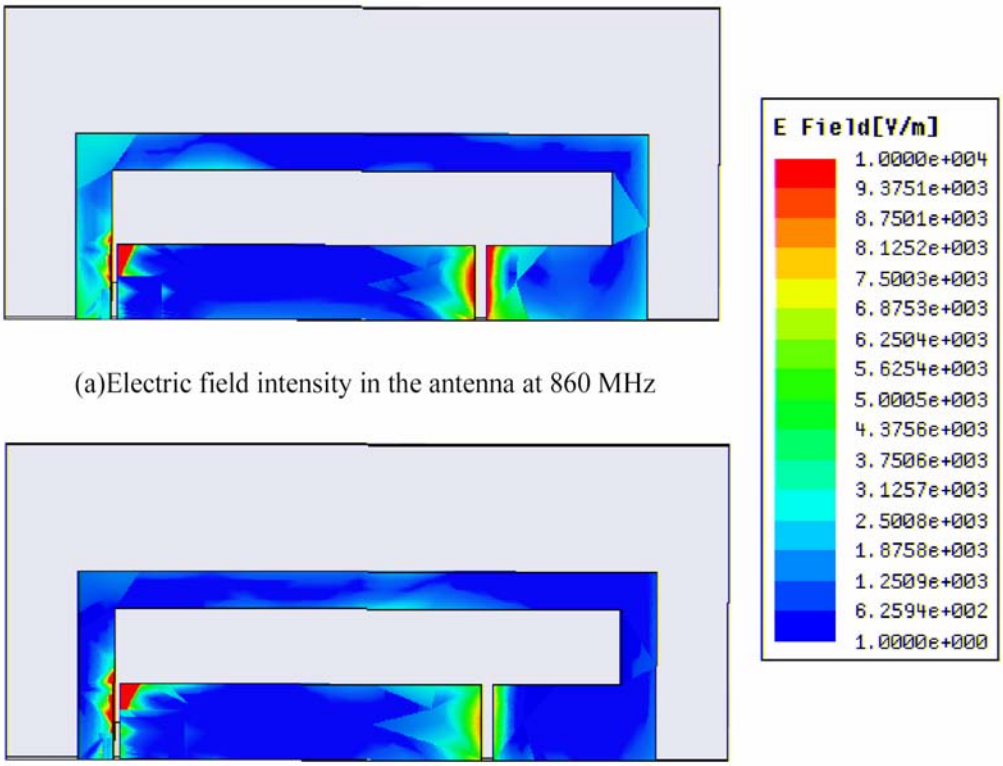

(a)Electric field intensity in the antenna at 860 MHz

(b)Electric field intensity in the antenna at 2.4 GHz

Fig.4.21. Electric field distribution in the dual band antenna
L_1=14 mm, L_2=48 mm, W_g=30.5 mm, L_3 =14 mm,L_4=13 mm, W =3 mm, Wg = 6 mm,L_g = 30.5 mm,c=1 mm, h=1.6 mm, ε_r =4.4.

From the electric field distributions it can be inferred that the predominant locations of minimum field intensity are along the strips L_2, L_3, L_4 and L_g for the two resonances (Fig.4.11).

Hence the additional strip may be attached to any of the strips L_2, L_3, L_4 or L_g. Considering the compactness of the antenna, the location of the additional strip is chosen to be at the intersection of the strips L_2 and L_3.The resulting antenna geometry is given in fig.4.22.

4.5.2 Modified Dual Band antenna for triple band operation

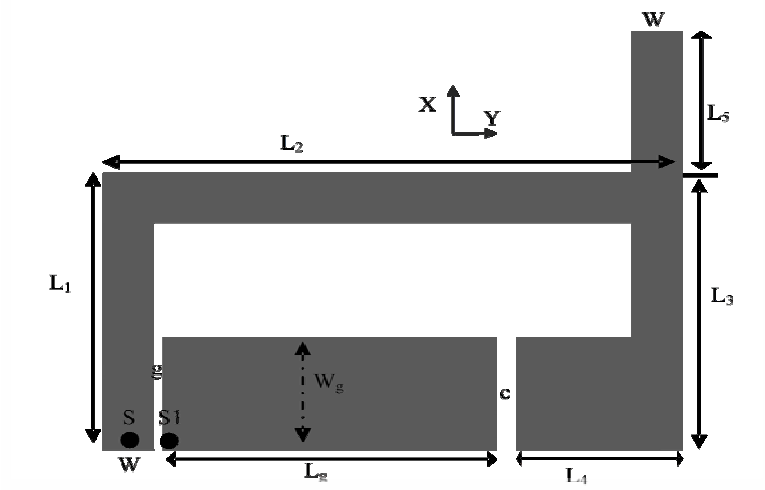

Fig.4.22. Geometry of the triple band antenna
L_1=14 mm, L_2=48 mm, W_g=30.5 mm, L_3 =14 mm,L_4=13 mm, L_5=11 mm, W =3 mm, Wg = 6 mm, L_g = 30.5 mm, c=1 mm, h=1.6 mm, ε_r =4.4.

The antenna shown above resonates in three bands centered at 855 MHz, 2.35 GHz and 4.92 GHz with good impedance matching The return loss characteristic of the antenna is shown in fig 4.23.

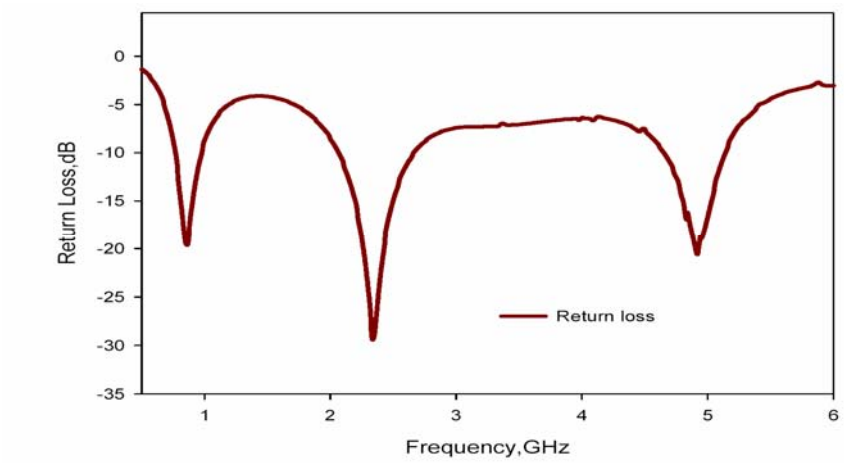

Fig.4.23. Return loss curve of the triple band antenna
L_1=14 mm, L_2=48 mm, W_g=30.5 mm, L_3 =14 mm,L_4=13 mm, W =3 mm, Wg = 6 mm,L_g = 30.5 mm, L_5=11 mm c=1 mm, h=1.6 mm, ε_r =4.4.

It can be seen that the first two resonances remains nearly unaltered even after the insertion of the additional strip.

It can be seen that the length of the additional arm, L_5 is equal to a quarter of the dielectric wavelength corresponding to the excited additional resonance at 4.9 GHz.

To bring down the additional resonance to the frequency band of interest the length of the additional strip has to be increased. Simply increasing the length of L_5, increases the overall dimensions of the antenna. Hence the additional strip is bent in the form of an inverted L as shown in fig.4.24.

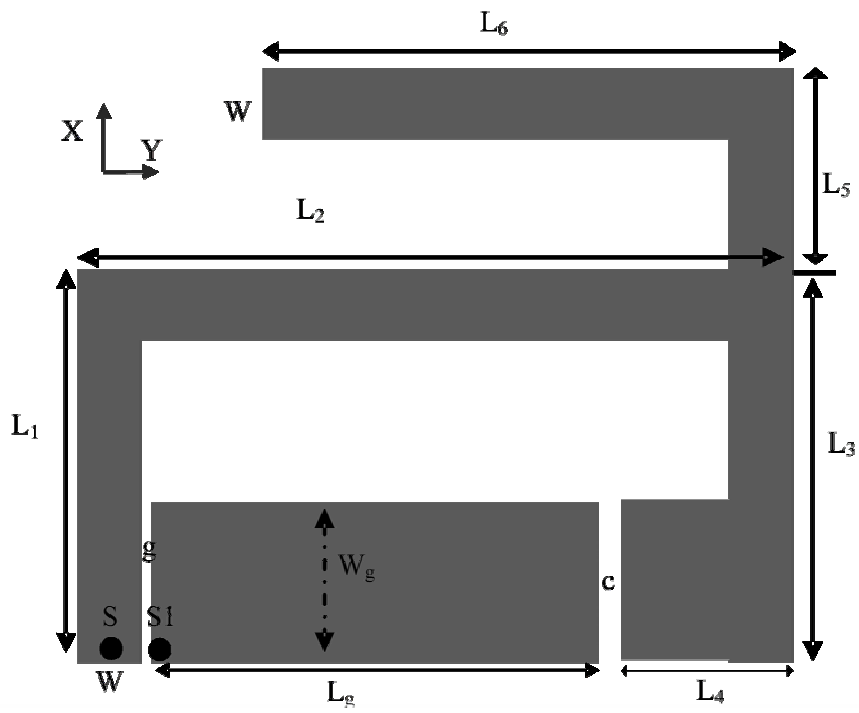

Fig.4.24. Geometry of the triple band antenna
L_1=14 mm, L_2=48 mm, W_g=30.5 mm, L_3 =14 mm,L_4=13 mm, L_5=11 mm, W =3 mm, Wg = 6 mm,L_g = 30.5 mm, c=1 mm, h=1.6 mm, ε_r =4.4.

But bending the strip as shown in figure deteriorates the matching of the new resonance .This is due to the coupling between the strips L_2 and L_6.

Hence to find an optimum spacing between the strips a series of variation studies have been performed keeping the total length of L_5 + L_6 as a constant. This is given in fig.4.25.

4.5.3 L_5 variation studies

The current length (Quarter wavelength) required for the additional resonance at 1.8 GHz is nearly 27.5 mm. Hence the total length of the strips L_5 + L_6 is taken as 27.5 mm and various lengths of L_5 are used to study its influence in antenna performance.

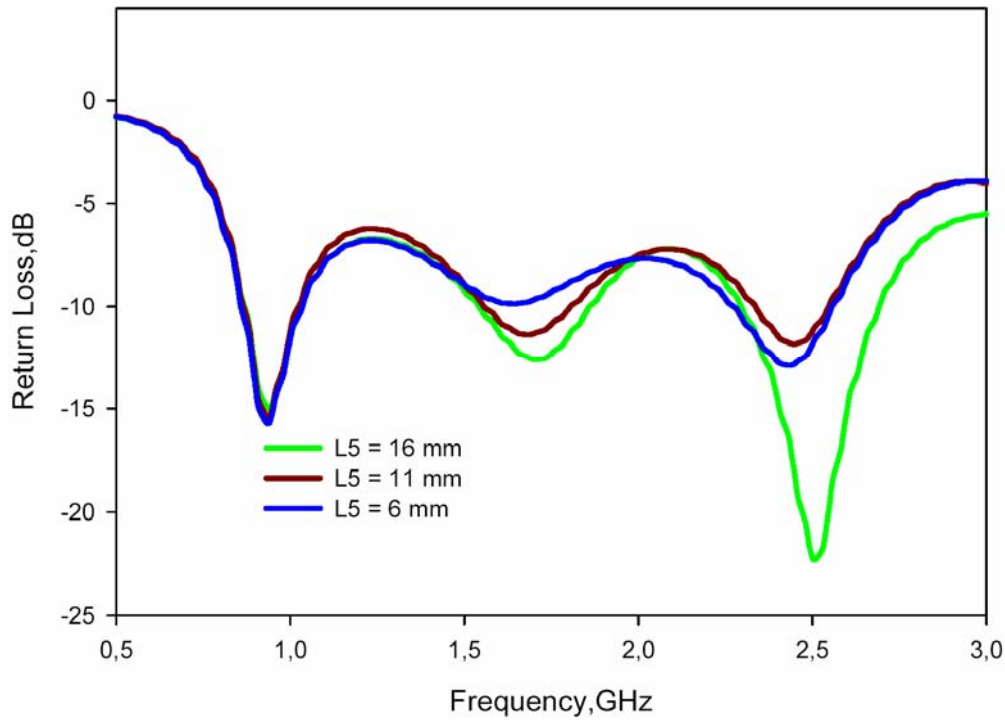

Fig.4.25. L_5 variation studies in the triple band antenna
L_1=14 mm, L_2=48 mm, W_g=30.5 mm, L_3 =14 mm,L_4=13 mm,
W =3 mm, Wg = 6 mm,L_g = 30.5 mm, c=1 mm, h=1.6 mm, ε_r =4.4.

From the variation study in fig.4.25, best performance is noted when L_5 is kept as 16 mm in this antenna. This is obvious since increasing the length of L_5 reduces the coupling between the strips L_2 and L_6. But this increases the overall size of the antenna. Therefore L_5 =11 mm is chosen for this antenna as an optimum length keeping in mind the coupling and compactness size of the antenna. The optimum value of L_5 /L_6 = 0.66 is selected for this antenna.

4.5.4 Final Ultra compact triple band antenna

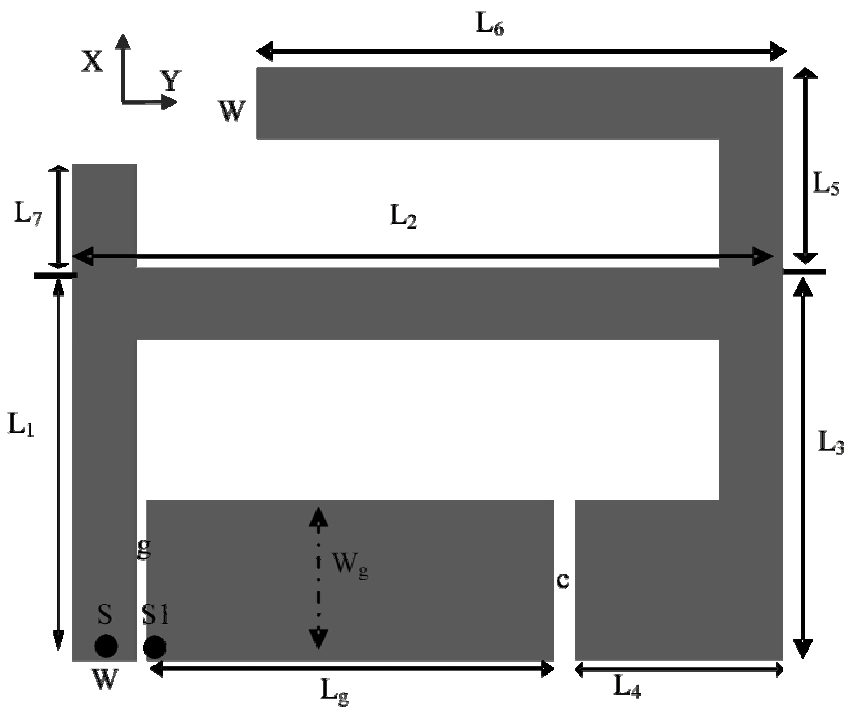

Fig.4.26. Geometry of the Final ultra compact triple band antenna
L_1=14 mm, L_2=48 mm, W_g=30.5 mm, L_3 =14 mm,L_4=13 mm,
W =3 mm, Wg = 6 mm, L_g = 30.5 mm, L_5=11 mm,L_6 =16.5 mm ,
c=1 mm, h=1.6 mm, ε_r =4.4.

From exhaustive simulation and experimental studies it is noted that the matching corresponding to the second resonance is still low. The input impedance corresponding to this resonance is capacitive. To compensate for this impedance the length of the strip L_1 is extended by a length L_7 as shown in fig.4.26.This method is found to be effective in improving the overall performance of the antenna without affecting the compactness. The strip L_7 acts as a stub thereby improving the matching of the antenna.

The variation of the return loss of the antenna with the length of the strip L_7 is shown in fig.4.27.This study is used to find the optimized dimension of the strip L_7.

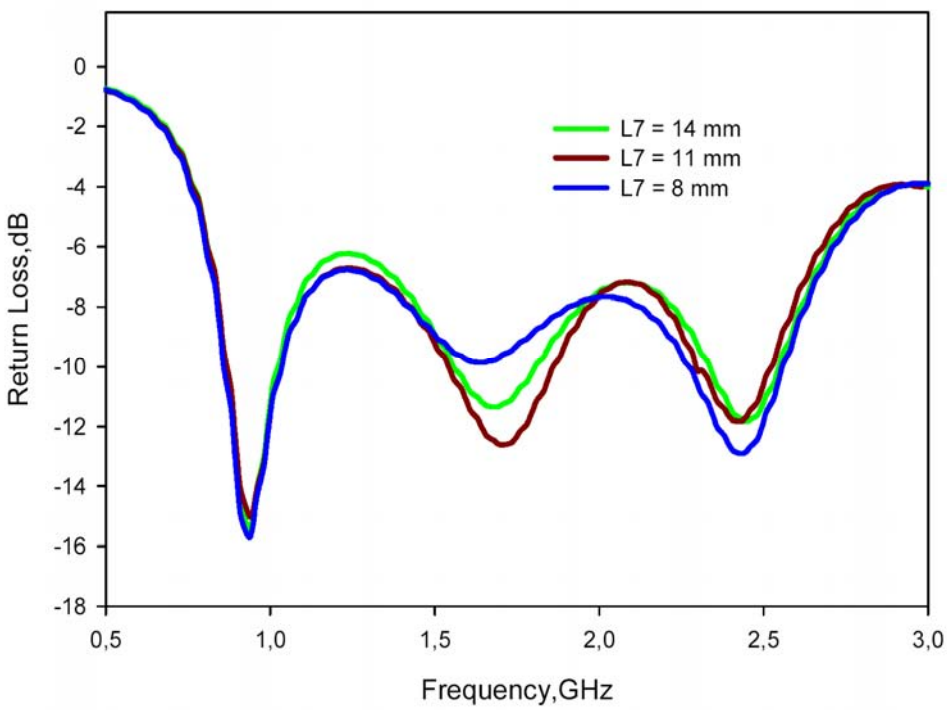

Fig.4.27. Variation of return loss characteristics with the length of the strip L_7
L_1=14 mm, L_2=48 mm, W_g=30.5 mm, L_3 =14 mm,L_4=13 mm, W =3 mm, Wg = 6 mm,L_g = 30.5 mm, L_5=11 mm,L_6 =16.5 mm , c=1 mm, h=1.6 mm

The experimental and simulated return loss curves of the final triple band antenna are shown in fig.4.28. The antenna resonates in three bands from 820 MHz to 1.09 GHz, from 1.69 GHz to 1.90 GHz and from 2.39 GHz to 2.58 GHz with a 2:1 VSWR bandwidth easily covering the GSM 900/1800 and 2.4 WLAN bands.

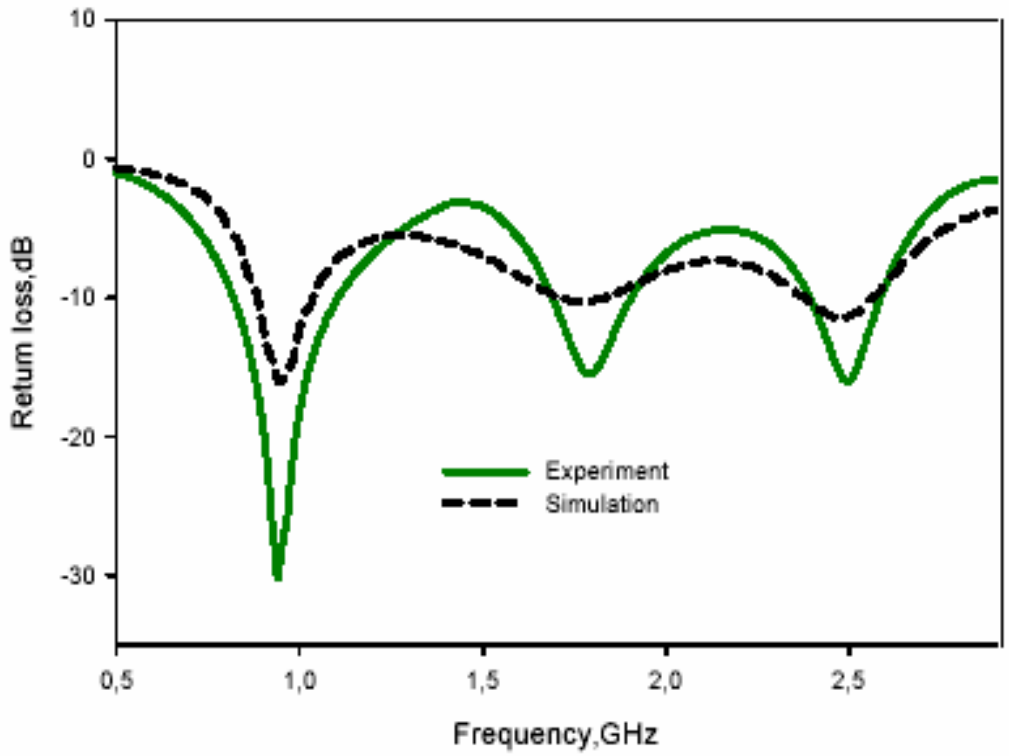

Fig.4.28. Experimental and simulated return loss curves of the final ACS fed ultra compact triple band antenna
L_1=14 mm, L_2=48 mm, W_g=30.5 mm, L_3 =14 mm,L_4=13 mm, W =3 mm,Wg = 6 mm, L_g = 30.5 mm, L_5=11 mm,L_6 =16.5 mm, L_7=8 mm, c=1 mm, h=1.6 mm, ε_r =4.4.

To confirm the resonant paths the surface current distributions in the antenna for the three resonances is studied and is shown in fig.4.29.

4.5.5 Surface current distribution in the antenna

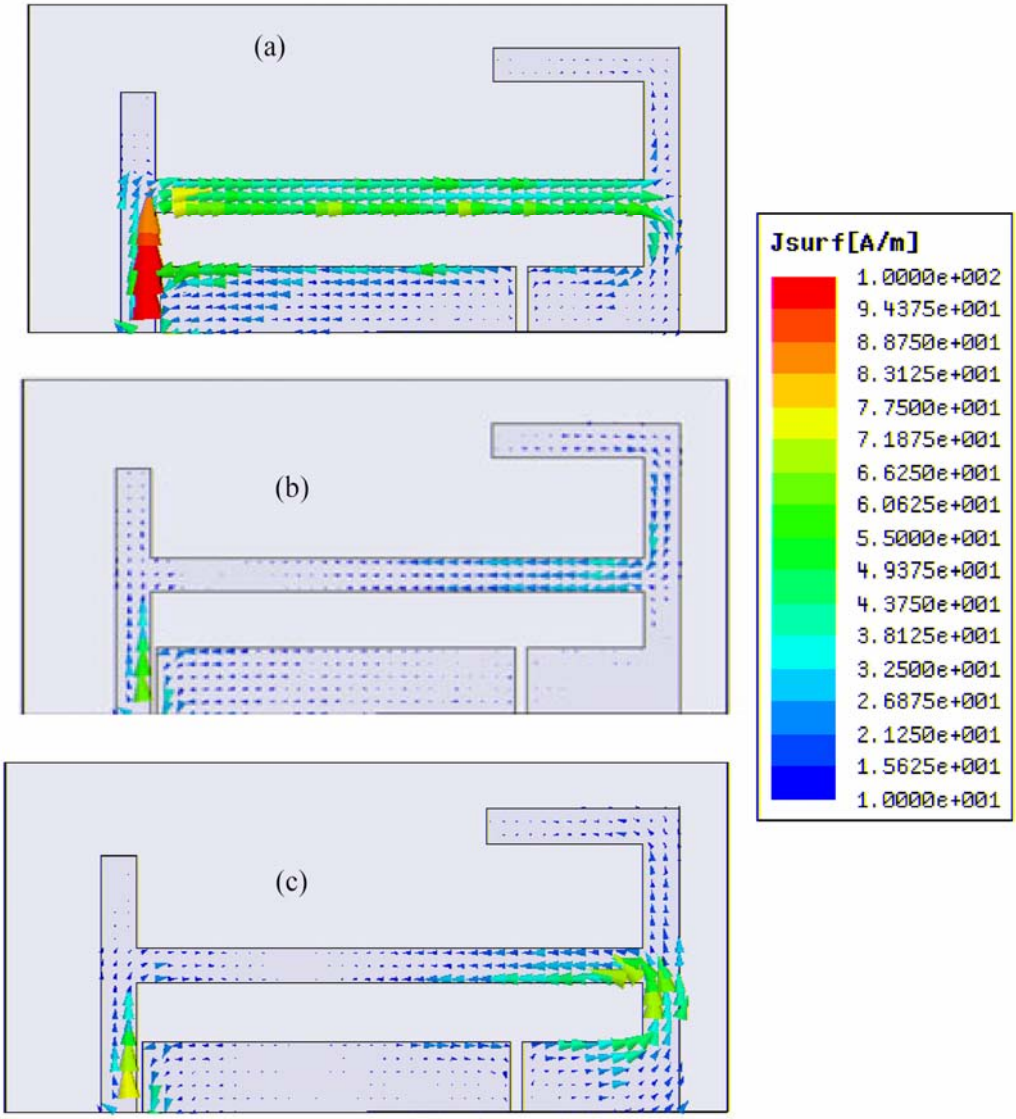

Fig.4.29. Surface current distribution in the antenna for the three resonances
(a)At 900 MHz (b) At 1.8 GHz. (c) At 2.4 GHz
L_1=14 mm, L_2=48 mm, W_g=30.5 mm, L_3 =14 mm,L_4=13 mm, W =3 mm, Wg = 6 mm, L_g = 30.5 mm, L_5=11 mm,L_6 =16.5 mm,L_7=8 mm,c=1 mm, h=1.6 mm, ε_r =4.4.

Fom the current distribution in the antenna the following design equations are derived

The first resonance is due to the total length of the loop structure

i.e, $L_1+L_2+L_3+L_4+Lg = 0.5\ \lambda_{d1}$ .....(4.5)

The second resonance corresponds to a quarter wave variation in the additional strip and is given by

$L_5+L_6 = 0.25\ \lambda_{d2}$ .....(4.6)

The third resonance can be calculated as

$L_1+L_2+L_3+L_4+Lg = 1.5\ \lambda_{d3}$ .....(4.7)

Where λ_{d1}, λ_{d2} and λ_{d2} are the dielectric wavelengths corresponding to the first, second and third resonant frequencies.

It has to be noted that in the case of the third resonant frequency, the resonant frequency can be varied by 10% by changing the position of the slot without deteriorating the matching the three resonances.

Another attraction is that the overall dimensions of the triple band antenna is of the order of $\lambda_d/5$ x $\lambda_d/10$ corresponding to the lowest operating frequency.

4.5.6 Radiation characteristics of the final triple band antenna

The 3 D radiation patterns of the antenna for the three bands are shown in fig.4.30.

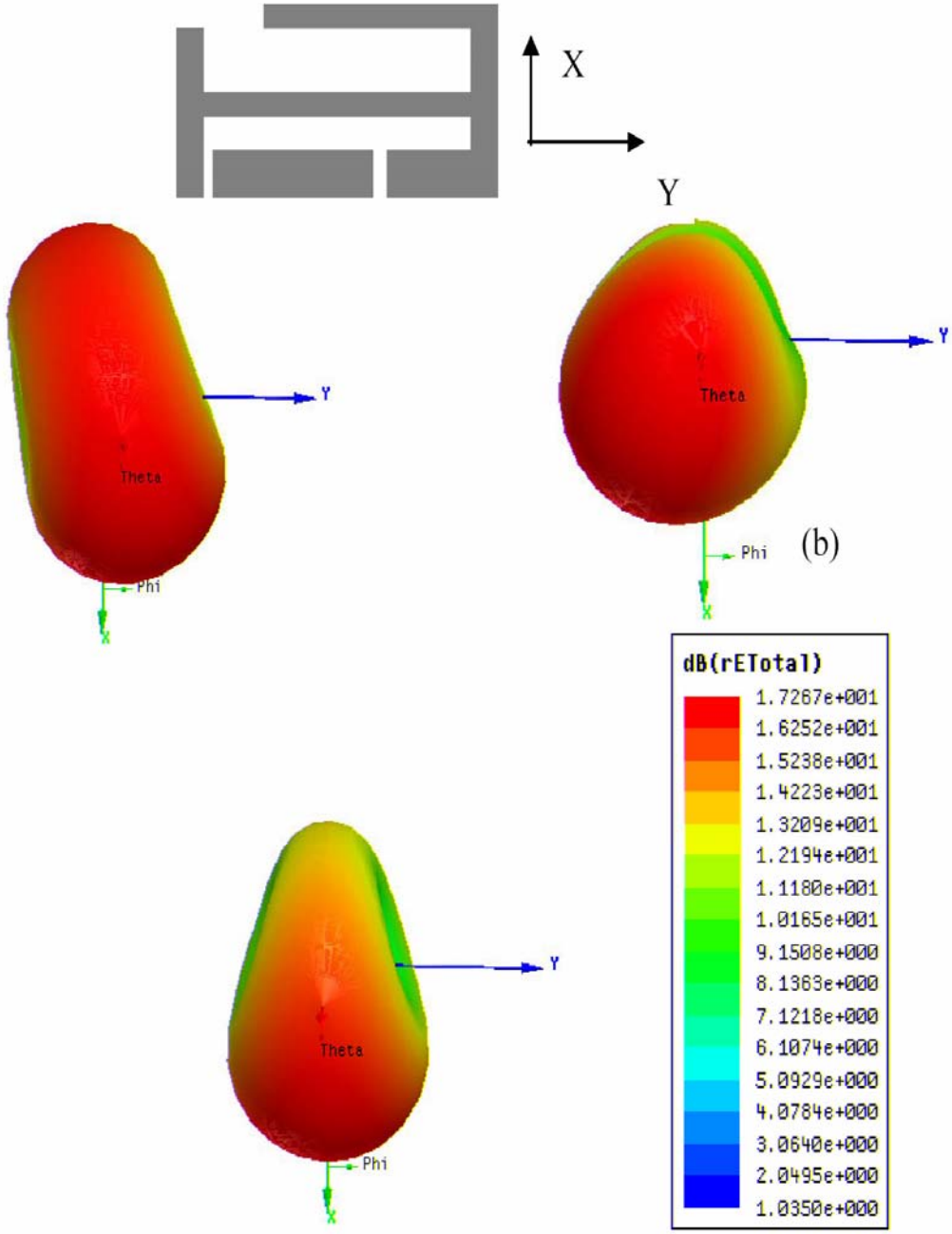

Fig.4.30. 3-D Radiation pattern of the antenna for the three resonances (a)At 900 MHz (b) At 1.8 GHz. (c) At 2.4 GHz

The measured 2 D radiation pattern for the three bands are also shown in fig.4.31.

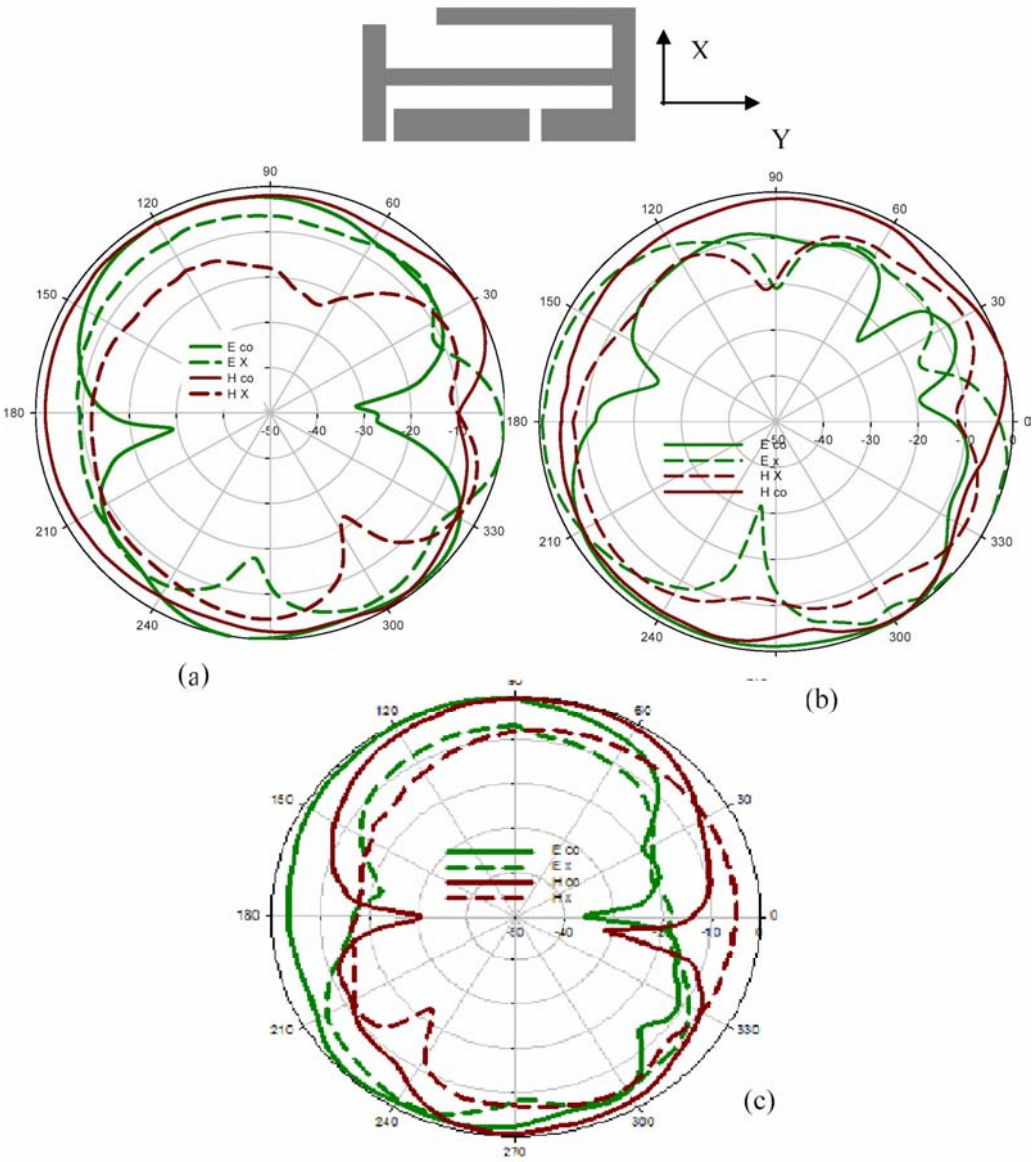

Fig.4.31. 3-D Radiation pattern of the antenna for the three resonances (a)At 900 MHz (b) At 1.8 GHz. (c) At 2.4 GHz

The average gain is found to be 0.7dBi at the 900 MHz, 2.5 dBi at 1.8 GHz and 2.2 dBi at 2.5 GHz with efficiencies of 43%, 69% and 74% respectively.

The above results prove that the antenna can be efficiently used for the design of compact multiband antennas for wireless devices. The overall dimensions of the triple band antenna on a substrate of dielectric constant 4.4 and height 1.6 mm is 24 mm x 48 mm. In terms of the lowest operating frequency the size comes to be around $\lambda_d/5$ x $\lambda_d/10$.

4.6 Asymmetric Coplanar Strip fed ultra compact antenna for low frequency wireless applications

The previous sections dealt with the design and development of ultra compact Asymmetric coplanar strip fed antennas in the 900/1800/2400 MHz bands. In this section the above technique is effectively used to design a highly demanding DVB-H antenna.

The evolution of multitude of services along with voice communication has created greater challenges to designers. Television was the only service missing from mobile phones until recently. But this deficit has also been cleared recently with the innovation of DVB-H services.

DVB-H stands for Digital Video Broadcast - Hand held. DVB-H comprises of not only television broad casting, but also data broadcasting for many users with a single service. It makes possible to provide movies, news, music, weather forecasts and other public services via a single service channel with a bandwidth of 8 MHz for each channel. DVB-H system uses the frequency range from 470 MHz to 702 MHz, i.e, a bandwidth of 40 percent in the lower UHF region. Today one of the most challenging task before antenna designers is the design of ultra compact antenna for DVB-H applications [2,3]

The antenna has to be compact and should be integrated inside the limited space available in a mobile phone. There is no specific criterion for the return loss, but the antenna gain should be better than -10 dBi to -7 dBi over the band 470-702 MHz. The typically realized designs occupy area of nearly 135 mm x 80 mm (Nokia 7700 DVB-H hand set) [4].

In this section an attempt is made to realize an ultra compact antenna which can operate in the DVB-H range. A modification of the previous shorted inverted L antenna with the slot may be an efficient choice for the above application (fig.4.32)

4.6.1 Ultra compact antenna for DVB-H applications

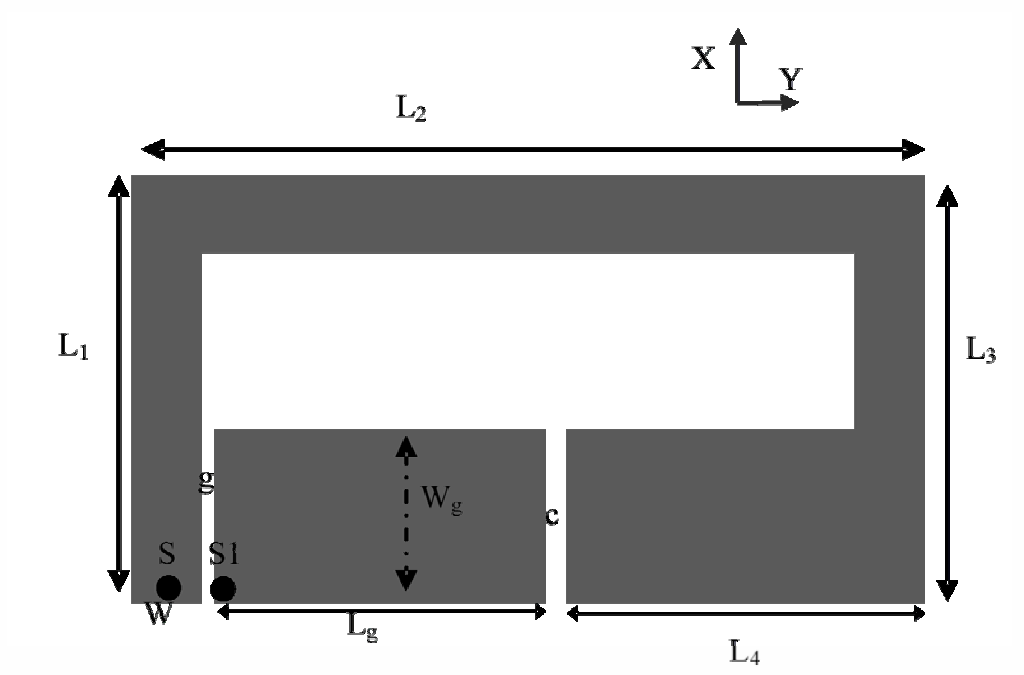

Fig.4.32. ACS fed inverted L antenna with the slot 'c'
L_1=20 mm, L_2=58 mm, L_3=20 mm, L_4 =25.5 mm, W=3 mm, c = 1 mm, L_g =28, Wg = 7 mm, h=1.6 mm, ε_r =4.4

The total length of the loop stricture is chosen to be nearly equal to a half of the dielectric wavelength corresponding to the centre frequency at 600 MHz. The return loss of the antenna is shown in fig.4.33. The 3.5:1 VSWR of the antenna ranges from 510 MHz to 710 MHz which is better than the currently reported compact designs.

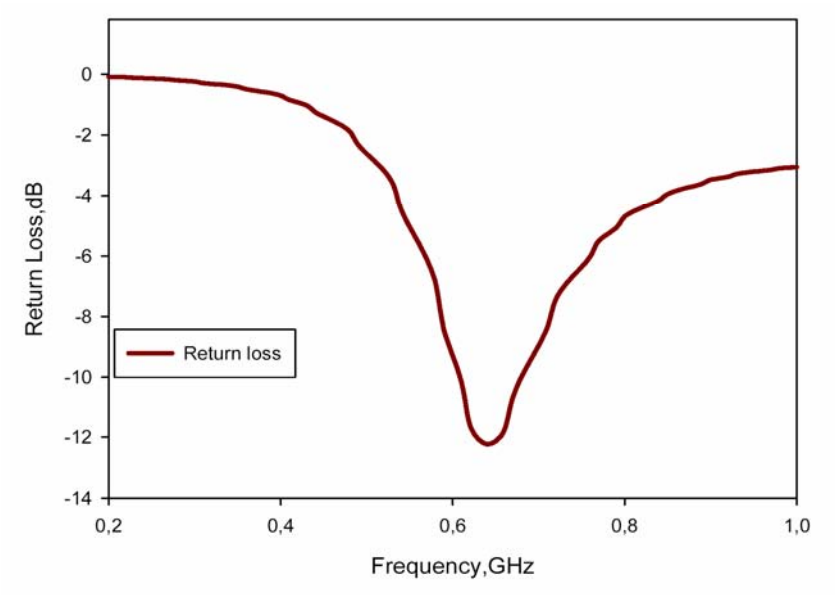

Fig.4.33. Return loss characteristic of the ACS fed inverted L antenna with the slot 'c'
L_1=20 mm, L_2=58 mm, L_3=20 mm, L_4 =25.5 mm, W=3 mm, c = 1 mm, L_g =28, Wg = 7 mm, h=1.6 mm, ε_r =4.4

The impedance matching needs to be improved in the entire DVB-H band. Increasing the width of the slot decreases the impedance band width along with increase in the resonant frequency as seen in fig.4.17.

After a series of Simulation and experimental studies it is found that inserting a small slit $S_x x S_y$ as shown in fig.4.34, increases the impedance matching along with decrease in resonant frequency. The position and dimensions of the slit is optimized for good impedance matching.

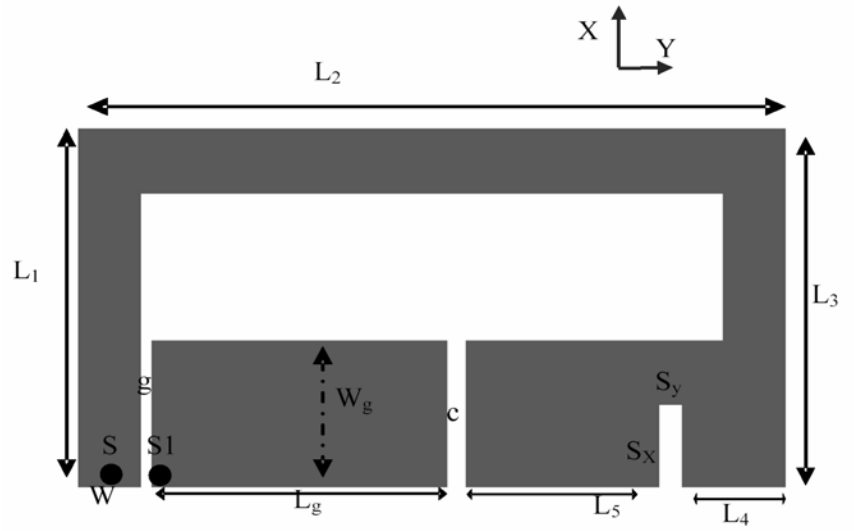

Fig.4.34. ACS fed inverted L antenna with the additional slit
L_1=20 mm, L_2=58 mm, L_3=20 mm, L_4 =5 mm, L_5 = 24 mm, S_x = 4mm, S_y = 1 mm, W=3 mm, c = 1 mm, L_g =28, Wg = 7 mm, h=1.6 mm, ε_r =4.4

The return loss curves of the two antennas are shown in fig.4.35.

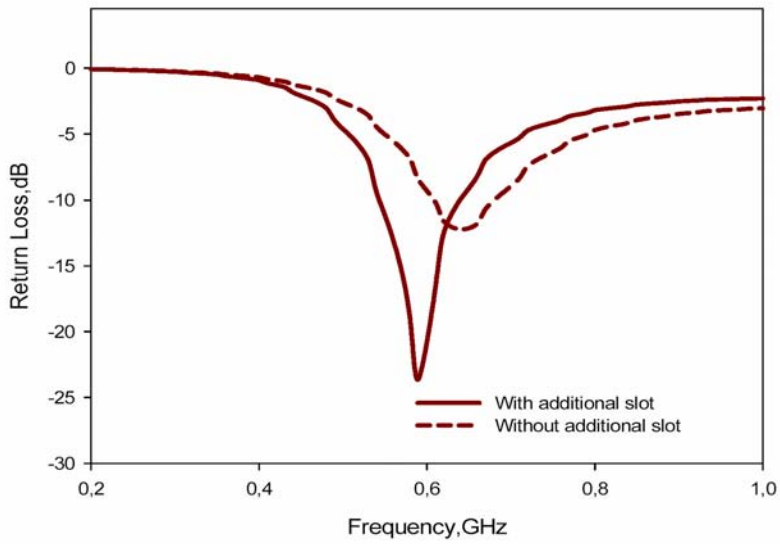

Fig.4.35. Return loss characteristics of the ACS fed antenna with and without the additional slit
L_1=20 mm, L_2=58 mm, L_3=20 mm, L_4 =5 mm, L_5 = 24 mm, C_x = 4mm, C_y = 1 mm, W=3 mm, c = 1mm, L_g =28, Wg = 7mm, h=1.6 mm, ε_r =4.4

4.6.2 Reflection characteristics of the Ultra compact antenna for DVB-H applications

The antenna is realized on a substrate of dielectric constant 4.4 and height 1.6 mm. The experimental and simulated return loss curves of the final antenna with the slot are also shown in fig.4.33.

The antenna exhibits a 3.5:1 VSWR from 460 MHz to 740 MHz covering the entire DVBH spectrum.

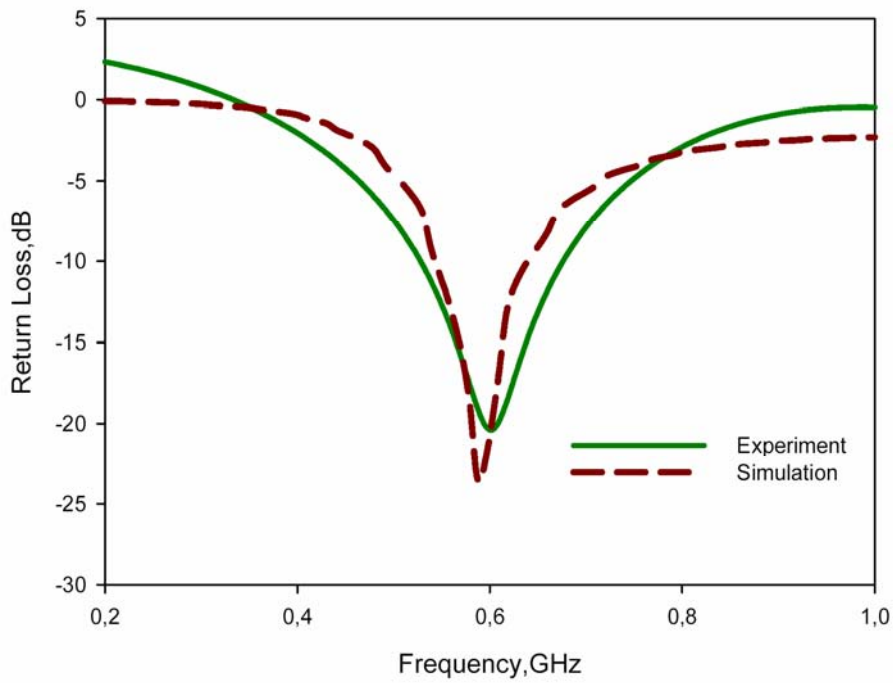

Fig.4.36. Return Loss characteristics of the ACS fed inverted L antenna with the additional the slit
L_1=20 mm, L_2=58 mm, L_3=20 mm, L_4 =5 mm, L_5 = 24 mm, C_x = 4mm, C_y = 1 mm, W=3 mm, c = 1 mm, L_g =28, Wg = 7 mm, h=1.6 mm, ε_r =4.4

The current distribution in the antenna for the resonant frequency is shown in fig.4.37.There is a half wave variation in the entire antenna structure corresponding to the resonance at 600 MHz.

It is interesting to note that the antenna occupies a dimension of only 58 mm x 20 mm on a substrate of dielectric constant 4.4 and height of 1.6 mm. In terms of the dielectric wave length of the lowest operating frequency the size comes to be only $\lambda_d/7$ x $\lambda_d/22$.

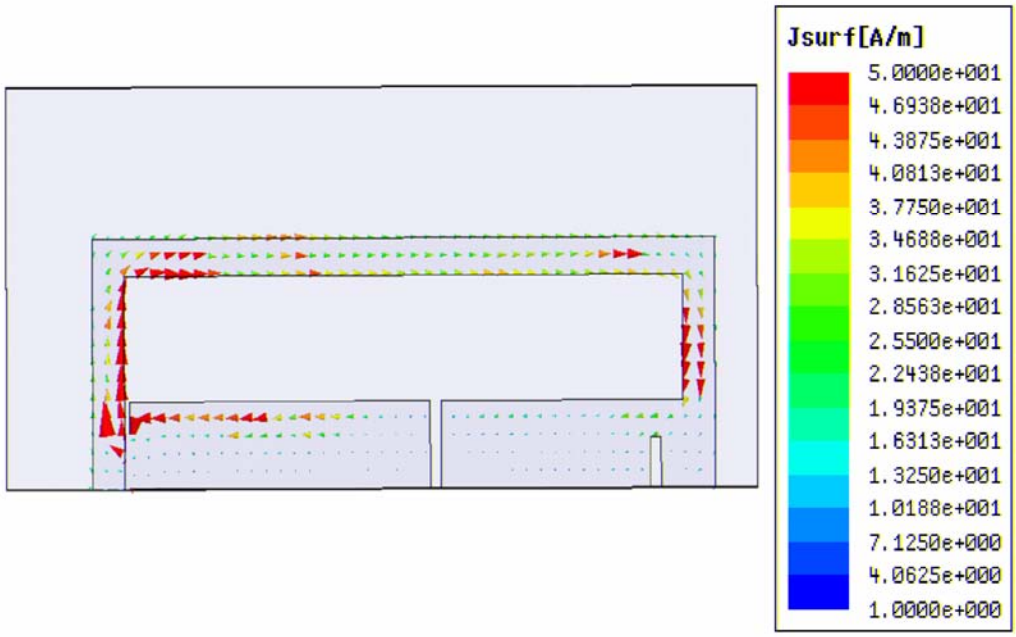

Fig.4.37. Current distribution in inverted L antenna with the additional slit L_1=20 mm, L_2=58 mm, L_3=20 mm, L_4 =5 mm, L_5 = 24 mm, C_x = 4mm, C_y = 1 mm, W=3 mm, c = 1 mm, L_g =28, Wg = 7 mm, h=1.6 mm, ε_r =4.4

4.6.3 Radiation characteristics of the Ultra compact antenna for DVB-H applications

The 3-D radiation pattern of the antenna at 600 MHz is shown in fig.4.38. It can be seen that the pattern is similar to the case of the previous dual band antenna.

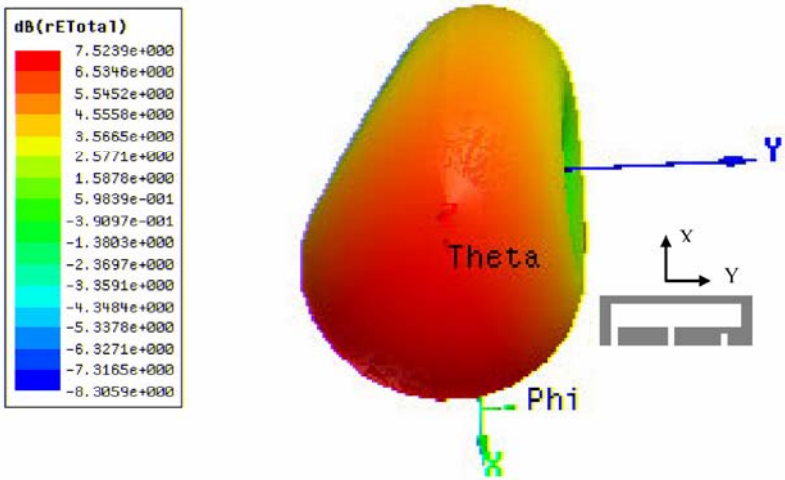

Fig.4.38. 3 –D radiation pattern of the final ACS fed antenna for DVBH applications at 600 MHz.

The 2-D radiation pattern of the antenna at 600 MHz is presented in fig.4.39. The antenna exhibits nearly dipole like pattern with a figure of eight in the E plane and nearly non directional in the H-plane. The E-plane HPBW is around 70°. The computed efficiency of the antenna is 23% at 600 MHz.

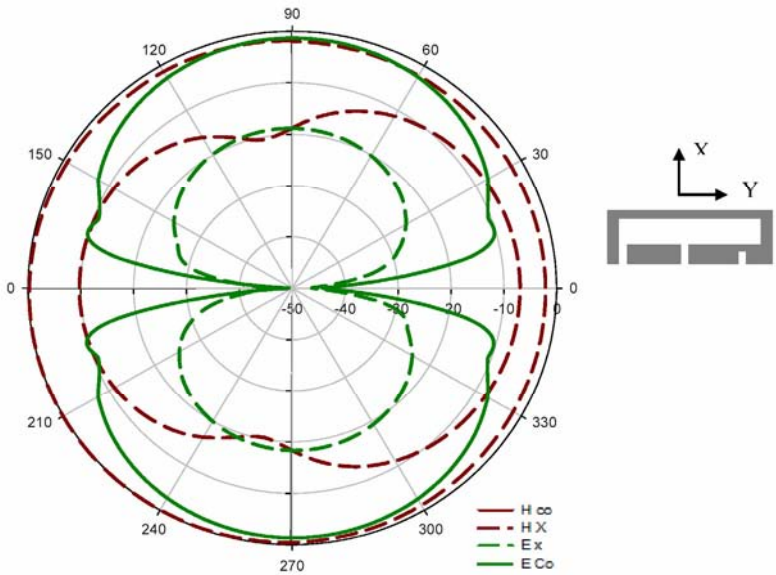

Fig.4.39. 2 – D radiation pattern of the ACS fed DVB-H antenna

The measured gain of the antenna is given in fig.4.40. The dotted line shows the required DVB-H specification. As mentioned earlier as per the DVBH specification the gain of the antenna should be better than -10 dBi to -7 dBi over the band from 470-702 MHz It can be seen that the ACS fed antenna has higher gain than the specification in the entire operating band.

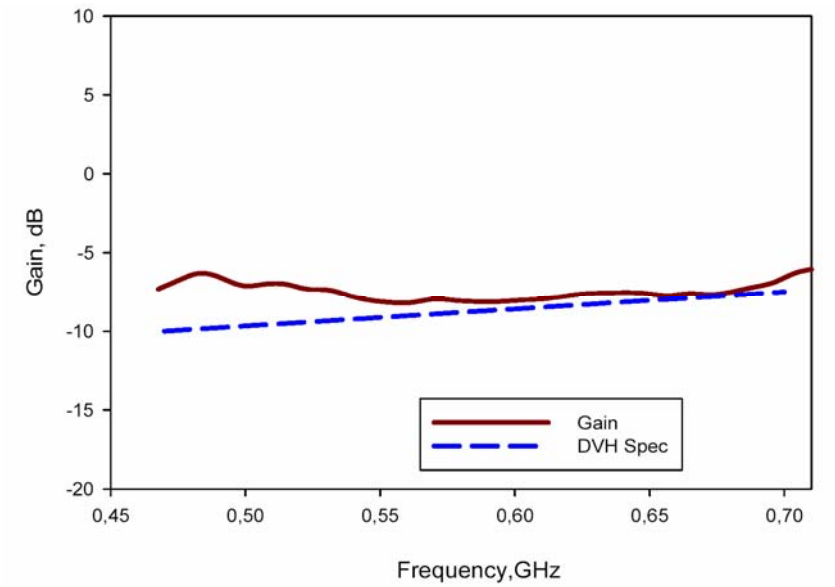

Fig.4.40. Realized gain of the antenna along with the DVB-H specification

4.6.4 Conclusion

The above studies depict the capability of the ACS fed antenna in low frequency applications. Note that the overall dimension of the antenna is only $\lambda_d/7$ x $\lambda_d/22$. But the radiation and reflection performance of the antenna is far better than the conventional designs. Moreover the simplicity in the design also portrays it as viable alternative to present day DVB –H antennas.

4.7 Modified Design of the DVBH antenna for mobile communication applications

The modified design of the ACS fed DVB-H antenna for mobile communication application is presented in this section. This modification is made

keeping in mind the use of the antenna in a typical handset. The modification is brought about by dividing the structure into two layers. One layer is printed on the side of the large reflector or the larger ground plane of the mobile gadget while the other layer is printed side by side along with other circuitry.

Description of Antenna Geometry: Fig 4.41 shows the geometry of the antenna. The antenna is fed directly using a 50 Ω coaxial cable. The central conductor is connected to the point s_1 and the ground is connected to the point s_2. The dimension of the top layer is 51.5 mm x 7 mm. The top layer is etched side by side in the PCB along with the other circuitry (fig.4.42.a)

The bottom layer is etched on the inner side of the mobile phone cover as shown in figure. Both the layers are connected by a via of diameter 0.5 mm and length, v = 4 mm. The antenna can be considered as a folded loop structure. A 1 mm slot is inserted in the top layer at Lg to enhance the matching (fig.4.42.b) as in the previous case.

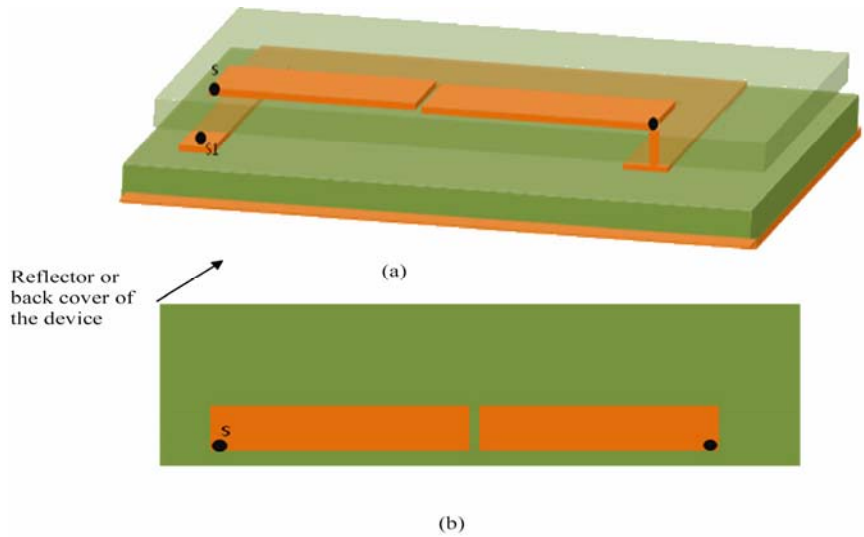

Fig.4.41. Geometry of the antenna
(a) Overall view of the final DVBH Antenna (b)Top view of the final DVBH Antenna

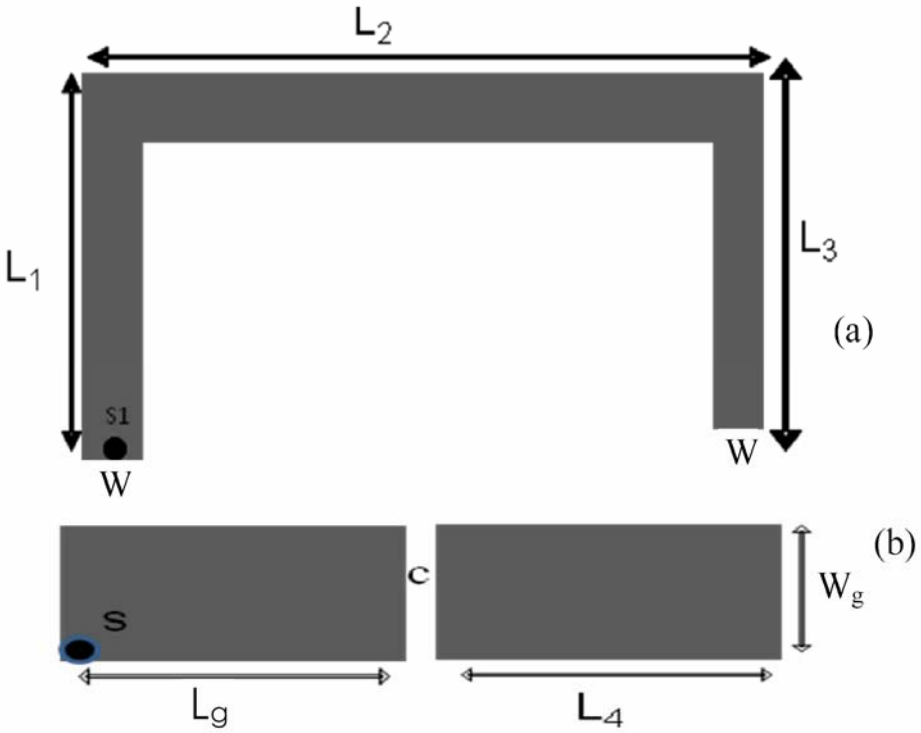

Fig.4.42. Geometry of the proposed antenna

a. Geometry of the bottom layer

b. Geometry of the Top Layer

L_1=20 mm, L_2=58 mm, L_3=17.5 mm, L_4 =25 mm, W=3 mm, c = 1 mm, L_g =7 mm, Lg = 25.5 mm, W_g =7mm, h=1.6 mm, ε_r =4.4, v = 4 mm

4.7.1 Reflection characteristics of the modified DVB-H antenna

The simulated and experimental return loss characteristics of the antenna are shown in fig.41.The The 3.5:1 VSWR of the antenna is from 436 MHz to 711 MHz covering the entire DVBH bands.

Note that the antenna gives good performance even without the insertion of the additional slot as in fig.4.43.

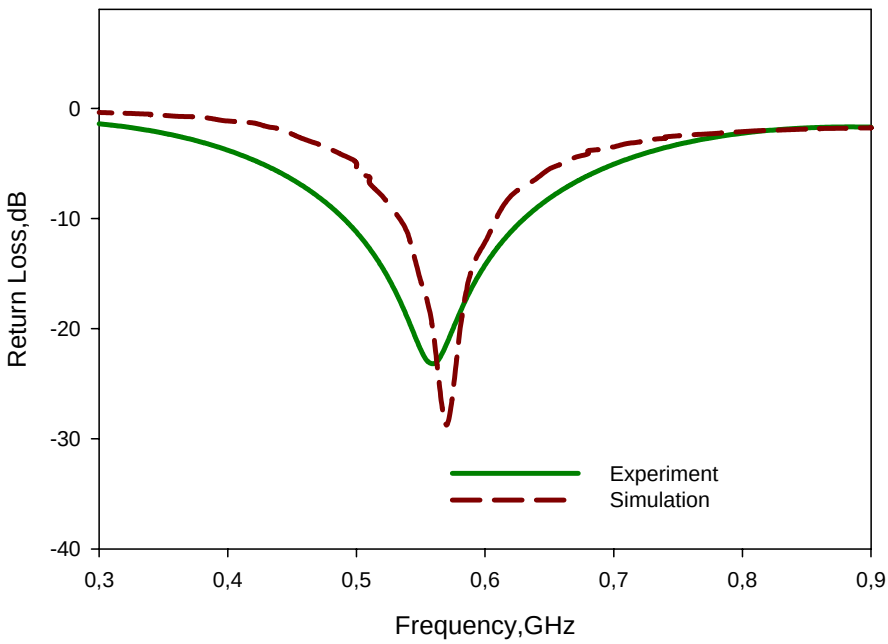

Fig.4.43. Experimental and simulated return loss curves of the modified DVB-H antenna
L_1=20 mm, L_2=58 mm, L_3=17.5 mm, L_4 =25 mm, w=3 mm, c = 1 mm, L_g =7 mm, Lg = 25.5 mm,Wg =7mm, h=1.6 mm, ε_r =4.4, via,v = 4 mm

In terms of the lowest operating frequency the size of the antenna comes to be $\lambda_d/8$ x $\lambda_d/23$.Also it is interesting to note that the dimensions of the top layer is only $\lambda_d/9$ x $\lambda_d/66$.

The current distribution in the antenna at the resonant frequency is shown in fig.4.44. A half wave variation of current intensity is observed in the entire structure.

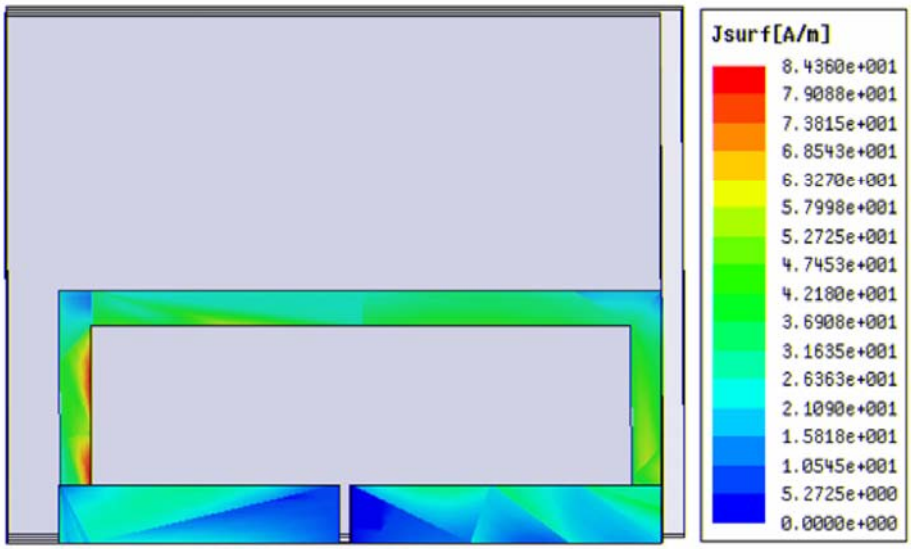

Fig.4.44. Simulated current distribution in the modified DVBH antenna
L_1=20 mm, L_2=58 mm, L_3=17.5 mm, L4 =25 mm, W=3 mm, c = 1 mm,
L_g =7 mm, Lg = 25.5 mm,Wg =7mm, h=1.6 mm, ε_r =4.4, v = 4 mm

After a series of experimental and simulation studies the design equation of the antenna is derived as

$$L_1+L_2+L_3+L_4+v+Lg = 0.5\,\lambda_d \quad \text{.....(4.8)}$$

Where λ_d corresponds to the wavelength in the substrate at the resonant frequency and v is the via length.

The ratio of L_1/L_2 is maintained as 0.3 for better performance.

4.7.2 Radiation characteristics of the modified DVB-H antenna

The 3-D radiation pattern of the antenna is shown in fig.4.45.It can be noted that there is no appreciable change in the radiation pattern of the antenna even after the modification of the geometry.

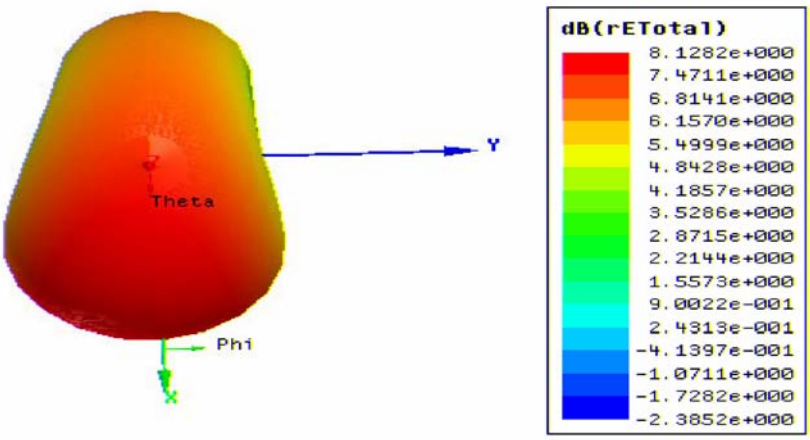

Fig.4.45. 3-D Radiation pattern of the antenna at 610 MHz
L_1=20 mm, L_2=58 mm, L_3=17.5 mm, L4 =25 mm, W=3 mm, c = 1 mm, L_g =7 mm, Lg = 25.5 mm,Wg =7mm, h=1.6 mm, ε_r =4.4, v = 4 mm

The 2-D radiation pattern of the antenna at 610 MHz is shown in figure.4.46. A Dipole like pattern is obtained. The pattern remains nearly the same as that of the previous design. The efficiency is computed as 26% at 610 MHz

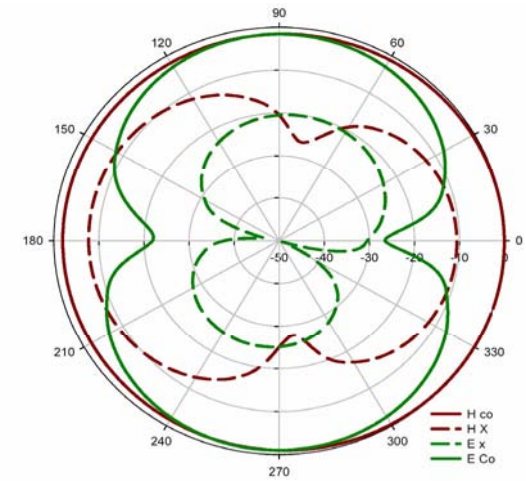

Fig.4.46. 2-D Radiation pattern of the antenna at 610 MHz
L_1=20 mm, L_2=58 mm, L_3=18 mm, L4 =25 mm, W=3 mm, c = 1 mm, L_g =7 mm, Lg = 25.5 mm,Wg =7mm, h=1.6 mm, ε_r =4.4, Separation = 4 mm

The measured gain of the antenna is plotted in fig.4.47. The gain is higher than the DVBH specifications (shown in dotted lines).

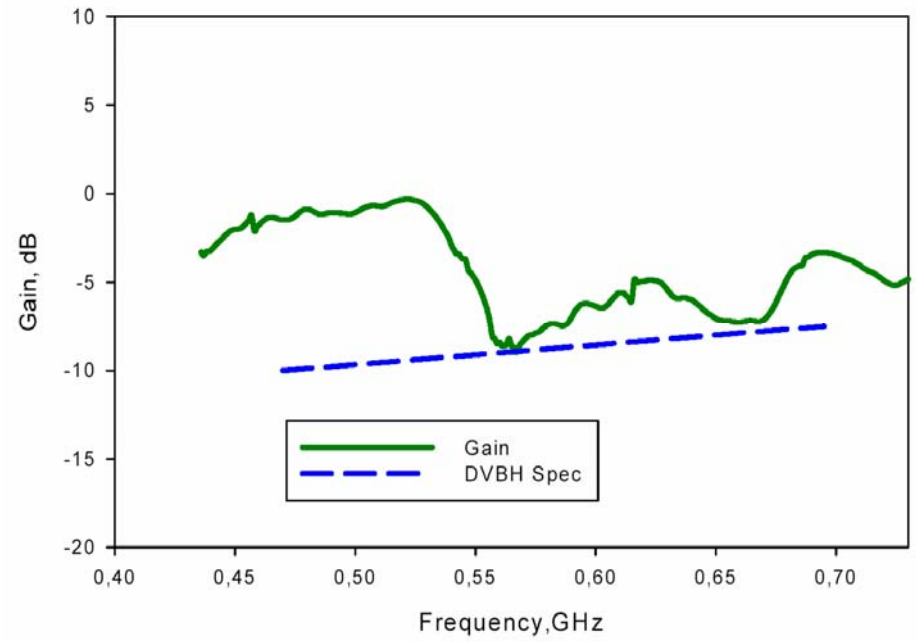

Fig.4.47. Gain of the modified DVB-Hantenna

4.7.3 Conclusion

An ultra compact DVBH antenna with overall dimensions of the order of $\lambda_d/8$ x $\lambda_d/23$ is presented. The bottom layer can be easily is printed on the back side of the mobile phone cover. The antenna has a 3.5:1 VSWR bandwidth from 436 MHz to 711 MHz covering the entire DVBH spectrum. The simple structure and high conformability of the antenna together with moderate reflection and radiation characteristics portray it as an ideal candidate for mobile DVB-H application.

These designs underlines the potential of ACS feed in compact antenna designs compared to conventional design techniques.

References

[1] Filiberto Bilotti,Andrea Ali and Lucio vegni, " Design of miniaturized metamaterial patch antennas with μ-negative loading",IEEE Trans Antennas and propogat.,Vol 56,No.6,June 2008

[2] www.dvb.org

[3] Ulrich H. Reimers, "DVB—The Family of International Standards for Digital Video Broadcasting", Proceedings of the IEEE, vol. 94, no. 1, January 2006

[4] http://www.nokia.com

Chapter 5

CONCLUSION AND FUTURE PERSPECTIVE

Contents

This chapter highlights the accomplishments and achievements of the research work. A sum up of the results and the directions for future study are also discussed

5.1 Thesis highlights and contributions

This chapter stands as a brief conclusion of the thesis. It also highlights the objectives of the study and the achievements attained.

The aim of the thesis was to design highly compact uniplanar antennas which can be easily fabricated. The conventionally used coplanar wave guide fed antennas cannot easily cater to the growing requirements of ultra compact antennas.

On a broader sense an antenna can be considered as composed of a feed and a radiator, even though they cannot be segregated in practice. The feed acts as an interface between the radiator and the coaxial connector and is essential for the proper functioning of the antenna. The radiating element primarily

determines the reflection and radiation characteristics of the antenna. But in compact antennas such a division is untrue since the feed as well as the radiator together determines the reflection and radiation characteristics.

In this thesis emphasis is given both to the design of the feed as well as the radiator. The Asymmetric coplanar strip (ACS) – a compact uniplanar feed is chosen in place of the conventional coplanar wave guide. Various designs are studied using this feed to design different compact and ultra compact antennas highly useful for practical applications.

5.1.1 The Asymmetric coplanar strip fed antennas

The choice of the Asymmetric coplanar strip (ACS) as a feed in place of the conventional coplanar wave guide (CPW) feed is one of the important highlight of the Thesis. From comparative studies it is proved that the ACS fed antennas exhibit nearly the same characteristic as compared to antennas fed by conventional feeding techniques like the CPW barring a tilt in the radiation pattern. For the efficient use of this feed in place of the conventional ones, exhaustive simulation and experimental studies are performed.

From the studies the following conclusions are reached upon in the case of ACS fed strip monopoles. These inferences are used to design compact Single band, Dual band and triple band antennas as discussed in chapter 3.

The following inferences are obtained from the study of the ACS fed strip monopole.

1) The resonance is due to the combined length of the signal strip and the ground plane.
2) Better performance is noted when the length of the ground plane is kept nearly equal to the signal strip length.

Thus the ground plane contributes to the radiation and acts as part of the feed. The designs with baluns are also studied. Much difference in the performance is not seen. It remains upto the designer to choose the antenna with or without the balun according to his constraints of area since the usage of balun requires larger area.

The strip monopole is then bent in the form of an inverted L to achieve further compactness (Fig.5.2.b). The dimensions of the inverted L antenna are optimized for better performance. It is interesting to note that the tilt in the pattern as in the previous case is removed in this design

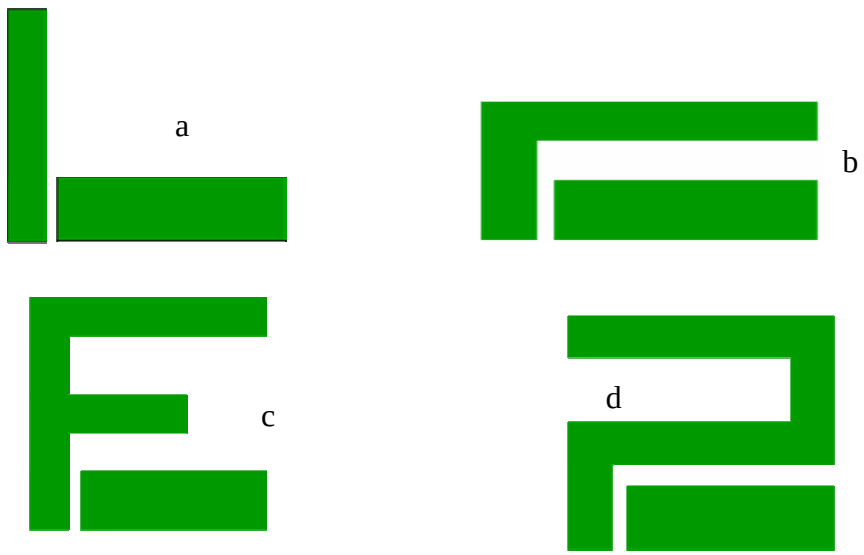

Fig.5.1. Asymmetric Coplanar Strip fed compact antennas

a. ACS fed Single band antenna b. ACS fed inverted L antenna
c. F shaped dual band antenna d. ACS fed Triple band antenna

This single band inverted L is further modified to a dual band antenna by adding an additional strip at the position of minimum current intensity. This gives an F shaped dual band antenna (Fig.5.1.c).

The width of the signal strip of the inverted L shaped antenna is further modified and along with the insertion of a slot to produce the multi band antenna in (Fig.5.1.d.).

All the above compact designs have an overall size of $\lambda_d/4$ x $\lambda_d/4$.These studies are elaborately presented in chapter 3. The rapid development of wireless communication demand further ultra compact designs. This is also discussed elaborately in the thesis in chapter 4.

5.1.2 Asymmetric coplanar strip fed Ultra compact antennas

The ACS feed can be used for the design of ultra compact antennas. The signal strip is bent in the form of a loop. The resulting reactance is balanced by the insertion of a proper slot at the appropriate position. This results in a ultra compact antenna with overall dimension in the order of $\lambda_d/5$ x $\lambda_d/18$ (Fig.5.2.a).

The above dual band antenna is properly modified to design a triple band antenna by adding an additional strip at the current minimum position as in the earlier case. The resulting antenna covers GSM 900/1800 and 2.4 GHz WLAN bands with dimensions of the order of $\lambda_d/5$ x $\lambda_d/10$ (Fig.5.2.b.).

Fig 5.2. Asymmetric Coplanar Strip fed Ultra compact antennas
(a) Dual Band b) Triple band

5.1.3 ACS fed Ultra compact antennas for DVB-H applications

The recent introduction of DVB-H services has fostered a great need for compact antennas for designing compact devices. The above designs are

suitably modified to design ultra compact antennas for DVBH applications. A highly compact antenna having dimensions of the order of $\lambda_d/7$ x $\lambda_d/22$ is presented (Fig.5.3.a). The antenna exhibits good reflection and radiation characteristics and is highly suitable for DVB-H applications.

The above design is further modified into a dual layer with a eye on practical applications (Fig.5.3.b). This facilitates further compact design so that only $\lambda_d/8$ x $\lambda_d/23$ of the PCB space is needed for the DVB-H antenna. The top layer is more compact of the order of $\lambda_d/9$ x $\lambda_d/66$.

Fig 5.3. Asymmetric Coplanar Strip fed Ultra compact antennas
(a) DVBH antenna 1 b) Top view of the modified DVBH antenna

5.2 Slot line fed antennas

In addition to the Asymmetric Coplanar Strip feeding technique another uniplanar feed which has received recent attraction is the Slotline feed.

The Slot line may be considered as a complementary of the coplanar wave guide. The main advantage of this transmission line is the ease for mounting active and passive circuits into these lines.

Two different slot line fed designs (slot line fed dipole (Fig.5.4.a) and slot line fed dual band antenna (Fig.5.4.b)) are also studied in the thesis and is given as appendix.

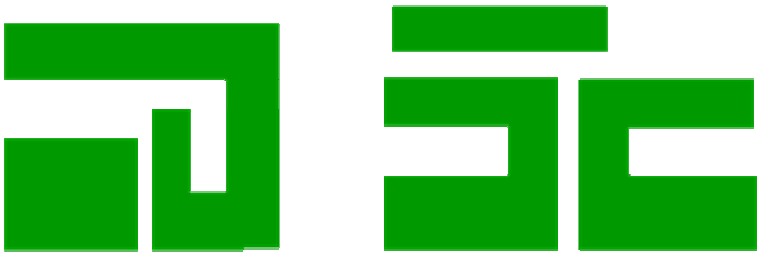

(a) Dual Band antenna (b) dipole antenna

Fig.5.4. Slot line fed antennas

5.3 Scope of future work……

The Asymmetric coplanar strip is an effective candidate for the design of compact antennas and it has been proved by the studies presented in the thesis. The practical use of the device into mobile phones and other compact devices require further optimizations. Also the introduction of the antenna into a practical circuitry with ICs, resistors, capacitors, cameras, speakers etc are expected to create variations in the performance. This has to be practically tested and the antenna has to be fine tuned for best performance.

Also the need for an “Universal Antenna” which can support the existing mobile communication bands along with the DVB-H bands is in a rise. As a future challenge the design of an ACS ultra compact “Universal Antenna” can be seriously looked upon.

The reduction of radiation towards users head while using the antenna in practical mobile phones may also be conducted by suitably loading with metamaterials. Other different compact designs using metamaterials can also be worked upon

In short the Asymmetric coplanar strip feed antennas opens up new and interesting arenas for the design of simple miniaturized antennas for an antenna designer which are cost effective and can be easily fabricated.

Appendix **I**

Slot line fed planar dipole antenna with a parasitic strip for wide band applications

In addition to the Asymmetric Coplanar Strip feeding technique another uniplanar feed which has received recent attraction is the Slotline feed.

As mentioned in chapter 3, the slot line may be considered as a complementary to the coplanar wave guide. The main advantage of this transmission line is in the ease of mounting active and passive circuits into these lines. Here the width of the slot and the height of the substrate determine the characteristic impedance of the slotline for a particular substrate.

In this section the use of the slot line to feed a dual band antenna and a dipole is discussed.

1. Introduction

Dipole antennas are attractive for wireless applications due to a host of applications like simple design, excellent radiation pattern etc. Normally printed dipoles are excited using a microstrip line [1-3]. Recently uniplanar dipoles have received wide attention due to advantages like ease of fabrication and integration of active circuit elements [4-5]. Most of the reported designs have either a double layer structure or a balun configuration [6]. Since antennas are nowadays embedded in the circuit boards, simple cost effective and easily printable designs are preferred.

While feeding the dipole with an balanced feed like a microstrip line or a coaxial cable, the need of a balun arises. This increases system complexity and

also the overall dimension of the antenna. Recently printed self balancing folded dipole antennas devoid of baluns have gained attraction [7-9] due to their compactness and simplicity.

In this section a simple planar dipole fed using a slot line [10 -11] is presented The antenna exhibits good matching and radiation characteristics similar to antennas using baluns even though it doesn't have any complicated baluns or other matching networks

The design and development of a slot line fed planar dipole antenna with a parasitic strip for wide band applications is presented in this section. The presented antenna offers a 2:1 VSWR bandwidth from 1.66 GHz to 2.71 GHz covering the DCS/PCS/UMTS and IEEE 802.11b/g bands with a gain better than 6.5 dBi. The uniplanar design, simple feeding technique and higher gain make it a versatile antenna for wireless applications.

Exhaustive experimental and simulation studies have been performed to understand the characteristics of the antenna.

2. Slot line fed Dipole antenna

A simple dipole fed by the slot line feed is shown in Fig. 1. The dimensions of the slot line are taken from standard design equations [12] The dipole arms have a total length of $\lambda_d/2$ (2 L_d) and width of 0.05 λ_d (w) where λ_d is the dielectric wavelength corresponding to the resonant frequency. The dipole is fed by a slot line of length slightly greater than $\lambda_d/2$ and width 0.1 λ_d with a separation gap 'g' =0.5 mm. The signal strip of the coaxial cable is connected to F1 and the ground to F2. The dimensions are chosen after a series of experimental and simulation studies.

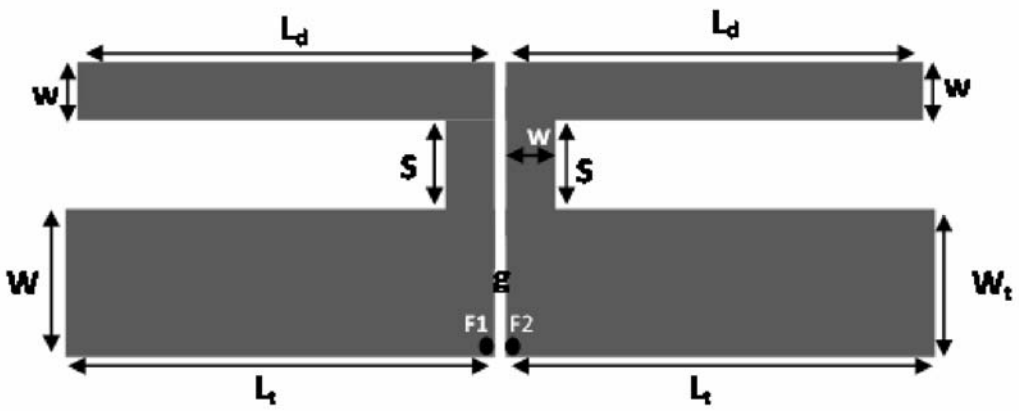

Fig. 1. Slot line fed Dipole, L_d=32 mm, w=5 mm, L_t=35 mm, W_t=10 mm, S=5 mm, g=0.5 mm ε_r=4.4 and h=1.6 mm

The return loss characteristic of the resulting antenna is shown in fig.2. The antenna resonates at 1.7 GHz with 22 % band width from 1.65 GHz to 2.05 GHz (Fig.2).

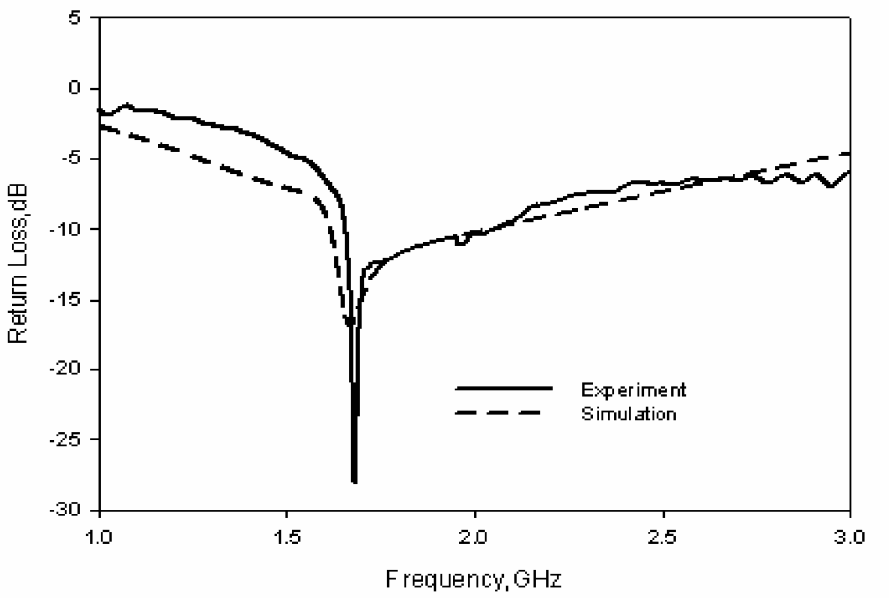

Fig. 2. Return loss characteristics of the dipole antenna shown in Fig.1. L_d=32 mm, w=5 mm, L_t=35 mm, W_t=10 mm, S=5 mm and g=0.5 mm ε_r=4.4 and h=1.6 mm

The measured radiation pattern is shown in fig.3. It can be seen that a normal dipole like pattern is obtained.

The gain of the antenna is also measured. A gain better than 4 dBi in the entire operating band is noted. The enhancement in gain may be due to the reflecting effect of the slot line feed.

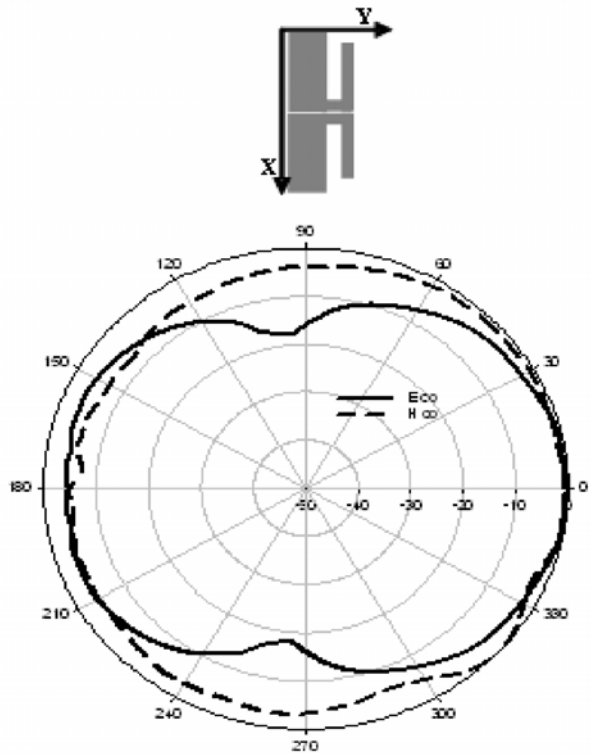

Fig.3. Principal E and H plane patterns of the dipole shown in Fig.1. L_d=32 mm, w=5 mm, L_t=35 mm, W_t=10 mm, S=5 mm and g=0.5 mm ε_r=4.4 and h=1.6 mm

To find out the resonant current path in the antenna the current distribution in the antenna is also studied (fig.4).

The Field distribution shows a half wave variation along the length of the strip at 1.7 GHz.

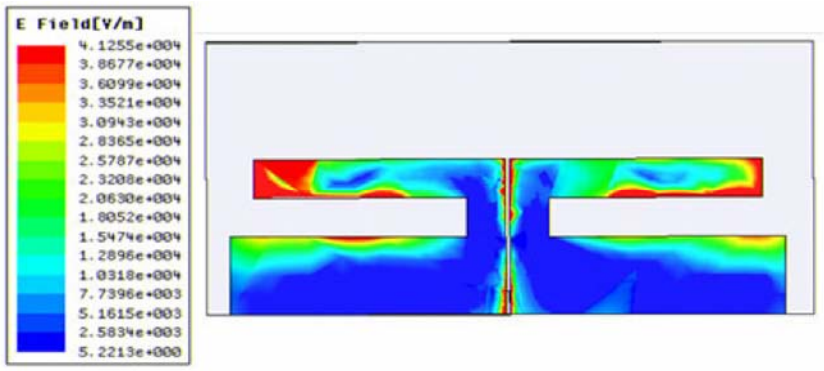

Fig. 4. Computed field distribution in the dipole antenna shown in Fig.1. L_d=32 mm, w=5 mm, L_t=35 mm, W_t=10 mm, S=5 mm and g=0.5 mm ε_r=4.4 and h=1.6 mm

3. Parametric analysis of the slot line fed dipole

The dependence of the resonant frequency on the slot line length L_t is shown in Fig. 5. There is only slight variation in the resonant frequency with L_t. But when the slot line length L_t is halved, the 3 dB beam width is increased by 30° due to increased radiation towards the slot line with a slight reduction in the gain by 0.8 dBi. The radiation patterns of the antenna for L_t and $0.5L_t$ are given in fig.6.

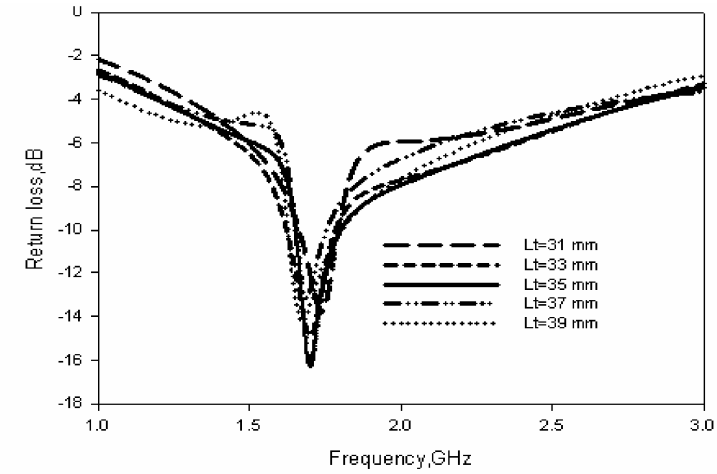

Fig.5. Variation of resonant frequency with lateral strip length L_t of the dipole antenna shown in Fig.1.
L_d =32 mm, w=5 mm, L_t=35 mm, W_t=10 mm, S=5 mm and g=0.5 mm ε_r=4.4 and h=1.6 mm

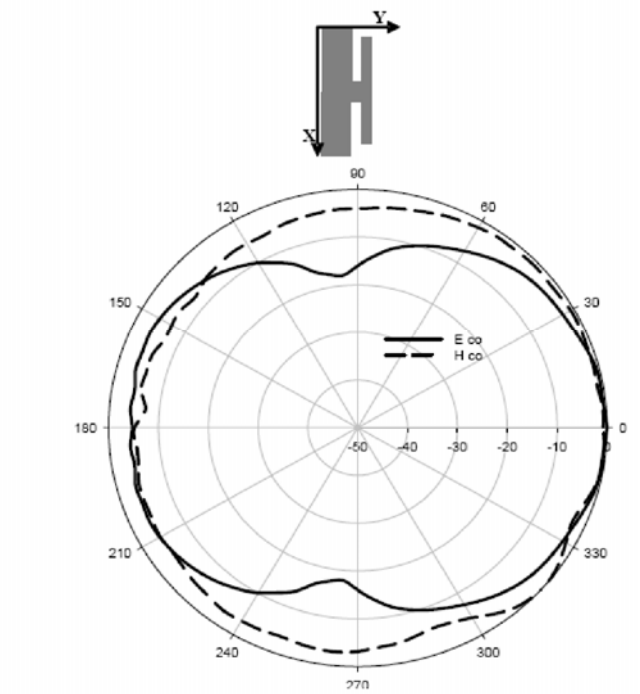

Principal E and H plane patterns with length L_t =35 mm

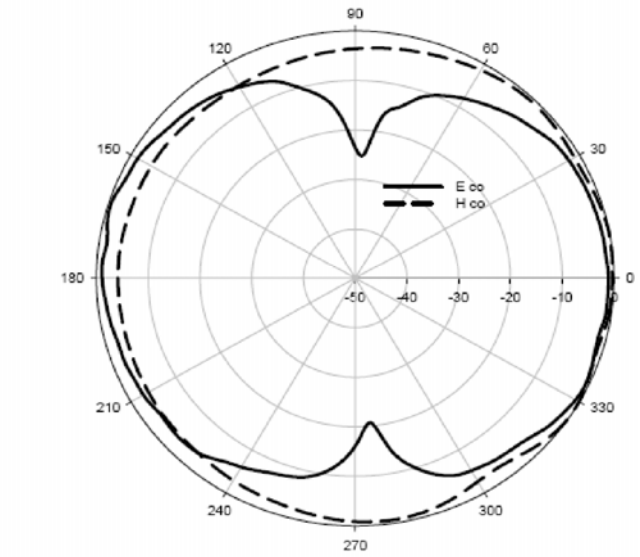

Principal E and H plane patterns with slot length L_t = 17.5 mm

Fig.6. Principal E and H plane patterns of the antenna with different slot line lengths L_t

The influence of the slotline length L_t on the resonant frequency was studied and it was observed that the resonant frequency decreases as the dipole length increases similar to an ordinary dipole.

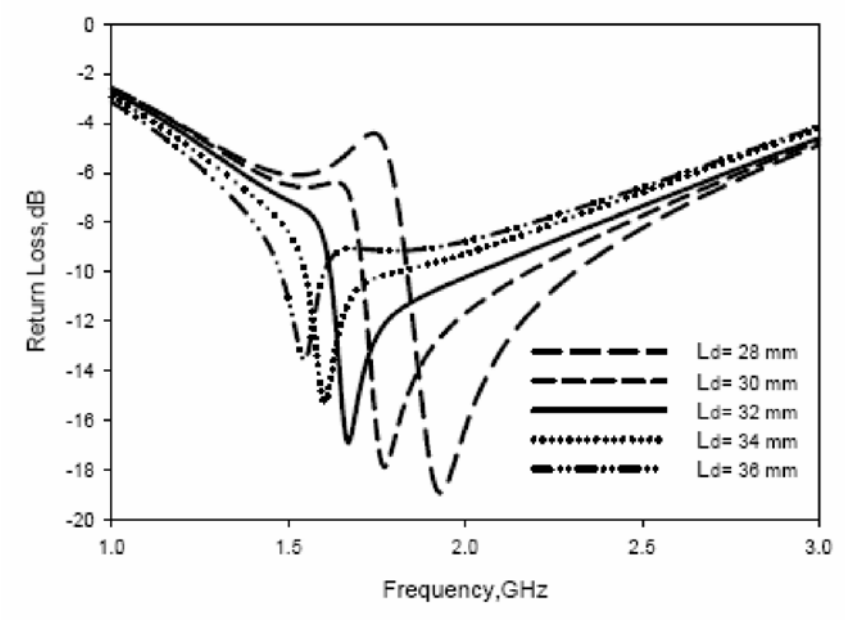

Fig.7. Variation of resonant frequency with lateral strip width W_t of the dipole shown in Fig.1.
L_d=32 mm, w=5 mm, L_t=35 mm, W_t=10 mm, S=5 mm and g=0.5 mm ε_r=4.4 and h=1.6 mm

The variation of the resonant frequency of the dipole with lateral slot width W_t and separation distance 'S' is shown in figures 8 and 9.In both cases there is no shift in the resonant frequencies but the matching conditions are severely affected Hence from parametric studies the optimum width is taken as Wt = 0.1 λ_d and'S' as 0.05 λ_d mm considering the compactness of the antenna.

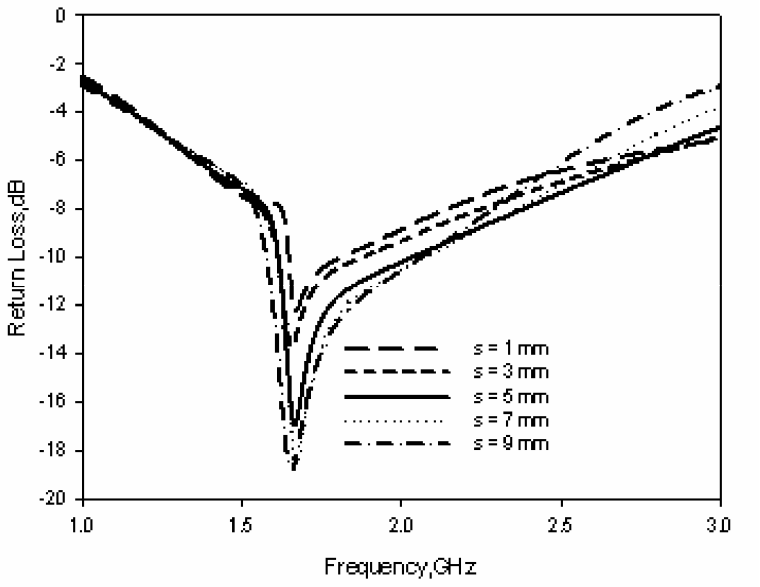

Fig.8. Variation of resonant frequency with the separation‘s’ of the dipole sh
L_d=32 mm, w=5 mm, L_t=35 mm, W_t=10 mm, S=5 mm and g=0.5 mm ε_r=4.4 and h=1.6 mm

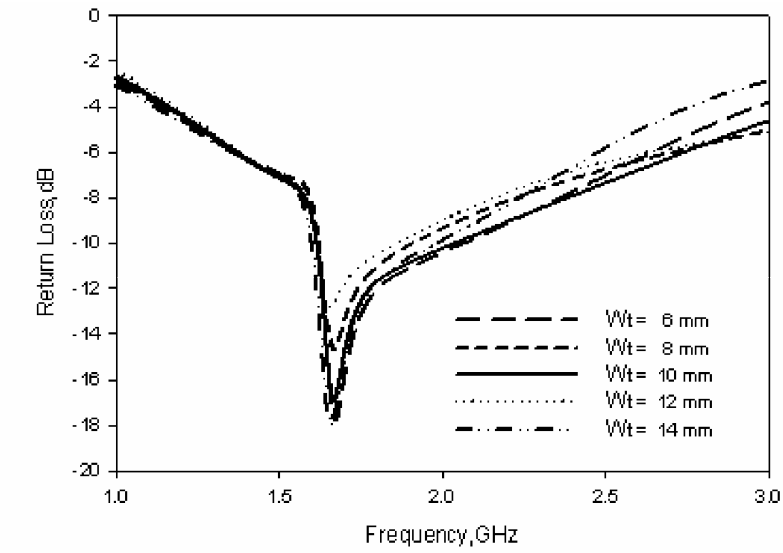

Fig.9. Variation of resonant frequency with lateral strip width W_t
L_d=32 mm, w=5 mm, L_t=35 mm, W_t=10 mm, S=5 mm and g=0.5 mm ε_r=4.4 and h=1.6 mm

The above studies confirm that the slot line as an efficient excitation for strip dipole and the resulting antenna retains all the characteristics of a dipole without the need of any additional circuitry. The lateral width L_t of the slot line can be chosen based on the user requirements like enhanced gain or pattern front to back ratio without affecting the resonant frequency.

4. Final antenna - Slot line fed dipole antenna with a parasitic strip

The dipole antenna mentioned above has relatively narrow bandwidth. To increase the bandwidth of the antenna a parasite is introduced in the structure [13]. The optimized design with the parasite exhibits nearly 50 % bandwidth with enhanced gain.

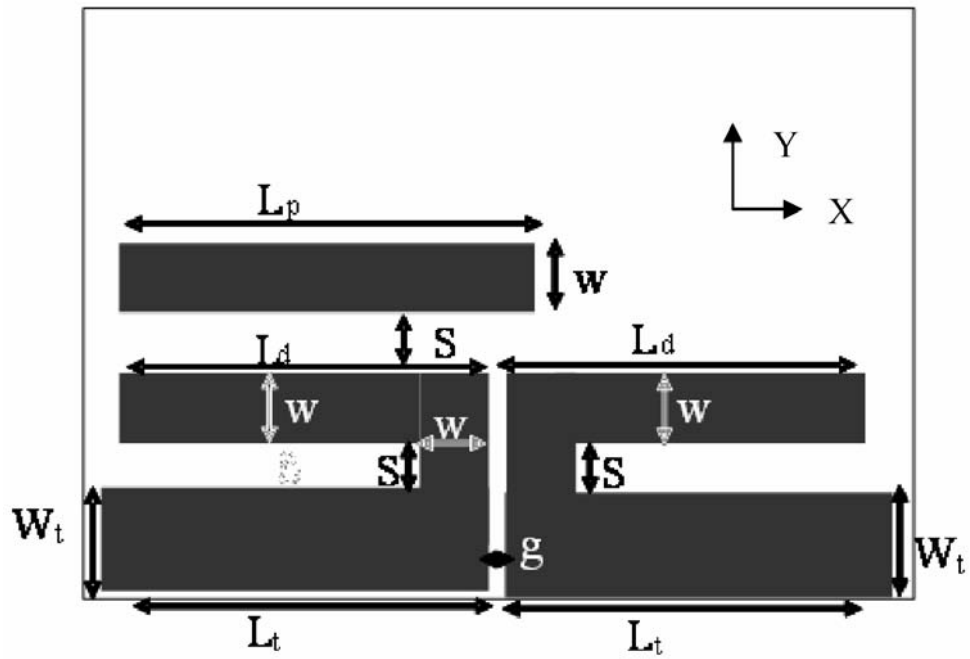

Fig. 10. Slot line fed Dipole with the parasitic strip
L_d=32 mm, w=5 mm, L_t=35 mm, W_t=10 mm S=5 mm and g=0.5 mm, Lp =35 mm, ε_r=4.4, h=1.6 mm.

The geometry of the antenna with the parasite is shown in Fig. 10. The dipole has a total length of λd/2 and width of 0.05 λ_d. The dipole is fed using a slot line having lateral slot length L_t = 0.27 λ_d W_t = 0.1 λ_d with a gap 'g' =0.5mm. A parasite having length Lp = 0.27 λ_d is placed at a separation 'S'equal to 0.05 λ_d from the dipole.

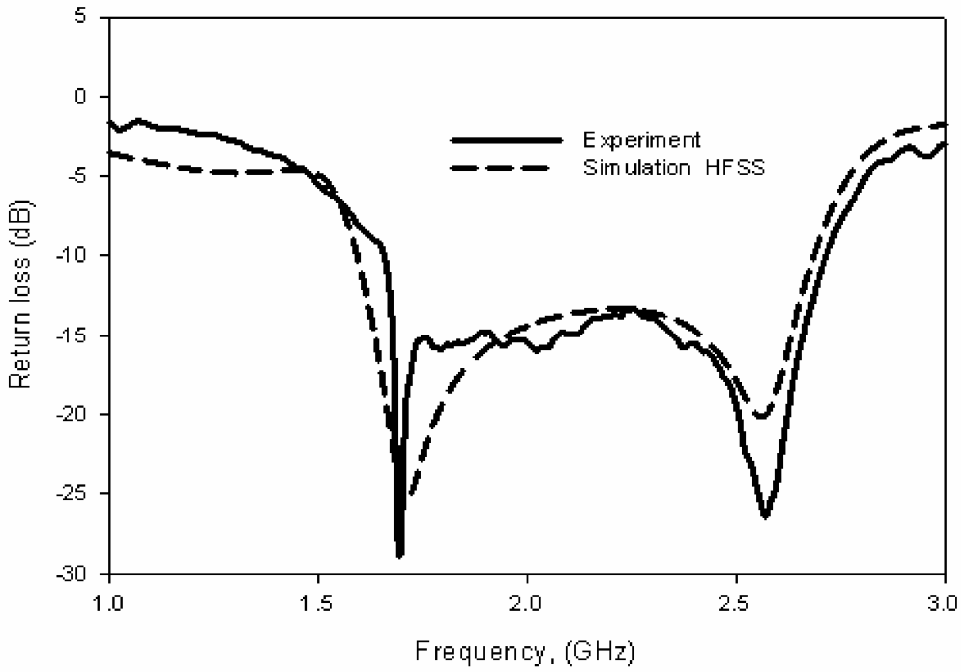

Fig.11. Return loss characteristics of the final antenna
L_d=32 mm, w=5 mm, L_t=35 mm, W_t=10 mm S=5 mm and g=0.5 mm, Lp =35 mm, ε_r=4.4, h=1.6 mm.

The measured return loss using HP 8510C network analyzer is compared with the simulation results in Fig 11. The 2:1 VSWR band of the antenna is from 1.66 GHz to 2.71 GHz, which offers a bandwidth of 50 %. A detailed study has been performed to determine the effect of the parasite in this case.

5. Parametric analysis of the final dipole with the parasite

It is well known that the position, length and loading height of the parasite determine the matching conditions of the antenna. The input impedance at the second resonance is greatly affected by the parasite length (fig12).

Similar effects are noted with variation in parasite position along Y axis (Fig.13.). The loading height of the parasite is also optimized to be equal to 'S'

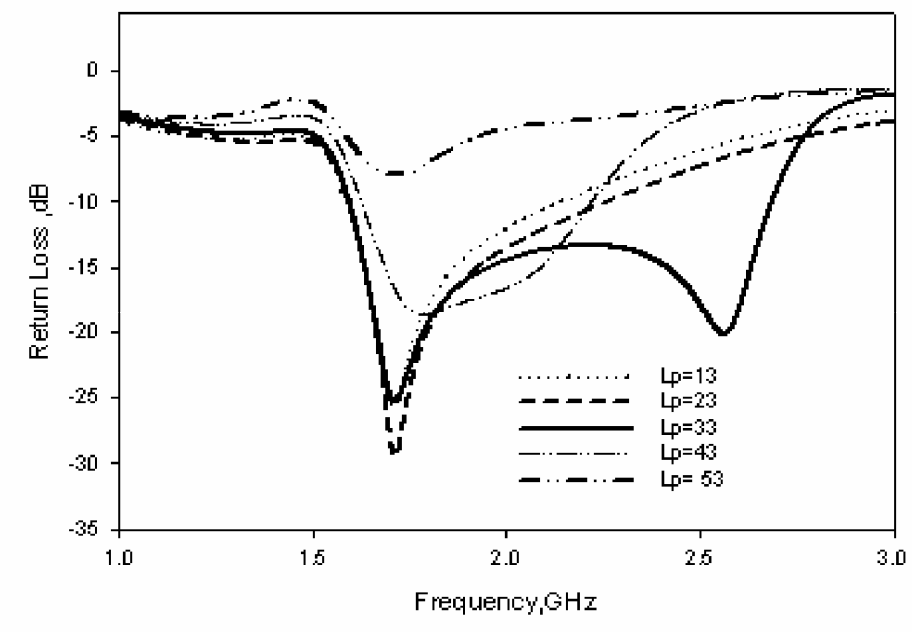

Fig.12. Variation of resonance with parasite length, Lp of the final antenna L_d=32 mm, w=5 mm, L_t=35 mm, W_t=10 mm S=5 mm and g=0.5 mm, Lp =35 mm, ε_r=4.4, h=1.6 mm

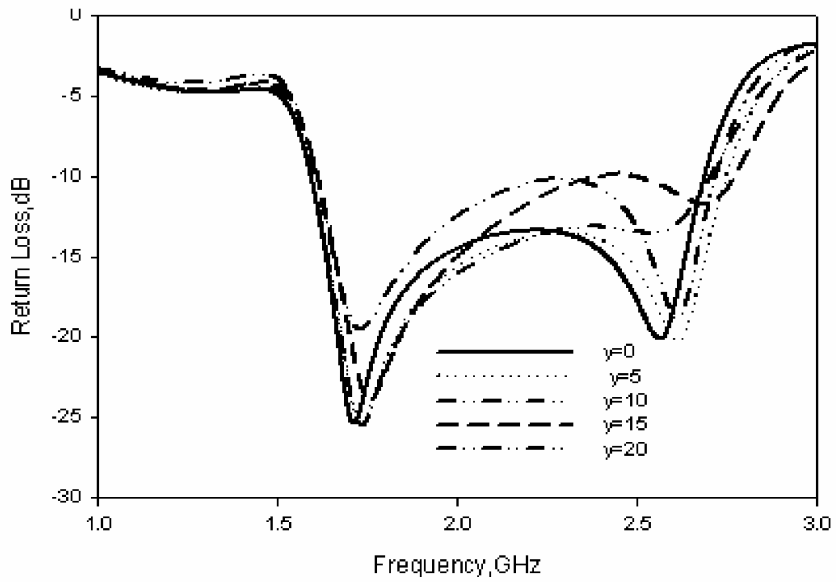

Fig. 13. Variation of resonances with the position of the parasite in the final antenna
L_d=32 mm, w=5 mm, L_t=35 mm, W_t=10 mm S=5 mm and g=0.5 mm, Lp =35 mm, ε_r=4.4, h=1.6 mm

In addition to impedance matching it can be seen that when the parasite is kept off centered, the 3 dB beam width gets reduced and the measured gain shows an increase of around 0.6 dBi. Hence the off centerd parasite is chosen in the final design.

The simulated field distribution in the antenna is shown in Fig. 14. Fig 14.a. shows the field variation at 1.69 GHz. The field is concentrated only on the dipole arms and a half wave variation corresponding to 1.69 GHz is observed along the length of the dipole. But at 2.56 GHz (14.b.) a half wave variation of the induced field is observed in the parasitic strip. These results confirm that the lower resonance is due to the dipole arm length and the higher resonance is due to the parasitic strip.

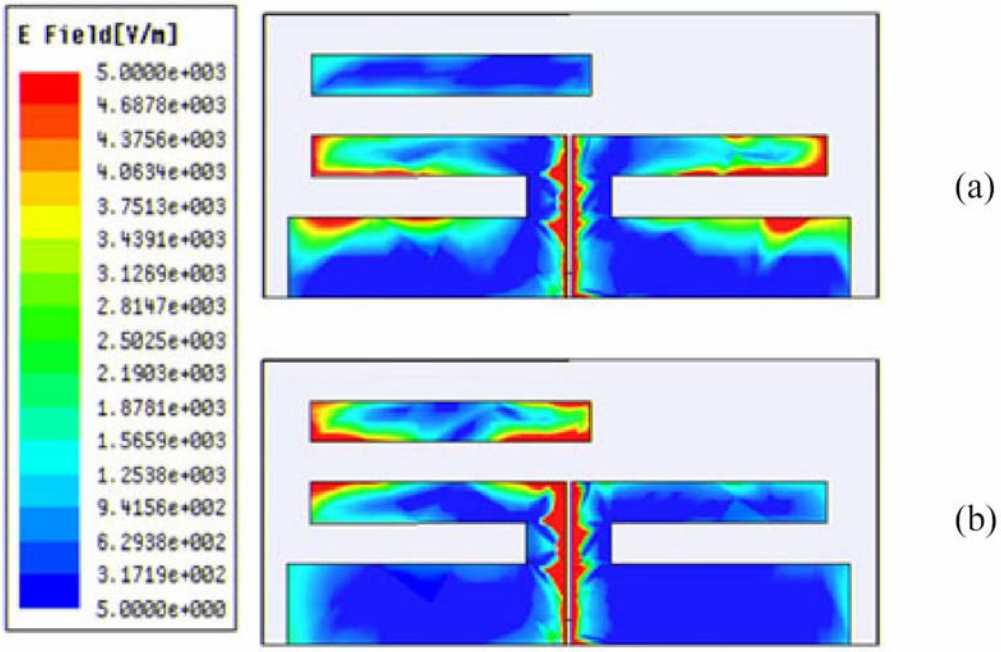

Fig. 14. Field distribution in the final antenna. (a) At 1.69 GHz (b) At 2.56 GHz
L_d=32 mm, w=5 mm, L_t=35 mm, W_t=10 mm S=5 mm and g=0.5 mm, Lp =35 mm, ε_r=4.4, h=1.6 mm

The principal E and H plane patterns of the antenna are shown in Fig. 15. It can be seen that the pattern remains almost stable in the entire operating band and polarized along the X axis for both the bands.

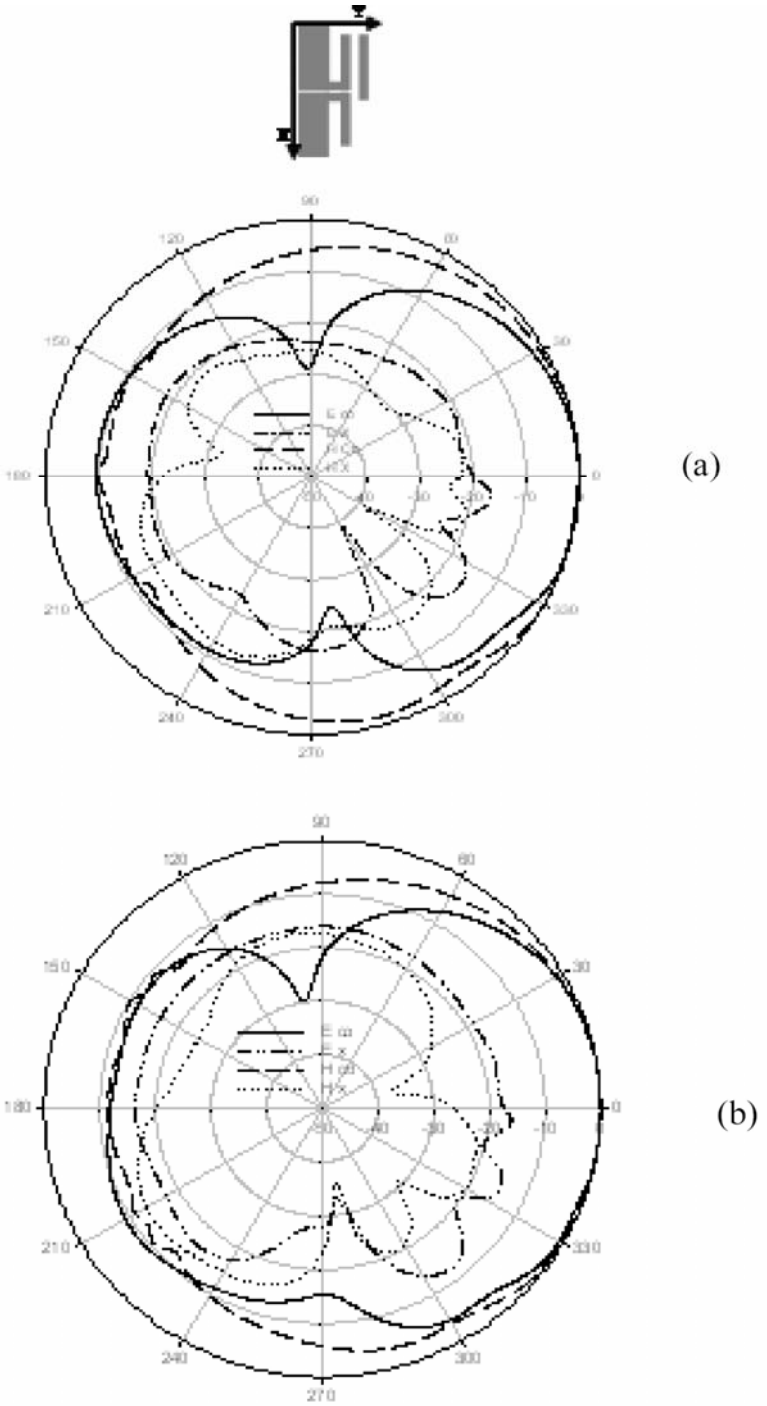

Fig 15. Principal E and H plane patterns of the antenna
(a)at 1.69 GHz (b) at 2.56 GHz

The measured gain of the antenna in the entire operating band is greater than 6.5 dBi (Fig. 16).This higher gain is due to the directive effect of the parasitic element. Also the addition of the parasite reduces the broadness of the pattern thereby increasing the gain of the antenna.

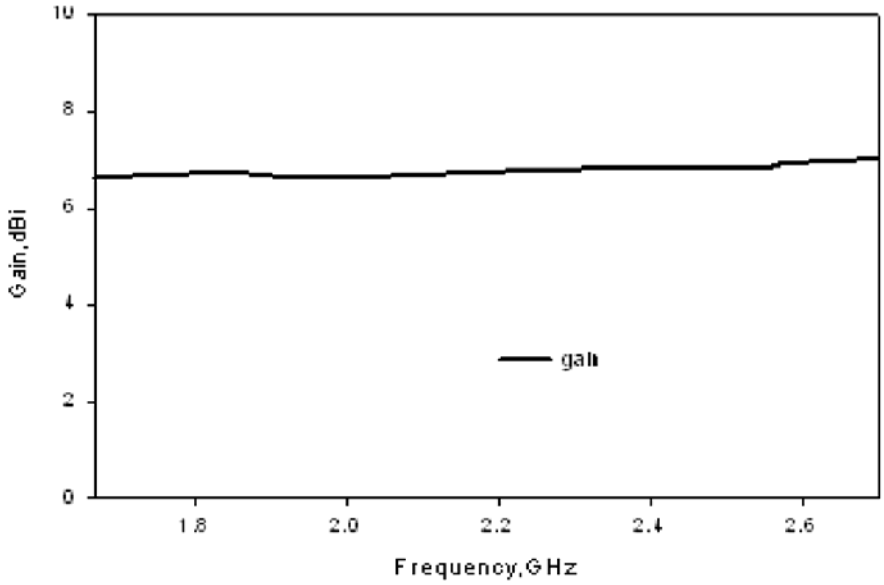

Fig. 16. Measured Gain of the final antenna

Conclusion

An uniplanar parasitic loaded wideband dipole antenna for DCS/PCS/UMTS IEEE802.11b/g applications is presented and discussed. The antenna is fed by a simple slot line without using baluns or other transitional structures. The dipole retains all the properties of an ordinary dipole but with an enhanced gain due to effect of the slot line and the parasitic strip A detailed study of the various parameters affecting the antenna characteristics is also presented. The design can be scaled and effectively used for the constructing high gain wideband printed antennas for wireless gadgets for Wi-Fi and WiMAX applications which is in a high demand.

References

[1] Young-Ho Suh and Kai Chang, "Low cost microstrip-fed dual frequency printed dipole antenna for wireless communications", *IEE Electron. Lett.*, 36, (2004)1177-1179.

[2] H.-M. Chen, J.-M. Chen, P.-S. Cheng and Y.-F. Lin, "Feed for dual-band printed dipole antenna", *IEE Electron. Lett.*, 40, (2004), 1320- 1321.

[3] Noriaki Kaneda, W. R. Deal, Yongxi Qian, Rod Waterhouse, and Tatsuo Itoh "A Broad-Band Planar Quasi-Yagi Antenna", IEEE Transactions on Antennas and Propagation,. 50, (2008), 1158-1160

[4] K. Tilley, X.-D. Wu and K. Chang,, "Coplanar waveguide fed coplanar strip dipole antenna", *IEE Electron. Lett.*, 30, (1994).

[5] C W Chiu,"Coplanar-Waveguide –fed uniplanar Antenna using a broadband balun", Microwave Opt.Technol .Lett.,40 (2004).70-73

[6] Y S Lin and C H Chen, "Novel Lumped Element Uniplanar transitions", *IEEE Trans. Antennas Propag.*, .49, (2001), 3833-3836.

[7] Shingo Tanaka, Yongho Kim, Hisashi Morishita,Satoru Horiuchi, Yasunori Atsumi, and Yoichi Ido," Wideband Planar Folded Dipole Antenna With Self-balanced Impedance Property" *IEEE Trans. Antennas Propag, 56, (2008)* 1223-1228

[8] H. K. Schuman, "Modeling folded dipoles and feedlines for radiation and scattering," *IEEE Trans. Antennas Propag.*, 38, (1990) . 30–39.

[9] H. K. Kan, R. B. Waterhouse, A. M. Abbosh, and M. E. Bialkowski, "Simple Broadband Planar CPW-Fed Quasi-Yagi Antenna", IEEE antennas and wireless propag lett, 6(2007)

[10] E A. Mariani, C P Heinzman, J P Agrios and S B Cohn , "Slot Line Characteristics", IEEE Trans. Microwave Theory Tech., 17,(1969), 1091-1096.

[11] V. Deepu, K.R. Rohith, J. Manoj, M.N. Suma, K. Vasudevan, C.K. Aanandan and P. Mohanan," Compact uniplanar antenna for WLAN applications", IEE Electron. Lett. Vol. 43 (2007)

[12] R Garg, P Bhartia and I Bahl, Microstrip antenna design hand book, 1st ed Boston. MA: Artech House, 2001, 786-789

[13] Xiao-peng Lu and Yan Li ,"Novel Broadband Printed dipole", Microwave and Optical Technology Lett., 48 (2006),1996-1998

Appendix **II**

Compact Uniplanar Antenna for WLAN Applications

This section describes the design and analysis of a compact slot line fed antenna for dual band applications. Here one of the lateral strips of the slotline feed is modified to excite dual band characteristics in the antenna. The compact dual-band uniplanar antenna operates in the 2.4/5.2/5.8 GHz WLAN/HIPERLAN2 communication bands. The dual-band antenna nature is brought by modifying one of the lateral strips of a slot line, to provide two different current paths. The antenna occupies a very small area of 14.5 x16.6 mm² including the ground plane on a substrate having dielectric constant 4.4 and thickness 1.6 mm at 2.2 GHz. The antenna resonates with two bands from 2.2 to 2.52 GHz and from 5 to 10 GHz with good matching, good radiation characteristics and moderate gain.

1. Introduction

With the tremendous increase in the number of laptops and other portable devices the need for wire-free communication, devoid of wires and interconnections, has become inevitable. The availability of the ISM band as licence free has paved the way for the design of various communication devices working at these frequencies for short-range communication. This has created great demand for suitable antennas working at these frequencies. Also, with the process of miniaturization in full swing, greater emphasis is given to compactness. Of available designs, planar antennas are preferred owing to advantages such as small volume, ease of fabrication and flush mounting facility.

Various types of antenna designs complying with these requirements have been reported. The printed double T monopole presented in [1] consists of two stacked T shaped monopoles for achieving dual resonance in the 2.4/5.2 GHz WLAN bands using a microstrip feed with a 50 x75 mm^2 ground plane. The planar monopole antenna [2] uses a shorted parasitic inverted L wire to obtain resonances in the 2.4/5.2/5.8 GHz bands. Compared to other designs, uniplanar antennas have advantages such as lack of soldering points, ease of fabrication and integration to MMICs on a single metallic layer structure. The compact dual-band antenna for ISM applications reported in [3] consists of an asymmetric dipole having a total area of 15x40 mm^2 and dual band is produced using the unbalanced current distribution in the asymmetric arms. The CPW fed dual-frequency antenna mentioned in [4] produces dual resonances connecting two monopoles to a single feed line.

A compact uniplanar antenna for WLAN applications is presented in this section. The proposed antenna design is obtained by modifying one of the lateral strips of a slot line. The proposed antenna resonates with two bands from 2.20–2.52 GHz and from 5.03–10.09 GHz which is wide enough to cover the IEEE 802.11b/g (2.400–2.484 GHz), IEEE802.11a (5.15–5.35, 5.725–5.825 GHz) and HIPERLAN2 (5.47–5.725 GHz) communication bands. Moreover, the antenna has a simple structure and occupies a very small area of 14.5 x16.6 mm^2 on a substrate of dielectric constant 4.4 and height 1.6 mm and can be easily printed into circuit boards.

2. Antenna Geometry

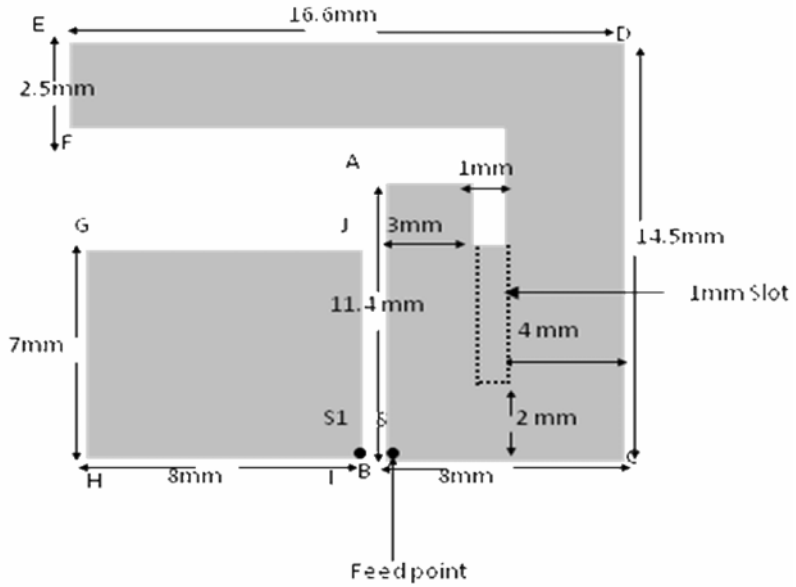

Fig.1. Geometry of the proposed slot line fed antenna

The geometry of the antenna is shown in fig.1. The basic geometry of the antenna is derived from a slot line having lateral strip width 8 mm and slot width 0.6 mm printed on an FR4 substrate of relative dielectric constant 4.4 and thickness 1.6 mm. The antenna is excited using a 50 Ω coaxial cable whose inner conductor is connected to the point S and the outer ground shielding to the point S1. Two arms (a shorter vertical strip and a longer inverted L strip) are first attached to one of the lateral strips of the slot line to introduce two different resonant paths. This results in a dual-band antenna resonating at 3.16 and 6.4 GHz.

To bring down the resonances to the required frequencies the structure is further modified. A narrow slot of 1 mm width is inserted in the structure to increase the resonant path and to bring down the resonances. The slot is shown in dotted lines in Fig. 1. The position of the slot is chosen to be at the position of minimum field intensity. It has to be noted that this technique does not affect the compactness of the antenna. The resulting antenna resonates at 2.44 GHz and 5.5 GHz.

3. Reflection and radiation characteristics of the antenna

The antenna is constructed on an FR4 substrate and tested. The simulated and experimental return loss characteristic of the final antenna is shown in Fig. 2. The experimental curve shows that a dual band is obtained from 2.2 to 2.52 GHz and from 5.03 to 10.09 GHz with good impedance matching.

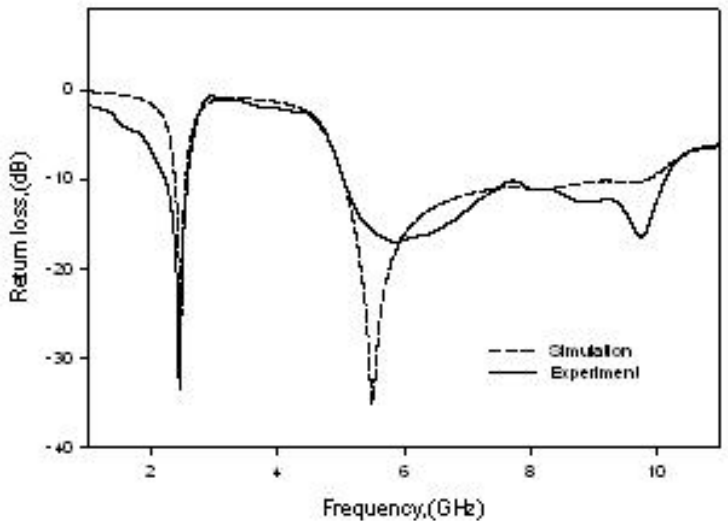

Fig.2. Experimental and simulated Return loss characteristic of the antenna

From simulation and experimental studies, it is found that for the first resonance the meandered length ABCDE acts as a quarter-wave monopole with GHIJ as the ground plane and for the second resonance the strip AB and GHIJ acts as the arms of an asymmetric dipole. i.e, the strips AB and GHIJ act as the arm of a $\lambda/2$ asymmetric dipole. The large width of the strip GHIJ is responsible for the high bandwidth in the second resonance. From simulation studies it is found that the strip CDE does not have much effect on the higher resonance

Also, it is noted that the horizontal strip DE has to be separated at least by a minimum distance of $0.2\lambda_1$ (where λ_1 corresponds to the first resonant wavelength) from the ground strip. This is to avoid coupling between the strip

DE and the ground strip so that the impedance matching is not deteriorated. The length and width of the strips are optimized to achieve good performance.

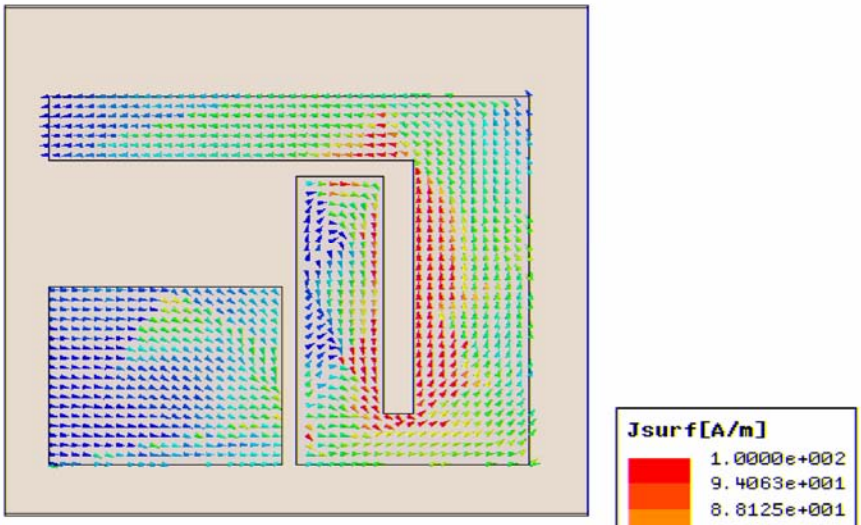

(a)

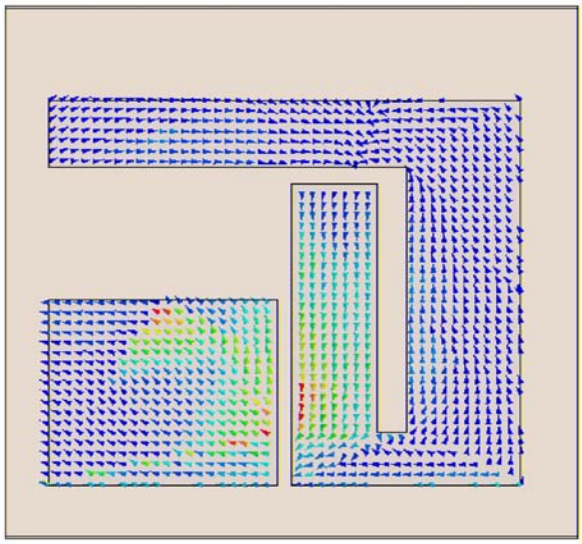

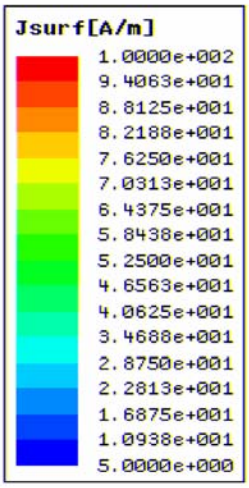

(b)

Fig. 3. Surface current distribution in the antenna

(a) 2.4 GHz (b) 5.2 GHz

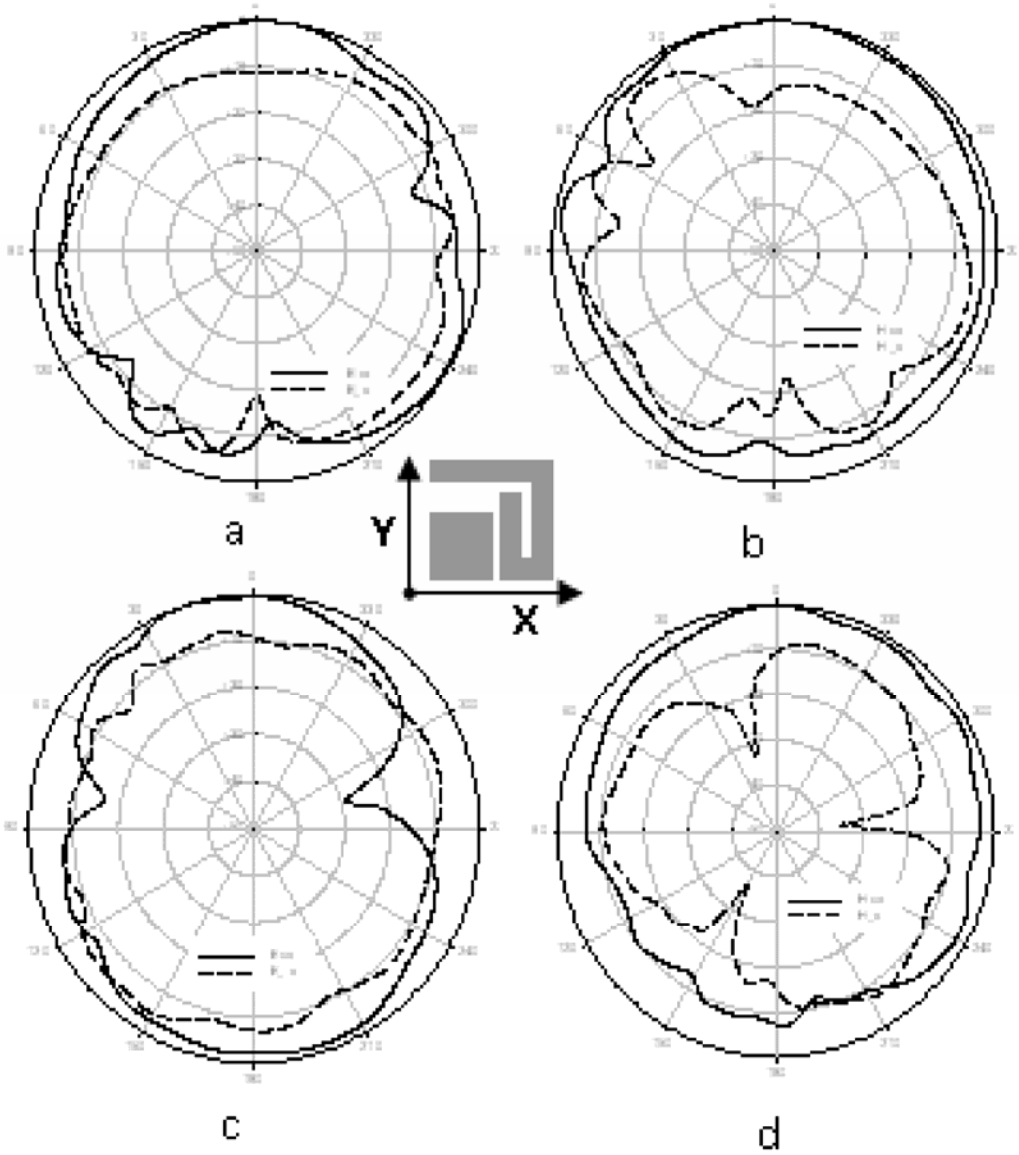

Fig.4. Radiation pattern of the antenna
(a) E plane at 2.44GHz (b) H plane at 2.44GHz (c) E plane at 5.5GHz (d) H plane at 5.5GHz

The principal E- and H-plane patterns of the antenna at 2.44 and 5.5 GHz bands are shown in Fig. 4. A near omnidirectional pattern is obtained in the two bands. This projects the suitability of the antenna in wireless applications.

The polarization of the antenna is determined experimentally. The antenna is polarized along the Y-axis in the lower band and along the X-axis in the higher band.

The gain of the antenna is measured in the two bands and is 1.9 dBi at 2.44 GHz, 1.6 dBi at 5.2 GHz, 1.8 dBi at 5.6 GHz and 1.9 dBi at 5.8 GHz, respectively.

4. Conclusion

A dual-band antenna for operation in the 2.4/5.2/5.8 GHz WLAN/HIPERLAN2 bands is presented and studied. The design is obtained by modifying a slot line thereby introducing two different current paths. The antenna has very compact dimensions of 14.5 x 16.6 x 1.6 mm^3 on an FR4 substrate. The simple, compact uniplanar structure and good radiation performance makes it useful in compact WLAN circuits.

References

[1] Kuo, Y.-L., and Wong, K.-L.: 'Printed double T monopole antenna for 2.4/5.2 GHz WLAN operations', IEEE Trans. Antennas Propag., 2003, 51, pp. 2187–2192

[2] Jan, J.-Y., and Tseng, L.-C.: 'Small planar monopole antenna with a shorted parasitic inverted-L wire for wireless communications in the 2.4-, 5.2-, and 5.8-GHz bands', IEEE Trans. Antennas Propag., 2004, 52, pp. 1903–1905

[3] Hwang, S.H., Moon, J.I., Kwak, W.I., and Park, S.O.: 'Printed compact dual band antenna for the 2.4 and 5 GHz ISM band applications', Electron. Lett., 2004, 40, (25),

[4] Chen, H.-D., and Chen, H.-T.: 'A CPW fed dual frequency monopole', IEEE Trans. Antennas Propag., 2004, 52, pp. 978–982

International Journals

1. Deepu V, Rohith K. Raj, Manoj Joseph, Suma M.N and P. Mohanan "Compact Asymmetric Coplanar Strip Fed Monopole Antenna for Multiband Applications", *IEEE Transactions on Antennas and Propagation*. Vol. 55, No. 8, August 2007.
2. Deepu V, Rohith K. Raj, Manoj Joseph, Suma M.N and P. Mohanan, "A Compact uniplanar antenna for WLAN applications". *IEE Electronics Letters* Volume 43, Issue 2, January 18 2007.
3. Deepu.V, S.Mridula, Sujith R and P.Mohanan, "Slot line fed dipole antenna for wide band applications", Microwave and Optical Technology Letters, Vol. 51, No. 3, March 2009
4. Deepu V,S Mridula,R Sujith and P Mohanan, ACS fed printed F shaped uniplanar antenna for Dual band WLAN applications, Microwave and Optical Technology Letters, (Accepted for publication May 2009).
5. Sujith R,Deepu.V,Laila D,C.K.Aanandan,K.Vasudevan and P.Mohanan, "A Compact Dual-Band Modified T-shaped CPW-Fed Monopole Antenna", Microwave and Optical Technology Letters, Vol. 51, No. 4, April 2009
6. Laila D, ,Deepu.V, Sujith R,, P.Mohanan,C.K.Aanandan, and K.Vasudevan "Compact asymmetric coplanar strip fed antenna for wide band applications" Microwave and Optical Technology Letters,(Accepted for publication May 2009).
7. Sumesh George, Prabhakaran Sreekumari Anjana, Vasudevan Nair Deepu, Pezholil Mohanan, and Mailadil Thomas Sebastian, Low-Temperature Sintering and Microwave Dielectric Properties of Li2MgSiO4 Ceramic for Low-Temperature Cofired Ceramic-Based Devices , Journal of the American Ceramic Society (accepted for publication March 2009)
8. Sherin Thomas, V. Deepu, P. Mohanan and M. T. Sebastian, "Effect of filler content on the dielectric properties of PTFE/$ZnAl_2O_4$-TiO_2 composites", *Journal of American Ceramic Society* Volume 91, Number 6, June 2008.
9. G,Subodh; V, Deepu; P, Mohanan; M. T., Sebastian ,"Polystyrene /sr2ce2ti5o15 composites with low dielectric loss for microwave substrate "Polymer Engineering and Science(Accepted for publication)
10. Nishamol M. S., Sarin V. P., Gigo Augustin, Deepu V., C. K. Anandan, P. Mohanan and K Vasudevan, "Compact Dual Frequency Dual Polarized Cross Patch Antenna with an X-slot", Microwave and Optical Technology Letters (December 2008.)

International and National Conferences

1. Deepu V, Rohith K.Raj,Manoj Joseph, Suma M.N , and P.Mohanan “Compact Dual band antenna for WLAN applications” Deepu V, Rohith K.Raj,Manoj Joseph, Suma M.N , and P.Mohanan .*IEEE APS-2007*,Honolulu,Hawaii,USA.
2. Deepu V, Rohith K.Raj,Manoj Joseph, Suma M.N ,C.K.Aanandan,K. Vasudevan and P.Mohanan “Compact asymmetric coplanar strip fed multiband antenna for wireless applications**”,** Proc. of the National Symposium on Microwave Antennas and Propagation, (APSYM-06). India **.**
3. Deepu.V, Sujith.R , Binu paul and P. Mohanan “Compact asymmetric coplanar strip fed Dual Band Antenna for WLAN applications” URSI GA 2008 ,USA
4. Deepu.V, S.Mridula, Sujith R and P.Mohanan, “Compact uniplanar antenna for multi band applications”, International conference on Aerospace Science and Technology, India 2008
5. Deepu.V, S.Mridula, Sujith R and P.Mohanan, “Asymmetric coplanar strip fed antenna for dual band applications”, IEEE International Microwave Conference Rajasthan,India ,November 2008
6. Laila D, ,Deepu.V, Sujith R,, P.Mohanan,C.K.Aanandan, and K.Vasudevan ,” Asymmetric coplanar strip fed wide band antenna “,IEEE International Microwave Conference Rajasthan,India,November 2008
7. P. S. Anjana , V. Deepu, P. Mohanan and M. T. Sebastian ,” Microwave dielectric properties of CeO_2 filled HDPE composites for microwave substrate applications”, Proc. of the National Symposium on Microwave Antennas and Propagation, (APSYM-08). India **.**
8. Laila D, ,Deepu.V, Sujith R,, P.Mohanan,C.K.Aanandan, and K.Vasudevan "Compact Uniplanar antenna for wide band applications", Proc. of the National Symposium on Microwave Antennas and Propagation, (APSYM-08). India
9. Sujith R,Deepu.V,Laila D ,Sarin V.P,NishaMol M.S,C.K.Aanandan, K.Vasudevan and P.Mohanan, ”Compact CPW fed antenna for Multiband applications”, Proc. of the National Symposium on Microwave Antennas and Propagation, (APSYM-08). India
10. Nishamol M S, Sarin V P, Deepu V, Sujith R, P Mohanan, C K Anandan and K Vasudevan,” Cross Patch Antenna with an X-slot for Polarization Switching”, Proc. of the National Symposium on Microwave Antennas and Propagation, (APSYM-08). India

11. Sarin V.P, Nisha mol M.S, Deepu V, Sujith R, P. Mohanan, C.K Aanandan and K. Vasudevan,” Broad band microstrip antenna for Wireless applications “,Proc. of the National Symposium on Microwave Antennas and Propagation, (APSYM-08). India
12. Thomas Sebastian, Sherin Thomas, G. Subodh, V. Deepu,P. Mohanan, and M. T. Sebastian,” Influence of Permittivity Contrast on the Properties of Microstrip patch Antenna Made of a Dual Substrate”, Proc. of the National Symposium on Microwave Antennas and Propagation, (APSYM-08). India **.**
13. Sumesh george , V. Deepu, P.Mohanan and M. T. Sebastian,” Microwave dielectric properties of ca[(li1/3nb2/3)0.8 ti 0.2]o3-_ – polyethylene composites for microelectronic applications”, National seminar on ferroelectric & dielectrics Patiala, India, November 2008.
14. Deepu V,S Mridula,Anju Pradeep Sujith R and P Mohanan An Ultra Compact Antenna for DVBH Applications, IEEE APS 2009 , (accepted)

Citations

a). **Paper :-** Deepu V, Rohith K. Raj, Manoj Joseph, Suma M.N and P. Mohanan, "A Compact uniplanar antenna for WLAN applications". *IEE Electronics Letters* Volume 43, Issue 2, January 18 2007.

1. **Compact dual-band printed monopole antenna for WLAN application**

   H Ma, QX Chu, Q Zhang - Electronics Letters, 2008 - ieeexplore.ieee.org

2. **CPW-FED shorted monopole antenna for broadband application**

   WC Liu, FM Yeh - Microwave and Optical Technology Letters, 2008 - interscience.wiley.com

3. **LTCC-based compact UWB antenna and its integration study**

   M Sun, YP Zhang - Microwave and Optical Technology Letters, 2008 - interscience.wiley.com

4. **Varactor-tuned microstrip bandpass filter with wide tuning range**

   J Kim, J Choi - Microwave and Optical Technology Letters, 2008 - interscience.wiley.com

5. **Very-low-cost copper-wire antenna for 2.4-GHz WLAN operation**

   JH Chou, SW Su - Microwave and Optical Technology Letters, 2008 - interscience.wiley.com

6. **Low-cost flat metal-plate dipole antenna for 2.4/5-GHz WLAN operation**

   SW Su, JH Chou - Microwave and Optical Technology Letters, 2008 - interscience.wiley.com

7. **Compact printed slot antennas for wireless dual-and multi-band operations**

   YC Lee, JS Sun - ceta.mit.edu

9. **Compact paper-clip-shaped wire antenna for 2.4 and 5.2 GHz WLAN operation**

   SW Su, JH Chou, YT Liu - Microwave and Optical Technology Letters, 2008 - interscience.wiley.com

10. **Broad dualband fork-shaped CPW-fed monopole antenna**

    WC Liu, CM Wu, YH Ho - TENCON 2007-2007 IEEE Region 10 Conference, 2007 - ieeexplore.ieee.org

11. **Slot line FED dipole antenna for wide band applications**

    V Deepu, S Mridula, R Sujith, P Mohanan - Microwave and Optical Technology Letters, 2009 – Iinterscience.wiley.com

12. **Design of Dual-band Planar Inverted-F Antennas with a Parasitic Element**

    W Nien - 2008 - thesis.lib.ncu.edu.tw

13. **New microstrip low pass filter with transmission zero and wide stopband**

    JK Xiao, QX Chu, HF Huang - Microwave and Optical Technology Letters, 2009 - interscience.wiley.com

14. **A bent, shorted, planar monopole antenna for 2.4 GHz WLAN applications**

    SW Su, FS Chang - Microwave and Optical Technology Letters, 2009 - interscience.wiley.com

15. **Compact multiband slotted antenna for wireless communication applications**

    YC Lee, JS Sun - Microwave and Optical Technology Letters, 2009 - interscience.wiley.com

b). Paper :- Deepu V, Rohith K. Raj, Manoj Joseph, Suma M.N and P. Mohanan "Compact Asymmetric Coplanar Strip Fed Monopole Antenna for Multiband Applications", *IEEE Transactions on Antennas and Propagation*. Vol. 55, No. 8, August 2007.

1. **Compact asymmetric coplanar strip-fed antenna for wideband applications**

   D Laila, V Deepu, R Sujith, CK Aanandan, K … - Microwave and Optical Technology Letters, 2009 - interscience.wiley.com

2. **Ultr a-Wideband Coplanar-Fed Monopoles: A Comparative Study**

   J JILKOVÁ, Z RAIDA - Radioengineering, 2007 - radioeng.cz

3. **Compact coplanar slot antenna fed by asymmetric coplanar strip for 2.4/5 GHz WLAN operations**

   Y Song, YC Jiao, XM Wang, ZB Weng, FS Zhang - Microwave and Optical Technology Letters, 2008 - interscience.wiley.com

4. **Compact dual-frequency double T-shaped slot antenna for RFID application**

   L Zhang, YC Jiao, K Song, FS Zhang - Microwave and Optical Technology Letters, 2009 - interscience.wiley.com

5. **A compact ultra-wideband bandpass filter with WLAN notch band**

   PY Hsiao, RM Weng - Microwave and Optical Technology Letters, 2009 - interscience.wiley.com

6. **Raman amplification impact in packet base networks**

   P Andre, B Neto, A Teixeira, N Wada - Microwave and Optical Technology Letters, 2008 - interscience.wiley.com

7. **Reconfigurable patch with switchable conductive edges**

   RL Haupt - Microwave and Optical Technology Letters, 2009 - interscience.wiley.com

8. **Millimeter wave conduct speech enhancement based on auditory masking properties**

   S Li, JQ Wang, M Niu, T Liu, XJ Jing - Microwave and Optical Technology Letters, 2008 - interscience.wiley.com

.....ꕥ.....

RESUME OF THE AUTHOR

DEEPU V
Senior Research Fellow
Centre for Research in Electromagnetics and Antennas
Department of Electronics
Cochin University of Science and Technology
Kerala, India,
Email: deepunairv@gmail.com

OBJECTIVE

To be part of an organization that will tap my potential to the fullest, emerge as a choice employee, and accelerate career growth in tandem with my organization.

AREAS OF INTEREST

Compact Planar antennas, DVBH Antennas,Mobile antennas, Printed Monopole Antennas, Microwave material characterisation.

WORK EXPERIENCE

1. Involved in the desining of various ultra compact wide band uniplanar antennas for multiband applications like WLAN, DVB-H and antennas highly suitable for compact mobile phones and RFIDs.
2. Successfully developed compact antennas for a Malaysian company as part of consultancy Project
3. Published papers in International Journals such as IEEE Transactions, IET Electronic lettersetc and various International/ National Symposia)
4. Designed various Uniplanar antennas for applications compatable for use in Laptops and similar wireless devices
4. Experience in design tools like Ansoft HFSS , CST and IE3D
5. Experienced in using Vector Network Analyzer HP 8510C, PNA 8362B Network Analyzer, Anechoic chamber measurements etc.
6. Experience in design and testing of compact low frequency antennas, uniplanar antennas, printed monopoles.
7. Experience in Microwave material characterisation

EDUCATION

Course	Year	University	Institution	Class
PhD	*Currently pursuing (In the final stage)*	*Cochin University of Science and Technology, Cochin(CUSAT), Kerala, India*	*Centre for Research in Electromagnetics and Antennas (CREMA), Department of Electronics, CUSAT, Kerala, India*	---
M.Sc Electronics	*2003-2005*	*Cochin University of Science and Technology(CUSAT), Cochin, Kerala, India*	*Department of Electronics,CUSAT, Kerala, India*	*First class with Distinction CGPA 8.28*
B.Sc Physics	*2000-2003*	*Kerala University Kerala, India*	*Mahatma Gandhi college, Thiruvananthapuram*	*First class (79.4%)*

PERSONAL INFORMATION

Date of Birth	:	27.05.1982
Languages	:	English, Malayalam, Hindi
Permanent Address	:	**21/1811, KADAVILAKATHU VEEDU KARAMANA P.O THIRUVANANTHAPURAM KERALA, INDIA,**

REFERENCE

Dr. P. Mohanan
Professor
Department of Electronics
Cochin University of Science and Technology
Cochin-22, Kerala, India.
drmohan@gmail.com

.....ꕥ.....

Index Words